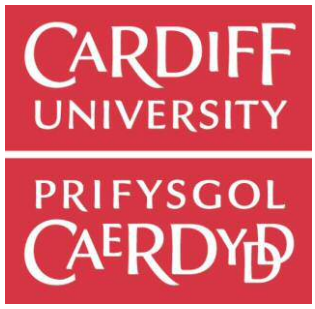

Exploring the role of the Notch signalling pathway in normal and malignant human haematopoiesis

Fábio Gabriel Pereira Lampreia

A thesis submitted for the degree of Doctor in Philosophy at

Cardiff University

School of Biosciences

Submitted: October 2019

Fábio Gabriel Pereira Lampreia was supported by Hodge Foundation studentships

Summary

Haematopoietic stem cells (HSCs) possess self-renewal capacity and give rise to the entire blood and immune systems. Notch is an evolutionarily conserved signalling pathway activated by cell-to-cell interactions with roles in stem cell maintenance, survival and differentiation. While studies in the murine haematopoietic system have proposed different roles for Notch signalling under stress and steady-state conditions, whether Notch is involved in the regulation of human haematopoietic stem/progenitor cells (HSPCs) has been scarcely explored. Here, we showed HSPCs express mainly Notch1 and Notch2 receptors and possess an active Notch pathway. We employed pharmacological inhibition by using the γ-secretase inhibitor DAPT and shRNA-mediated silencing of Notch pathway members (*NCSTN* and *RBPJ*) in human HSPCs. Notch inhibition led to reduced colony forming capacity *in vitro* and reduced frequency of immunophenotypic HSCs. Additionally, Notch inhibition caused decreased myelo-lymphoid engraftment *in vivo* along with deregulation of most stem/progenitor cell compartments, of which the HSC fraction was the most affected. Silencing *RBPJ* additionally impaired B cell development both *in vitro* and *in vivo*. These data contrast with the studies on the mouse haematopoietic system and suggest an essential role for Notch in the regulation of human HSCs. Malignant transformation of HSPCs lead to the development of haematological malignancies such as leukaemias. Here, we characterised Notch signalling in Acute Myeloid Leukaemia (AML) and showed that this pathway appears to be mostly silenced in this context. Reactivation of the pathway via membrane-bound Notch ligand and via a soluble Jag1 based peptide decreased proliferation and induced apoptosis in various AML cell lines. Furthermore, small molecule agonists of Notch were tested for their potential therapeutic value. All in all, our data further support the notion that Notch reactivation may exhibit therapeutic significance in some instances of AML.

Statements and Declarations

STATEMENT 1

This thesis is being submitted in partial fulfilment of the requirements for the degree of PhD (*insert PhD, MD, MPhil, etc., as appropriate*)

Signed _____
Date: 30th October 2019

STATEMENT 2

This work has not been submitted in substance for any other degree or award at this or any other university or place of learning, nor is it being submitted concurrently for any other degree or award (outside of any formal collaboration agreement between the University and a partner organisation)

Signed _____
Date: 30th October 2019

STATEMENT 3

I hereby give consent for my thesis, if accepted, to be available in the University's Open Access repository (or, where approved, to be available in the University's library and for inter-library loan), and for the title and summary to be made available to outside organisations, subject to the expiry of a University-approved bar on access if applicable.

Signed _____
Date: 30th October 2019

DECLARATION

This thesis is the result of my own independent work, except where otherwise stated, and the views expressed are my own. Other sources are acknowledged by explicit references. The thesis has not been edited by a third party beyond what is permitted by Cardiff University's Use of Third Party Editors by Research Degree Students Procedure.

Signed _____
Date: 30th October 2019

WORD COUNT 36595

(Excluding summary, acknowledgements, declarations, contents pages, appendices, tables, diagrams and figures, references, bibliography, footnotes and endnotes)

Table of contents

List of figures

List of tables

Acknowledgments

I would like to first thank Dr. Fernando dos Anjos Afonso for giving me the opportunity to undertake this challenge, for his guidance and teachings throughout these years. Many thanks also to Dr. Neil Rodrigues, Professor Andrea Brancale, Dr. Salvatore Ferla, Julija Jotautaite and António de Soure for the contributions made to this work.

I would also like to thank The Hodge Foundation for financially supporting this project and for continuing to support other research thereby having a very positive and big impact in research promotion and development. Without their support this work would not be possible.

I am also deeply grateful for all my colleagues and friends at the European Cancer Stem Cell Research Institute, especially Ana Jimenez, Andreas Zaragkoulias, Aleix Puig, Carlotta Olivero, Giusy Tornillo, Joana Carmelo, Juan Menendez and Leigh-Anne Thomas. Many thanks also to Aisha Al-Sabah, Aled Bryant, Chelsea Kendall, Pedro Gomez, Simone Lanfredini. Thanks Marco Marques, Salomé Magalhães and Gustav!

Thank you to all my Portuguese friends, from the Alentejo to the Margem-Sul crews for making the trips back home extra special. Especially João Ortiz and Yvonne Pacheco, Mário Oliveira, Carol Biasoli and Ísis; Tiago Dias and Mariana; Cláudia Miranda, Renato Penas and Cláudia Dias, Liliana Marques, Mariana Monteiro, Alice Portela, Filipe Catarino and Marta; Carlos Marques and Leslie; João Dias, Joana Barracosa and Maggie! Carla Dias and Valter; Viviana and Tatiana Duarte and Francisco Carrega! Love you all!

A very special thanks to all my family (Antonio, Maria, Michael, Catarina, Avó Catarina, Avô Francisco, Avó Joaquina and Avô Manuel) for their endless support, understanding and simply being the best people I know.

Thank you to my second family Mena Neves, André Simões, Sofia da Cruz, and the Neves family (Aurora, Manuel, Fátima, Ricardo and Carol).

At last but not the least, thank you Irina Neves Simões, for being my guiding light for all these years.

“You steer the ship the best way you know. Sometimes it’s smooth. Sometimes you hit the rocks. In the meantime, you find your pleasures where you can.”

— Junior Soprano

Abbreviations

aHSCT	Allogeneic haematopoietic stem cell transplantation
AML	Acute myeloid leukaemia
ANK	Ankyrin
APH	Anterior pharynx-defective
APL	Acute promyelocytic leukaemia
Ara-C	Cytarabine
B	B cell
B-ALL	B cell Acute lymphoblastic leukaemia
BFU-E	Burst forming unit-erythroid
bHLH	Basic helix-loop-helix
BiTE	Bi-specific T cell engagers
BM	Bone marrow
BMEC	Bone marrow endothelial cells
BMP	Bone morphogenetic protein
BSA	Bovine serum albumin
CAFC	Cobblestone area forming cell
CAR	Chimeric antigen receptor
CB	Cord blood
CFU	Colony forming unit
CFU-E	Colony forming unit-erythroid
CFU-GEMM	Colony forming unit-granulocyte, erythroid, macrophage, megakaryocyte
CFU-GM	Colony forming unit-granulocyte, macrophage
CFU-S	Colony forming unit-spleen
ChIP	Chromatin immunoprecipitation
CIC	Cancer initiating cell
CLL	Chronic lymphocytic leukaemia
CLOUD	Continuum low primed undifferentiated cells
CLP	Common lymphoid progenitor
CML	Chronic myeloid leukaemia
CMML	Chronic myelomonocytic leukaemia
CMP	Common myeloid progenitor
CNS	Central nervous system
CR	Complete remission

CSL	CFB1, Su(H), Lag-1
DAPI	4′,6-diamidino-2-phenylindole
DAPT	N-[N-(3,5-Difluorophenacetyl)-L-alanyl]-S-phenylglycine t-butyl ester
DC	Dendritic cell
DMEM	Dulbecco's Modified Eagle's Medium
DMSO	Dimethyl sulfoxide
DNA	Deoxyribonucleic acid
DNMAML	Dominant negative Mastermind-like
DNXSUH	Dominant negative Xenopus Supressor of Hairless
DOS	Delta and OSM-11 like proteins
DSL	Delta, Serrate and Lag2
EC	Endothelial cell
EDTA	Ethylenediaminetetraacetic acid
EF1α	Elongation factor α
EFS	Event-free survival
EGF	Epidermal growth factor
EGFP	enhanced Green fluorescent protein
ELN	European LeukaemiaNet
EP	Erythroid progenitor
Er	Erythroid
FAB	French American British
FACS	Fluorescence-activated cell sorting
FBS	Foetal bovine serum
FCM	Flow cytometry
FGF	Fibroblast growth factor
FISH	Fluorescence *in situ* hybridisation
FLT3	Fms-related tyrosine kinase 3
FLT3-ITD	Fms-related tyrosine kinase 3-internal tandem duplication
FSC-A	Forward scatter area
G	Granulocyte
G-CSF	Granulocyte colony stimulating factor
GFP	Green fluorescent protein
GM-CSF	Granulocyte macrophage colony-stimulating factor
GMP	Granulocyte macrophage progenitor
HD	Heterodimerisation domain
HEK	Human embryonic kidney

HPC	Haematopoietic progenitor cell
HSC	Haematopoietic stem cell
HSPC	Haematopoietic stem/progenitor cell
IDH1/2	Isocitrate dehydrogenase 1/2
IL	Interleukin
IL2Rγc	Interleukin-2 receptor common gamma chain
IMDM	Iscove's Modified Dulbecco's Medium
JAG	Jagged
KD	Knockdown
L	Litre
LB	Lennox broth
LBA	Long bone area
LIC	Leukaemia-initiating cell
Lin	Lineage
LMPP	Lymphoid primed multipotent progenitor
LNR	Lin12/Notch repeats
LSK	$Lin^{-}Sca^{-}1^{+}c^{-}Kit^{+}$
LTC-IC	Long-term culture initiating cell
LT-HSC	Long-term culture Haematopoietic stem cell
Luc	Luciferase
Ly	Lymphoid
M	Macrophage
MAML	Mastermind-like
MAP	Mitogen activated protein
M-CSF	Macrophage colony-stimulating factor
MEP	Megakaryocyte erythrocyte progenitor
MFI	Median fluorescence intensity
miRNA	micro ribonucleic acid
Mk	Megakaryocyte
mL	millilitre
MLP	Multi-lymphoid progenitor
mM	millimolar
MNC	Mononuclear cell
MOI	Multiplicity of infection
MPD	Myeloproliferative disease
MPP	Multipotent progenitor

mRNA	Messenger ribonucleic acid
MSC	Mesenchymal stem cell
My	Myeloid
NCSTN	Nicastrin
NFKB	Nuclear factor kappa B
NGFR	Nerve growth factor receptor
NGS	Next generation sequencing
NICD	Notch intracellular domain
NK	Natural killer cell
NLS	Nuclear localisation signal
NMHC	N-methylhemeanthidine chloride
NOD	Non-obese diabetic
NOD/SCID	Non-obese diabetic/severe combined immunodeficient
NRR	Negative regulatory region
NSG	Non-obese diabetic/severe combined immunodeficient gamma
OS	Overall survival
OXPHOS	Oxidative phosphorylation
PAR	Partitioning defective protein
PB	Peripheral blood
PBS	Phosphate buffered saline
PCR	Polymerase chain reaction
PEN	Presenilin enhancer
PEST	Proline-glutamine-serine-threonine rich domain
PFA	Paraformaldehyde
PNS	Peripheral nervous system
PS	Penicillin/Streptomycin
qRT PCR	quantitative real-time polymerase chain reaction
RBPJκ	Recombination signal binding protein for immunoglobulin kappa J region
RNA	Ribonucleic acid
ROS	Reactive oxygen species
RPMI	Roswell Park Memorial Institute
RSAP	Recombinant shrimp alkaline phosphatase
RT	Room temperature
SCF	Stem cell factor
SHRNA	Short hairpin ribonucleic acid
SKIP	Ski-interacting protein

SOP	Sensory organ precursor
SRC	Severe combined immunodeficient repopulating cell
SSC-A	Side scatter area
T	T cell
TACE	Tumor necrosis factor alpha converting enzyme
TAD	Transcriptional activation domain
T-ALL	T cell acute lymphoblastic leukaemia
TBA	Trabecular bone area
TCR	T cell receptor
TET	Ten-eleven-translocation enzyme
TGFβ	Transforming growth factor β
TMN	Transmembrane
TNFα	Tumour necrosis factor α
TPO	Thrombopoietin
TRM	Treatment-related mortality
UCB	Umbilical cord blood
µL	microlitre
µM	micromolar
VEGF	Vascular endothelial growth factor
WB	Western blot
WGS	Whole genome sequencing
WHO	World Health Organization
WNT	Wingless
YY	Yin Yang

Chapter 1 – Introduction

This thesis is focused on human haematopoiesis and all aspects discussed here concern the human system, except when the murine haematopoietic system is referred to at times for comparison purposes.

1.1. Normal haematopoiesis

1.1.1. Brief history of Haematopoietic stem cell (HSC) discovery

HSCs are the founders of the entire blood and immune system. These are multipotent cells with the ability to self-renew and to generate both a pool of stem cells and more committed progenitors. The latter differentiate into different mature blood and immune cells. The story of haematopoietic stem cell discovery came about with the advent of atomic warfare at the later stages of the second world war. The seminal works of Jacobson and colleagues, who at the time were studying the effects of ionizing radiation in mice, first showed that the animals could be protected from the lethal effects of ionizing radiation by shielding their spleens with lead (Jacobson *et al*., 1951). Later, Lorenz and colleagues showed that this type of protection could also be conferred by intravenous infusion of bone marrow (BM) cells (Lorenz *et al*., 1951). Soon after, scientists understood that this protection was conferred by transplanted stem cells, which launched the platform for the use of these cells in the treatment of several diseases. The understanding that the damage caused by myeloablation could be overcome, led to discovery of transplantable bone marrow cells capable of regenerating the haematopoietic system. This was originated from the attempt to quantify the minimal number of cells that would protect a lethally irradiated recipient. In these pivotal experiments, a key observation was made: the appearance of nodules at the surface of the spleens from the recipient animals; more importantly, the fact that the number of nodules was linearly correlated to the number of cells transplanted suggested that there must be a subpopulation within the transplanted cells with the capacity to generate splenic nodules (Till and McCulloch, 1961). From these early experiments, crucial observations led to several important conclusions: within the bone marrow of these mice lie haematopoietic cells of mixed myeloid origin, but also with some lymphoid differentiation potential, that could generate splenic nodules in secondary recipients (Wu *et al*., 1967). In this way, the concept of a multilineage repopulating cell with apparent self-renewal capacity was born, and in fact with it, so did the concept of a stem cell.

1.2. Hierarchy of the human haematopoietic system, a brief note

1.2.1. Haematopoietic stem cells

In the classical view, the haematopoietic system is believed to be organised in a hierarchical manner. It is commonly viewed that the most primitive cells sitting at the top of the hierarchy successively give rise to more committed progenitors which differentiate into the mature blood and immune cells, and supposedly progress from multipotent to oligopotent to unipotent cells. As they differentiate, cells gradually lose self-renewal capacity. The earliest bifurcation in cell fate decision is thought to be between the myeloid (granulocytes (G), monocytes (M), erythrocytes (Er) and megakaryocytes (Mk)) and the lymphoid (B, T, Natural Killer (NK) cells) lineages. A multipotent progenitor (MPP), which retains multilineage potential, gives rise to either a common myeloid progenitor (CMP) responsible for generating all the myeloid cell types, or to a common lymphoid progenitor (CLP) that gives rise to lymphocytes and NK cells.

There are three main sources of human post-natal HSCs: umbilical cord blood (UCB), peripheral blood (PB) and BM (Sirinoglu Demiriz *et al*., 2012). However, for instance it is estimated that only 1 in 10^6 cells in the BM is a transplantable HSC (Wang *et al*., 1997). To study such rare cells, HSCs must be isolated from the bulk of mononuclear cells (MNCs). This was made possible by technological advances in the field of fluorescence-activated cell sorting (FACS) by which the isolation of HSCs can be achieved with specific cell surface markers. The CD34 antigen was the first used to isolate a compartment of immature haematopoietic cells (Civin *et al*., 1984). Only about 1-4% of the total BM MNCs express CD34 (Civin *et al*., 1984). The CD90 (Thy-1) surface antigen was later found to further refine this primitive population (Baum *et al*., 1992). However, this is still a heterogeneous population containing many progenitors, which can be further enriched by the lack of CD38 (cyclic ADP ribose hydrolase) (Bhatia *et al*., 1997) and CD45RA (an isoform of protein tyrosine phosphatase, receptor type C) expressions (Lansdorp *et al*., 1990). For a while, the $CD34^+CD38^-CD45RA^-CD90^+$ was considered the population where HSCs could be confidently identified and indeed, transplantation of these cells into immunocompromised mice led to successful engraftment in most mice using as few as 100 cells (Majeti *et al*., 2007). In the same report, the authors suggested that the $CD34^+CD38^-CD45RA^-CD90^-$ compartment contained candidate progenitor cells, since these cells were also shown to have multilineage reconstitution but with a higher transplanted cell number (Majeti *et al*., 2007). However, more than 30% of the cells in the $CD34^+CD38^-CD45RA^-CD90^-$ compartment are also able to reconstitute secondary recipients, which raises the question of whether CD90 is in fact a reliable marker capable of segregating true HSCs from MPPs. To address this, Notta and colleagues used CD49f (integrin α6) antigen as an additional surface antigen for further purifying human HSCs. $CD49f^+$ cells were shown

to yield an almost 7-fold higher human chimerism in transplantation assays as compared to CD49f$^-$ cells and as little as ten CD34$^+$CD38$^-$CD45RA$^-$CD90$^+$CD49f$^+$ cells resulted in successful multilineage engraftment. This study has redefined the HSC immunophenotype and certified CD34$^+$CD38$^-$CD45RA$^-$CD90$^-$CD49f$^-$ into bona fide MPPs instead (Notta *et al*., 2011) (**Figure 1.1**).

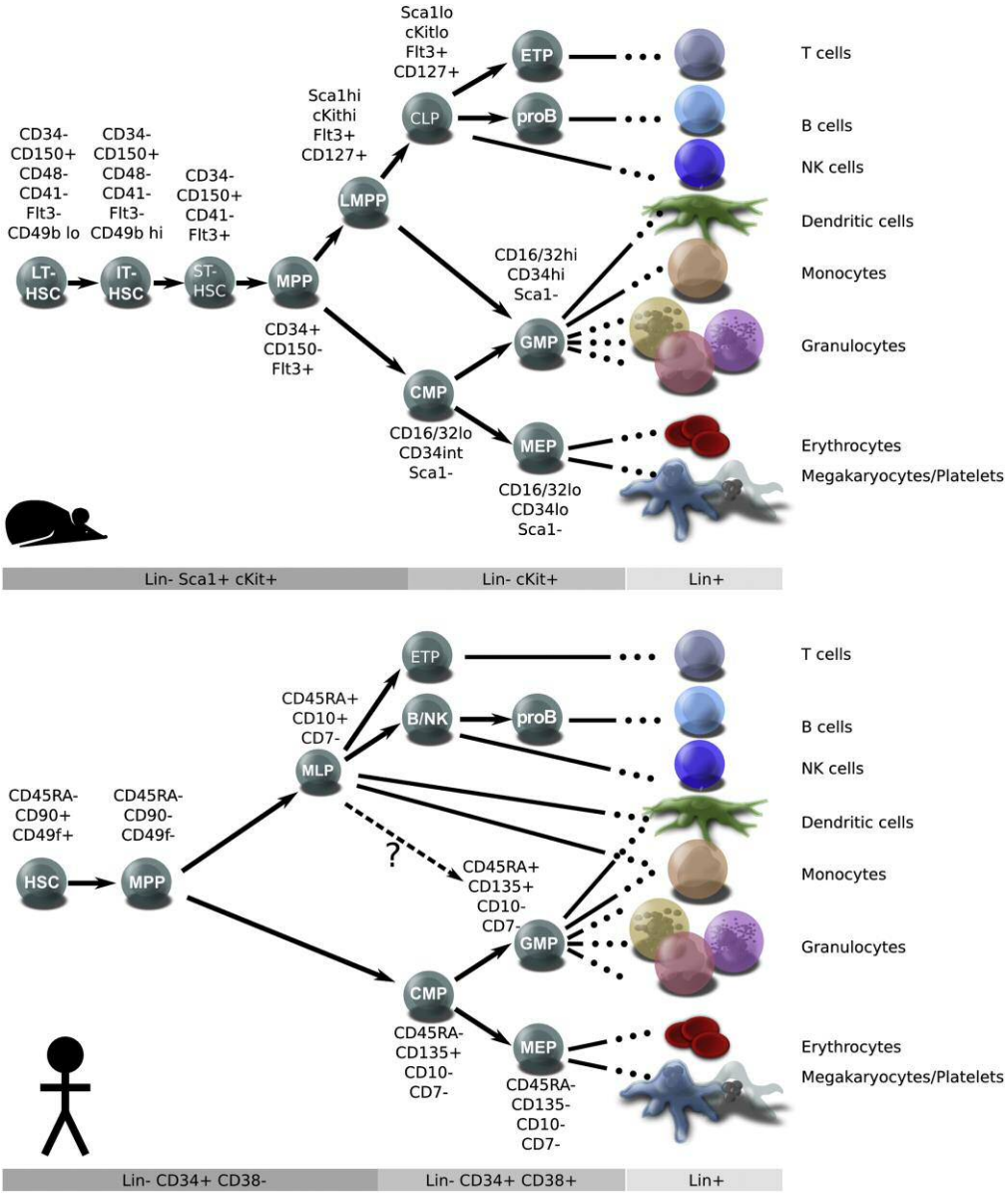

Figure 1.1 – Models of adult Mouse and Human Haematopoietic Hierarchies. The different populations discovered by functional assays are showed for both systems, with the immunophenotypes associated with each. In both models, gradual lineage restriction progresses from the left starting at the HSCs, through intermediate progenitors until mature cells on the right. (Lin: cocktail containing cell surface markers for all terminally differentiated populations (B cell; T cell; NK; dendritic cell, monocyte, granulocyte, megakaryocyte, and erythrocyte). (Reprinted from "Hematopoiesis: A Human Perspective", volume 10, Issue 2. Doulatov *et al*., P120-136, February 03, 2012 Copyright (2012), with permission from Elsevier).

So far, this immunophenotype has remained the gold standard for isolating highly purified human HSCs, although undoubtedly new markers will be discovered that will allow the isolation of populations progressively more enriched for true HSCs. On the other hand, a highly quiescent type of HSC can also be found in the $CD34^-$ compartment and can be placed at the top of the human hierarchy. Over 20 years ago, Bhatia and colleagues found a new $CD34^-$ population capable of repopulating non-obese diabetic/severe combined immunodeficient (NOD/SCID) mice which the authors termed $CD34^-$ SCID-repopulating cells (Bhatia *et al*., 1998). These cells were found at a proportion of one repopulating cell per 125,000 Lin^-CD34^- cells and were shown to have a very different behaviour under culture conditions as compared to $CD34^+$ cells. For example, human umbilical vein endothelial cell (HUVEC)-conditioned media co-culture increased the number of $CD34^-$-SRCs, while these conditions led to differentiation of $CD34^+$ cells (Bhatia *et al*., 1998). In addition to this, mice transplanted with UCB-derived $Lin^-CD34^-CD38^-$ showed human myelo-lymphoid engraftment at 24 weeks (Ishii *et al*., 2011). Later on, $CD34^-$ cells with engraftment potential were shown to be confined in the $CD93^+$ (C1qRp) fraction (Danet *et al*., 2002). Recent evidences suggest that they comprise highly quiescent cells, regulated in part by Notch and TGFβ signalling, which not only are able to give rise to but also possess higher repopulating potential than $CD34^+$ HSCs (Anjos-Afonso *et al*., 2013). All this suggests that $CD34^-$ HSCs are a rarer form of stem cells that can be placed at the top of human haematopoietic tree, are functionally very distinct and present different repopulation kinetics from $CD34^+$ HSCs. It is believed they represent a reservoir of very primitive cells that only contribute to haematopoiesis under stress conditions.

1.2.2. Haematopoietic progenitor cells

1.2.2.1. Multipotent progenitors (MPPs)

Downstream of HSCs lie the MPPs. These cells retain multilineage differentiation potential but are only capable of short-term engraftment. Early studies showed that CB $CD34^+CD38^{lo}$ cells were able to generate transient myelo-lymphoid engraftment in NOD/SCID mice at 2 weeks post-transplantation (Mazurier *et al*., 2003). This very lose definition of MPP population was later refined as being contained in the $Lin^-CD34^+CD38^-CD45RA^-CD90^-$ population as mentioned above (Majeti *et al*., 2007) and later, specifically demarcated as being $CD49f^-$ (Notta *et al*., 2011). These cells are capable of short-term multipotential engraftment in NOD/SCID/γc^{null} (NOD/SCID gamma chain null; NSG) mice at 4 weeks but disappear by week 12 (Majeti *et al*., 2007), (Notta *et al*., 2011). These data reinforce the idea that multilineage capacity is retained in MPPs, but self-renewal is limited when compared to HSCs, which are able to generate multilineage repopulation by week 12 and later. In a similar fashion to the

murine MPP population, these cells appear to display early lineage bias whereby MPPs can be further fractionated based on the expression of CD71 (transferrin receptor) and BAH-1 (also known as CD110 or thrombopoietin receptor), of which the F1 fraction ($CD71^-$ $BAH\text{-}1^-$) retains multilineage potential, while F2 ($CD71^+$ $BAH\text{-}1^-$) and F3 ($CD71^+$ $BAH\text{-}1^+$) predominantly give rise to Mk and Er lineages (Notta *et al*., 2016).

1.2.2.2. Lineage-restricted progenitors

Under the classical view of haematopoiesis, it is believed that a bifurcation occurs following the MPP stage, after the loss of lymphoid clonogenic potential, that segregates these cells by myeloid potential (via CMP) or lymphoid potential (via CLP). Efforts to isolate human CMPs have shown these cells to be the direct progenitors of GMP and MEPs. While CMPs can initiate a mix of colonies containing all the GM, M, G, Mk and Megakaryocyte/Erythrocyte (MkE) lineages in colony assays, GMPs can only give rise to GM colonies, while MEPs mostly originate colonies of the Er, Mk and MkE lineages (Manz *et al*., 2002). Transplanting human CMPs or MEPs into sub-lethally irradiated NOD/SCID/β2m mice led to 30% or 3% of human $CD45^+$ and/or $CD71^+$ cells, respectively. CMPs have been shown to differentiate into $CD15^+$ (3-fucosyl-N-acetyl-lactosamine) myelomonocytic cells and glycophorin-A^+ erythroid cells *in vivo*, whereas MEPs have been demonstrated to only generate glycophorin-A^+ erythroid cells at 3 weeks, reinforcing the concept of a gradual progression towards lineage commitment (Manz *et al*., 2002). These immunophenotypes were further refined by Doulatov and colleagues that argued the GMP population is confined in the $CD34^+CD38^+CD10^-$ (Neprilysin) $CD45RA^+CD135^+$ (Fms-related tyrosine kinase 3) compartment (Doulatov *et al*., 2010). Later, the previously described CMP fraction was revealed to still be heterogeneous. It was then demonstrated to contain an almost unbiased $CD71^-CD105^-$(endoglin) fraction that generated a $CD71^+CD105^-$ Mk/Er-biased population or GMPs (Mori *et al*., 2015). Using these markers, MEPs were further fractionated into a $CD71^+CD105^-$ subpopulation of erythrocyte-biased MEPs still capable of Mk production, and a true erythroid progenitor (EP) defined as $CD71^{int/+}CD105^+$ responsible for the generation of red blood cells (Mori *et al*., 2015). Yet, according to Notta and colleagues, the CD71 and BAH-1 markers are able to further partition the CMPs present in the $CD34^+CD38^+CD10^-Flt3^+CD45RA^-$ fraction, revealing three distinct populations: F1 ($CD71^-BAH\text{-}1^-$), F2 ($CD71^+BAH\text{-}1^-$), and F3 ($CD71^+BAH\text{-}1^+$). As assayed by co-culturing on MS5 stroma in the presence of cytokines SCF (stem cell factor), TPO (thrombopoietin), interleukin-7 (IL-7), interleukin-2 (IL-2), G-CSF (granulocyte-colony stimulating factor) and GM-CSF (granulocyte/macrophage-colony stimulating factor), CMPs found in CB or BM were shown to generate mostly myeloid colonies, showing no lymphoid potential. The F1 fraction was determined to be myeloid-biased while both F2 and F3 were

shown to preferentially generate erythrocytic progeny, suggesting that these newly uncovered fractions are functionally diverse from one another (Notta *et al*., 2016).

Over twenty years ago, a $Lin^{-}CD34^{hi}CD45RA^{+}CD10^{+}$ primitive lymphoid progenitor present in the BM was described (Galy *et al*., 1995). This population was described to have B, T, NK and DC differentiation potential, but lack any myeloid, Er, and Mk lineage capacity. On the other hand, Hao and colleagues reported an early human lymphoid progenitor contained in the $CD34^{+}CD38^{-}CD7^{+}$ (T-cell antigen CD7) compartment instead. However, this population was reported to give rise to B and NK but not myeloid or erythroid cells (Hao *et al*., 2001). More recently, a $CD34^{+}CD10^{+}CD24^{-}$ (small cell lung carcinoma cluster 4 antigen) human post-natal lymphoid progenitor was shown to be present in both CB and BM, with T, B and NK cells lineage capacity (Six *et al*., 2007). At around the same time, Hoebeke and colleagues argued that human CLPs could be found in the $CD34^{+}CD38^{-}CD7^{+}$ fraction (Hoebeke *et al*., 2007) instead. The identification of true human CLPs has been particularly problematic rendering very divergent opinions which can be due to the historical absence of reliable assays.

More recently, a population of multi-lymphoid progenitors (MLPs) emerging from MPPs has been described. MLPs are considered to have B, T and NK lineage potential while retaining some myeloid potential. In fact, MLPs are not lymphoid restricted and may, under the right conditions, give rise to dendritic cells (DCs) and macrophages (Doulatov *et al*., 2010). In this work, the authors have defined a $CD34^{+}CD38^{-}CD10^{+}$ population possessing B and NK cell potential with a bias towards NK cells but no myeloid potential, excluding these cells from the MLP compartment. On the other hand, two other populations defined as $CD34^{+}CD38^{-}CD90^{-/lo}CD45RA^{+}CD10^{+}CD7^{-}$ or $CD7^{+}$ were demarcated. The former cell fraction was defined as MLPs by the authors, and was described to produce B and NK cells, as well as $CD33^{+}$ (sialic acid-binding Ig-like Lectin 3) $CD11b^{+}$(integrin, alpha M (complement component 3 receptor 3 subunit or Mac-1) myeloid cells. Additionally, this population was reported to give rise to T-cells on OP9-Delta1 stroma. Importantly, these MLPs appear to only have B, T, NK and DC/macrophage potential but no G or Er potential. *In vivo* transplantation assays confirmed that MLPs showed a bipotent lymphoid/monocytic potential but not a granulocytic one (Doulatov *et al*., 2010).

The perception of the human haematopoietic system has been challenged in more recent years. We now hold that the first bifurcation in the human tree is not a clear separation of myeloid and lymphoid cells as previously thought. In the murine haematopoietic system, cells with lymphoid potential that can still generate granulocytes and macrophages, but no Mk or Er have been described. These have been termed lymphoid-primed multipotent progenitors (LMPPs) (Adolfsson *et al*., 2005). Conversely, a human LMPP-like population was uncovered

in acute myeloid laeukemia (AML) (Goardon *et al*., 2011). It can be defined as $CD34^+CD38^-CD45RA^+CD10^+$ and produces granulocytes, unlike the MLPs described in Doulatov *et al.* (Doulatov *et al*., 2010). In agreement with these findings, Görgens and colleagues hypothesised that CD133 (Prominin-1) could further demarcate functionally different subsets of progenitors (Gorgens *et al*., 2013). Cells with long-term *in vitro* and *in vivo* potentials are specifically defined as $CD34^+CD133^+$. Within this population, CB-derived $CD45RA^+CD10^-$ LMPP-like cells were demonstrated to originate MLPs ($CD45RA^+CD10^+$) or GMPs ($CD45RA^+CD7^-CD10^-$) (Gorgens *et al*., 2013). However, no phenotypically defined $CD34^+CD38^-CD45RA^+CD10^+$ MLP population is detected in human BM. Instead, another BM-derived population similar to CB MLPs, devoid of clonogenic myelo-erythroid potential, was isolated from the $CD34^+CD38^+CD45RA^+CD10^-$ fraction, based on high expression of L-selectin (CD62L) (Kohn *et al*., 2012). In summary, this implies that the earliest bifurcation in the human system does not entirely segregate myeloid and lymphoid potential. Rather, all lymphoid and some myeloid cells are still generated in a lympho-myeloid arm, while the remaining myeloid cells originate in the myelo-erythroid restricted branch.

1.2.3. Brief notes on the evolving view of a dynamic hierarchy

The depiction of the human hierarchical system has shifted over the recent years from the view of a somewhat rigid structure with very well-defined stages of differentiation, towards a more gradual and plastic process. Current work from John Dick's lab exposed a different interpretation on the roadmap for lineage commitment in human haematopoiesis (Notta *et al*., 2016). A key observation was that this hierarchy changes its shape when moving from foetal to adult haematopoiesis. The former is dominated by the presence of oligopotent progenitors with My-Er-Mk and Er-Mk potential (Notta *et al*., 2016). On the other hand, the authors suggest that adult haematopoiesis is organised as a two-tier system, with the top tier comprising multipotent cells such as HSCs and MPPs and the bottom tier containing mainly unipotent progenitors. They also suggest that Mk and Er commitment occurs very early and arises directly from stem cells, dismissing the likelihood of existing intermediate oligopotent progenitors, although claiming that if such cells exist, they are probably very short lived and could not be detected with the experimental setup used (Notta *et al*., 2016). In agreement with this view, human haematopoiesis is now proposed to be a continuum process where a "continuum of low primed undifferentiated cells (CLOUD)-HSPCs" contains phenotypic MPPs and MLPs (Velten *et al*., 2017). Such progenitors do not constitute stable and discrete cell types but rather transitory states where CLOUD-HSPCs acquire transcriptional programmes driving them into a specific direction. The authors suggest that transcriptomic priming is linked to the restriction of differentiation potential at an early stage both *in vitro* and *in vivo*.

Interestingly, early transcriptional priming events that drive differentiation into the lympho-myeloid, or into the Mk-Er direction are present in the most primitive HSCs, suggesting lineage bias very early on (Velten *et al*., 2017). A study from the Camargo's lab used transposon tagging to perform lineage tracing and appreciated the fates of stem and progenitor cells in steady state murine haematopoiesis. Under homeostatic conditions, part of the Mk population was described to arise independently from other lineages whereby a subset of long-term HSCs (LT-HSCs) contributed actively to Mk output directly, without seemingly going through any intermediate MPP stage, which means the roadmap concept is more flexible than previously realised (Rodriguez-Fraticelli *et al*., 2018).

1.2.4. Molecular regulation of HSCs - a brief summary

To maintain a balanced daily production of blood, HSCs must decide whether to divide or maintain their usual quiescence, and if division is undertaken, do they self-renew or differentiate into more mature progenitors. This is regulated by a complex system of intrinsic (e.g. cell cycle, chromatin modifiers, etc.) and extrinsic (e.g. integrins, cytokines, etc.) regulators. When this balance is skewed, diseases such as leukaemia may develop.

HSCs reside in the haematopoietic niche – a very rich microenvironment encompassing numerous molecular cues. The BM is the primary site of haematopoiesis, but other niches such as the spleen and the liver are also the home for haematopoietic cells. The BM is particularly rich, comprising of many cell types (Crane *et al*., 2017) Of those, the most abundant are the osteoblasts – a bone-lining endosteal cell type. Additionally, CXC-chemokine ligand 12 (Cxcl12)-abundant (CAR) cells, leptin receptor-expressing ($Lepr^+$) stromal cells, immune cells such as macrophages, monocytes and megakaryocytes, paired-related homeobox 1 ($Prrx1^+$) stromal cells and to a lesser extent, nervous system components such as neurons and Schwann cells have all been shown to contribute to the regulation of HSCs in mice (Crane *et al*., 2017). Thus, it is easy to appreciate the complexity of such a rich microenvironment where many different types of cell-to-cell interactions regulate HSCs via specific surface molecules, as well as indirectly through the secretion of molecules into the BM.

Among the myriad of signalling molecules present in this niche, SCF, CXCL12 and TPO appear to be particularly relevant. Scf from haematopoietic cells, osteoblasts and Nestin-expressing stromal cells were shown not to be required for HSC maintenance (Ding *et al*., 2012). But deletion of *Scf* directly in endothelial cells (ECs) and $Lepr^+$ perivascular cells were demonstrated to lead to depletion of HSCs and ultimately overall loss of myeloid and lymphoid cells (Ding *et al*., 2012). CXCL12, through its receptor CXCR4 found on HSCs, is an important

factor in HSCs retention in the BM niche. Loss of either *Cxcl12* or *Cxcr4* was described to deplete HSCs from the BM (Sugiyama *et al*., 2006), (Tzeng *et al*., 2011). Mice lacking either Tpo – a well-known regulator of platelet production, or its receptor c-Mpl are deficient in multiple haematopoietic lineages including the stem cell compartment (Kimura *et al*., 1998), which is due, at least in part, to a decrease in cell cycle regulators $p57^{kip2}$ (p57) and $p19^{ink4d}$ and Hox transcription factors (Qian *et al*., 2007). TPO is also required both in the initial expansion of HSCs following transplantation as well as in the maintenance of adult quiescent HSCs (Qian *et al*., 2007), through its close interaction with TPO-producing osteoblasts (Yoshihara *et al*., 2007).

Many of the major signalling pathways including FGF1/2, BMPs, WNT, TGF-β and Notch have also been implicated in HSPCs regulation (Crane *et al*., 2017). Conditional deletion of *Smad1* and *Smad5* in BM cells was shown to contribute normally to the re-establishment of the haematopoietic system (Singbrant *et al*., 2010). Instead, wild type (WT) HSCs were verified to have reduced activity in a BMP4-deficient background (Goldman *et al*., 2009). Loss of β or γ-catenin has been revealed to have little impact in the murine haematopoietic system. However, the WNT signalling pathway regulates foetal haematopoiesis, as well as both murine and human adult HSCs, whereby stimulation of these cells by WNT ligands increases self-renewal capacity (Van Den Berg *et al*., 1998). Additionally, non-canonical WNT signalling appears to play a role in the maintenance of quiescent HSCs (Sugimura *et al*., 2012). Quiescence is one of the cellular hallmarks of stem cells. Such a dormant state is imposed, at least in part, by TGF-β signalling. TGF-β can upregulate potent cell cycle inhibitors such as $p21^{Waf1}$ (p21) and p57 and block the expression of cytokine receptors such as KIT, FLT3, c-MPL and IL-6R (Fortunel *et al*., 2003). FGF1 produced by megakaryocytes aids in haematopoietic system recovery following injury. Indeed, FGFR1-specific inactivation was shown to prevent CXCL12/CXCR4-induced HSPC mobilisation following BM damage (Zhao *et al*., 2012). FGF2 on the other hand, appears not to be required in steady state conditions, but it seems to be essential in recovery under stress conditions. In fact, FGF2 induction was shown to trigger the expansion of $Nestin^{+}$ MSCs that induced Scf expression in the niche (Itkin *et al*., 2012). Interestingly, human $CD34^{+}$ HSPCs are also in close contact with $CD271^{+}$ (nerve growth factor receptor) MSCs and a balance in CXCL12 exposure of HSPCs in that microenvironment is important to maintain a healthy bone marrow (Flores-Figueroa *et al*., 2012). Finally, Notch signalling, being the focus of this thesis will be described in greater detail later.

Due to evident difficulties in studying the human haematopoietic system, most of what is understood about the BM niche comes from studies on the murine system. However, despite the many differences between the two systems, some similarities can be appreciated. For example, when comparing human BM biopsies and mouse BM xenografts, Guezguez and

colleagues showed that human HSPCs were preferentially detected in the endosteal region either in the native human BM or in the mouse BM following transplantation (87% and 85%, respectively) rather than the vascular region (13% and 15%, respectively) (Guezguez *et al*., 2013). Moreover, HSCs were described to be enriched in the trabecular bone area (TBA) and with higher SRC activity than HSCs localised in the long bone area (LBA) as addressed by secondary transplantation. Interestingly, TBA-HSCs were reported to have increased Notch activity which appeared to be mediated by the close interactions with TBA-residing Notch ligand- expressing osteoblasts (Guezguez *et al*., 2013).Nevertheless, the cell fate decision ultimately made by HSPCs are not fully imposed by external cues. Microarray data (Laurenti *et al*., 2013) and RNA-sequencing technology have allowed for a deeper look into the transcriptional programmes of human haematopoietic cells revealing new or reinforcing the roles of known intrinsic regulators of human haematopoiesis. As a result of the increasing applicability of this new technology, a great deal of research has focused on HSCs transcriptional programmes to show these are very dynamic throughout the differentiation journey, and possess a specific signature that is different from lineage-restricted progenitors (Novershtern *et al*., 2011), (Buenrostro *et al*., 2018), (Karamitros *et al*., 2018).

Despite different studies having established different specific gene expression modules for each haematopoietic population, the general view is that different populations share many of these modules at diverse stages of differentiation, suggesting that changes in the transcriptional states are a gradual process (Novershtern *et al*., 2011), (Buenrostro *et al*., 2018), (Karamitros *et al*., 2018). Of these, HSCs have a prevalent module containing surface markers including CD34, and transcription factors such as GATA2, HOXA9, HOXA10, MEIS1 and N-MYC (Novershtern *et al*., 2011). This module, although particularly prevalent in HSCs, persists through many steps of differentiation. Of note, GATA2, HOXA9 and HOXA10 have been described as Notch targets (Robert-Moreno *et al*., 2005), (Weerkamp *et al*., 2006). Other studies have also reinforced the idea of “lineage priming” as imposed by key transcription factors that direct lineage specification early on (Novershtern *et al*., 2011). Nevertheless, HSCs and MLPs share many transcriptional programmes, especially regarding the expression of transcription factors (Laurenti *et al*., 2013). As briefly mentioned, a study undertaking single cell RNA-seq analysis of different HSPCs cells revealed that, apart from particular sets of transcription factors, the most primitive HSCs were described to possess prevalent modules associated with typical features of primitive stem cells such as quiescence, low gene expression machinery, low RNA content, low cellular respiration, low CD38 and high CD90 expression (Velten *et al*., 2017). Thus, not only transcriptional landscapes associated with HSCs persist for a few stages of differentiation, but HSCs also express sets of genes associated with myeloid/lymphoid (*FLT3/SATB1*) and megakaryocyte/erythrocyte

(*GATA2/NFE2*) lineage commitment. This has been interpreted as the occurrence of lineage priming at the very early stages of HSC development (Velten *et al*., 2017). Even though changes in transcriptional profiles are also imposed by external cues, the extent to which these landscapes are part of intrinsic properties of certain cells is unknown.

Molecular regulation of stem and progenitor cells goes beyond the expression of hallmark TFs and is indeed very complex. Chen and colleagues believe that different cell types utilise the expression of transcripts and their respective isoforms as well as a myriad of splice junction alterations differentially (Chen *et al*., 2014). Additionally, it is now recognised that other layers of regulation that control cells including epigenetics and non-coding RNAs have emerged as players in the regulation of HSCs as well. As an example, G9a/GLP promotes H3K9me2 patterning in HSPCs generating a specific chromatic structure landscape that prevents the activation of lineage-affiliated genes (Chen *et al*., 2012). Non-coding RNAs such as miR-22 increases self-renewal in HSCs (Song *et al*., 2013), and interestingly miR-126 seems to play a differential a role in HSCs and leukaemia initiating cells (LICs) opening potential therapeutic avenues (Lechman *et al*., 2016).

1.2.5. *In vitro* assays

1.2.5.1. Colony-forming unit (CFU) assay

The CFU assay focuses on the detection of haematopoietic progenitor cells, with limited self-renewal capacity. It is carried out by seeding test cells onto semi-solid media, such as methylcellulose, collagen, agar or fibrin clots supplemented with nutrients and growth factors. Methylcellulose – a commonly used medium consists of a gelling agent that is chemically inert and which properties do not change with pH (Miller and Lai, 2005). Progenitors present in the initial cell suspension give rise to recognisable colonies of different lineages, such as the colony-forming-unit erythroid (CFU-E), burst-forming unit-erythroid (BFU-E), CFU-granulocyte/macrophage (CFU-GM) and mixed lineage CFU-granulocyte, erythroid, megakaryocyte, macrophage (CFU-GEMM). For instance, the generation of more colonies of the mixed CFU-GEMM lineage indicates the presence of more primitive cells with multilineage capacity. Under an optimal plating condition, the number of colonies formed is derived from single progenitors, hence the assay gives an idea not only of the type but also the frequency of progenitors present in the initial mix (Miller and Lai, 2005).

1.2.5.2. Long-term culture-initiating cell (LTC-IC) assay

The most relevant *in vitro* assay for HSCs is the LTC-IC assay. During the 1970s, when building on the colony-forming unit spleen (CFU-S) assay for murine HSCs, it was discovered that certain human haematopoietic cells can be maintained in *in vitro* cultures for several weeks given the adequate conditions (Dexter *et al*., 1977), (Gartner and Kaplan, 1980), (Sutherland *et al*., 1990). Minimally manipulated cells containing prospective HSCs are co-cultured in the presence of an irradiated stromal feeder layer, frequently the MS5 cell line, which supports human HSCs and allows differentiation of progenitors (Issaad *et al*., 1993). After irradiation, a test population of haematopoietic cells can be deposited on top of the stromal layer and cultured for many weeks. More mature progenitors differentiate and eventually disappear from the culture. The more primitive cells remain in culture, proliferate and originate more mature progenitors. By the fifth week of culture, progenitors present in the mix have differentiated and died off and the remaining cells capable of generating colonies are the most primitive ones and these are designated the long-term culture-initiating cells (LTC-IC). In addition, these cells migrate underneath the stromal layer and form cobblestone-like areas - the number of which correlates to the number of primitive cells present. Usually, at the end of the five-week period, the cells are harvested and seeded in a semi-solid medium such as methylcellulose, containing cytokines that support the growth and differentiation of the progenitors present similarly to a CFU assay. The *in vitro* culture system has remained the surrogate assay for multipotent cells for a long time. However, the real difference between these LTC-ICs and bona fide HSCs could not be discovered without *in vivo* experiments, which in humans is understandably not possible. This has been overcome by the development of xenogeneic transplantation models, where strains of successively more immunodeficient mice have been used as hosts for testing human cells such as HSCs.

1.2.6. *In vivo* assays

1.2.6.1. Xenotransplantation mouse models

The first attempt to xenograft human cells was focused on transplantation of acute myeloid leukaemia (AML) cells into immunocompromised mice (Palu *et al*., 1979) and athymic nude mice (Flanagan, 1966). These nude mice are homozygous for the nude (*nu*) gene (*Foxn1*^{nu}) and allowed for the first transplantation studies of human cells in immunocompromised mice (Segre *et al*., 1995). However, the outcomes were frequently inconsistent and unreliable, and worked preferentially using cell lines. Further improvements in 1983, led to the development of SCID mice (Bosma *et al*., 1983). These mice have a disrupted protein kinase DNA-activated catalytic polypeptide (*Prkdc*) gene, which results in the lack of expression of rearranged

antigen receptors, and therefore these mice lack functional B and T cells (Bosma *et al*., 1983). However, residual NK cells and macrophages impair human engraftment in these mice. The generation of the NOD/SCID mice by crossing SCID mice with NOD mice, led to more defects in adaptive and innate immunological cells, lacking functional B and T cells and decreased macrophage activity as a consequence of poor secretion of interleukin-1 (IL-1) (Shultz *et al*., 2005). These mice allow a higher human engraftment compared to SCID mice. However, even with this already severe compromised mouse model, only 70% of AML samples can engraft (Ailles *et al*., 1999). In addition, a major drawback is that these animals have a short lifespan of 8.5 months as a result of frequent development of thymic lymphomas, which limits the observation of human engraftment (Shultz *et al*., 2005), and the presence of NK cells also limit long term studies (Prochazka *et al*., 1992). To overcome these limitations, the IL-2 receptor common gamma chain (IL2Rγc) which interferes with IL-15 signalling that is necessary for NK cell development was deleted (Ito *et al*., 2002). The NOD/SCIDγc^{null} (NSG) mouse strain was then generated, which is devoid of B, T, and NK cells. These mice do not develop thymic lymphomas and are overall better recipients for human cells, making it a popular model for xenotransplantation studies. More recently, cutting edge models have been developed. In 2010 the generation of the NSGS mouse model, by crossing NGS with NSS mice (NOD/SCID SCF, GM-CSF, interleukin-3 (IL-3)), which lacks the IL2Rγc and produces human SCF, GM-CSF and IL-3, that allows a better homing of leukemic cells as compared to the NGS and NSS models (Wunderlich *et al*., 2010). In 2014, the MISTRG (standing for M-CSF, IL-3/GM-CSF and TPO in a *Rag2*$^{-/-}$*Il2rg*$^{-/-}$background) mouse model was developed and this strain supports the development of human innate immune cells such as monocytes, macrophages and NK cells through the expression human cytokines (M-CSF; IL-3, GM-CSF and TPO) (Rongvaux *et al*., 2014). We can expect in the future newer strains of immunocompromised mice that better mimic the human haematopoietic niche that will allow a better understanding of normal and leukaemic human haematopoiesis.

1.3. Acute Myeloid Leukaemia (AML)

1.3.1. Brief description of AML

Acute myeloid leukaemia (AML) is an aggressive type of blood cancer characterised by the block in myeloid differentiation from HSPCs into mature myeloid cells and uncontrolled growth of abnormal myeloid cells. It is the second most common type of adult leukaemias. It can arise following an underlying haematological malignancy but most of the times it appears as a *de novo* disease in healthy individuals. In the UK, around 3100 people were diagnosed in 2015 (www.cancerresearchuk.org). Even though the tremendous research effort in the field has

significantly increased the survival and quality of life of the patients, the overall survival (OS) at 5-years is still very low, especially in older patients. While the OS at 5-years is more than 65% in children aged 14 or younger and around 60% in patients aged between 15 and 24, this number drops to 40% in patients aged between 25 and 64 and to a staggering 5% in people aged 65 or older (https://www.cancerresearchuk.org/about-cancer/acute-myeloid-leukaemia-aml/survival). The diagnosis is usually done by morphological detection of blasts, which must represent at least 20% of cells in blood smears (Dohner *et al*., 2017). In addition, cytogenetics and immunophenotyping are employed by using specific markers such as CD34 precursors, CD65 granulocytic, CD14 monocytic or CD41 megakaryocytic markers (additional information on the markers can be found in Dohner *et al.,* 2017 (Dohner *et al*., 2017)). AML is characterised by genomic changes such as translocations and emergence of complex karyotypes discussed later in the text. Standard metaphase chromosomal profiling is still routinely used to detect such alterations (Grimwade *et al*., 1998). Fluorescence *in situ* hybridisation (FISH) represents another method for detecting these large-scale genomic alterations. Fluorescent DNA probes designed to target specific *loci* allow for the visualisation and quantification of specific translocations (Wertheim, 2015). Still, a low number of cells are analysed when using FISH or cytogenetics. Real-time polymerase chain reaction (RT-PCR) using primer pairs covering the two loci involved in the translocation is a common alternative diagnostic tool (Bacher *et al*., 2009). More recently, the development of next generation sequencing (NGS) strategies has helped uncover novel genetic alterations in AML by detecting specific translocations and mutations in AML-related genes. Whole genome sequencing (WGS), based on NGS allows for the identification of complete genomic alterations encompassing point mutations, indels, copy number changes, translocations, cryptic rearrangements, inversions and complex rearrangements in the whole genome (Ilyas *et al*., 2015). The first whole cancer genome sequencing to be performed was in an AML patient in 2008 by Ley and colleagues (Ley *et al*., 2008). This led to the detection of recurrent somatic mutations in *FLT3* and *NPM1* and the finding of other eight novel somatic mutations. The same group soon after found that *DNMT3A* mutation is a recurrent event in patients with de novo AML of intermediate risk category (Ley *et al*., 2010). Interestingly, Welch *et al.* have employed WGS strategies to detect acute promyelocytic leukaemia (APL) fusion genes which could not be detected using FISH, which resulted in the patient being successfully treated for APL (Welch *et al*., 2011). The development of “bench-top” NGS instruments means this technology will be available to an increasing number of researchers and clinicians for the diagnosis of AML.

Occasionally, stem and progenitor cells with mutations arise which upon expansion generate a sub-clone of cells with a different genetic background in a process called clonal

haematopoiesis. Some argue that this process might contribute to disease initiation although this is debatable. Clonal haematopoiesis-harbouring mutations in AML-associated genes was found in 95% of 50-70-year-olds with clonal haematopoiesis (Young *et al*., 2016), which is higher than previously thought. However, these clonal mutations appear to confer higher self-renewal capacity without increasing proliferation (Young *et al*., 2016). Furthermore, it is not known whether clonal haematopoiesis occurs due to certain clones being selected for or if on the other hand, random fluctuations in HSC states such as cell cycle and contributions from different HSCs is at the root of this condition (Mupo *et al*., 2013).

1.3.2. Characterisation of AML

AML arises due to abnormal proliferation and differentiation of primitive myeloid cells that sustain genetic abnormalities. The current model of leukemogenesis proposes that three different classes of mutations must occur (De Kouchkovsky and Abdul-Hay, 2016),(Gruszka *et al*., 2017). An early model hypothesis had been proposed as a mechanism for the emergence and progression of AML (Kelly and Gilliland, 2002). Within this view, two types of mutations must occur for the disease to develop. Class I type of mutations give a subset of cells a proliferative advantage. These frequently arise from mutations in the FLT3 gene, yielding a FLT3-internal tandem duplication mutation (commonly known as FLT3-ITD). This results in constitutive activation of the FLT3 receptor, leading to activation of downstream targets STAT5 and mitogen-activated protein (MAP) kinase (Hayakawa *et al*., 2000). Other genes commonly involved are *KIT*, *N/KRAS* and *TP53*. Class II mutations on the other hand block the natural differentiation process. These occur in genes such as *NPM1* and *CEBPA*. More recently, a third type of mutations in DNA modifiers such as *DNMT3A*, *TET2* and *IDH1/2* have been identified (De Kouchkovsky and Abdul-Hay, 2016). Beyond point mutations, other genetic lesions such as aneuploidies, fusion genes and complex karyotypes arise in the context of AML. In one study analysing some of the largest patient cohorts so far has consolidated the landscape of driver mutations in AML (Papaemmanuil *et al*., 2016). These genetic alterations are summarised in **Figure 1.2**.

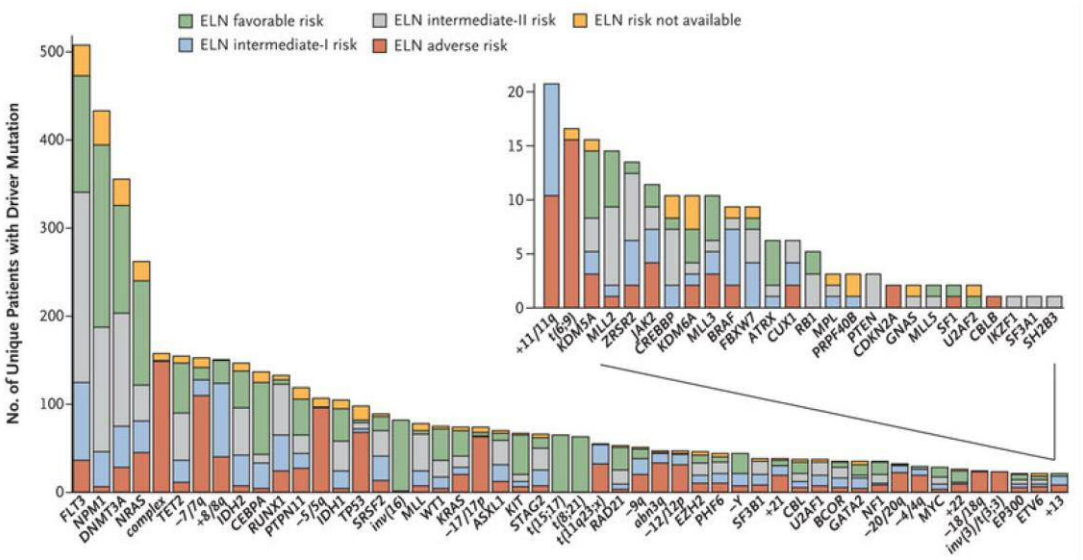

Figure 1.2 – Landscape of driver mutations in AML. Each bar is a driver lesion which may include mutations, chromosomal aneuploidies, fusion genes and complex karyotypes. The Y axis shows the number of unique patients containing the driver mutation. A total of 1540 patient samples were analysed. The colours indicate the risk stratification according to the European LeukemiaNet (ELN) classification. As in (Pappamanuil *et al*., 2016). (Reproduced with permission from Papaemmanuil, Elli *et al*. "Genomic Classification and Prognosis in Acute Myeloid Leukemia." *The New England journal of medicine* vol. 374,23 (2016): 2209-2221, Copyright Massachusetts Medical Society).

First established in 1976, the French-American-British (FAB) classification system divided leukaemias into one of eight (M0-M7) subtypes based on the cytological and chemical properties of the blasts (Bennett *et al*., 1976). These are summarised in **Table 1.1**:

Table 1.1 – French-American-British (FAB) classification of AML (Bennett *et al*., 1976).

FAB subtype	Name
M0	Undifferentiated acute myeloblastic leukaemia
M1	Acute myeloblastic leukaemia with minimal maturation
M2	Acute myeloblastic leukaemia with maturation
M3	Acute promyelocytic leukaemia (APL)
M4	Acute myelomonocytic leukaemia
M4eos	Acute myelomonocytic leukaemia with eosinophilia
M5	Acute monocytic leukaemia
M6	Acute erythroid leukaemia
M7	Acute megakaryoblastic leukaemia

Technological advances led to the creation of another classification system by the World Health Organization (WHO) that goes beyond morphological classification and includes information on genomic alterations. The latest update from the WHO classification of AMLs is depicted on **Table 1.2** (Arber *et al*., 2016).

Table 1.2 – World Health Organisation (WHO) classification of acute leukaemias and myeloid neoplasms (Arber *et al*., 2016).

WHO classification of AML
AML with recurrent genetic abnormalities
AML with t(8;21)(q22;q22.1);RUNX1-RUNX1T1
AML with inv(16)(p13.1q22) or t(16;16)(p13.1;q22);CBFB-MYH11 APL
APL with PML-RARA
AML with t(9;11)(p21.3;q23.3);MLLT3-KMT2A
AML with t(6;9)(p23;q34.1);DEK-NUP214
AML with inv(3)(q21.3q26.2) or t(3;3)(q21.3;q26.2); GATA2, MECOM
AML (megakaryoblastic) with t(1;22)(p13.3;q13.3);RBM15-MKL1
Provisional entity: AML with BCR-ABL1
AML with mutated NPM1
AML with biallelic mutations of CEBPA
Provisional entity: AML with mutated RUNX1
AML with myelodysplasia-related changes
Therapy-related myeloid neoplasms
AML, not otherwise specified (NOS)
AML with minimal differentiation
AML without maturation
AML with maturation
Acute myelomonocytic laeukemia
Acute monoblastic/monocytic laeukemia
Pure erythroid laeukemia
Acute megakaryoblastic laeukemia
Acute basophilic laeukemia
Acute panmyelosis with myelofibrosis
Myeloid sarcoma
Myeloid proliferations related to Down syndrome
Transient abnormal myelopoiesis (TAM)
Myeloid laeukemia associated with Down syndrome
Blastic plasmacytoid dendritic cell neoplasm
Acute laeukemias of ambiguous lineage
Acute undifferentiated laeukemia
Mixed phenotype acute laeukemia (MPAL) with t(9;22)(q34.1;q11.2); BCR-ABL1
MPAL with t(v;11q23.3); KMT2A rearranged
MPAL, B/myeloid, NOS
MPAL, T/myeloid, NOS

Patients can be stratified according to their risk of treatment resistance or treatment-related mortality (TRM). In general, age and performance status help predicting the risk of TRM and these factors are taken into consideration when deciding on a treatment plan. But the cytogenetic profile is the most important prognostic factor for complete remission (CR) and overall survival (OS) in AML. In a simplified manner, AML patients can be stratified into

favourable, intermediate or adverse risk groups (Dohner *et al*., 2017), (De Kouchkovsky and Abdul-Hay, 2016) (**Table 1.3**).

Table 1.3 – Current Stratification of Molecular Genetic and Cytogenetic Alterations – according to ELN Recommendations. Adapted from (Dohner *et al*., 2017).

Risk profile	Subsets
Favourable	t(8;21)(q22;q22); *RUNX1-RUNX1T1* inv(16)(p13.1q22) or t(16;16)(p13.1;q22); *CBFB-MYH11* Mutated *NPM1* without *FLT3-ITD* (normal karyotype) Biallelic mutated *CEBPA* (normal karyotype)
Intermediate-I	Mutated *NPM1* and *FLT3-ITD* (normal karyotype) Wild-type *NPM1* and *FLT3-ITD* (normal karyotype) Wild-type NPM1 without *FLT3-ITD* (normal karyotype)
Intermediate-II	t(9;11)(p22;q23); *MLLT3-KMT2A* Cytogenetic abnormalities not classified as favourable or adverse (insufficient data)
Adverse	inv(3)(q21q26.2) or t(3;3)(q21;q26.2); *GATA2–MECOM* (*EVI1*) t(6;9)(p23;q34); *DEK-NUP214* t(v;11)(v;q23); *KMT2A* rearranged −5 or del(5q); −7; abnl(17p); complex karyotype

The chromosomal translocations t(8,21), t(15,17) and inv(16) all fall into the favourable group. Patients with normal cytogenetics usually fall in the intermediate group, while adverse cytogenetics comprise abnormalities such as monosomy 5 or 7, t(6,9) and inv(3) and complex karyotype which is defined as three or more chromosomal abnormalities. A summary on the stratification of patients based on cytogenetics and molecular profile can be found in (De Kouchkovsky and Abdul-Hay, 2016).

In the initial step of leukemogenesis, the driver mutation occurs in a normal stem or progenitor cell that may possesses other mutations that do not necessarily play a role in the disease. The driver mutation confers advantage to the affected cell, and with the expansion of this clone, all the other passenger mutations are retained. When a new driver mutation further confers advantage to the founding clone, it acquires more passenger mutations during the disease progression. At the time of diagnosis, the founding clone contains few drivers, but many passenger mutations. Indeed, it is known that AML progression is driven by relatively few driver mutations when compared to other types of cancers. Hence, understanding which driver and passenger mutations are important is imperative. As an example, *FLT3-ITD* is one of the most common of these genetic abnormalities (Welch *et al*., 2012). We now know that the tandem duplication of this gene alone does not initiate overt leukaemia, but additional driver mutations that are acquired leads to propagation of the disease (Kelly and Gilliland, 2002), (Li *et al*., 2008), (Sallmyr *et al*., 2008). Using exome-sequencing for leukaemia-specific mutations,

a model for *FLT3*-mutated AML progression was proposed in which a series of mutations or epigenetic events occur in self renewing HSCs, acquiring new mutations throughout the disease progression (Jan *et al*., 2012).

The authors found pre-leukemic mutations in residual non-leukaemic HSCs in all the cases of normal karyotype AML analysed. For example, in 2 out of 5 cases *TET2* mutations were found in residual HSCs whereas *FLT3* mutation was not found in any of the cases (Jan *et al*., 2012). Therefore, it is currently viewed that *FLT3* mutations are secondary events. It has also been highlighted that mutations in epigenetic modifiers such as *DNMT3A*, *ASXL1*, *IDH1/2* and *TET2* genes are often acquired earliest (Papaemmanuil *et al*., 2016). These are usually present in the founding clone and are very rarely found alone in leukaemic cells suggesting the clone requires additional mutations to cause overt leukaemia. Another example relates to *NPM1* mutation which is usually considered a primary event (Falini *et al*., 2011), although in some cases *DNMT3A* mutations can precede *NPM1* mutations (Shlush *et al*., 2014), (Kronke *et al*., 2013). Altogether, this suggests that AML is not the sum of random genetic abnormalities but rather follows a defined multi-step leukaemogenic trajectory (Papaemmanuil *et al*., 2016).

1.3.3. The Leukaemic Initiating Cell (LIC)

A major problem in cancer biology is identifying the cell of origin capable of replicating the tumour – the cancer initiating cell (CIC). This concept - now widely accepted in a variety of cancer types was first introduced in the context of AML via two seminal works from John Dick's group (Lapidot *et al*., 1994), (Bonnet and Dick, 1997). In Lapidot *et al.*, the authors showed that cells from all the AML subtypes tested engrafted in SCID mice (Lapidot *et al*., 1994). Importantly, cells from the M4 and M5 FAB subtypes proliferated more aggressively and disseminated to extramedullary sites more readily than M1 and M2 cells, showing that the SCID-leukaemia model was able to accurately reflect the aggressiveness of the various AML subtypes. Importantly, only $CD34^{+}CD38^{-}$ cells were demonstrated to be capable of extensive leukaemic engraftment and the authors concluded that AML developed in these mice due to extensive proliferation and differentiation of these LICs or Leukaemic Stem Cells (LSCs) *in vivo*. Later, Bonnet and colleagues suggested that AML is organised in a hierarchical manner (Bonnet and Dick, 1997). In this view, a leukaemogenic event targeting HSCs ($CD34^{++}CD38^{-}$) generates LICs that produce committed leukaemic progenitors that ultimately lead to the detection of the several subtypes of AML. Importantly, the authors demonstrated that LICs were exclusively present in the $CD34^{++}CD38^{-}$ compartment irrespective of subtype or lineage markers expressed on the blasts. We now know this consisted of a simplified version of a much more complex picture. A third of AML cases are in fact $CD34^{-}$ AMLs (defined as the presence of <10% $CD34^{+}$ cells) in which the bulk of LICs are found in the $CD34^{-}$ fraction,

although LICs can be at times detected in a minor fraction of $CD34^+$ cells (Quek *et al*., 2016). Contrary to LICs arising from the $CD34^+$ compartment, these are not believed to represent hierarchically related cells but are rather the consequence of plastic expression of the CD34 antigen, which in AML is not a cell immaturity marker (Quek *et al*., 2016). It was shown in a study that within the $CD34^+$ fraction, two subpopulations of LICs could be found: LMPP-like $CD34^+CD38^-$ and GMP-like $CD34^+CD38^+$ cells, whose names derived from the similarity to their healthy counterparts (Goardon *et al*., 2011). Remarkably, LMPP-like LICs were reported to give rise to GMP-like cells, but not the contrary, reinforcing the notion of a hierarchical organisation (Goardon *et al*., 2011). These authors further suggested that these LICs were found to be more closely related to normal haematopoietic progenitors that gained self-renewal capacity, rather than stem cells, which was validated by gene expression profile analysis (Goardon *et al*., 2011). Interestingly, a study showed that the experimental setup used may influence the outcome of the experiments. Anti-CD38 antibodies, routinely used in the isolation of putative LICs, may lead to the clearing of LICs by innate immune cells in transplantation models (Taussig *et al*., 2008). The authors showed that LICs could be mostly found in the $CD34^+CD38^+$ compartment in all the AML samples tested but can also be found in the $CD34^+CD38^-$ compartment.

Disease relapse following complete remission is the major hurdle in AML management. Shlush and colleagues combined genetic and functional approaches and performed whole-genome sequencing (WGS) of AML samples harvested at diagnosis and relapse (Shlush *et al*., 2017). The authors showed that in some patients, the cellular origin of relapse lies in a rare population of cells with a primitive phenotype resembling HSPCs. In others, relapse originates from cells with a more committed immunophenotype (Shlush *et al*., 2017). Regardless, relapse in both patient groups seems to be closely linked to stem cell properties whereby in the first case, primitive LICs are responsible for relapse, while stemness transcriptional programmes that are retained in the bulk of the leukaemia population are the culprit when more committed progenitors are at the origin of relapse (Shlush *et al*., 2017). It was further suggested that chemotherapy does not induce mutations leading to emergence of new clones, but it rather selects for pre-existing subclones that were already resistant to therapy due to their quiescence (Shlush *et al*., 2017). In agreement with this, a stemness transcriptional signature has been demonstrated to predict therapy success (Ng *et al*., 2016). Gene expression analysis of LSC^+ versus LSC^- fractions of AML samples revealed a 17-gene list comprising a transcriptional signature that is predictive of overall performance (Ng *et al*., 2016). A high LSC17 score was associated with poor overall survival and event-free survival. High LSC17 score patients were also found to present higher percentage of bone marrow blasts at diagnosis, higher rates of relapse and lower response rates to standard induction

chemotherapy. Interestingly, in one AML cohort, the LSC17 signature proved to be the strongest predictive factor of resistance to therapy, ahead of variables such as age, *de novo* vs secondary AML, total white blood cell count and cytogenetics (Ng *et al*., 2016).

It seems increasingly clear that in order to eradicate the disease, both bulk blasts and LICs need to be effectively targeted. Even though LICs can resemble their normal HSPCs counterparts in many aspects of their biology, they possess some unique features that may be the focus of therapeutic intervention. Some LICs, just as normal HSCs, appear to be quiescent. In fact, in a study from the 1960s, patients were injected with tritiated thymidine (a radioactive nucleoside – 3H-thymidine, used to measure the extent of cell division) revealed the presence of cells with different kinetic properties within the disease (Clarkson *et al*., 1967). It was hypothesised that slowly cycling cells could perhaps show increased resistance to anti-proliferative therapies. More recently, AML cells from 6 out of 7 samples tested were shown to capture leukaemic progenitors that engrafted in NOD/SCID mice and were resistant to killing by tritiated thymidine (Guan *et al*., 2003). Isolated quiescent AML cells were shown to exit G0 after 24-72 hours of serum-free culture without cytokines, which did not happen in normal lineage-negative BM cells (Guan *et al*., 2003). The notion that their quiescence may help escaping chemotherapy has remained a popular concept for a long time. However, this is not always the case. A subset of CD93-expressing LICs found in the $CD34^{+}CD38^{-}$ fraction was reported to be actively cycling in MLL-rearranged AMLs (Iwasaki *et al*., 2015). These cells, which were found in the G1 phase of the cell cycle, were demonstrated to have serial transplantation capacity while the G0 phase $CD34^{+}CD38^{-}CD93^{-}$ cells were inefficient in engrafting in primary recipients (Iwasaki *et al*., 2015).

Whether LICs' metabolism compares to that of normal HSPCs is also debatable. LICs were shown to possess lower levels of reactive oxygen species (ROS) and oxygen consumption - typical of a low oxidative phosphorylation profile (Lagadinou *et al*., 2013). Additionally, these cells were described to be more reliant on oxidative phosphorylation and were determined to have an upregulated *BCL2* expression pattern when compared to high oxidative phosphorylation LICs and normal haematopoietic cells (Lagadinou *et al*., 2013). In the same study, the authors used BCL-2 inhibitors and demonstrated a selective eradication of LICs while normal HSCs were mostly spared and this was due, at least in part, to the higher glycolytic reserve capacity of HSCs (Lagadinou *et al*., 2013). More recently however, challenging this idea, Farge and colleagues described that chemotherapy-resistant AML cells have a high oxidative phosphorylation (OXPHOS) status (Farge *et al*., 2017). They proposed that chemoresistance might be more strongly driven by cellular metabolism rather than quiescence or maturity of the cells. These high OXPHOS cells, in contrast to low OXPHOS cells were found to be chemo-resistant *in vivo*. Targeting mitochondrial protein synthesis,

electron transfer or fatty acid oxidation was able to shift the cells towards low OXPHOS, enhancing their susceptibility to the anti-leukemic effects of cytarabine. All in all, this demonstrates metabolic heterogeneity in the LIC compartment.

Altered epigenetics is another important hallmark of LICs. Pre-leukemic HSCs very frequently contain mutations in epigenetic regulator genes such as *TET2*, *DNMT3A* and *IDH1/2*, that ultimately alter their metabolism and confer self-renewal capacity to haematopoietic progenitor cells (Wouters and Delwel, 2016). The natural process of DNA methylation influences gene expression. Aberrant DNA methylation patterns have been recognised as contributors to leukemogenesis. DNMT3A mutated proteins are believed to act as a dominant negative over wild-type DNMT3A and lead to abnormal methylation patterns (Russler-Germain *et al*., 2014). Ten-Eleven-Translocation (TET)-enzymes catalyse the oxidation of 5-methylcytosine into 5-hydroxymethlycytosine (5hmC). *TET2* mutations results in decreased levels of 5hmC. Although the biological relevance of this metabolite is not fully understood, *TET2* mutations ultimately confer poor prognosis in intermediate-risk AML (Metzeler *et al*., 2011). Isocitrate dehydrogenase (IDH) enzymes catalyse the conversion of isocitrate to α-ketoglutarate. Mutations in *IDH1* and *IDH2* result in the production of the aberrant metabolite 2-hydroxyglutarate which competes with α-ketoglutarate, ultimately inhibiting TET2 (Wouters and Delwel, 2016).

In addition to the cellular features mentioned, several surface markers that are upregulated in $CD34^{+}CD38^{-}$ AML LICs compared to normal HSPCs could be the target for therapeutic intervention. These include CD123, CD44, CD47, TIM3, CD96, CD99, CLL-1, CD32, CD25, IL1RAP, GRP56 and CD93 (Thomas and Majeti, 2017). Some of these have been the target of a more specific therapeutic approach briefly described in the following section.

1.3.4. Treatment and management of AML, a brief note

The standard induction therapy employed to treat AML comprises administration of cytarabine (Ara-C) in combination with an anthracycline. Cytarabine is a nucleoside analog that is incorporated into cells during the S phase of the cell cycle and inhibits DNA synthesis. Anthracyclines intercalate between adjacent DNA base pairs and are believed to inhibit the nuclear enzyme topoisomerase II. Standard induction therapy leads to a complete response in 60-85% of the patients younger than 60 years old. For patients older than 60, complete response is 40-60% (Dohner *et al*., 2017). This has remained the standard therapy for nearly fifty years. **Figure 1.3** summarises the major approvals for AML treatment, including newly identified drugs. Noticeably, few agents have been introduced for AML management in nearly 25 years following the introduction of the 7+3 regimen (7 days standard dose cytarabine and

3 days anthracycline). However, the last three years have seen a very promising boost in the number of approvals towards AML treatment (**Figure 1.3**).

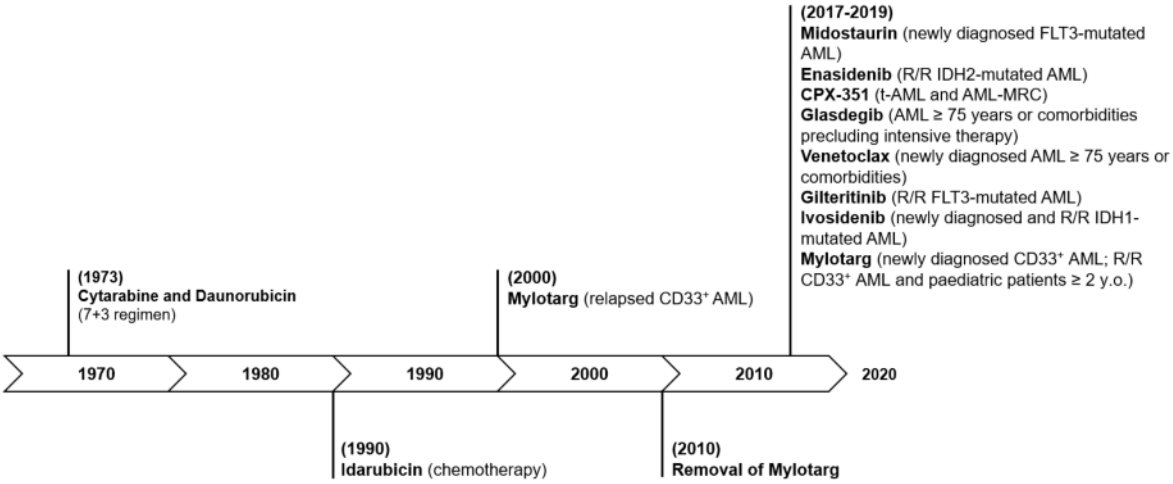

Figure 1.3 – Timeline of major approvals for the treatment of AML. R/R – relapsed/refractory; MRC – myelodysplasia-related changes; y.o. – years old.

Newer agents aimed at improving on this have been tested as potential alternative therapies targeting various aspects of cellular features. Among these are drugs targeting epigenetic modifiers, such as IDH1/2 mutant enzyme inhibitors. AG-120 is an IDH-1 mutant inhibitor that yielded haematological responses in half of IDH-1 positive patients including four CR (DiNardo *et al*., 2015). For IDH-2 mutants, AG-221 demonstrated benefits in survival of an IDH-2 mutant AML xenograft model (Stein *et al*., 2015). Recent approvals for this subclass of AML include enasidenib and ivosidenib. Enasidenib has emerged as a treatment option for relapsed/refractory (R/R) IDH2-mutated AML. This drug led to complete remission and complete remission with partial hematologic recovery rate of 23% and median remission duration of 8.2 months (Stein *et al*., 2019). Ivosidenib is a small molecule inhibitor of mutated IDH1 enzyme, which showed a complete remission rate of 21.6% and median duration of 8.2 months (DiNardo *et al*., 2018). In 2019, this drug was approved for treatment of newly diagnosed AML patients 75 years old and older or with comorbidities (Lai *et al*., 2019). Tyrosine kinase inhibitors, such as FLT3 and KIT inhibitors are also of relevance. Well-known first generation FLT3-ITD inhibitors include sorafenib and midostaurin, and second-generation agents include quizartinib and crenolanib, some of which have shown improvements on OS and event-free survival (EFS) (De Kouchkovsky and Abdul-Hay, 2016),(Dohner *et al*., 2017). Midostaurin is a multi-targeted kinase inhibitor, which has shown activity in FLT3-mutated cell lines and mouse models (Weisberg *et al*., 2002). A phase III clinical trial studied the efficiency of midostaurin combined with standard chemotherapy. Compared to placebo, this drug was associated with longer OS and EFS (Stone *et al*., 2017). In 2018, gilteritinib was approved in

the United States and Japan for the treatment of R/R FLT3-mutated AML, which has shown to prolong OS compared to the control arm of the study (Perl, 2019). Venetoclax - a potent BCL-2 inhibitor, was approved for the treatment of patients 75 years and older. It showed promising results regarding the rate and duration of CR and its combination with hypomethylating agents or low-dose cytarabine is now an option for this group of patients (Lai *et al*., 2019),(Estey *et al*., 2020). Also noteworthy is CPX-351 – a liposomal formulation containing a fixed 1:5 M ratio of daunorubicin and cytarabine, capable of bypassing drug efflux pumps, entering the cells as liposomes. This drug was approved by the FDA in 2017 and the European Medicines Agency (EMA) in 2018 for the treatment of therapy-related AML (t-AML) and AML with myelodysplasia-related changes (AML-MRC) (Lai *et al*., 2019). CPX-351 displayed improved CR and OS when compared to standard 7+3 therapy (Lancet *et al*., 2018). Other approaches include cell cycle and signalling inhibitors and nuclear export inhibitors (Wouters and Delwel, 2016). Additionally, antibody-based therapies have resurfaced as potential candidates. These include antibody-drug conjugates such as Gemtuzumab ozogamicin (GO, trade name Mylotarg) – an anti-CD33 and calicheamicin conjugate. Even though FDA approval was rescinded prematurely for this drug, a later analysis showed a decrease in relapse and improved survival in patients treated with Mylotargwhen combined with standard chemotherapy (Hills *et al*., 2014). The more recent approval for Mylotarg is for a lower recommended dose and schedule than its previous approval and is aimed at a different patient population. Immunotherapy strategies employing bi- and trispecific antibodies such as anti-CD33 and anti-CD3 bispecific T-cell engagers (BiTE) conjugates aim to engage T-cells into attacking leukemic cells (Jitschin *et al*., 2018). Additionally, engineered chimeric antigen receptor (CAR) have been explored. CARs are genetically engineered membrane receptors capable of activating T cells by linking an extracellular tumour antigen-recognising fragment to an intracellular signalling component comprising the T-cell receptor (TCR) primary domain and additional co-stimulatory endodomains (Shang and Zhou, 2019). CAR T cells targeting CD33 and CD123 are being investigated in early clinical trials (Dohner *et al*., 2017). Yet, the most effective therapy to prevent relapse is allogeneic HSC transplantation (aHSCT) (Cornelissen *et al*., 2012). T-cells present in the donor graft have a strong anti-leukaemic effect due to the graft-versus-leukaemia effect. However, these can also attack healthy tissue in the recipient leading to graft-versus-host disease which is associated with high level of transplant-related mortality.

1.4. The Notch signalling pathway

1.4.1. The Notch pathway members and mechanism

Over 100 years ago, John S. Dexter observed aberrant fly wing phenotypes (Dexter, 1914) that were later on shown to be the result of mutant alleles. Only around 70 years later, Spyros Artavanis-Tsakonas and Michael Young identified that the wing phenotype was due to Notch gene haploinsufficiency (Kidd *et al*., 1986), (Wharton *et al*., 1985). In mammals, there are four Notch receptors (Notch-1*,* 2*,* 3, and 4) and five structurally related, single-pass membrane Notch ligands (Delta-1*, 3* and 4 and Jagged-1 and 2, simply termed Jag-1 and Jag-2 from now on) (D'Souza *et al*., 2010). Canonical Notch signalling is activated when a canonical transmembrane ligand interacts with a canonical transmembrane receptor on contacting cells, instigating the first cleavage of the Notch receptor, which is mediated by metalloproteases like the tumor necrosis factor alpha converting enzyme (TACE). This licenses a second cleavage mediated by the γ-secretase complex (comprising of Nicastrin, Presenilin 1/2, PEN2 (presenilin enhancer 2) and APH1 (anterior pharynx-defective 1)). Upon this second cleavage it generates the intracellular Notch receptor domain (NICD), which subsequently translocates into the nucleus and cooperates with the DNA-binding protein RBPJκ (Recombination signal binding protein for immunoglobulin kappa J region; also known as CSL (standing for CBF1, Su(H), Lag-1)). Subsequently, this allows the conversion of the transcriptional repressor complex into an activator complex together with its co-activator Mastermind-like 1 (MAML1), and other specific co-activators (Bray, 2006), (Andersson *et al*., 2011). MAML1 also recruits the histone acetylase p300, which promotes assembly of initiation and elongation complexes (Bray, 2006). Another member that interacts with NICD is SKIP (ski-interacting protein) that gets recruited to spliceosomes (Bray, 2006). In the absence of Notch activity, CSL proteins recruit histone deacetylases instead, such as SMRT, SHARP, which in turn recruit CtBP (Borggrefe and Oswald, 2009). The activation of Notch signalling triggers the expression of various target genes, such as members of the *HES* and *HES*-related (HESR/HEY) family of basic helix-loop-helix transcription factors (Iso *et al*., 2003) and subsequently regulates the expression of other genes (**Figure 1.4**). Notch signalling can also be orchestrated in a non-canonical manner via HES- or RBPJk/HES-independent axis or by other means (Andersen *et al*., 2012).

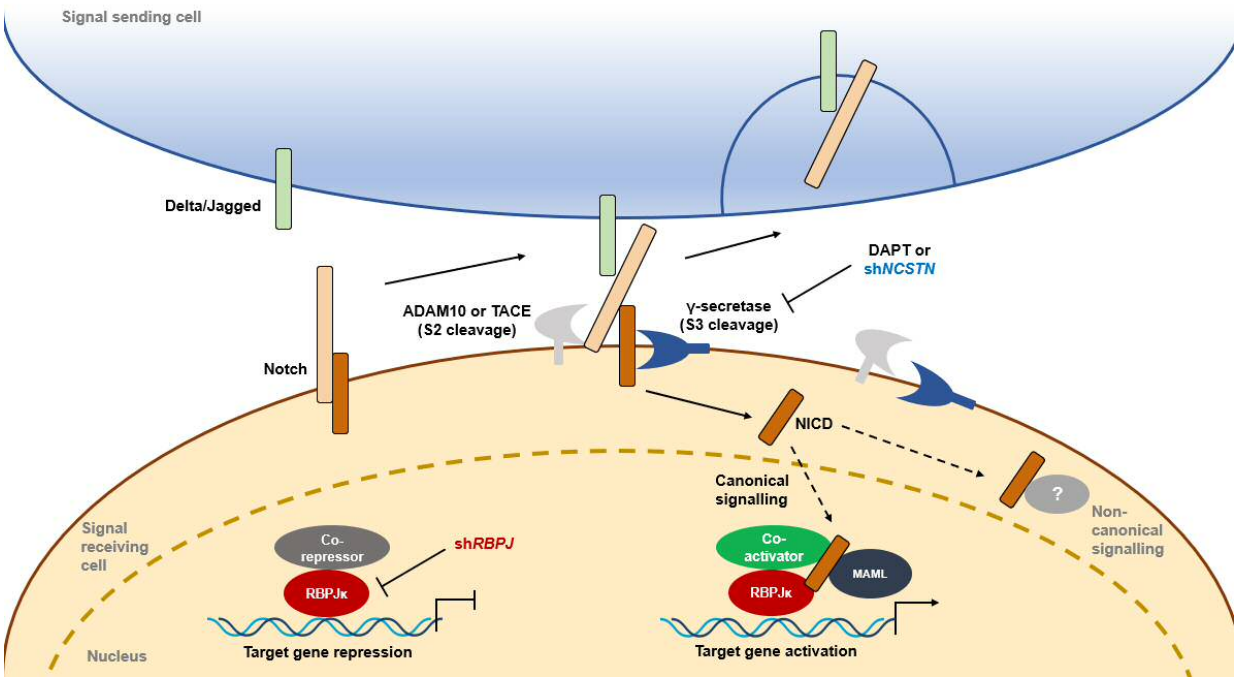

Figure 1.4 – A simplified illustration of the Notch signalling pathway. Binding of a Notch ligand on one cell to the Notch receptor on another cell results in two proteolytic cleavages of the receptor. Metalloproteases catalyse the S2 cleavage, generating a substrate for S3 cleavage by the γ-secretase complex. This releases the Notch intracellular domain (NICD), which upon binding with the CSL domain, the Mastermind (Maml1) and others, relieves repression on target genes. The γ-secretase inhibitor DAPT and shRNA targeting *NCSTN* used in this project block Notch receptor processing, therefore acting as pan-Notch inhibitors. shRNAs targeting *RBPJ*, inhibit canonical Notch signalling.

1.4.2. Notch ligands and receptors

The Notch genes encode for ~300 kDa type 1 transmembrane proteins. These contain around 36 tandem EGF-like repeats (Wharton *et al*., 1985). EGF-like repeats 11 and 12 in particular, are thought to be necessary for binding to ligands in Drosophila (Rebay *et al*., 1991). Additionally, they have three Lin12/Notch repeats (LNR) which are cysteine rich regions; a heterodimerisation domain (HD); a negative regulatory region (NRR) responsible for preventing activation of the pathway in the absence of ligands (Gordon *et al*., 2007); a transmembrane subunit (TMN) that is anchored to the plasma membrane; a RAM domain that binds to CSL and seven ankyrin repeats responsible for binding to downstream effector proteins (Andersson *et al*., 2011). A proline-glutamine-serine-threonine rich domain (PEST) is required for Notch degradation (in fact its frequent mutations in Notch-1 leads to T-ALL (Weng *et al*., 2004). A C-terminal transcriptional activation domain (TAD) modulates epigenetic regulation of gene expression (Kurooka and Honjo, 2000). The latter is only present in Notch-1 and Notch-2 receptors (**Figure 1.5**).

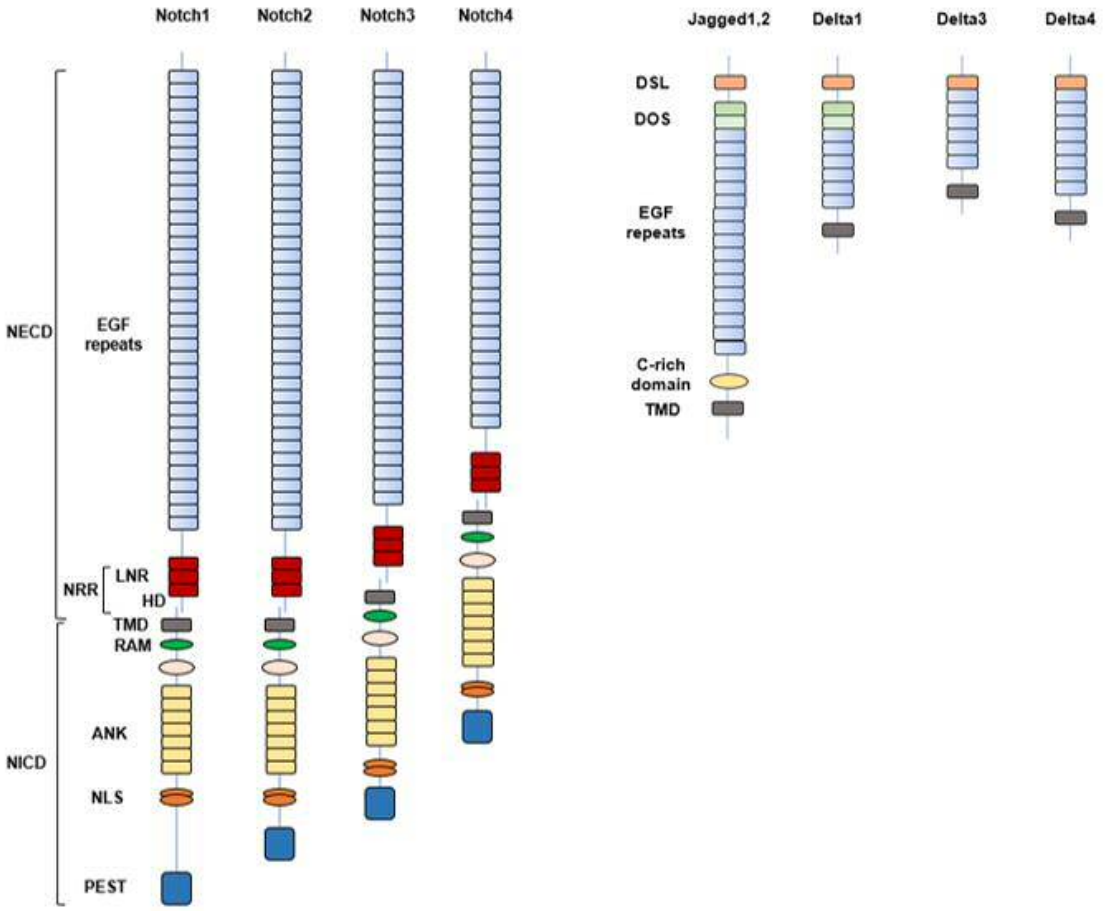

Figure 1.5 - Notch receptors and ligands. Notch receptors are type I transmembrane proteins. They contain multiple EGF-like repeats. A negative regulatory region (NRR) is composed of three cysteine-rich Lin repeats (LNR) and a heterodimerization domain (HD). They also contain a transmembrane domain (TM), a RAM domain, a nuclear localization sequence (NLS), seven ankyrin repeats (ANK) and a transactivation domain (PEST). The canonical DSL ligands contain DOS and EGF-like repeats.

The canonical DSL (for Delta, Serrate and Lag2) ligands are type I cell-surface proteins. Just as the receptors, the ligands contain multiple EGF-like repeats; an N-terminal (NT) domain, followed by the DSL domain. The latter is necessary but not sufficient for interaction with Notch (Shimizu *et al*., 1999). Also, a Delta and OSM-11-like proteins (DOS) domain located within the first two EGF-like repeats cooperates with the DSL domain (Komatsu *et al*., 2008) in certain ligands (Delta-4 and Delta-3 do not possess this domain). Jag-1 and Jag-2 ligands have additional cysteine-rich (CR) regions not present in Delta-like ligands. Many of the intracellular regions of DSL ligands contain multiple lysine residues and a C-terminal PDZ ligand motif. They are required for signalling activity and interactions with cytoskeleton

respectively (D'Souza *et al*., 2010) (**Figure 1.5**). Although these ligands are structurally very similar, they are not functionally equivalent. Interestingly, Delta-3 ligand does not activate Notch signalling in *trans*, and seems to function exclusively as an antagonist (Ladi *et al*., 2005).

1.4.3. The role of the Notch pathway

The Notch pathway has been implicated in several systems described in more detail in the review by Sarah Bray (Bray, 2006). For instance, it plays a role in the effect of lateral inhibition. This arises from the concept that equivalent populations of cells have roughly the same amount of Notch receptors and ligands at the cell surface. However, small differences where a certain cell expresses slightly more Notch receptors than its neighbours, will turn into a Notch-receiving cell, reinforcing this pathway and inhibiting the expression of ligands. This is on the other hand, turns the surrounding cells into Notch-sending cells that mainly express Notch ligands as opposed to receptors. Such differences regulate cell fate determination by creating boundaries of cells based at least in part, on Notch receptor and ligand expressions (Bray, 2006). Therefore, another role for this pathway can be found in lineage determination and asymmetric division. This arises from the principle that the asymmetrical inheritance of Notch regulators on a certain bi-potent cell, such as a sensory organ precursor (SOP) cell from the Drosophila peripheral nervous system (PNS), will determine the Notch activity in each daughter cell (Guo *et al*., 1996). If one such cell receives a higher concentration of the negative Notch regulator Numb, this will lead to a higher turnover and degradation of the receptors thus, making this cell have less Notch activity than a surrounding neighbour that inherited less Numb (Guo *et al*., 1996). Notch signalling also has a role in self-renewal *versus* differentiation decisions. In radial glial cells from the central nervous system (CNS), the polarity of partitioning defective protein 3 (PAR3) segregates Mindbomb (Mib-1) to the apical daughter cell, therefore restricting Notch signalling to the basal daughter cell, hence promoting self-renewal, while the apical daughter cell with low Notch signals differentiates (Dong *et al*., 2012). Not only different Notch receptor/ligand pairings have shown to determine diverse outcomes (Ramasamy and Lenka, 2010), but also the strength of such interactions is important in certain contexts. Specification of HSCs in the mouse haemangiogenic endothelium requires low-strength Jag1 ligand mediated signalling, while specification of endothelial arterial cells requires high-strength Delta4 mediated signalling (Gama-Norton *et al*., 2015). Remarkably, a recent study documented different outcomes of Notch1 receptor mediated signalling depending on the ligand engaged (Nandagopal *et al*., 2018). While Delta1/Notch1 interactions were shown to lead to pulsatile activation of Notch1 receptor with preferential *Hes1* upregulation, the outcome on Delta4/Notch1 interactions were demonstrated to sustain activation of the pathway through *Hey/L* upregulation in CHO-K1 cells (Nandagopal *et al*., 2018). An additional way by which a

seemingly simple pathway can become complex is by CSL interaction with factors from other signalling pathways. For example, in the mouse forkhead box p3 (*Foxp3*) gene, an overlapping CSL-NFκB binding site in the promoter helps the cooperative regulation by Notch3 receptor and NF-κB signalling (Barbarulo *et al*., 2011). Furthermore, Notch has been shown to interact with many other pathways such as Wnt, Hedgehog, TGF-β/BMP, Hippo/Yap as well as stress and hypoxia-related pathways (Bigas and Espinosa, 2016).

1.4.4. Notch target genes

Among the many Notch target genes, the best characterised is *HES1* - a member of the Hes-related family (Iso *et al*., 2003). Other members such as *HES5, HES7, HEY1, HEY2* and *HEYL* are also upregulated by Notch (Iso *et al*., 2003). HES and HEY proteins function mainly as transcriptional repressors. There are two possible mechanisms by which HES1 promotes transcriptional repression: HES1 can form non-DNA binding complexes with other bHLH factors through its bHLH domain, thereby preventing these factors from carrying out their functions. A second mechanism is active repression: HES1 can bind to N-boxes by forming complexes with co-repressors (Iso *et al*., 2003). The recruitment of histone deacetylases (HDACs) promotes transcriptional inhibition (Liu *et al*., 2015). HES1 has many known targets, such as *PTEN* (phosphatase and tensin homolog). By binding to its promoter, HES1 strongly silences *PTEN* expression (Palomero *et al*., 2007). In the mouse embryo, HES1 protein represses *Gata2* – a necessary process for emerging HSCs (Guiu *et al*., 2013). However, HES1 has been shown to be more than a repressor. As an example, HES1 amplifies *Runx2* expression by cooperating with pRb (Lee *et al*., 2006), as well as binding to *CDKN1A* promoter thus, inducing p21 expression and consequently HSPCs' growth arrest (Yu *et al*., 2006). Other identified Notch targets comprise *CD25*, *GATA3*, *NRARP* and *DTX1*, the latter of which is a Notch pathway regulator (Borggrefe and Oswald, 2009). In the context of cancer, *MYC* has been found to be a target of Notch-1 in T-ALL (Weng *et al*., 2006). Still in the cancer context, other implicated genes in the Notch signalling have been *CCND1* (Ronchini and Capobianco, 2001) and *CDKN1A* (Rangarajan *et al*., 2001) linking Notch to cell cycle regulation.

1.4.5. The roles of Notch in haematopoiesis

Notch signalling has been shown to be active in very primitive human $CD34^-$ (Anjos-Afonso *et al*., 2013) and in $CD34^+$ HSCs (Kojika and Griffin, 2001), (Ohishi *et al*., 2002), being gradually downregulated as the cells progress towards more committed cell fates therefore, suggesting a role in the maintenance of an undifferentiated state. The Notch pathway is known to be essential in the developing haematopoietic system (Kumano *et al*., 2003) and in T-cell differentiation (Radtke *et al*., 1999). However, whether it is necessary for the maintenance of

adult HSCs is still a matter of controversy. A review from our group has discussed this topic in a greater detail (Lampreia *et al*., 2017). Gain-of-function approaches have shown that inducing Notch signalling leads to an increase in the self-renewal capacity of stem cells which is accompanied by a decrease in differentiation (**Table 1.4**).

Table 1.4 – Notch signalling gain-of-function studies.

Study	Species	Outcome
Exposure of KSL cells to membrane bound or immobilised Jag1 (Varnum-Finney *et al*., 1998)	Mouse	Increased self-renewal of HSPCs / Decreased differentiation
Constitutively active *Notch1* allele (Carlesso *et al*., 1999)	Human	
Exposure of progenitors to Notch ligands *in vitro* (Karanu *et al*., 2001)	Human	
Exposure of human $CD34^+CD38^-$ cells to immobilised Delta1 (Ohishi *et al*., 2002)	Human	
Overexpression of Notch downstream target *Hes1* in mouse KSL (Kunisato *et al*., 2003)	Mouse	
Activation of Jag-1 expression through osteoblast stimulation (Calvi *et al*., 2003)	Mouse	
Exposure of KSL cells to immobilised Delta-1 (Varnum-Finney *et al*., 2003)	Mouse	
Exposure of human $CD34^+CD38^{low}$ cells on membrane bound Delta4 (Lauret *et al*., 2004)	Human	

KSL, c-$Kit^+Sca\text{-}1^+Lin^-$ cells (containing mouse HSCs).

This has been demonstrated through the direct exposure of stem/progenitors to ligands *in vitro* (Varnum-Finney *et al*., 1998), (Karanu *et al*., 2001), (Ohishi *et al*., 2002), (Varnum-Finney *et al*., 2003), (Lauret *et al*., 2004) or by the overexpression of the constitutively active form of Notch1-intracellular domain (N1-ICD) (Carlesso *et al*., 1999) or the Notch target *HES1* (Kunisato *et al*., 2003). Exposure of UCB $CD34^+CD38^-$ cells to immobilised Delta1 in the presence of SCF, FLT3L, TPO, interleukin-6 (IL-6) and IL-3 was shown to inhibit differentiation while expanding $CD34^+$ cells as compared to cultures without the ligand (Ohishi *et al*., 2002). As stated before, quiescence is a hallmark of HSCs and Notch appears to play a role in cell cycle regulation. As an example, enforced expression of *HES1* was demonstrated to induce cell cycle arrest *in vitro* and to block expansion *in vivo*, partially through upregulation of p21, a potent cell cycle inhibitor (Yu *et al*., 2006). Yet in another report, JunB was shown to control

the responsiveness of HSCs to Notch and TGFβ signalling whereby, limiting the expansion and myeloid differentiation of HSPCs (Santaguida *et al*., 2009). Importantly, it was observed that JunB-deficient HSPCs failed to respond to Notch and TGFβ, leading to a reduction in Hes1, p57 and Smad7 thus, triggering the overproduction of myeloid progenitors *in vivo* and consequently contributing to myeloproliferative disease (MPD) development (Santaguida *et al*., 2009). In the context of AML, *HES1* expression induced by Notch activation was shown to downregulate BCL-2 and upregulate p53 and p21 resulting in leukaemic cell growth arrest (Kannan *et al*., 2013). On the other hand, loss-of-function approaches on the role for Notch signalling in the maintenance of murine adult HSCs have led to conflicting results (**Table 1.5**).

Table 1.5 - Evidences of Notch signalling in HSPC regulation.

Study	Species	Outcome
Notch1 loss of function (*Mx1-Cre*) (Radtke *et al*., 1999)	Mouse	Blockage in T cell development Notch1-deficient cells contribute normally to other lineages
RBPJk loss of function (*Mx1-Cre*) (Han *et al*., 2002)	Mouse	Blockage in T cell development Notch1-deficient cells contribute normally to other lineages
Notch inhibition (dnRBPJk-transduced LSK cells) (Duncan *et al*., 2005)	Mouse	Depletion of LT-HSCs
Notch1 and Jag-1 loss of function (*Mx1-Cre*) (Mancini *et al*., 2005)	Mouse	No effect on self-renewal Normal repopulation on Notch1/Jag1 deficient animals after 5FU
***RBPJk* deletion (*Mx1-Cre*) (Maillard *et al*., 2008)**	Mouse	No effect on HSC maintenance
Notch1/2 loss of function (*Mx1-Cre*) (Varnum-Finney *et al*., 2011)	Mouse	Notch2 mediates SK^+ self-renewal Notch2 mediates HSC/MPP repopulation after irradiation
Notch inhibition (γ-secretase inhibitor) (Anjos-Afonso *et al*., 2013)	Human	Higher engraftment capacity (increased generation of $CD34^+CD38^-$ from $CD34^-$ HSCs)
dnMAML1-transduced HSCs (Benveniste *et al*., 2014)	Human	Reduction in HSC frequency but increase in number
Rbpjk loss of function (*Rbpjk*$^{fl/fl}$/*Vav-Cre*$^+$; *Rbpjk*$^{fl/fl}$/*Mx1-Cre*$^+$) (Duarte *et al*., 2018)	Mouse	Unperturbed haematopoiesis in steady state. Rbpjκ-deficient BM cell capable of normal reconstitution

RBPJk, (Recombination signal binding protein for immunoglobulin kappa J region); 5-FU, fluorouracil; LSK, $Lin^-Sca^-1^+c\text{-}Kit^+$ HSCs; SK, $Sca^-1^+c^-Kit^+$ cells; dnMAML1, dominant negative form of Mastermind-like1.

Loss of Notch1 receptor or Jag1 ligand studies resulted with no apparent phenotype in HSCs function (Mancini *et al*., 2005), which has been attributed to the hypothetical compensation by other receptors and ligands. However, the deletion of *Rbpjk*, a key component of Notch signalling activation was also showed to have no role of Notch signalling in HSCs self-renewal (Maillard *et al*., 2008). Despite these early results, more recent reports have shown a role for Notch2 in regulating mouse short and long-term repopulating cells during transplantation (Varnum-Finney *et al*., 2011). Jag1 ligand has been recently shown to support self-renewal of HSCs in the adult bone marrow vascular niche (Poulos *et al*., 2013). Immortalised endothelial cells expressing Jag1, Jag2, Delta1 and Delta4 ligands were determined to support Notch-mediated expansion of long-term HSCs and supported long-term reconstitution in lethally irradiated mice (Butler *et al*., 2010). Notably, knocking down different members of the Notch pathway has been correlated with the initiation of different types of leukaemias which is discussed in greater detail below.

In an interesting study, it was reported that the loss of *Itch* (an E3 ubiquitin ligase which negatively regulates Notch signalling by controlling Notch receptor degradation) led to sustained levels of Notch-1 receptor-mediated signalling (Rathinam *et al*., 2011). Mice transplanted with *Itch*-deficient $Lin^{-}Sca1^{+}c\text{-}Kit^{+}$ (LSK) HSPCs had an expanded stem cell pool with enhanced haematopoietic contribution up to 24 weeks as compared to control LSK cells (Rathinam *et al*., 2011). Early studies have established the Notch1/RBPJk/HES1 axis as a major regulator of T cell differentiation. However, disturbing this axis had no effect on myeloid and B cell lineage commitment (Radtke *et al*., 1999), (Han *et al*., 2002). Duncan and colleagues showed that LSK cells from a transgenic Notch reporter (TNR-GFP) mouse have high Notch activity as evidenced in bone marrow sections by co-localisation of $c\text{-}kit^{+}$ and GFP^{+} cells and by flow cytometric analysis of primitive LSK cells showing GFP expression (Duncan *et al*., 2005). Interestingly, transplanting murine lineage negative (Lin^{-}) cells transduced with dominant-negative suppressor of Xenopus Rbpj homologue (dnXSu(H)) resulted in the depletion of the HSC population after long-term reconstitution compared to control transduced cells (Duncan *et al*., 2005). Although Jag1 ligand is expressed in the osteoblastic niche, loss of Jag1 and Notch1 in the bone marrow does not affect HSC homeostasis (Mancini *et al*., 2005). These studies do not rule out possible redundant effects from other Notch receptor/ligand pairs. In fact, Notch2 but not Notch1 receptor mediates LSK cell self-renewal and repopulation following transplantation and inhibits myeloid differentiation (Varnum-Finney *et al*., 2011). However, it was reported that neither the loss of Notch1 nor Notch2 receptor had any effect on the number of HSC in steady state conditions (Varnum-Finney *et al*., 2011). Perhaps more convincingly is a study undertaking a pan-inhibition of all canonical Notch signalling approach mediated by the overexpression of a dominant negative form of

mastermind-like 1 (dnMAML1), the authors reported no effect on LSK cell function (Maillard *et al*., 2008). They also proposed that under homeostatic conditions LSK cells are normally exposed to very low levels of Notch signalling *in vivo* (Maillard *et al*., 2008) which contrasts the observations by Duncan *et al*. In one of the few studies with human HSCs, Benveniste *et al.,* directly compared the impact of canonical Notch signalling on human HSCs *in vitro* and *in vivo* by overexpressing dnMAML1 (Benveniste *et al*., 2014). Repopulation capacity was comparable in both Notch-inhibited and control HSCs. More recently, using pan-haematopoietic (*Vav-Cre*) and inducible (*Mx1-Cre*) mouse models driving the deletion of *Rbpj*, Duarte and colleagues reported unperturbed haematopoiesis in steady state conditions upon Notch inhibition. Additionally, apart from the expected lack of T cell development, *Rbpj*-deficient BM cells reconstituted recipients without any defects (Duarte *et al*., 2018).

Outside the stem cell compartment however, Notch pathway appears to play a role in cell fate decisions at different nodes of the haematopoietic hierarchy. This has been best demonstrated in the murine system, where Notch1 and Notch2 receptors represent the two main regulators of early adult haematopoiesis (Oh *et al*., 2013). Notch1 drives lymphopoiesis through thymic epithelium-bound Delta4 (Hozumi *et al*., 2008). Alternatively, Notch2 receptor drives erythropoiesis at an early progenitor stage, presumably the pre-MkE. Also, it promotes marginal zone B-cell differentiation at the expense of follicular B cells (Tanigaki *et al*., 2002), (Saito *et al*., 2003). Most notably, Notch has been associated with the promotion of T cell development at the expense of B cell production. Specifically, Notch 1 receptor overexpression by retrovirally transduced haematopoietic progenitors was demonstrated to lead to the appearance of ectopic T cells in the BM (eventually leading to T-ALL) while inhibiting B cell formation (Pear *et al*., 1996). Conversely, blocking Notch 1 receptor in the bone marrow was confirmed to inhibit thymic T cell development while inducing ectopic appearance of B cells in the thymus (Wilson *et al*., 2001). This implies that one the roles for Notch signalling is to promote a bias towards T cell differentiation at the expense of B cell production. In addition, Notch 1 receptor has also been implicated in myelopoiesis (Schroeder *et al*., 2003) and megakaryopoiesis (Mercher *et al*., 2008). Using FDCP-mix cells – that contain haematopoietic progenitor cells derived from murine BM, Schroeder *et al.,* indicated that Notch1 receptor signalling caused the decrease in self-renewal of FDCP cells while promoting differentiation towards the myeloid lineage with concomitant increase in *Spi1* expression (Schroeder *et al*., 2003). The Notch1/Delta1 pathway mediates megakaryocyte development from HSCs *in vivo* (Mercher *et al*., 2008). This axis leads to induction of a megakaryocytic transcriptional programme that includes transcription factors GATA-1, GATA2 and FOG1 which have been shown to play a role in megakaryopoiesis (Shivdasani *et al*., 1997), (Tsang *et al*., 1997), (Chang *et al*., 2002). Remarkably, Notch4 receptor only promotes megakaryocyte

development when is induced in MEPs, meaning there are different requirements for the Notch receptors at the various nodes of differentiation.

As stated before, the BM tightly regulates HSPCs, partly through Notch signalling. Co-culture of HSPCs with bone marrow endothelial cells (BMECs) expressing Jag1 ligands leads to expansion of haematopoietic progenitors via Notch signalling. Interestingly, pro-inflammatory signals such as TNFα and LPS promote Jag2 ligand expression on ECs, which in turn activate Notch1/2-mediated signalling in haematopoietic progenitors *in vivo* (Fernandez *et al*., 2008). ECs were also shown to support long-term expansion of LSK cells through Notch signalling in another study (Butler *et al*., 2010). In an interesting study of signalling crosstalk, the secretion of vascular endothelial growth factor A (VEGF-A) by HSPCs was reported to stimulate cell surface expression of Jag2 ligand on ECs which in turn supported HSPCs expansion via Notch1/2 signalling (Butler *et al*., 2010). More evidences for EC-mediated support of HSPCs came from Poulos and colleagues' work: although ECs-specific *Jag2* deletion had no effect on HSPCs under homeostasis, Notch2 receptor signalling was shown to be essential for haematopoietic recovery under myelosuppressive conditions. Interestingly, Jag2 ligand-mediated signalling enhanced *Hey1* expression via Notch2 receptor, while suppressing *Hes1* instead (Poulos *et al*., 2013). Other types of cells have been implicated in Notch-mediated regulation of HSPCs. High Jag1 ligand expressing $CD146^+$ MSCs were determined to support long-term culture of HSPCs (Corselli *et al*., 2013). In contrast, osteoblast ablation was shown to reduce quiescence, long-term engraftment and overall self-renewal capacity of HSCs (Bowers *et al*., 2015). Interestingly, co-culture of osteoblasts expressing Jag1 ligand was described to reduce cell cycling and overall cell numbers of both leukaemic and normal HSCs (Bowers *et al*., 2015). In summary, these studies focusing on the haematopoietic niche provide strong evidence for the regulation of HSPCs by a variety of cell types involving crosstalk between Notch signalling and other pathways.

1.4.6. A general view of Notch signalling in haematological malignancies

In contrast to the above results, suggesting the role for Notch is still not clearly understood in the human haematopoietic system, several mouse models where different members of the pathway have been deleted consistently show that defective Notch in the BM microenvironment is a major player in the development of different myeloproliferative disease (MPD) phenotypes (**Table 1.6**).

Table 1.6 – Loss of Notch pathway members frequently results in myeloproliferative disease in mouse models

Mouse model	Phenotype	Effect on stem cells
***Psen1*$^{+/-}$/*Psen2*$^{+/-}$ (Qyang *et al*., 2004)**	MPD (expanded granulocytes)	Normal side population
***MMTV-Cre/Mib*$^{f/f}$ *Mx1-Cre/Mib*$^{f/f}$ (Kim *et al*., 2008)**	MPD (expanded granulocytes)	Expanded LSK
***FX*$^{-/-}$ (Zhou *et al*., 2008)**	MPD	Normal LSK
***Mx1-Cre/Pofut*$^{f/f}$ (Yao *et al*., 2011)**	Increased neutrophils	ND
***Mx1-Cre/Adam10*$^{f/f}$ (Yoda *et al*., 2011)**	MPD (increased neutrophils)	Expanded LSK
***Mx1-Cre/Ncstn*$^{f/f}$ (Klinakis *et al*., 2011)**	CMML-like disease	Expanded LSK
***Mx1-Cre/Rbpj*$^{f/f}$ *Tie2-Cre/Rbpj*$^{f/f}$ (Wang *et al*., 2014)**	MPD	Expanded LSK

ND, Not determined; MPD, myeloproliferative disease; CMML, Chronic myelomonocytic leukaemia; LSK, Lin$^-$Sca$^-$1$^+$c-Kit$^+$

One of the earliest reports linking Notch signalling to MPD showed that presenlinin-1 haplo and presenilin-2-deficient (*Psen1*$^{+/-}$ *Psen2*$^{-/-}$) mice had an expanded granulocytic compartment and the animals developed signs of MPD (Qyang *et al*., 2004). Also, *FX*$^{-/-}$ mice (FX mediates addition of N-acetylglucosamine residues to Notch receptors, which is essential for proper interaction with ligands) develop a myeloproliferative phenotype with expanded granulocytes and erythrocytes (Zhou *et al*., 2008). Similarly, *Pofut*-deficient marrow progenitors were revealed to have defective O-fucosylation of Notch receptors and no ability to bind to Delta-like ligands (Yao *et al*., 2011). Thus, Pofut-deficient mice have increased numbers of neutrophils and reduced lymphocytes. In addition, loss of Mib1 - essential for ligand endocytosis, was shown to cause MPD originated from the LSK population (Kim *et al*., 2008). Especially, this report showed that defective Notch signalling between the cells that make up that microenvironment caused the MPD phenotype. Granulopoiesis can also develop following *Adam10* deletion in the BM (Yoda *et al*., 2011). Loss of *Adam10* further resulted in both cell-autonomous and non-cell-autonomous enlargement of the HSC pool and MPD (Yoda *et al*., 2011).

In addition to this, Nicastrin-deficient HSCs were demonstrated to develop a human chronic myelomonocytic leukaemia-like (CMML) disease with expanded LSK compartment, with the Notch-suppressed cells showing a de-repressed myeloid transcriptional program (Klinakis *et al*., 2011). Finally, an elegant study from the Carlesso lab showed that mice that were

conditionally deleted of *Rbpj* using *Mx1-Cre* developed myeloproliferative disease (Wang *et al*., 2014). By performing reciprocal experiments, the authors showed that the mutant-LSK cell pool was significantly expanded but multiple progenitor subsets were unaffected thus, having no consequences in the WT recipient mice. However, when transplanting WT HSPCs into mutant mice, CMPs and GMPs in the BM and spleen were significantly increased, resulting in a lethal MPD (Wang *et al*., 2014). This study demonstrated that cell-autonomous loss of Notch activation was not sufficient to develop myeloid disease, but the loss of Notch signalling in the microenvironment induced lethal MPD in a non-cell autonomous manner. Mechanistically, the loss of *Rbpj* led to increased expression of mir-155 and consequently upregulated NFκB signalling by targeting one of its main regulators Kb-RAS1. This led to increased expression of G-CSF and TNFα, inducing a persistent inflammatory state in the BM (Wang *et al*., 2014).

All these results suggest that a proper activation of Notch signalling must be maintained not only in HSPCs but also in the BM niche. It is rather remarkable that inhibition of Notch, through the loss of several different members of the pathway leads to the expansion of the most primitive HSCs impairing their repopulating capacity. This is probably due to the early differentiation induced by the loss of a quiescent state partly imposed by Notch signalling. Altogether these studies highlight the importance of maintaining a proper Notch signalling in the BM for a proper regulation of hematopoiesis.

Activating *NOTCH1* mutations are found in half of T-ALL cases (Weng *et al*., 2004),(Chiaramonte *et al*., 2005) where they act as a well-known oncogene. These mutations result in ligand independent activation of the receptor and enhanced stability of the Notch1-ICD by removing the destabilizing PEST domain (Weng *et al*., 2004). Similarly, Notch mutations have also been implicated in chronic lymphocytic leukaemia (CLL) (Puente *et al*., 2011a),(Fabbri *et al*., 2011), whereby *NOTCH1* mutations prevent FBW7 E3 ligase degradation of the Notch1 receptor. These events are associated with poor prognosis in this disease (Rossi *et al*., 2012). Contrastingly, Notch appears to be a tumour suppressor in B-cell leukaemias. Constitutive expression of truncated forms of all four Notch receptors or downstream effector *HES1* prevented growth and induced apoptosis of various B-cell acute lymphoid leukaemia (B-ALL) cell lines including Hodgkin, myeloma and mixed-lineage leukaemia (Zweidler-McKay *et al*., 2005). Others have found that 8% of large B-cell lymphomas and 5% of marginal zone lymphomas possess activating Notch2 mutations (Lee *et al*., 2009). As mentioned earlier, deletion of *Ncstn* results in CMML-like disease in mice (Klinakis et al., 2011). The authors further identified additional mutations in Notch pathway components and have suggested a tumour suppressing role for Notch in this disease.

1.4.7. The role of Notch in AML

As mentioned earlier, it is well established that Notch signalling acts as oncogene in T-ALL (Weng *et al*., 2004), (Chiaramonte *et al*., 2005), (Aster *et al*., 2008). However, it is still a matter of debate whether the Notch pathway plays an oncogenic or tumour suppressor in other haematological diseases (Nowell and Radtke, 2017).

Early studies on the role of Notch in myeloid malignancies revealed that certain AML cell lines and primary AML samples express the Notch1 receptor (Tohda and Nara, 2001). The same group later demonstrated that stimulation of primary AML cells with immobilised Jag1 or Delta1 ligand caused mixed outcomes on proliferation but Notch activation appeared to promote blast differentiation (Tohda *et al*., 2005). Conversely, activation of Notch1 receptor in the HL60 cell line impaired monocyte and granulocyte differentiation under pro-differentiative stimuli (Carlesso *et al*., 1999). A mechanism for this emerged later, when stimulation of Notch signalling by its cognate ligand Delta4 was shown to induce *SKP2* up-regulation in HL60 cells and primitive haematopoietic cells, regulating the balance between proliferation and differentiation (Sarmento *et al*., 2005). Notch activation was also shown to cause inhibited cell cycle kinetics in erythroleukemic cell line TF1 (Chadwick *et al*., 2008) and in CML cell line K562 (Yin *et al*., 2009). Even though Notch components are rarely mutated in AML (for example, MAML1 is frequently deleted in 5q AMLs) (Jerez *et al*., 2012), *NOTCH2* and *FLT3* are the most frequently mis-spliced genes in AML (Adamia *et al*., 2014). The authors reported that as much as 73% of the AML samples analysed expressed a Notch2 splice variant named Notch2-Va. Expression of this variant was correlated with decreased Notch target gene expression and associated with poor outcome (Adamia *et al*., 2014).

A few research groups have reported tumour suppressor roles for Notch signalling in myeloid leukaemias. As briefly mentioned, loss of Nicastrin led to enlargement of the GMP population and development of a CMML-like disease in a mouse model (Klinakis *et al*., 2011). This was thought to be mainly driven by the loss of Notch1 and Notch2. The authors believed that Nicastrin, through Notch, repressed a myeloid-specific programme which was de-repressed upon Nicastrin loss. Ectopic expression of *Hes1* prevented granulocyte/monocyte lineage differentiation through repression of *Cebpa* and *Spi1* (Klinakis *et al*., 2011). Notch1-IC knock-in mice bred with *Ncstn*$^{-/-}$ mice supressed GMP enlargement and disease progression (Klinakis *et al*., 2011). Additionally, exon sequencing of CMML patient samples uncovered somatic heterozygous mutations in *NCSTN*, *APH1*, *MAML1* and *NOTCH2* (all members of the Notch pathway). In another study, AML cell lines were reported to have undetectable levels of active Notch receptors despite expressing Notch receptors on the cell surface (Kannan *et al*., 2013). Re-activation of Notch signalling by retrovirally transducing AML cell lines with ICN1-4 resulted in growth arrest and increase in *HES1* expression. Interestingly, a similar effect was observed

when *HES1* was overexpressed (Kannan *et al*., 2013). Notch reactivation caused caspase-dependent apoptosis, along with a decrease in *BCL2* expression and increase in p53/p21, although it was unclear whether HES1 had a direct involvement in these effects. Overexpression of N1-ICD or HES1 was also shown to reduce leukaemic burden *in vivo*, which on the other hand, seemed to be aggravated by using the Notch inhibitor dnMAML1. A Notch agonistic peptide (Jag1 DSL) was also used to demonstrate significant apoptotic induction in both primary and AML cell lines *in vitro* (Kannan *et al*., 2013). Similarly, another group showed that the Notch pathway was silenced in AML by performing microarray gene expression analysis of normal BM cells compared to AML cells (Lobry *et al*., 2013). The effect seen was in part due to hypermethylation of Notch target gene promoters such as *HES1* and *NRARP*. The authors also complemented their studies by showing that an MLL-AF9 driven mouse model of AML also had silenced Notch signalling, with methylation of Notch target gene promoters *Hes1*, *Nrarp* and *Gata3* (Lobry *et al*., 2013). Reactivation of Notch pathway by crossing the MLL-AF9-driven AML mouse to a model containing inducible N1-ICD expression, resulted in decreased leukaemic burden *in vivo* and overall increased survival (Lobry *et al*., 2013). The reactivation of Notch induced in this experimental setting led to increased apoptosis and differentiation of AML LICs. Moreover, *HES1*-low cohorts of AML patients seem to have a worse outcome in terms of overall survival and relapse free survival than *HES1*-high groups, suggesting HES1 may serve as an independent prognostic factor in this disease (Tian *et al*., 2015).

Surprisingly, Notch has also been shown to act as an oncogene. In a mouse model with an activating mutation in β-catenin, this caused increased Jag-1 ligand expression on osteoblasts that triggered Notch signalling in LSK cells, resulting in AML development (Kode *et al*., 2014). These mice were seen to have increased GMP and decreased MEP populations, with no apparent change in CMPs. Interestingly, transplanting BM cells from the *Ctnnb1*^{CAosb} leukaemic mouse model into WT recipients generated AML. Conversely, when WT BM cells were transplanted into mutant mice, the recipient mice also generated AML. These results reinforce the notion that in some cases, AML may be induced by defective niche signals that are restricted to the BM cells such as osteoblasts (Kode *et al*., 2014). By deleting one *Jag1* allele in osteoblasts, the authors of this work also demonstrated the rescued of anaemia previously seen and also prevented AML development (Kode *et al*., 2014). The authors of this work also found localisation of activated β-catenin in osteoblasts in 40% of human primary AML samples, while this was not observed in healthy BM controls (Kode *et al*., 2014).

More recently however, a research group inter-crossed dnMAML1-GFP mice with *Vav-Cre* animals to disrupt Notch in haematopoietic cells (Francis *et al*., 2017). Double heterozygous dnMAML1$^{f/-}$Vav$^{+/-}$ mice displayed a reduction in the CMP compartment and an expanded GMP

fraction at 15-18 months. Despite GMP expansion, the authors did not report the emergence of a myeloid neoplasm thus, contrasting with the work from Klinakis and colleagues (Klinakis *et al*., 2011). Also, *TRIB2* expression, encoding for Tribbles homolog 2 is modulated by Notch1 and was shown to contribute to AML pathogenesis (Keeshan *et al*., 2006) even though Notch1 activation does not cause AML in mice. The authors suggested that Notch1 regulation of Trib2 may be context dependent and not operational in myeloid progenitors (Keeshan *et al*., 2006), (Puente *et al.,* 2011). This reveals the complexity of Notch signalling modulation. In any case, re-activation of the Notch pathway has supported the notion of a tumour suppressor role for Notch signalling in this context.

1.5. Aims of the Thesis

Some studies mentioned here reveal that Notch signalling has been mainly exploited to expand HSPCs *in vitro*. However, the functions of this pathway in the regulation of human HSPCs and in AML have not been clearly elucidated yet. The objectives of this work are to:

- Characterise the expression and activity of Notch signalling in human HSPCs.
- Block Notch signalling (canonical only and pan-inhibition) via a γ-secretase inhibitor and shRNAs targeting *NCSTN* and *RBPJ* in human HSPCs.
- Gauge the effects of Notch inhibition on the maintenance and differentiation capacity of HSPCs *in vitro*.
- Gauge how inhibiting Notch impacts myelo-lymphoid engraftment and frequencies of HSPCs and mature blood cells *in vivo*.
- Characterise the expression and activity of Notch signalling in primary AML and AML cell lines.
- Activate Notch through membrane-bound ligands, small molecules and peptides in primary AML and AML cell lines and assess its effect on cell proliferation and apoptosis.
- Determine whether activation of distinct Notch receptors impacts AML cell proliferation and apoptosis differently.

Chapter 2 – Materials and Methods

2.1 Materials and Methods

2.1.1 General laboratory equipment

Suppliers of materials and reagents are provided below in the relevant methods sections. All plastic-ware and tissue culture vessels were purchased from Greiner Bio One, UK and VWR, USA. Centrifugation of cell suspensions were performed in a Beckman Allegra 6R (Beckman Coulter, USA). The centrifuges used for molecular biology work were a Heraeus™ Fresco™ 21 Microcentrifuge (Thermo, USA) and a Heraeus™ Megafuge™ 40R (Thermo).

2.1.2 Buffers and stock solutions

See **Appendix I.**

2.2 Cell culture

All tissue culture was performed in a Safe 2020 Class II Biological Safety Cabinet (Thermo) and the cells were incubated in HeraCell 150 (Thermo) incubators at 37°C with 20% O_2 and 5% CO_2.

2.2.1 Human cell lines

The adherent cell lines HeLa, Saos2 and HEK293TLTX (LentiX^{TM}-293T) were maintained in Dulbecco's Modified Eagle's Medium – high glucose (DMEM; Merck, USA) supplemented with 10% foetal bovine serum (FBS, LSP, UK), 1% Penicillin/Streptomycin (P/S) (Gibco, USA) and 1X GlutaMAX (Gibco). This formulation is herein termed "complete DMEM". Cells were passaged every 2 to 3 days when reached a 70-90% confluency. The leukaemia cell lines HL60, THP1, OCI-AML3, KG1, Kasumi, Molt4 and Raji were cultivated in RPMI 1640 (Merck) supplemented with 10% FBS and 1% P/S (formulation simply called "complete RPMI"). Cells were split every 3 to 4 days to a cell density of $3x10^5$ cells/mL. All cell lines were originally acquired from the cell service of Cancer Research UK – London Research Institute. To passage adherent cells, growth media was removed, and cells were washed once with pre-warmed PBS (Merck). Then, trypsin-ethylenediaminetetraacetic acid (EDTA) (0.05%), phenol red (Thermo) was added for 5 min at 37°C. Two volumes of complete growth media were then added to neutralise trypsin and cell suspension was harvested and centrifuged. Cell pellet was resuspended in complete growth media and re-plated at ratios between 1:4 and 1:6 every 3 days until use.

2.2.2 Murine cell lines

The MS5, S17, and S17-Delta4 murine stromal cell lines were a kind gift from Dr. Evelyn Lauret (University of Paris). Cells were maintained in alpha-MEM (Gibco) + 10% FBS + 1% P/S (termed “complete alpha-MEM”). Cells were passaged every 2 to 3 days when reached a 70-90% confluency and passaged three times before were used in experiments.

2.2.3 Thawing and Cryopreservation

Cells were thawed in a 37ºC water bath and transferred dropwise to a 15 mL tube with the respective culture medium. Cell suspensions were centrifuged at 300× *g* for 5 min, resuspended in the respective culture medium as described and plated at apropriate density. Cells were counted using a haemocytometer and trypan blue exclusion method. Adherent cells were plated on tissue culture-treated surfaces at densities around 1.5-2.5 × 10^4 cells/cm^2 and split upon reaching 70-80% confluence as described. Suspension cells were plated on tissue culture-treated wells or flasks in vertical position at densities around 1-2×10^6 cells/mL and split after 2 days.

Human and murine cell lines were preserved in 90% of their respective growth media with 10% of dimethyl sulfoxide (DMSO, Fisher Scientific, USA). Cells were resuspended in the appropriate freezing media and 1 mL of cell suspension was added per cryovial (Merck) and stored in Nalgene® Mr. Frosty freezing containers (Merck) at -80°C, allowing for gradual cooling process. Adherent cells were frozen at cell densities between 2-5×10^6 cells/mL and suspension cells at 8-10×10^6 cells/mL. The cells were then later transferred to a liquid nitrogen storage unit for long-term preservation.

2.3 Molecular biology

2.3.1 Cloning of lentiviral constructs

The plasmids, primers and oligonucleotides used for the cloning of the various constructs are listed in **Tables II.1**-**5** of **Appendix II**.

2.3.1.1 shRNA Design for miR-30-based and H1 promoter-driven shRNA lentiviral constructs

shRNA design was based on sequences commercially available (**Table II.1** of **Appendix II**). and were mostly based on sequences available at Dharmacon™, USA. The 19-mer oligonucleotides that presented the least complementarity to non-desired targets were chosen (**Table 2.1**).

Table 2.1 – shRNA target sequence and location. Based on Nicastrin accession number NM_015331.3 and RBPJκ accession number NM_005349.3.

Clone	Target sequence (5' > 3')	Location
sh*NCSTN-1*	ACTGTACAACATAAGTGGT	1701
sh*NCSTN-3*	GAGTCAACATTCTCTAACT	1078
sh*RBPJ-2*	TTTGGAGTGAAATTCTGTC	1360
sh*RBPJ-3*	TGGAGTGAAATTCTGTCCT	1358

To adapt the 19-mer sequences to the miR-30 backbone few modifications were made: 1- by relying on the anti-sense sequence, the sense sequence was generated by complementarity; 2- two nucleotides at position -1 and +20 were added based on their complementarity to the desired mRNA. As shown in **Figure 2.1**, that the anti-sense sequence aligns with 100% complementarity to the *NCSTN* (highlighted sequence). When reading the *NCSTN* mRNA, the nucleotide -1 is a C, while nucleotide +20 is an A. Therefore, the sense sequence becomes 5' - **C**ACCACTTATGTTGTACAGT**A** -3'; 3- the nucleotide at position -2 was used to generate a mismatch using nucleotides A or C with the nucleotide at position +21 when the RNA structure folds onto itself. Since, the nucleotide +21 in this case is a T, this means the nucleotide at position -2 will be a C. The sense sequence now becomes 5'-**CC**ACCACTTATGTTGTACAGT**A**-3' and the anti-sense sequence is instead 5'-**T**ACTGTACAACATAAGTGGT**GT-3'.**

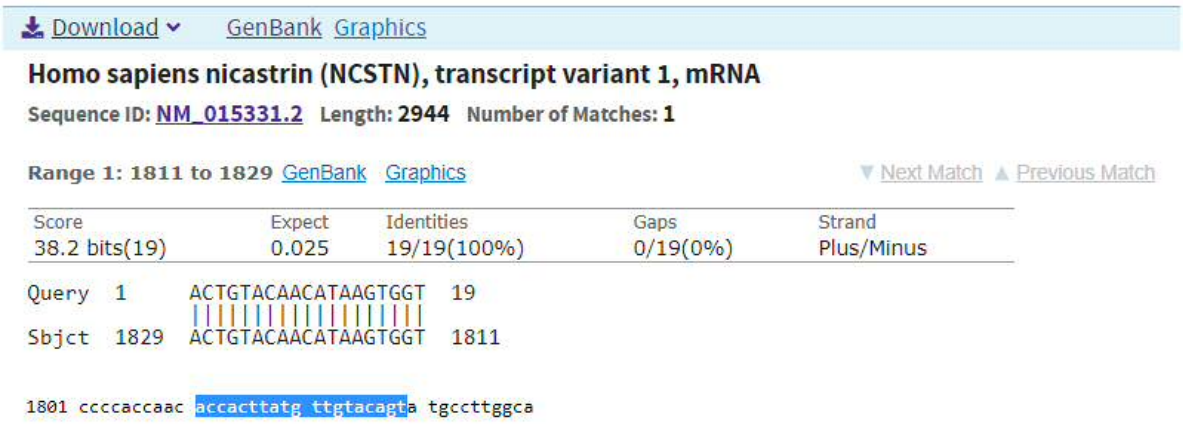

Figure 2.1 – Example of alignment of anti-sense sequence to target gene. Alignment of anti-sense sequence number 1 targeting the *NCSTN* gene using BLAST® tool (National Center for Biotechnology Information database)

A loop with the sequence TAGTGAAGCCACAGATGTA was introduced in between the sense and anti-sense sequences (based on the design of the pGIPZ™ construct (Dharmacon™)).

The forward and reverse oligos with the sequence below (with phosphate group on 5' end) were purchased from Merck and were reconstituted to 1 mM in molecular grade water. Then, 2 µL of each oligo were added to 48 µL of annealing buffer (see **Appendix I**). The mix was incubated for 4 min at 95°C, then 10 min at 70°C. The oligos were then allowed to cool slowly at room temperature (RT) for several hours.

For the H1 promoter-driven shRNA lentiviral constructs, the shRNA sequences used were based on the 19-mer sequences that were validated with the miR-30-based system, with small modifications (according to the recommendations from the Riken Institute, Japan): 1-the sense sequences starting with a C or a T were changed to an A or G (preferably A) by shifting the sequence in any direction for one or two nucleotides until this condition was reached; 2- a BglII-5' overhang and a XbaI-3' overhang were added; 3- a loop with the sequence TTCAAGAGA was introduced in between the sense and anti-sense sequences. Phosphorylated oligos were purchased from Merck.

2.3.1.2 Cloning of a miR-30-based lentiviral vector

The lentiviral vector for constitutive expression of miR30shRNA containing specific shRNA sequences along with a GFP reporter was generated based on the vector pLV.EF1α-premiRNA30a-rPuro. First, the enhanced GFP (eGFP) gene was amplified by polymerase chain reaction (PCR) from the plasmid pSIN.Tet-HPGK-rtTA2-hDKK-Ires-GFP (available in the lab), using the primers to insert the XbaI and SalI restriction sites. Briefly, PCR amplification was performed using the HotStarTaq® (Qiagen, Germany) at 70°C. The PCR product was cleaned up by running the DNA in a 1% UltraPure Agarose (Thermo) gel, from which the band of interest was excised. The DNA was extracted from the gel using the PureLink™ Quick Gel extraction kit (Thermo), according to manufacturer's instructions. Then, the DNA was then digested with the *XbaI* and *SalI* restriction enzymes (all restriction enzymes were purchased from New England Biolabs, USA). The pLV.EF1α-premiRNA30a-rPuro plasmid was also digested with *XbaI* and *SalI* and then dephosphorylated using the Shrimp Alkaline Phosphatase (rSAP) (New England Biolabs). The linearised vector was separated by gel electrophoresis and DNA extracted from the gel. The eGFP sequence was ligated to the linearised pLV.EF1α-premiRNA30a-rPuro vector at a molar ratio of 3:1, respectively, by using the Quick Ligation™ kit (New England Biolabs), according to manufacturer's instructions. The ligation was transformed in NEB® Stable competent bacteria (New England Biolabs). Briefly, one vial of bacteria was thawed on ice for a few minutes. Then, 2 µL of ligation reaction was added to the bacteria and the mix was incubated on ice for 30 min. Then, heat-shock transformation was performed by placing the mix in a Thermo Mixer® (Eppendorf) at 42°C for 30 seconds and then placing back on ice for 5 min. Then, 1 mL of pre-warmed S.O.C. medium

(Thermo) was then added to the mix which was incubated at 37°C while shaking at 225 rpm for 1 h. Lastly, 200 µL of the pre-growth was added to solidified Lennox broth (LB)-Agar (Thermo) plates with ampicillin and incubated at 30°C overnight. The next day, several bacterial colonies were picked and cultivated in LB medium (Merck) at 37°C while shaking at 225 rpm for approximately 16 h. The next day, bacteria were harvested by centrifugation and plasmid DNA was extracted using the PureLink™ miniprep kit (Thermo). Successful ligation was confirmed by sending the DNA to be sequenced at Eurofins Genomics (Ebersberg, Germany) with the primer "Seq GFP Fwd". This generated the vector simply termed pLV. Then, the miR30 precursor sequence was replaced by a miR30shRNA sequence. The mir30 backbone used for shRNA integration was obtained from the pGIPZ™ vector (Dharmacon™).

Since *XhoI* and *EcoRI* sites are not single restriction sites within the pGIPZ™ vector, the fragment containing the mir30shRNA sequence from pGIPZ™ was first cloned into an intermediate vector (pECFP-C1; already available in the lab). Briefly, the miR30shRNA sequence was PCR amplified using the HotStarTaq®. The primers were modified to introduce *BamHI* and *NheI* recognition sites. The mir30shRNA was then transferred to pECFP-C1 via *BamHI*/*NheI*. Then, 1 µL of annealed oligos was then used for direct ligation with pECFP-C1-mir30shRNA via *XhoI*/*EcoRI*. The ligation product was transformed in OneShot™ TOP10 (Thermo) bacteria. The transformation protocol used was the same as the one used for NEB Stable competent bacteria, except for the selection plates being incubated at 37°C instead of 30°C. To select positive clones, DNA from the various colonies were sent for DNA sequencing with the primer "Seq Fwd shmir30 pECFP". Lastly, the mir30-shRNA backbone containing the shRNA of interest was transferred into the pLV vector via *BamHI*/*NheI*. The ligation product was transformed into NEB® Stable bacteria. Successful cloning was confirming by sequencing with the primer "Seq Rev shmir30 EF1". Clones with the correct DNA sequences were then propagated in larger scale and DNA was extracted using the PureLink™ Maxiprep or Megaprep kits (Thermo) according to manufacturer's instructions.

2.3.1.3 Cloning of H1 promoter-driven shRNA lentiviral constructs (CS-shRNA)

The lentiviral vector CS-RfA-EG (RIKEN BRC DNA Bank, Japan) backbone was used to overexpress shRNA under the control of the H1 promoter. This construct contains a GFP reporter protein under the control of the EF1α promoter. The pENTR4-H1 (RIKEN BRC DNA Bank) plasmid was linearised via *BglII*/*XbaI* restriction enzymes, followed by dephosphorylation and gel purification. The annealed oligos were ligated into the linearised pENTR4-H1 plasmid and transformed in OneShot™ TOP10 bacteria. Successful cloning was confirmed by sequencing with the primer "pH1up2seq". Finally, the H1-shRNA sequences from the pENTR4-H1-shRNA were transferred into the destination vector CS-RfA-EG through

Gateway® LR cloning. The reactions were incubated for 6 h and then transformed into OneShot™ TOP10 bacteria. Successful cloning was once more confirmed by sequencing with the primer “pH1up2seq”.

2.3.1.4 Cloning of a Notch reporter lentiviral vector

The mCherry sequence was amplified by PCR from the pmCherry plasmid (TakaraBio, Japan) and transferred via *AgeI* and *HindIII* into the pHes1-GFPd20 plasmid (Addgene; plasmid #14808), generating pHes1-mCherry. From the latter plasmid, the sequence spanning the *Hes1* promoter and mCherry was amplified by PCR and transferred into an intermediate *in-house* generated plasmid (plasmid A) which contained a cassette with the SFFV promoter driving another gene of interest, via XhoI and SalI restriction sites. This generated another intermediate plasmid (plasmid B). The truncated NGFR sequence was amplified by PCR from the pCCL-NGFR plasmid (a gift from Prof. Luigi Naldini) via *XhoI* and *NdeI*, and cloned into plasmid B. Lastly, a third *in-house* generated plasmid (plasmid C, a modified version of the plasmid CSII-EF-MCS; Riken) containing the sequence for the EF1α promoter was digested with *SanDI*/*XhoI* restriction sites in order to transfer the fragment containing the sequence for EF1α into plasmid B therefore, generating the final Notch reporter lentiviral vector containing the EF1α promoter driving the expression of the truncated NGFR and further downstream, a Hes1 promoter driving the expression of the mCherry reporter protein. The construct was propagated in NEB® Stable competent bacteria as described before. Successful cloning was confirmed by using the primers “Fwd Seq NGFR”, “Rev Seq NGFR”, “Rev Seq Hes1”, “Fwd Seq cherry” and “Rev Seq cherry”.

2.3.2 Quantitative real-time PCR

RNA extraction was performed using the Direct-Zol RNA miniprep or microprep kits (Zymo Research, USA) depending on the starting number of cells, according to manufacturer’s instructions. cDNA was generated by performing reverse transcription of the mRNA using either the OmniScript or Sensiscript kits (Qiagen) depending on starting RNA quantity. Briefly, 20 µL reactions containing 1 µL of reverse transcriptase enzyme, 2 µL of 2X reverse transcriptase buffer, 1 µL of Oligo-dT 14-mer (10 µM; Merck), 2 µL of dNTPs and varying amounts of mRNA, topped up with molecular grade water were incubated at 37°C for 1 h. The reaction was stopped by incubating at 93°C for 5 min. The cDNA solution was then placed on ice for a few minutes. For quantitative real-time PCR, between 3-6 ng of the original equivalent mRNA were used per RT-PCR reaction (10 µL) using *Power*SYBR™ (Thermo) according to manufacturer’s instructions. Primers were added at a final concentration of 600 nM (Primer list can be found in **Table II.6** of **Appendix II**). The reactions were amplified using QuantStudio

7 Flex Real-Time PCR system (Thermo). The targets were amplified using the following protocol: Hold stage – 2 min at 50°C, then 10 min at 95°C; PCR stage (40 times) 15 sec at 95°C then 1 min at 60°C; Melt curve stage – 15 sec at 95°C, 1 min at 60°C, 15 sec at 95°C.

The analysis was performed by using the ΔΔCt method (Livak and Schmittgen, 2001), (Schmittgen *et al*., 2000), (Winer *et al*., 1999). The ΔCt for a certain gene represents the difference in the cycle threshold (Ct) value for the gene of interest and the Ct value of the housekeeping gene and was calculated by using the formula ΔCt = Ct value (gene of interest) – Ct value (housekeeping gene). The ΔΔCt value represents the difference in Ct values between the gene of interest in two different conditions, normalised to the housekeeping gene within their respective conditions and was calculated according to the formula: ΔΔCt = ΔCt (gene of interest in condition A) – ΔCt (gene of interest in condition B). Lastly, to quantify the fold-change in the expression of the gene of interest in relation to a control condition, the formula $2^{(-\Delta\Delta Ct)}$.

2.4 Western-Blot (WB)

2.4.1 Preparation of cell lysates

Adherent cells were harvested by trypsinisation and washed twice with PBS. Conversely, the appropriate number of suspension cells were harvested and washed twice with PBS. The pellet was then resuspended in the appropriate volume of RIPA buffer (Merck) containing 1% of Proteinase Inhibitor Cocktail (Merck). The cell lysate was incubated on ice for 30 min while mixing several times during the incubation period. The cell lysate was then cleared by centrifuging for 10 min at 4°C at 16,000x *g* and harvesting the supernatant. The protein was quantified using the DC Protein assay (Biorad, USA). Briefly, 5 µL of the protein suspension was added into a 96-well plate. Then, 25 µL of a mixture of Reagent S and Reagent A was added to the sample. Then, 200 µL of Reagent B was added to the sample and mixed. Known concentrations of stock BSA (bovine serum albumin; Merck) protein were used to generate a calibration curve. The samples were then incubated at room temperature (RT) for 10 min on a shaker, and after that, absorbance of each sample was measured using a CLARIOstar Plus microplate reader (BMG Labtech, Germany). The concentration of the samples was extrapolated using the calibration curve generated.

2.4.2 Preparation of the gel

The desired quantity of protein was mixed with water and 6X Laemmli buffer (Merck) in 20 µL solutions. The mix was incubated for 5 min at 95°C and then let cool down at RT for 10 min.

Before loading, the suspension was mixed and briefly centrifuged. Then, 20 µL of cell suspension was loaded per well of NuPAGE™ 4-12% Bis-Tris Protein gels (Thermo). The gel was embedded in SDS Running buffer solution (**Appendix I**) and was run for 2.5 h at 100 volts (V) using a PowerPac basic (Biorad).

2.4.3 Membrane transfer and immunoblotting

After the gel run, a piece of PDVF membrane (Maine Manufacturing LLC, USA) with the same size of the gel was cut and activated by incubating in methanol (Merck) for 3 min. After that, a sandwich composed of (in order): sponge, blotting paper, gel, PDVF membrane, blotting paper and sponge was put together. The sandwich was mounted on a cassette and transferred in Transfer buffer (**Appendix I**) for 1.5 h at 100 V at 4°C. The membrane was then blocked for 2 h with blocking solution (**Appendix I**) at RT while shaking. After that, the membrane was incubated in primary antibody solution (diluted in blocking solution) overnight at 4°C while rotating. The next day, the membrane was washed five times with TBS-T solution (**Appendix I**) and incubated with an appropriate secondary antibody solution for 1 h at RT while rotating. The membrane was washed three times with TBS-T and then incubated with Immobilion HRP substrate (Millipore, USA) solution for 5 min. The proteins were detected using Hyperfilm™ ECL™ (Merck) developed in the ECOMAX X-ray processor (ClassicXRay, USA). Information on the antibodies used can be found in **Table III.2** of **Appendix III**.

2.5 Flow cytometry (FCM) and immunostaining

2.5.1 General extracellular staining

Adherent cells were harvested by trypsinisation, whereas in the case of suspension cells, the desired number of cells were simply collected. Cells were centrifuged at 300x *g* for 5 min and resuspended in PBS + 2% FBS. Antibodies were added at x µL of antibody (see **Appendix III**) per $1x10^6$ cells in 50 µL of staining solutions. The staining solutions were usually PBS + 2% FBS + γ-Human globulins from Cohn fraction II, III (HAG, Merck, at 1:5 final dilution from a 20 mg/ml of stock), unless two or more Brilliant Violet (BV) fluorochrome-conjugated antibodies were used in the same master mix, in which case the staining solution was the BV staining buffer (BD Biosciences, USA). The list of antibodies used in this study are summarised in **Table II.7** of **Appendix III**. Cells were incubated with the desired antibodies for 30 min at 4°C in the dark. After staining, the cells were washed with PBS + 2% FBS, then resuspended in PBS + 2% FBS + 4′,6-diamidino-2-phenylindole (DAPI, Thermo, at 1:2000 final dilution from a 2 mg/mL of stock) and were kept on ice until analysis. Samples were acquired on a BD LSRFortessa™ Flow cytometer (BD Biosciences) and analysis was

performed using the FlowJoV10 (software (FlowJo LLC, USA). Manual compensation was performed by using single-stained samples for each fluorochrome used in the experiment. Compensation was performed by adjusting the median fluorescence intensity (MFI) of each fluorochrome against that of all other fluorochromes used in the experiment. As seen on **Figure 2.2**, when analyzing a sample only stained with an antibody conjugated to the APC-Cy7 fluorochrome, there was spillage of signal into the PE-Cy7 channel. Therefore, using the compensation matrix, this spectral overlap was discounted. This was performed for all fluorochromes until each is properly compensated against all others. For all analyses, at least $1x10^4$ events were recorded. For immunophenotypic characterisation of stem/progenitor cell populations $2.5x10^5$-$5x10^5$ events were recorded.

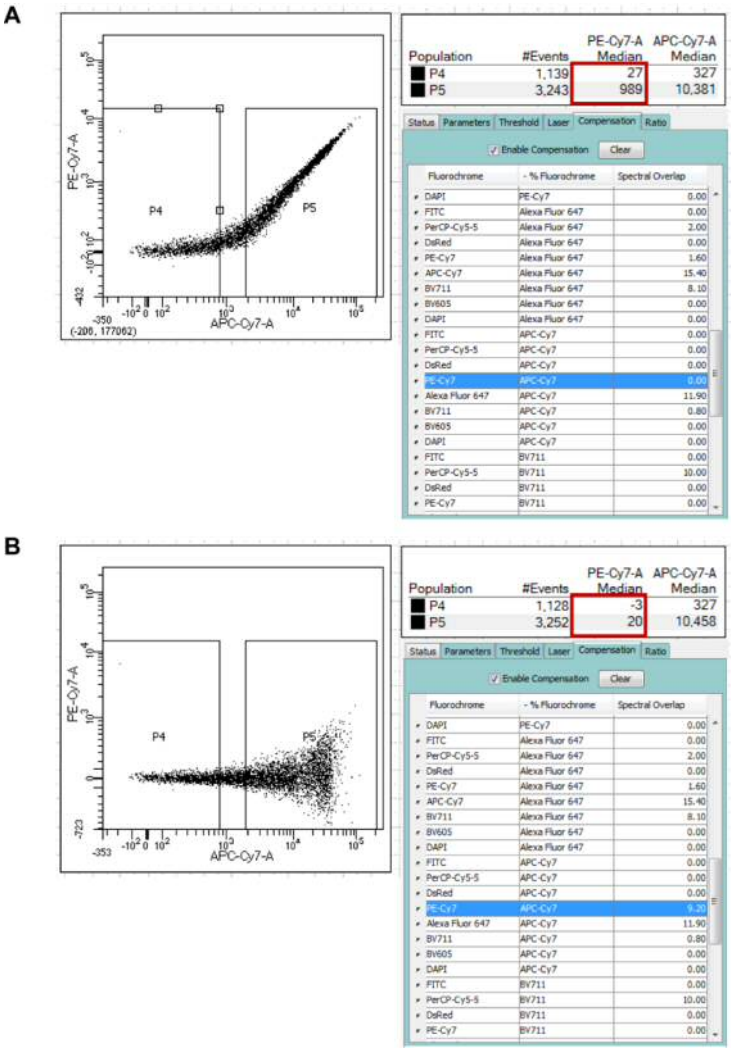

Figure 2.2 – Compensation strategy. Dot plot and MFI values of an APC-Cy7-conjugated single-stained sample plotted against PE-Cy7 (A) before and (B) after compensation. In (A), population P5 has an MFI of 989 for PE-Cy7, compared to population P4 with an MFI of 27. After applying compensation (B), the MFI of P5 was reduced to similar MFI levels of P4 before compensation, to discount spill over. In this example, the spectral overlap was 9.2.

2.5.2 Quantifying of apoptosis by Annexin-V staining

To quantify the degree of apoptosis, the cells were harvested and washed twice with PBS to remove traces of serum. These were then resuspended in 1X Annexin V binding buffer (BD Biosciences). Then, 5 µL of recombinant AnnexinV-APC (Biolegend, USA) was added per tube in 100 µL staining solutions and incubated for 15 min at RT in the dark. Then, 300 µL of 1X binding buffer containing DAPI (1:2000) was added to each tube and analysed by FCM. To quantify apoptosis, cells were gated using FSC-A and SSC-A. Early and late apoptotic events were distinguished using Annexin-V and DAPI staining (**Figure 2.3**).

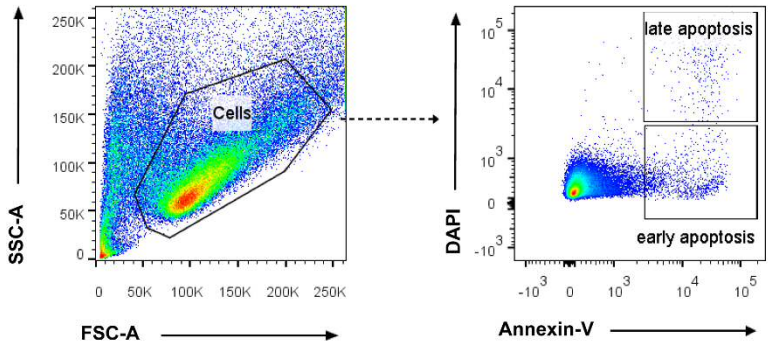

Figure 2.3 – Analysis of apoptosis by FCM. For analysis, the cells were gating using the forward scatter and side scatter parameters, and apoptosis was quantified by using DAPI and Annexin-V. Early apoptotic events are Annexin-V$^+$DAPI$^-$ while late apoptotic events are Annexin-V$^+$DAPI$^+$.

2.5.3 Intracellular staining

The methods described in this section had already been optimised and performed by António de Soure, a former student in the lab. The whole procedure was performed in 15 mL tubes. When necessary, cells were stained for extracellular surface antigens first. Cells were then washed once in PBS and resuspended in 500 µL PBS at a density of 1x10^6 cells/ml. Then, 500 µl of 4% methanol-free formaldehyde (PFA; TAAB Laboratories, UK) were added and cells were fixed at RT or at 37°C for 10 min and then washed with PBS and centrifuged at 300x *g* for 10 min. Cells were resuspended in 250 µL PBS then 250 µL of 0.2% Triton X-100 solution (Merck; made in PBS) were added. Then, cells were permeabilised at RT for 10 min and afterwards washed by filling up the tube with PBS and 1 mL of FBS and centrifuged at 300x *g* for 10 min. Fixed/permeabilised cells were then resuspended in a desired volume of PBS + 2% FBS (50-100 µL) and each sample was divided into different tubes depending on the preferred number of testing conditions but each containing ~2.5x10^5 cells in 25 µL. Cells were incubated with primary intracellular antibodies (2 µL of each antibody) at 4ºC for 1 h, washed, then stained with appropriate secondary antibodies (0.25 µL) in the same staining

conditions. Following staining washes, cells were then resuspended in PBS + 2% FBS containing DAPI (1:200). For the quantification of the activated forms of Notch1 and Notch2, samples were acquired in an Amnis® ImageStream® (Luminex, Austin, TX, USA) image flow cytometer and analysed using the IDEAS® softwarea FCM and analysis was performed as described above in section **2.5.1**. As for determining the percentage of cells with a nuclear-translocated Notch4 receptor, the cell nucleus was stained with a DAPI solution (final concentration of 1.6 ng/mL), samples were acquired on an ImageStream® (Amnis®) and analysis performed using the IDEAS® software.

2.6 Fluorescence activated cell sorting (FACS)

All cell sorting was performed in a BD FACSAria™ Fusion (BD Biosciences) and using the BD FACSDiva™ software (BD Biosciences). Cells were prepared in the same way as for FCM analysis. All cells were sorted into PBS + 2% FBS + 1% P/S. After sorting, cells were centrifuged and resuspended in their respective complete growth medium.

2.7 Generation of lentiviral particles and viral transductions

2.7.1 Production of lentiviral particles

Lentiviral particles were produced using the calcium phosphate transfection method. Briefly, 10^7 HEK293LTX cells were seeded on 15 cm^2 dishes in complete DMEM. The next day, the medium was replaced by Opti-MEM (Merck) + 2% FBS without antibiotics and 2 h later the cells were transfected. The transfecting particles were produced by mixing the pMD2G plasmid (envelope), pCMVdR8.74 plasmid (packaging) (a kind gift from Dr. Didier Trono; École Polytechnique Fédérale de Lausanne) and the transfer vector of interest at a 1:1:2 molar ration, respectively, in tissue culture-grade water. Then, 122 µL of $CaCl_2$ (2.5M) were added to the mix dropwise followed by 1250 µL of 2x HEPES (Merck) dropwise topping up to 2500 µL volume solutions, while mixing mildly. The mix was incubated for 10 min at RT and then added to the cells. After 8 h, the medium was replaced by Opti-MEM + 2% FBS + 1% P/S (Thermo) + HEPES (25 mM) (Merck). The viral supernatant was collected 48 h post-transfection.

2.7.2 Concentration of lentiviral particles

The lentiviral particles were concentrated by collecting the viral supernatant and centrifuging for 5 min at 300x *g* at 4°C to remove cells and debris. The supernatant was then filtered through Millex-HV syringe filter units (0.45 µm; Merck) and concentrated by ultracentrifugation for 2.5 h at 4°C at 90,000x *g*, in thin-wall polypropylene conical tubes (Beckman Coulter, USA)

using an Optima™ XPN-80 Ultracentrifuge (Beckman Coulter), with the SW32Ti rotor (Beckman Coulter). Following ultracentrifugation, the supernatant was discarded, and the pellet of viral particles was resuspended in the appropriate medium (same growth medium for the cells to be transduced). After a 2 h incubation period on ice, the suspension was then collected and aliquoted at -80°C until further use.

2.7.3 Determination of virus titres

To determine viral titres, HeLa cells were seeded at $5x10^4$ cells/cm^2 on 24-well plates in complete DMEM. After 8 h, virus solutions were centrifuged for 3 min. Then, the cells were infected with various dilutions of the viral suspension. HeLa cells were incubated at 37°C and analysed 3 days post-transduction by FCM to quantify the percentage of transduced cells. The viral titre was calculated using the formula:

$$\textit{virus titre (TU/ml)} = \frac{\textit{[\%GFP] x [dilution factor (eg 1000)] x [no of cells (ie } 5x10^4\textit{)]}}{100}$$

2.7.4 Lentiviral transduction of cell lines

For transduction of adherent cell lines, cells were seeded at $2.5x10^4$ cells/cm^2. After 8 h, cells were infected at a multiplicity of infection (MOI) of 10. Cells were then incubated with virus overnight and the next day were washed with PBS + 2% FBS + 1% P/S to remove viral particles. Fresh complete media was then added. The AML cell lines used were diluted to a cell density of $3x10^5$ cells/mL 1.5 days before transduction. Cells were recounted before lentiviral was added at a MOI of 10. Cells were then incubated with virus overnight and the next day were washed with PBS + 2% FBS + 1% P/S to remove viral particles. Suspension cells were then resuspended in a 1:1 mix of fresh complete RPMI medium and conditioned RPMI (from growing cells) to help recovery.

2.7.5 Generation of Notch reporter AML cell lines

Following the above the protocol, cells were then cultured for several days until enough numbers of cells were achieved for positive selection using FACS. For this, cells were washed with PBS + 2% FBS + 1% P/S and then stained with anti-CD271-AF647 antibody (5 µL of antibody/$1x10^6$ cells) for 30 min at 4°C in the dark. After this time, cells were washed and resuspended in PBS + 2% FBS + 1% P/S + DAPI (1:2000) and sorted for $NGFR^+$ cells by FACS. After sorting, cells were resuspended in complete RPMI and cultured for several days,

until enough numbers were reached for freezing down. To generate Notch reporter AML cell lines with sh*Luc* or sh*NOTCH1* or sh*NOTCH2*, the various Notch reporter AML cell lines were transduced with the respective lentivirus as above (the latter two constructs were generated/validated by a colleague, Joana Carmelo in the lab). Cells were then cultured for several days until enough numbers of cells were achieved for GFP selection using FACS as described. After sorting, cells were resuspended in complete RPMI and cultured for several days, until enough numbers were reached for freezing down.

2.8 Human primary cells

2.8.1 Isolation and culture of CB-derived human HSPCs

Human CB/CB-MNCs were obtained from different sources (Anthony Nolan Cord Blood Bank, Stem Cell Technologies and The Royal London Hospitals) and were obtained after informed consent approved by their respective local ethical committees and the Declaration of Helsinki. HSPCs were isolated mostly from frozen cord blood mononuclear cells (CB-MNCs) and at some occasions from fresh CB. Briefly, CB-MNCs from fresh CB was obtained by transferring the blood to a T175 flask and diluting at 1:3 ratio with PBS. Then, 15 mL of Lymphoprep™ (Stem Cell Technologies, Canada) were added to a 50 mL Falcon™ tube. The diluted blood was then added carefully on top of the Lymphoprep™ at an angle. Two parts blood were added to one-part Lymphoprep™. The mix was centrifuged for 30 min at 20°C at 550x *g* with the brakes of the centrifuge on the "Off" position. After centrifugation, 3 distinct layers could be seen: a top layer of serum, a bottom layer of red blood cells and a thin middle layer containing the MNCs. The MNCs layer was carefully harvested by using a transfer pipette (Fisher). Collected MNCs were then diluted 1:2 with PBS and centrifuged at standard speed for 7 min at 5°C. The supernatant was discarded, and the pelleted cells were all pooled together into a new 50 mL falcon tube with PBS (enough to wash all tubes used). Next, 15 mL ammonium chloride solution (NH_4Cl) (Stem Cell Technologies) were added to the cell suspension (approximately 3 to 4 volumes of cell suspension). The mix was incubated at 4°C for 7 min to lyse red blood cells. Then, 2 mL of FBS were added balance osmolarity, and PBS was then added to top up the solution. Cells were centrifuged, resuspended in PBS + 2% FBS and counted. Cells were used right away or frozen in FBS containing 10% DMSO.

Frozen CB MNCs were thawed at 37°C, washed once with PBS + 2% FBS, centrifuged at 300x *g* and counted. $CD34^+$ cells were selected using the EasySep™ Human CD34-positive selection kit (StemCell™ Technologies) according to manufacturer's instructions. Briefly, cells were resuspended in 1 mL PBS + 2% FBS at 1-5x10^8 cells/mL, to which 100 µL of $CD34^+$ selection reagent were added. The mix was incubated for 10 min at RT. Then, 50 µL of

magnetic particles were added and incubated for another 10 min. The tube was then placed into the EasySep™ magnet for 5 min and the supernatant was discarded while in the magnet. An additional 2.5 mL of PBS + 2% FBS were added and a total of 4 rounds of selection were performed.

2.8.2 Sorting of $CD34^+CD38^-$ HSPCs

After $CD34^+$ cell selection, cells were counted, resuspended in 50 µL of PBS + 2% FBS and stained with anti-CD34-APC and anti-CD38-PE-Cy7 antibodies (5 µL of antibody/$1x10^6$ cells) for 30 min at 4°C in the dark. After washing with PBS + 2% FBS and resuspension in PBS + 2% FBS + 1% P/S + DAPI (1:2000), cells were filtered and the $CD34^+CD38^-$ cells were sorted as described in 2.6.

2.8.3 Culture of $CD34^+CD38^-$ HSPCs

After sorting, cells were pre-stimulated for approximately 16 h in a 96-well plate in StemSpan™ (Stem Cell Technologies) containing SCF 100 ng/mL, Flt3L 100 ng/mL, G-CSF 25 ng/mL, IL-3 10 ng/mL and IL-6 10 ng/mL (all from Peprotech, USA), 1% P/S and HEPES (10 mM) (Merck). After this period, HSPCs were transduced at a MOI of 50 with the respective lentiviral particles for 10-12 h. Then, a few drops of FBS were added to the cells to inactivate the viral particles. Then, cells were washed three times with PBS to remove excess of viral particles and serum and resuspended in StemSpan™ containing SCF 300 ng/mL, Flt3L 300 ng/mL and TPO 20 ng/mL, 1% P/S and HEPES (10 mM) for an additional 4 days. After the 4-day expansion period, GFP^+ HSPCs were sorted as described above. For expansion of primitive cells after lentiviral transduction, HSPCs were cultured with the latter condition and cultures were divided at 1:2 to 1:4 ratios every 3 days for 12 days.

2.8.4 Long-term culture initiating-cell (LTC-IC) assay

The MS5 stromal cell line was cultured in complete αMEM for three passages before use. T96-well plates were coated with collagen (StemCell Technologies) at 0.3 mg/mL for 1 min. Collagen solution was then removed from the wells, which were then left to dry for 1 h. Next, the wells were washed with PBS twice to neutralise the collagen pH before use. Then, MS5 cells were seeded at a density of 3000 cells per well in Iscove's Modified Dulbecco's Medium (IMDM) (Merck) supplemented with 10% FBS and 1% P/S (complete IMDM). Two days later, MS5 cells were irradiated at 6.8 Gys (Grays; using a ^{137}Cs source). After irradiation, cells were incubated for at least 8 h at 37°C to allow for recovery, time after which the medium was replaced by MyeloCult™ H5100 medium (StemCell Technologies) + 1% P/S. Following

sorting, GFP^+ HSPCs were resuspended in complete IMDM medium, and various cell quantities were dispensed on top of the MS5 feeder layer. On average 5 to 15 wells were used per cell dose in one independent experiment. Co-cultures were maintained in MyeloCult™ H5100 medium + 1% P/S for a total of 5 weeks with weekly half-medium changes. By the fourth week of the co-culture, CAFCs could be observed as exemplified in **Figure 2.4**. Only large colonies of >50 densely packed haematopoietic cells were counted in each condition.

Figure 2.4– A cobblestone-area at week 4 of LTC-IC co-culture of human HSPCs and MS5 stromal cells. Highlighted in red, two large colonies of packed haematopoietic cells form cobblestone-resembling patterns.

2.8.5 Colony-forming unit (CFU) assay

At the end of the 5-week co-culture, both human HSPCs and murine MS5 stromal cells were harvested by trypsinisation. For this, the supernatant was also collected prior the harvest of the adherent fraction. Then, both non- and adherent fractions were mixed together. Depending on the number of wells per cell dose used in each experiment, the collected cells were resuspended in an equivalent volume of 100 µL complete IMDM/well. Then, 100 µL of this mix were added to 1 mL of MethoCult™ H4435 (StemCell Technologies) + 1% P/S. The mix was briefly vortexed to ensure proper distribution of the cells. Then, the mix was dispensed into two wells of a 12-well plate. Cultures were maintained for a total of 2 weeks, time after which the colonies were counted.

2.8.6 Immunophenotypic characterisation of LTC-IC cells

The information of the antibodies used in this study can be found in **Table III.1** of **Appendix III**. At the end of the 5-week co-culture period, cells were harvested as described above. After washing, cells were resuspended and a fraction of the cells was incubated with the HSPC panel of markers (CD34, CD38, CD90, CD45RA, CD135) and another fraction with the differentiated cell panel of markers (CD34, CD14, CD19, CD33, CD56 and CD11c). Another fraction of cells was incubated with Rabbit IgG isotype control-PE or Nicastrin-PE (dilution 1:4) antibodies to assess the knockdown levels of Nicastrin. In all the staining conditions, 5 µL of each crude or diluted antibody was used and stainings were performed as depicted in section 2.4.1.

2.8.7 Immunophenotypic characterisation of AML cells

Before immunophenotypic characterisation, samples were depleted of Annexin-V$^+$ cells using the Annexin-V MicroBead kit (Miltenyi Biotec, Germany). For this, AML primary samples were thawed at 37°C, added to PBS + 2% FBS and centrifuged at 300x *g* for 10 min. After two additional washing steps with PBS, cells were then resuspended in 1X Annexin-V binding buffer at 80 µL/10^7 cells. Annexin-V beads were added at 20 µL/10^7 cells and the mix was incubated for 15 min at 4°C. After this step, 2.5 mL of 1X Annexin-V binding buffer were added and magnetic separation was carried out by placing the tube into the EasySep™ magnet for 5 min at 4°C. The supernatant (containing live cells) was collected and the magnetic separation process was repeated for a total of 4 times. At the end, cells were washed and resuspended in PBS + 2% FBS. Next, 4x10^6 cells were stained with a panel of antibodies containing 20 µL of each anti- CD34, CD38, CD90, CD45RA and CD99 antibodies. Then, the whole mix was divided into 4 tubes to assess the expression of single Notch receptors. For this, different fractions of cells were stained separately with anti-Notch1-PE (5 µL/1x10^6 cells), Notch2-PE (5 µL/1x10^6 cells), Notch4-PE (2,5 µL/1x10^6 cells) or the mouse IgG isotype control-PE (10 µL/1x10^6 cells). The remaining staining protocol can be seen in section 2.4.1 Detailed information on the antibodies used is listed in **Table III.1** of **Appendix III**.

2.8.8 Activation of Notch signalling using ligand-overexpressing stroma

S17 and S17-Delta4 stromal cells were cultured in complete αMEM and passaged three times before use. For the co-culture assay, each stromal cell line was seeded at 2x10^4 cells/cm^2 on 24-well plates. All the AML cell lines used were resuspended in complete αMEM and added to stromal cells at 2.5x10^4 cells/well.

2.8.9 Testing small molecules interacting with Notch signalling

A collaboration with Professor Andrea Brancale at the School of Pharmacy of Cardiff University was setup, aiming to obtain candidate small molecule agonists of Notch signalling. The methods described in this section have been performed by the Master student Julija Jotautaite, who was a member of the Brancale's research group. Briefly, virtual screening is a computational docking technique which screens libraries of small molecules to identify those with highest probability of binding to a given target. This can be done via structure-based virtual screening, which uses the 3D structure of the target to find cognate partners, whereas ligand-based virtual screening uses the 3D structure of the ligand to filter a library of small molecules. No three-dimensional information on Notch2-4 exist. Therefore, the crystallised 3D structures of Notch1 EGF11-13 region (code 2VJ3) were used along with that of Jag1 DSL and EGF1-3 region (code 2JV2) (obtained from RCSB protein data bank (www.rcsb.pdb.org)) to obtain a model of the Notch1/Jag1 complex, which the docking procedure could use to screen potential ligands. A total of 3,300,000 compounds available from libraries were virtually screened between the structure-based and ligand-based virtual screening techniques. A series of molecular docking filters using different docking scoring functions were applied. The best scoring compounds were then visually inspected for their ability to interact and occupy with the selected binding site (i.e. number of hydrogen bond formations, hydrophobic interactions, etc.). Compliance with Lipinski's rule of five (which determines the likeliness that a chemical compound can be used as an orally active drug in humans) (Lipinski *et al*., 2001) and absence of potential toxic groups, further reduced the number of compounds, generating a final selection of 177 molecules as potential binders of Notch. Of those, 19 compounds were purchased for biological evaluation, and 6 of those were evaluated in our lab **(Table IV.1 of Appendix IV).**

All the small molecules were reconstituted to either 50 mM or 25 mM, depending on their solubility in DMSO. Small molecules were added to the culture medium at a concentration of 10 μM. In some testing conditions, the Notch inhibitor CompE (Merck) was added at a final concentration of 2 μM 2 h prior treatment with the drugs to ensure blocking of Notch receptor cleavage.

2.8.10 Activation of Notch signalling with Jag1 based peptide

The CDDYYYGFGCNKFCRPR Jag1 peptide (Genscript, USA) was reconstituted to 5 mg/mL in 1:1 water:DMSO and stored at -20°C. The Jag1 peptide was added to the culture at the final concentration mentioned in the text. In some testing conditions, the Notch inhibitor CompE was added at a final concentration of 2 μM 2 h prior treatment with the Jag1 peptide to ensure blocking of Notch receptor cleavage. Treated cells were analysed 48 h after Jag1 treatment.

2.9 *In vivo* analysis of HSPCs

2.9.1 Xenotransplantation of HSPCs into NSG mice

Due to the lack of an appropriate animal facility at Cardiff University to breed the number of pathogen-free immunodeficient mice required for this project, both the animal adoptive transfer and the schedule-1 sacrifice procedures were performed by Dr. Fernando dos Anjos Afonso at The Francis Crick Institute in London. All the animal procedures were performed in accordance with the UK Home Office regulations after The Francis Crick Institute ethics committee approval.

NSG mice aged 8-12 weeks were sub-lethally irradiated at 3.75 Gy (^{137}Cs source) up to 24 h before tail vein injection of cells. For experiments of pan-Notch inhibition, 5000 FACS purified $CD34^+CD38^-$ HSPCs were transplanted. Six to seven weeks post-transplant mice were randomly split into two groups: one group received 5 doses of α-secretase IX (DAPT; 12 mg/Kg; Tocris Bioscience, UK), and another group received vehicle (DMSO), all dissolved in oil. Mice were intra-peritoneally injected every other day. Five and a half weeks later, the recipients were sacrificed, and their BMs analysed. To test the cell-autonomous Notch inhibition, 3800-5000 FACS purified GFP^+ HSPCs were injected into the tail vein of sub-lethally irradiated NSG mice. After 12 weeks the recipients were sacrificed, and their BMs were harvested and analysed.

2.9.2 Immunophenotypic characterisation of engrafted cells

To analyse the bone marrow content of transplanted animals, three pairs of bones (tibiae, femurs and ileum) from NSG mice were flushed with 1 ml PBS + 2% FBS several times until the marrow had a white appearance, indicating successful removal of the marrow. Cell suspensions were submitted to red blood cell lysis by adding two times the initial volume of NH_4Cl. The mix was incubated for 3 min at RT. Then, a few drops of FBS were added to balance the osmolarity, and the mix was centrifuged. Cells were resuspended in 200 µL of PBS + 2% FBS and their numbers were determined. In the experiments with DAPT, to quantify the level of human myelo-lymphoid engraftment, a fraction of the cell suspension (containing $5x10^5$ to $1x10^6$ cells) was stained with anti-CD45, CD19 and CD33 antibodies. In the experiments injected with GFP^+ HSPCs, cells were stained with the differentiation cell panel markers (anti- CD34, CD11c, CD19, CD33 and CD14 antibodies). Human engraftment was quantified as the proportion of live cells that were $CD45^+CD33^+$ and $CD45^+CD19^+$. For immunophenotypic characterisation of engrafted immature populations in mice, cells were also stained with a panel of antibodies to detect different HSPC fractions (anti- CD34, CD38, CD90, CD45RA, CD10, CD135, CD62L and Lineage). Staining conditions can be seen in the

section 2.5.1. Dead cells and debris were excluded from the analysis and the maximum number of lived effects were acquired.

2.10 Statistical analysis

All statistical analyses were performed using the Prism8 software (Graphpad, USA). Unpaired t-tests were used for the analyses. Statistical analysis of all engraftment data was performed by using the Mann-Whitney test, as the values within the groups being compared cannot be assumed to be normally distributed. The level of significance used was: *$p<0.05$, **$p<0.005$ and ***$p<0.0005$.

Chapter 3 - Exploring the effects of pan-Notch inhibition in human HSPCs

3.1 Brief introduction

Beyond the divergent data in mice discussed in **Chapter 1**, only recently some light has been shed on the role of Notch pathway in human HSCs *in vivo*. Similarly to Maillard *et al.,* (Maillard *et al*., 2008), Benveniste and colleagues showed that human HSPCs have different requirements for Notch *in vitro* and *in vivo* (Benveniste *et al*., 2014). Specifically, stem cells seem to depend more on Notch signals *in vitro*, as it was shown by the blockade in T cell development and HSC maintenance/expansion *in vitro*, while only T cell lineage specification was impaired in transplanted Notch-inhibited HSCs *in vivo* (Benveniste *et al*., 2014). In contrast, Bhatia's group showed that HSCs with superior regenerative and self-renewal capacity tend to localise to endosteal regions of the trabecular bone area (TBA) (Guezguez *et al*., 2013). These HSCs have distinct molecular activation enriched with Notch signalling signature compared to HSCs localising in the long bone area (LBA). Particularly within the TBA, phenotypic human HSCs and HPCs preferentially locate in the endosteal over vascular regions. The authors of this work also showed that osteoblasts from the TBA have increased expression of Notch ligands Jag1, Jag2, and Delta4 compared to osteoblasts from the LBA, consistent with the HSC activation profile (Guezguez *et al*., 2013). Of interest, a three-fold higher proportion of osteoblasts expressing Jag1 ligand was detected in the TBA compared to the LBA. Additionally, Jag1-binding HSPCs were found to have higher CFU capacity and repopulating capacity. Upon Notch inhibition with DAPT treatment *in vivo*, total human engraftment and HSPC numbers were not affected in the LBA, whereas there was a significant reduction in the TBA, suggesting that only this region is sensitive to Notch inhibition (Guezguez *et al*., 2013). These observations support a critical role of Notch signalling in human HSC regulation through interactions with specific bone marrow niche cells.

As still little is known on the importance of the Notch pathway in regulating human HSC and HPC functions, the aim of this chapter is to establish the role of Notch signalling by first employing pharmacological inhibition of the pathway using the well-known γ-secretase inhibitor DAPT and later by cell-autonomous shRNA-mediated knockdown of Nicastrin – a key member of the pathway and one of the few non-redundant members of the pathway Additionally, targeting *NCSTN* has been well documented to inhibit the Notch pathway (Klinakis et al., 2011).The use of shRNAs to silence genes of interest has been widely employed and has been greatly refined since its discovery (Hannon and Rossi, 2004), (Mohr and Perrimon, 2012). MicroRNA-30 can be excised from mRNA transcripts containing the 71 nucleotide miR-30a precursor and when is introduced into an expression plasmid is able to

strongly silence target transcripts (Zeng *et al*., 2002). In this work, we first attempted to employ a tailored miR-30 backbone's ability to be processed by the cells in order to silence genes of interest, along with the expression of fluorescent protein reporter genes (Fellmann *et al*., 2013). Aiming at addressing the role of Notch signalling in human HSPC, we started by characterising Notch receptor expression and activity in the different stem and progenitor populations and by challenging Notch-deficient HSPCs under rigorous assays *in vitro* and *in vivo*. Importantly, no studies on the potential role of non-canonical Notch signalling have been performed so far. Blocking Nicastrin will prevent both non-canonical and canonical Notch signalling. On the other hand, silencing of *RBPJ* only affects canonical Notch signalling, which will be discussed in **Chapter 4**.

Aims of Chapter 3

- Measure the expression levels of Notch receptors and their active domains in human HSPCs.
- Determine the impact of Notch inhibition in human HSPCs *in vivo* by using γ-secretase inhibitor DAPT on myelo-lymphoid engraftment and frequencies of stem/progenitor cells.
- Block pan-Notch signalling in HSPCs by using shRNA lentiviral vectors that inhibit the expression of *NCSTN* – a member of the γ-secretase complex.
- Assess *in vitro* effects of Notch inhibition by measuring colony-forming and differentiation capacity under the LTC-IC assay.
- Assess *in vivo* effects of Notch inhibition by measuring myelo-lymphoid engraftment and frequencies of stem/progenitor and mature cells.

3.2 Characterisation of the Notch signalling pathway in human HSPCs

As a first step, the Notch pathway activity in human HSPCs was characterised. To do this, the various sub-populations were defined through their immunophenotypic surface markers. As previously mentioned, the broad stem and progenitor cell compartment comprises a very heterogeneous population of cells. These can be divided into their respective self-renewal and differentiation potentials partially based on the expression of key surface markers. The immunophenotypic profile used was based on the work by Weissman's group (Majeti *et al*., 2007) and further adjusted by others (Notta *et al*., 2011) and is illustrated in **Figure 3.1**.

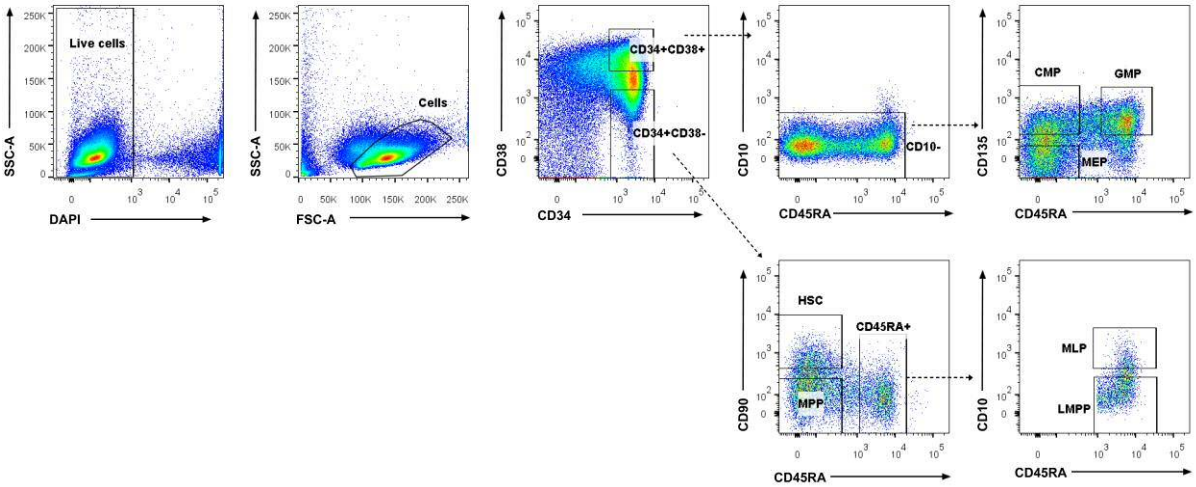

Figure 3.1 – Gating strategy for HSPCs. Within the $CD34^{+}CD38^{+}$ compartment, $CD10^{-}$ cells are selected, which can be separated into CMP, GMP or MEP based on CD45RA and CD135 expressions. Within the $CD34^{+}CD38^{-}$ sub-population, HSCs and MPPs can be divided based on their CD90 and CD45RA expressions. The $CD45RA^{+}$ cells can further be portioned into MLP or LMPPs based on CD10 surface expression. FSC-A – Forward scatter-area; SSC-A – Side scatter-area.

By first selecting live cells and excluding cell debris, a subset of $CD34^{+}CD38^{+}$ cells can be subdivided into the CMP, GMP and MEP compartments based on their CD135 and CD45RA expressions. Conversely, within the $CD34^{+}CD38^{-}$ fraction, HSC, MPP and MLP/LMPP populations can be found based on CD90 and CD45RA expressions. MLPs and LMPPs can be further fractionated based on CD10 expression. This is the gating strategy that will be followed throughout the entire thesis unless specifically stated otherwise. To begin with, the extracellular expression of each Notch receptor was determined in the various primitive haematopoietic stem and progenitor cell compartments using FCM (**Figure 3.2**).

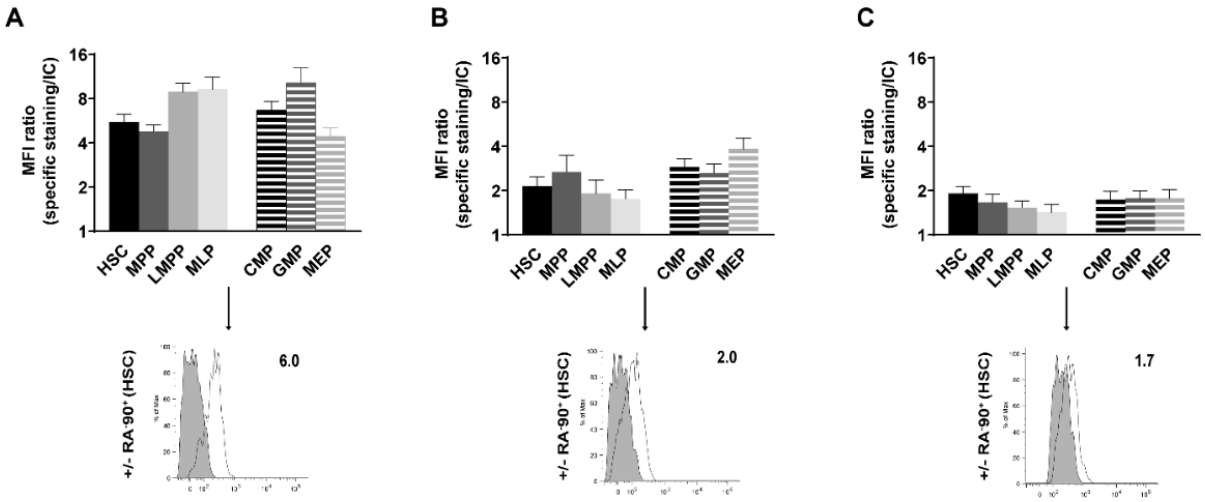

Figure 3.2 – Human HSPCs highly express Notch1 and Notch2 receptors. FCM analysis of surface Notch receptors. The surface expression of (A) Notch1, (B) Notch2 and (C) Notch4 receptors was evaluated for each CB-derived HSPC sub-population by determining the MFI ratio of each receptor (anti-Notch/isotype controls). Results are presented as the mean ± standard error (SD) (n=4-5).

All stem and progenitor cell populations were found to express Notch1 and Notch2 receptors but low/absent levels of Notch4 (**Figure 3.2**). The expression of the Notch3 receptor was not assessed, as previous studies have shown that this receptor is absent on human HSPCs (Anjos-Afonso *et al*., 2013). The sub-populations with the highest Notch1 expression were the CD45RA^{+} sub-populations (LMPP, MLP and GMP), while the lowest was observed for HSC, MPP and MEP fractions. As for Notch2 receptor, its highest expression was observed in the CMP and MEP sub-populations. Altogether, this reveals the different HSPC sub-populations have distinct Notch expression profiles, indicating that different signalling responses to Notch ligands might occur within the various populations. This contrasts with the mouse haematopoietic system, in which HSPCs mainly express low levels of Notch2 while the Notch1 receptor is almost absent (Oh *et al*., 2013).

Yet, cell surface expression of Notch receptors alone does not imply activation of the pathway. To fully assess its degree of activation, the cleaved forms of the Notch receptors, which are indicative of Notch activity, were assessed by FCM. For this, antibodies that detect the Notch intracellular domain of Notch1 and Notch2 specifically following the S3 cleavage were used. Importantly, these antibodies do not recognize the full-length Notch receptors, but rather their cleaved form. To determine the optimal staining conditions, each antibody was titrated using different cell lines or primary cells as positive and negative controls for the expression of each of the Notch receptors (conditions had already been established in the lab). Regarding Notch4, no antibody that specifically detects the cleaved form of this receptor was commercially available at the time of the experiments. To devise that, an antibody that detects the C-

terminus domain of Notch4 was used, and the percentage of translocation of N4-IC into the nucleus was measured using imaging flow cytometer ImageStream®X. N1-ICD, N2-ICD and nuclear Notch4 were present in all HSPC sub-populations (**Figure 3.3**), further supporting the notion that Notch is active in the broad $CD34^+$ HSPC pool and may play an important role in controlling HSC biology.

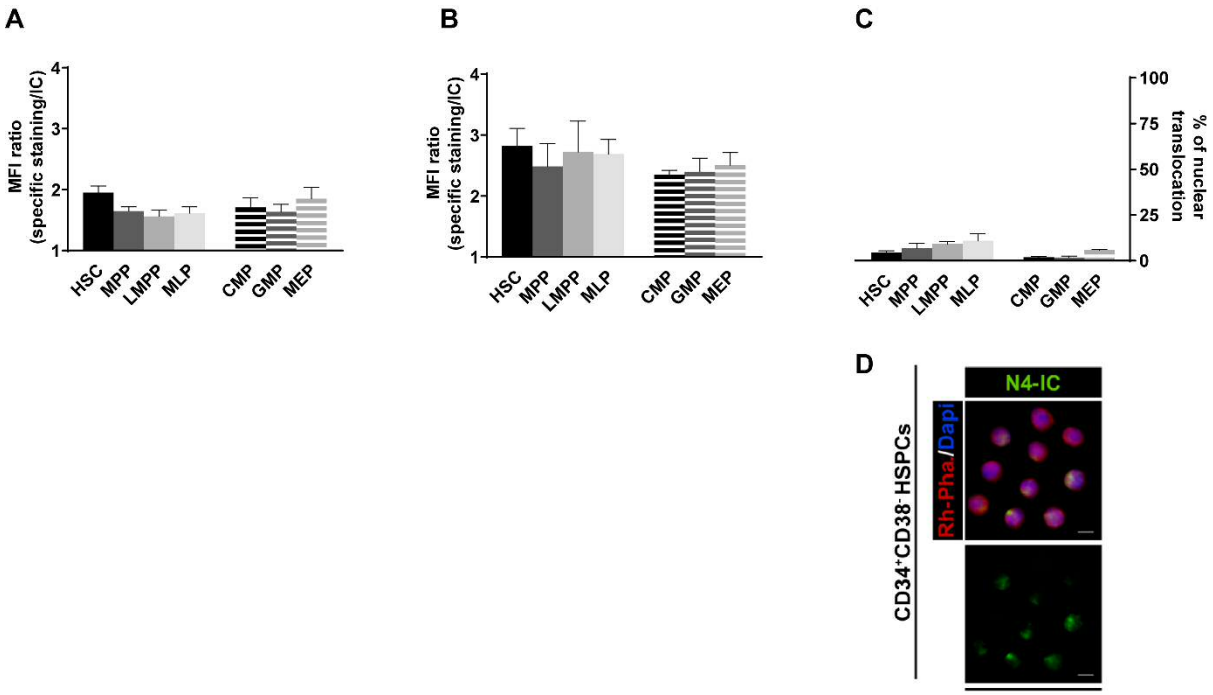

Figure 3.3 – Human HSPCs have Notch activity. The levels of activated (A) Notch1 (N1-ICD), (B) Notch2 (N2-ICD) and (C) the percentage of cells with nuclear-translocated of Notch4 receptor was also calculated (N4-IC) for each HSPC sub-population**,** (D) detection of intracellular Notch4. Scale bars 5μm. Results are presented as mean ± SD (n=4). Rh-Pha – Rhodamine Phalloidin. (Note: the nuclear-translocation of Notch4 experiments were performed by a former lab member – António de Soure).

Interestingly, all these populations appear to display a preferential level of Notch2 receptor activation. The reason for this has yet to be elucidated. However, some aspects of Notch regulation can be at play in this case. It is believed that different ligands have different affinities towards the different Notch receptors. For example, the Delta4 extracellular domain has an at least one order of magnitude higher affinity towards Notch1 than Delta1 does (Andrawes *et al*., 2013). Even though the nature of all possible interactions between the various ligand/receptor pairings has been the subject of much investigation, this remains a largely unclear aspect of Notch signalling biology. Nonetheless, it can be argued that this outcome can be explained if ligands with a higher propensity to interact with Notch2 are present in the niche. In addition to the well characterised activation of Notch through the *trans*-interaction of

ligands and receptors, *cis*-interaction leads to inhibition instead. Delta3 ligand appears to be unable to activate Notch in a *trans* fashion and instead, inhibits Notch when co-expressed on the same cell (Ladi *et al*., 2005). In addition, Notch ligands and receptors are susceptible to a great amount of post-translational modifications that modulate their responsiveness to one another (a great detailed review on the topic can be found on (Fortini, 2009)). The Fringe family of glycosyltransferases catalyses the elongation of O-fucose (a moiety added by Pofut-1 in mammals) by adding N-acetylglucosamines at specific EGF-like repeats on the Notch extracellular domain. Although best characterised in Drosophila, these have been shown to impact Notch activity in mammalian cells as well. Lunatic-Fringe (one of the Fringe family members) appears to enhance Delta-induced Notch1 signalling over Jagged-induced Notch1 signalling in C2C12 myoblasts and NIH3T3 cells. With these we can appreciate the additional layer of complexity that post-translational modifications impart in Notch signalling. To the best of our knowledge, no studies of the topic have been performed in human HSPCs, but it can be argued that these modifications probably occur in this system as well and might alter the responsiveness of the receptors to different DSL ligands.

A higher level of N1-IC was observed in HSCs when compared to other sub-populations, suggesting that this receptor may be particularly important in regulating this population. As for the activation of Notch2, the broad $CD34^{+}CD38^{-}$ HSPC fraction had higher N2-IC levels than the $CD34^{+}CD38^{+}$ HPC fraction, with a trend of higher expression in the most primitive HSCs (**Figure 3.3**). The Notch4 receptor was found to be minimally processed in $CD34^{+}$ HSPCs (**Figure 3.3**). Of note, this contrasts again with the very rare primitive $CD34^{-}$ HSCs which show a unique Notch4 expression and cleavage pattern (Anjos-Afonso *et al*., 2013). In summary, this data consolidates the idea that human $CD34^{+}$ HSPCs possess Notch activity, possibly relying on differential Notch receptor expression/activation for their regulation. Furthermore, at the technical level, it highlights the importance of assessing the extent of receptor cleavage in such sub-population, rather than solely relying on cell surface expression for a more complete appreciation of pathway activity.

3.3 Pharmacological inhibition of Notch leads to depletion of haematopoietic stem and progenitor cell fractions *in vivo*

To test whether the Notch signalling pathway plays a role in HSPCs *in vivo*, sub-lethally irradiated NSG mice were transplanted with 5000 FACS purified human $CD34^{+}CD38^{-}$ HSPCs. After six to seven weeks, DAPT or vehicle was administered to the animals five times every other day (**Figure 3.4 A**). The BMs of the recipients were analysed five and a half weeks post-

DAPT treatment (for a total of 12 weeks post-transplantation) (**Figure 3.4 B**). Notch was not inhibited at least six weeks after transplantation to ensure the adequate regeneration of the vascular endothelial system which is disrupted following irradiation (Lee *et al*., 2012) and is dependent on Notch signalling for regeneration (Krebs *et al*., 2000), (Kim *et al*., 2015).

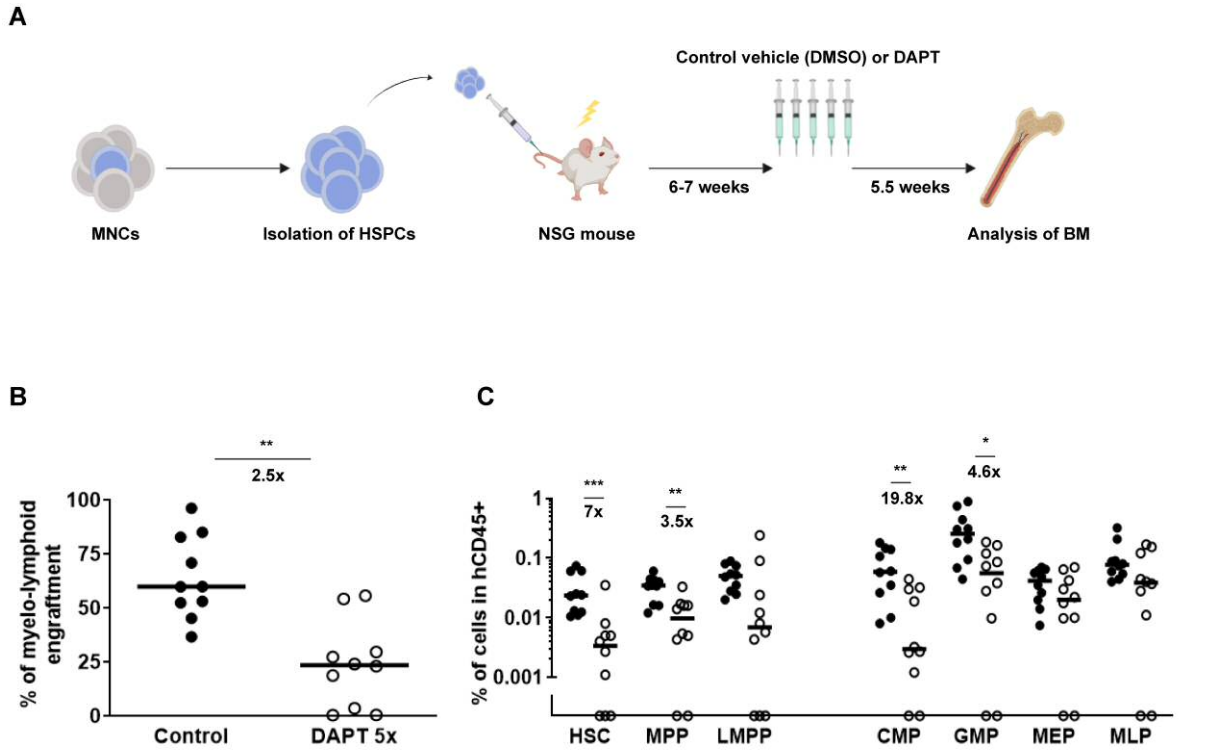

Figure 3.4 – Pharmacological inhibition of Notch signalling leads to depletion of stem and progenitor cells *in vivo*. (**A**) Schematic representation of the experimental workflow: sub-lethally irradiated NSG mice were transplanted with CB HSPCs. Six to seven weeks later, the animals were treated five times with DAPT (12 mg/Kg) or vehicle (DMSO) every other day. Five and a half weeks later, the animals were sacrificed, and their bone marrows were analysed. (**B**) Percentage of myelo-lymphoid engraftment at five and a half weeks post-transplantation. (**C**) Percentage of stem and progenitor cell compartments in the human cell fraction at five and a half weeks post-DAPT treatment. Each dot represents a mouse, and the bars the medians of the values. Median bars are shown (n=10). DAPT - N-[N-(3,5-Difluorophenacetyl)-L-alanyl]-S-phenylglycine t-butyl ester. Mann-Whitney test. *p<0.05; **p<0.005; ***p<0.0005.

Following transplantation, human HSPCs home to the BM, where they self-renew and begin the differentiation process into mature blood cells. The percentage of myelo-lymphoid engraftment represents the percentage of cells with B lymphoid ($CD19^+$) and myeloid ($CD33^+$) lineage that were generated. A 2.5-fold reduction in myelo-lymphoid engraftment was observed in the animals treated with DAPT when compared to vehicle-treated recipients (**Figure 3.4 B**). This indicates that Notch inhibition impaired stem and progenitor cell

repopulating and/or differentiation capacity. When examining the BMs for the presence of human haematopoietic stem and progenitor cells, an overall reduction in the frequency of many subsets of cells was observed (**Figure 3.4 C**). The major reductions occurred in the HSC and the CMP compartments, with a 7- fold and a 20-fold decrease in their frequency compared to the control cohort, respectively. Still, in general, all progenitors downstream of HSCs were affected albeit to different degrees. Of note, phenotypically defined MLPs ($CD34^+CD38^-CD45RA^-CD10^+$) commonly found in CB were not detected after engraftment in NSG mice. Instead, phenotypic MLPs generated after transplantation adopted an immunophenotype similar to human BM MLPs ($CD34^+CD38^+CD45RA^-CD10^-CD62L^+$) (Anjos-Afonso, personal observations). Hence, this phenotype was used to define human MLPs in NSG mice. As mentioned earlier, a previous study has reported a reduction in the total engraftment in mice transplanted with human Lin^- cells and treated with DAPT (Guezguez *et al*., 2013). Specifically, trabecular bone area (TBA)-HSCs in the BM which were particularly affected. $CD34^+CD38^-$ HSPCs from the TBA had decreased frequencies when Notch was inhibited, while $CD34^+CD38^+$ progenitors were expanded, which the authors attributed to a likely induction of differentiation from stem to progenitor cells (Guezguez *et al*., 2013). In agreement with this, we have found a significant reduction in myelo-lymphoid engraftment and HSC pool in DAPT-treated animals. On the contrary, we did not find an expansion in $CD34^+CD38^+$ cells. This disparity may be related to the timings of the analyses. Guezguez and colleagues analysed the BM 5 days following initial treatment. Following Notch induction, enforced release of HSCs from quiescence induces a rapid expansion of progenitors. In our setup, we have analysed BMs almost 6 weeks following Notch inhibition, time by which this initial expansion may have ended, and instead both stem and progenitor cell compartments suffered exhaustion of their respective pools due to Notch inhibition. Although these results strongly suggest that maintenance of physiological levels of Notch signalling in the BM is fundamental for haematopoietic homeostasis, we cannot rule out the possibility that the effects seen may in part be non-cell autonomous. To address this question, Notch signalling needs to be inhibited exclusively in HSPCs.

3.4 shRNA-mediated silencing of *NCSTN* in human HSPCs

3.4.1 Testing a miR-30-based shRNA system in human HSPCs

To study the potential functions of Notch signalling in human HSPCs, and to assess whether the previously observed effects were cell-autonomous, lentiviral vectors overexpressing shRNAs targeting the *NCSTN* gene were generated. *NCSTN*, encoding for the Nicastrin protein - a member of the γ-secretase complex, is responsible for the S3 cleavage of Notch

receptors (Bray, 2006). Even though the dominant negative form of MAML1 (dnMAML1) has been used in a few reports (Maillard *et al*., 2008), (Maillard *et al*., 2008), (Duncan *et al*., 2005) it only blocks canonical signalling. Furthermore, this protein has the potential to affect other non-Notch related pathways, as evidenced by its interaction and co-activator function of p53 (Zhao *et al*., 2007). On the other hand, a Nicastrin mutant that appears to act as a dominant negative protein has been reported (Klinakis *et al*., 2011). However, no other studies have validated the functionality of this mutant protein. Hence, a vector (pLV.EF1α-miRNA30-shRNA-GFP) was developed to express premiRNA30-shRNA and GFP reporter protein under the EF1α promoter. Embedding the shRNA into the context of endogenous miRNAs has been used to overcome saturation of endogenous miRNA pathways and to increase Dicer processing accuracy by using natural substrates in the miRNA biogenesis pathways (Gu *et al*., 2012). These structures can trigger potent knockdown and their efficacy has been shown for various miRNA backbones, including miRNA30, yielding less off-target effects (Fellmann *et al*., 2013). miR-30 based systems have been shown to trigger potent cognate mRNA knockdown in mammalian cells (Zeng *et al*., 2002), (Stegmeier *et al*., 2005). A similar system has also been reported to efficiently transduce murine LSK cells (Holmfeldt *et al*., 2016). More recently, a study took advantage of a different miR-30 based system to transduce human $CD34^+$ cells at high levels (Xiao *et al*., 2019). Cloning of the premiRNA30-shRNA sequence inside the EF1α intron allows it to be spliced out from the transcript. Following processing and stabilization, the reporter gene can be translated. The schematic representation of the construct used is depicted in **Figure 3.5**.

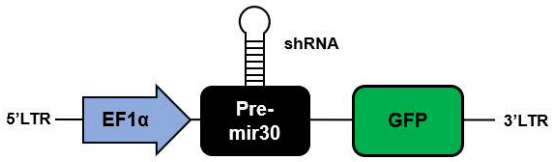

Figure 3.5 – Schematic representation of the pre-miR30 lentiviral construct. The EF1α promoter controls the expression of the shRNA embedded into the pre-mir30 intron and the GFP reporter protein.

In this system, the elongation factor alpha (EF1α) promoter drives the expression of the reporter GFP protein. Along with it, the shRNA embedded into the pre-miR30 backbone is generated through the processing of the pre-miR30 via the natural miRNA processing machinery found in the cells. To test this system, a shRNA sequence targeting the Luciferase gene (sh*Luc*) was used as a control (the Luciferase gene is only found in the common firefly and therefore this sequence has no targets in mammalian cells) and sequences targeting *NCSTN* (sh*NCSTN*) (listed in **Appendix II**) were cloned into the intermediate vector

(pECFPc1) using XhoI/EcoRI restriction sites. Then, those sequences, now flanked by the mirRNA30 backbone were then transferred into pLV.EF1α-miR30shRNA-GFP using BamHI/NheI restriction sites. The correct cloning of the different sequences was confirmed by plasmid sequencing. Lentiviral particles for the various constructs were produced as described in the **Chapter 2**. Next, HEK293T cells were transduced with the different pLV.EF1α -miR30-shRNA-GFP clones. After 8 days in culture, the cells were analysed by FCM to assess GFP expression, and afterwards, both protein and RNA were extracted. GFP expression was found in more than ~94% of the cells analysed after transduction (**Figure 3.6**).

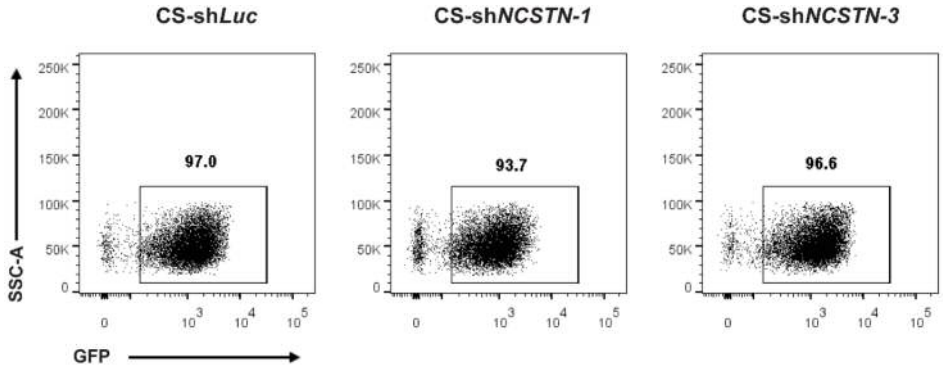

Figure 3.6 – HEK293T cells transduced with CS-shRNA constructs. HEK293T cells were analysed for their GFP expression 8 days post-transduction with CS-shRNA constructs.

Measurement of knockdown efficiency was carried out by assessing the decrease in the Nicastrin protein levels by Western-blotting (WB) and at the mRNA level by quantitative real-time PCR (qRT-PCR). A total of 7 shRNAs were tested for their ability to silence the *NCSTN* gene. The constructs termed sh*NCSTN-1* and sh*NCSTN-3* were found to be the most effective. For this reason, these two constructs were used for the remaining work. sh*NCSTN-1* and sh*NCSTN-3* resulted in a decrease of 58% and 57% of the Nicastrin protein, respectively (**Figure 3.7 A and B**) and 52% and 72% at the mRNA level, respectively (**Figure 3.7 C**).

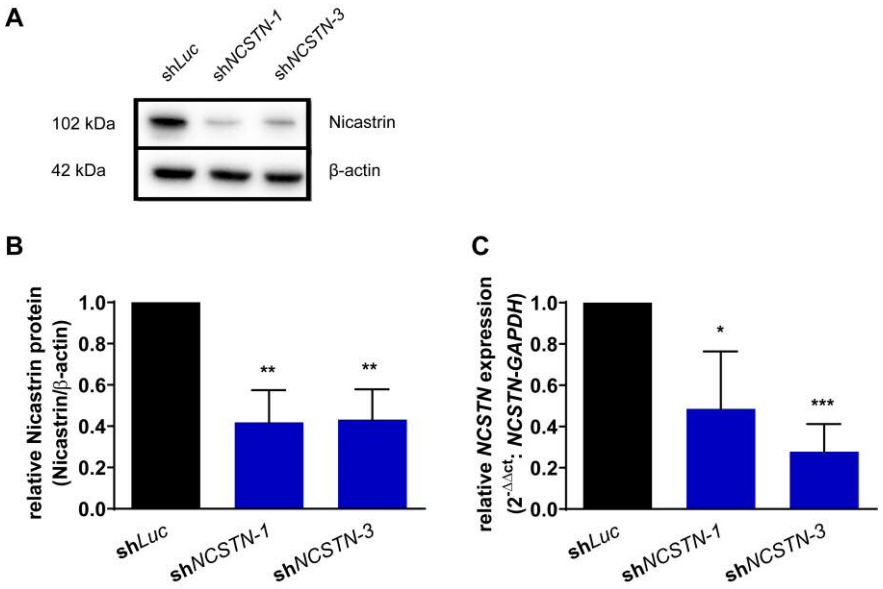

Figure 3.7 – shRNA-mediated knockdown of Nicastrin in HEK293T cells. (**A**) Representative WB of shRNA-mediated knockdown of the Nicastrin protein. Quantification of (**B**) protein and (**C**) mRNA knockdown of *NCSTN*. Results are the mean ± SD (n=4). Unpaired t-test. *p<0.05; **p<0.005; ***p<0.0005.

Following validation of silencing efficiency from these constructs in the HEK293T cell line, the clones were tested for their efficiency to silence their targets in human HSPCs. Firstly, HSPCs were isolated from CB MNCs. An initial round of $CD34^+$ cell selection was performed. $CD34^+$ cells were incubated with magnetic beads that possess affinity to the CD34 antigen. In this manner, the CD34-expressing cells were magnetically separated from the bulk of the population. Following this initial enrichment step, the cell suspension was stained with anti-CD34 and anti-CD38 antibodies conjugated to fluorochromes. The $CD34^+CD38^-$ fraction was then sorted by FACS. The sorted cells were pre-stimulated in serum-free StemSpan culture medium containing cytokines (SCF, FLT3L, G-CSF, IL-3 and IL-6) (Haylock *et al*., 1997), (Conneally *et al*., 1997). The cells were then transduced with the lentiviral constructs at a multiplicity of infection (MOI) of 50. The next day, the cells were washed to remove excess viral particles and were cultured for an additional four days in StemSpan containing a combination of high concentration of cytokines (SCF, FLT3L and TPO) that was demonstrated to maintain stemness (Arrighi *et al*., 1999), (Vanheusden *et al*., 2007). After the four-day expansion period, the HSPCs were sorted based on their GFP reporter protein expression by FACS. However, despite many attempts only maximum of ~9% of transduction efficiency was achieved (**Figure 3.8**).

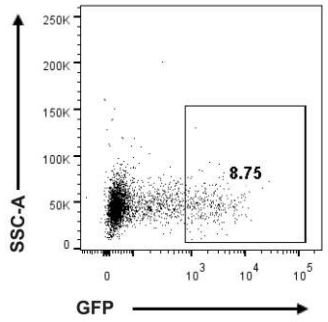

Figure 3.8 – miR-30 based shRNA lentiviral vector has low infectivity potential of human HSPCs. Representative dot plot of human CB $CD34^{+}CD38^{-}$ cells transduced with the miR-30 lentiviral vector at MOI 50. At day 4 post-transduction, the cells were analysed for their GFP expression.

Hence, even though miR-30 based strategies have been employed to transduce murine LSK cells (Wang *et al*., 2012), (Holmfeldt *et al*., 2016) and more recently human haematopoietic progenitor cells (Xiao *et al*., 2019) at high efficiencies, this reveals that this specific construct is not a good option for human HSPCs or may need further optimisation. Importantly, this miR-30 based system also inefficiently transduced HSPCs when shRNA sequences targeting different genes were used (data not shown), indicating that this is not exclusive to Nicastrin knockdown. At this point, a different shRNA-mediated silencing method was sought out to carry out the remaining work.

3.4.2 Silencing of *NCSTN* using an H1 promoter-driven shRNA system

To circumvent the previous issue, a system using the well-established H1 promoter-driven shRNA expression was utilised (Hannon and Rossi, 2004). The H1 promoter drives the expression of the shRNA sequence of interest while GFP is controlled by the EF1α promoter (**Figure 3.9**). The same sequences tested in the pre-miR30 system were used. The shRNA sequences were cloned into the pENTR4 plasmid. Afterwards, the pENTR4-H1 constructs now carrying the shRNAs, were recombined with the destination vector CS-RfA-EG by gateway cloning, generating the final products. HEK293T cells were once more used to assess knockdown potential.

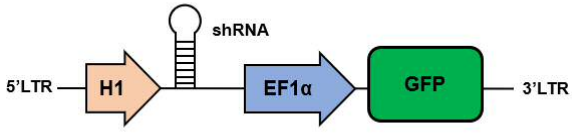

Figure 3.9 – Schematic representation of the CS-shRNA lentiviral construct. The H1 promoter drives the expression of the shRNA. The EF1α promoter controls the expression of the GFP reporter protein.

After transducing HEK293T cells with the various constructs, these were cultured for 8 days. At this point, the cells were analysed by FCM to measure GFP expression, and in parallel, both protein and RNA were extracted. GFP expression was found in more than 90% of cells analysed (data not shown) after transduction. A greater than 90% decrease in the protein (**Figure 3.10 A and B**) and mRNA (**Figure 3.10 C**) levels were observed for both sh*NCSTN*-1 and sh*NCSTN*-3. Following validation in the HEK293T cell line, HSPCs were transduced with the lentiviral constructs at a MOI of 50. In contrast to the low infectivity potential from miR30-based viral particles, the transduction efficiency using the CS-shRNA system was significantly higher (**Figure 3.11**) and was used for the remaining work.

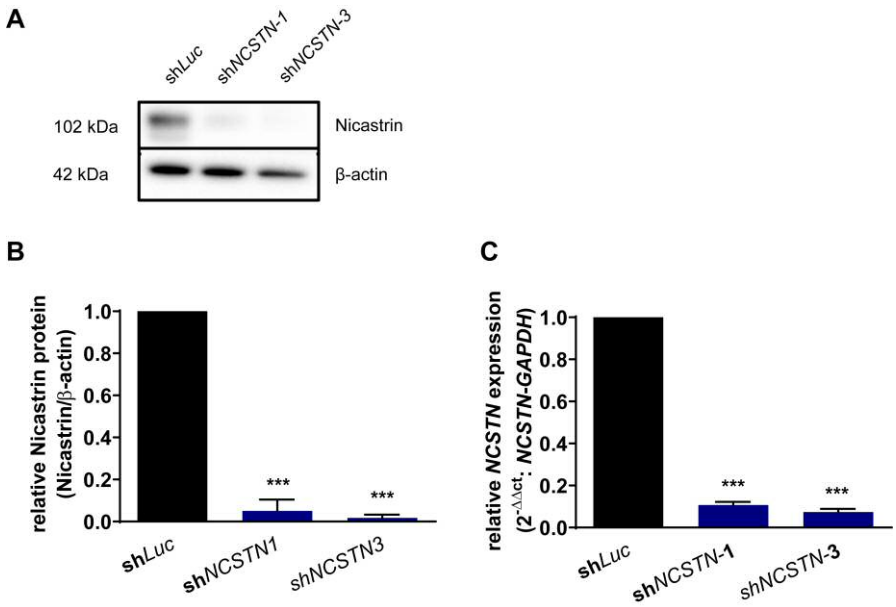

Figure 3.10 – The CS-shRNA lentiviral construct yields potent Nicastrin knockdown in HEK293T cells. (**A**) Representative western blot of shRNA-mediated knockdown of the Nicastrin protein. Quantification of (**B**) protein and (**C**) mRNA knockdown of Nicastrin. Results shown are the mean ± SD (n=4). Unpaired t-test. ***p<0.0005.

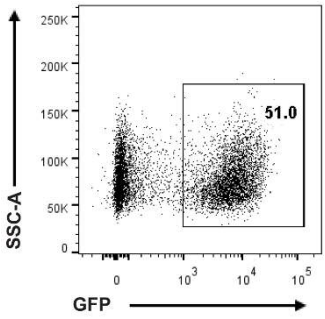

Figure 3.11 – The CS-shRNA lentiviral vector yields high transduction efficiency in human HSPCs. CD34⁺ HSPCs were enriched from MNCs which were then FACS sorted based on CD34 and CD38 expression. After transduction, GFP⁺ HSPCs were FACS sorted 4 days post-transduction.

3.5 Pan-Notch inhibition leads to HSC pool depletion and perturbed myeloid/lymphoid balance *in vitro*

Following GFP$^+$ HSPCs selection (transduction efficiencies obtained were up to ~50%) a fraction of the cells was co-cultured along with murine stromal MS5 cells to initiate the LTC-IC assay to address the role of Notch in human HSPCs *ex vivo* (**Figure 3.12**).

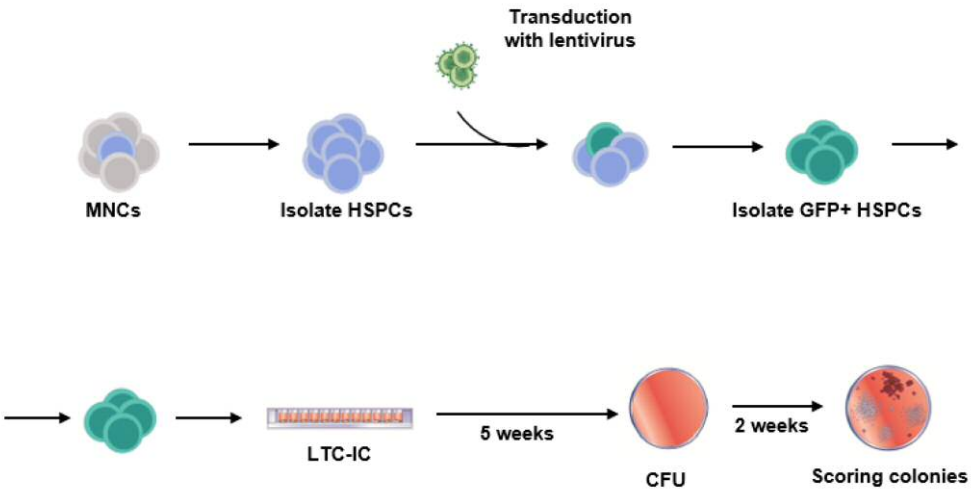

Figure 3.12 – Schematic representation of workflow. HSPCs were isolated from mononuclear cells by sorting CD34$^+$CD38$^-$ cells which were then transduced with lentivirus at MOI 50. GFP$^+$ HSPCs (as exemplified in **Figure 3.10**) were sorted 4 days following transduction and co-cultured with MS5 stromal cells for 5 weeks, following by methylcellulose sub-culturing for a further 2 weeks to measure the colony output of the LTC-IC assay.

The remaining cells were cultured for an additional 8 days in StemSpan containing SCF, FLT3L and TPO. At the end of this period, the number of cells in each condition was monitored throughout the culture. The Nicastrin-knockdown (Nicastrin-KD) HSPCs divided at a similar rate to the control cells, indicating that the constructs had no apparent toxic effects to the cells (**Figure 3.13**).

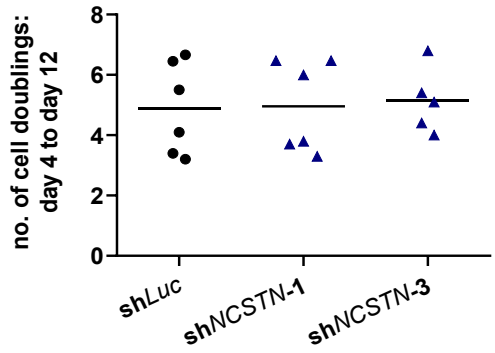

Figure 3.13 – Nicastrin-KD HSPCs proliferate at a similar rate to control cells. The number of cell doublings from day 4 to day 12 of HSPCs expansion was evaluated. Each dot represents an independent experiment and the bars are the mean of the values.

In addition, knockdown efficiencies were determined at day 12 of the culture at the mRNA and protein levels. While the sh*NCTSN-1* construct yielded a knockdown of ~50%, sh*NCSTN-3* consistently resulted in almost 100% knockdown, as determined by FCM analysis (**Figure 3.14 A and B**). Also, a reduction of approximately 55% and 65% of the *NCSTN* gene was achieved with sh*NCSTN*-1 and sh*NCSTN*-3, respectively (**Figure 3.14 C**).

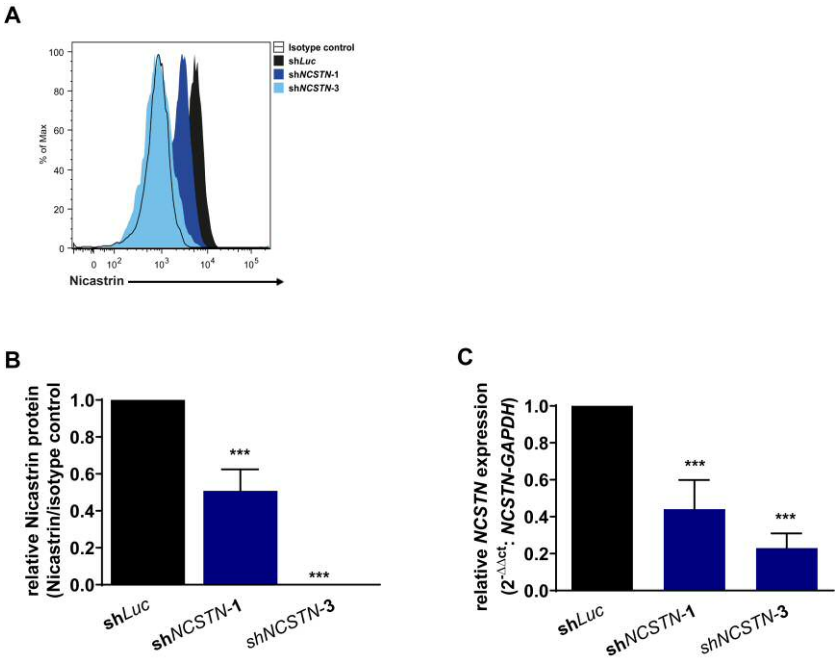

Figure 3.14 – The CS-shRNA lentiviral vector imparts potent Nicastrin knockdown in human HSPCs. (**A**) Representative histogram demonstrating Nicastrin knockdown. Quantification of Nicastrin (**B**) protein knockdown by FCM and (**C**) mRNA levels. Results shown are the mean ± SD (n=4-5). Unpaired t-test. ***p<0.0005.

A portion of the sorted GFP$^+$ HSPCs were tested under the LTC-IC assay. The cultures were maintained for a total of 5 weeks. It is well established that during this assay, HSPCs migrate underneath the stromal feeder layer which supports HSPCs survival and maintenance. Primitive cells present in the mix are then able to divide and generate cobblestone-resembling colonies. First, both HSPCs and murine MS5 cells were harvested and analysed for the expression of GFP. We observed a trend suggesting a reduction in the frequency of human cells generated in the Nicastrin-KD conditions at the end of assay, which is suggestive of a diminished capacity to maintain primitive cells when Notch pathways was inhibited (**Figure 3.15**).

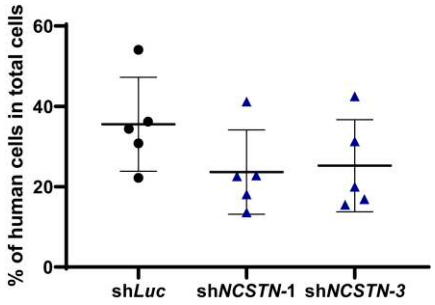

Figure 3.15 – Silencing of *NCSTN* reduces total human haematopoietic cell output in LTC-IC assay. Frequencies of GFP$^+$ cells in the total number of cells present at the end of the LTC-IC assay. The data represents the combination of preliminary optimisation and subsequent validated experiments (n=5).

An impaired increase in the number of CAFCs was detected at the various cell dosages, with significant reduction in the sh*NCSTN*-3 condition (**Figure 3.16**).

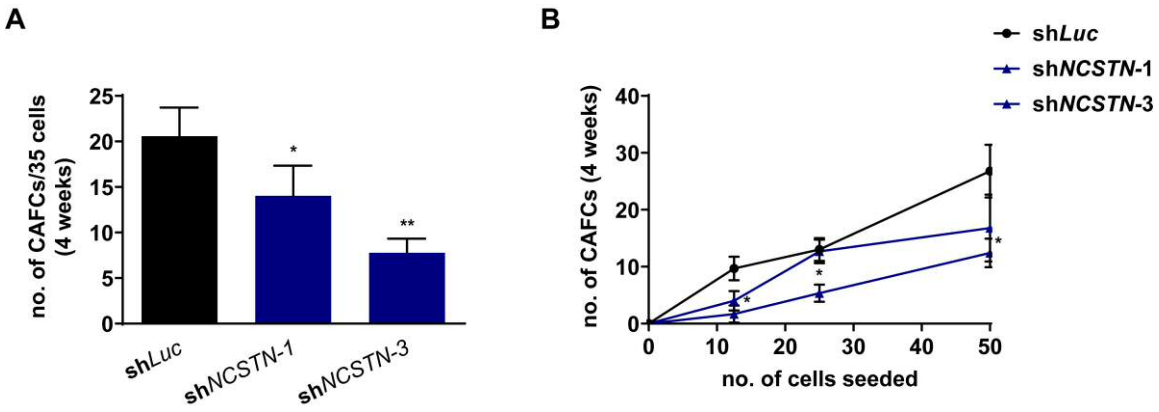

Figure 3.16 – Nicastrin-KD HSPCs have defective CAFC capacity. (**A**) Total number of CAFCs generated at 4 weeks after HSPCs seeding and (**B**) number of CAFCs generated at various cell doses at 4 weeks after seeding. The results are the mean ± SD (n=3). Unpaired t-test. *p<0.05; **p<0.005.

This data also suggests a dose dependent effect of the Notch inhibition and demonstrates that Notch is essential for the long-term maintenance of cells with primitive features *in vitro*. However, this data does not prove impaired differentiation potential. Hence, at the end of the five-week co-culture period, the cells were harvested and re-plated onto methylcellulose for an additional two weeks to measure the number of differentiated progenies generated from LTC-ICs that remained in culture (**Figure 3.17**). At the end of the LTC-IC assay, progenitors present in the initial suspension had differentiated and died off.

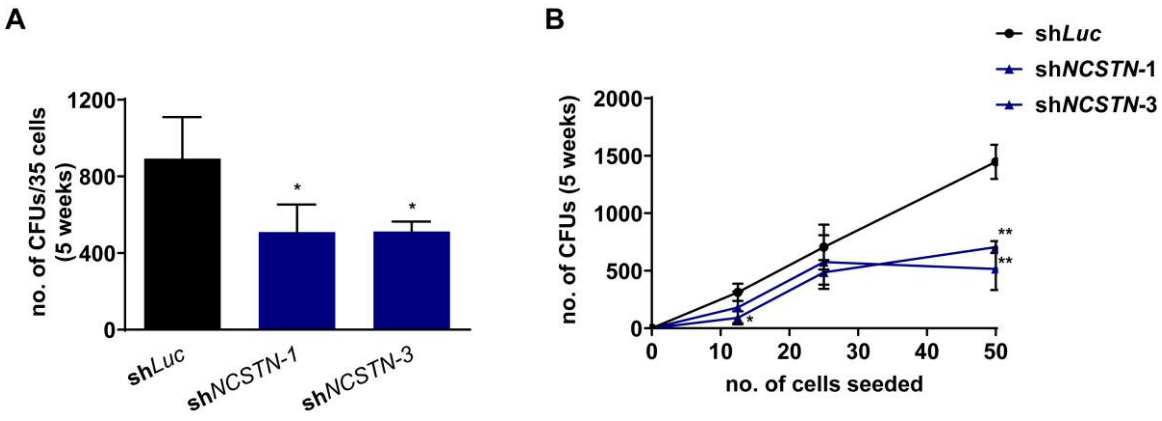

Figure 3.17 – Nicastrin-KD HSPCs have defective LTC-IC derived CFU capacity. (**A**) The total number of CFUs generated two weeks after re-plating in methylcellulose (**B**) and the number of CFUs generated at the corresponding cell dose. The results are the mean ± SD (n=3-4). Unpaired t-test. *p<0.05; **p<0.005.

Therefore, this measures the capacity of more primitive cells that were retained in the five-week culture period to generate differentiated progenies. We observed an almost 2-fold reduction in the total number of colonies in both conditions (**Figure 3.17 A**) compared to the control – an effect which was especially evidenced at the higher cell dose (**Figure 3.17 B**). Indeed, a decrease of approximately 50% and 65% was observed in the number of colonies generated in the sh*NCSTN-1* and sh*NCSTN-3* conditions compared to the control, respectively (**Figure 3.17 B**).

To complement this functional assay, the remaining cells were characterised immunophenotypically at the end of the LTC-IC assay. A fraction of the cell suspension was stained with a panel of antibodies aimed at the detection of primitive populations and analysed by FCM (**Figure 3.18**).

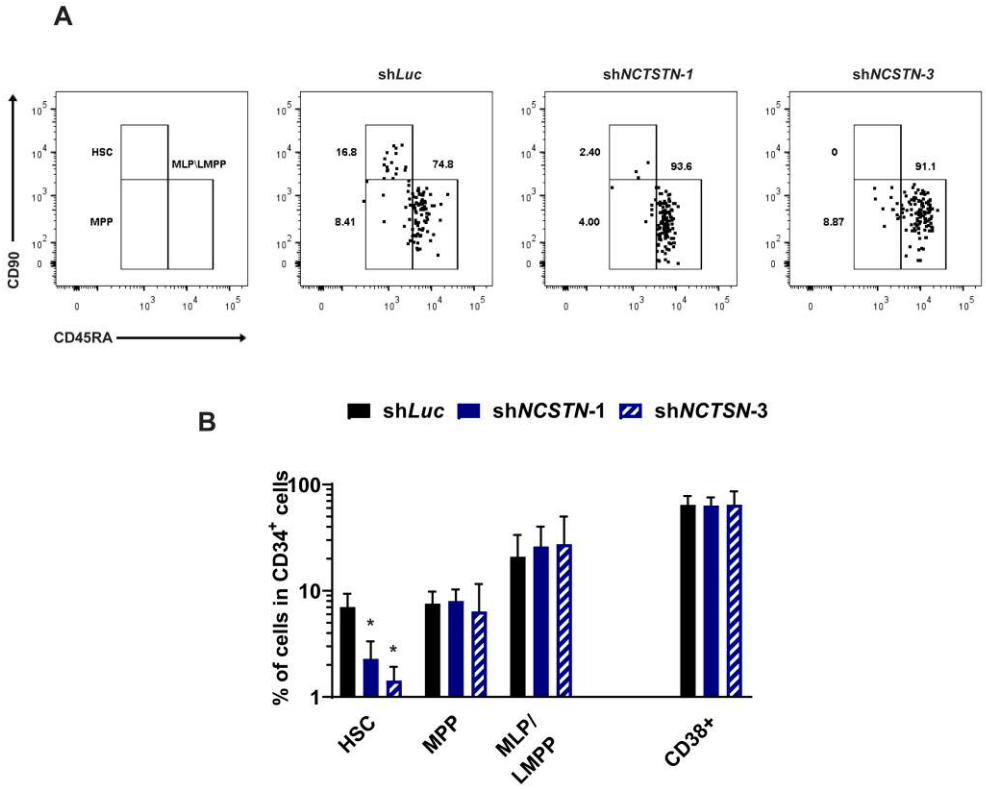

Figure 3.18 – Cell-autonomous Notch inhibition leads to reduced HSC compartment *in vitro*. (**A**) Representative dot plot of stem and progenitor cell frequencies. The cells were gated on the $GFP^+CD34^+CD38^-$ compartment. (**B**) Quantification of stem and progenitor cell frequency in control and Nicastrin-KD HSPCs. The results are the mean ± SD (n=3). Unpaired t-test. *p<0.05.

Hence, by gating on $GFP^+CD34^+CD38^-$ cells, the frequencies of the three most primitive cells compartments were analysed. In support of the effects observed, we detected a greater than 4-fold and 5-fold decrease in the frequency of phenotypic HSCs in sh*NCSTN-1* and sh*NCSTN-3* conditions compared to sh*Luc*, respectively (**Figure 3.18 A and B**). The reduction of HSCs appeared to have left the balance of downstream progenitors unaffected. Nonetheless, a trending increase in the MLP/LMPP compartment was observed in Nicastrin-KD HSPCs. Due to the large variation in the frequencies of $CD38^+$ progenitors (including CMPs, GMPs and MEPs) among the three independent experiments that would prevent a more rigorous analysis, these subpopulations were grouped in the larger collective $CD38^+$ population which revealed to be at comparable frequency to the control group. Nevertheless, the significant reduction in CAFCs and LTC-IC-derived CFUs observed could be mostly accounted for by the reduced HSCs frequencies (and total numbers, given the reduction in the total human GFP^+ cells generated - **Figure 3.15**) when Notch signalling was reduced. In addition to this, another fraction of cells was stained with a panel of antibodies that allowed the detection of differentiated cells. The LTC-IC assay has been modified over the years, initially confined to the support of granulocyte and macrophage differentiation (Dexter *et al*., 1977) and it was later

modified to support broad myeloid and B cell differentiation (Berardi *et al*., 1997). T-cell differentiation requires a different co-culture system (La Motte-Mohs *et al*., 2005) and therefore was not analysed. By excluding primitive $CD34^+$ cells from the analysis, more mature progeny could be detected based on various markers. CD19 is an early B cell marker. Monocytes can be detected in the $CD19^-CD33^+CD14^+$ fraction. Within the $CD33^+CD14^-CD11c^+$ compartment we can find DC-like cells. NK cells are the $CD56^+$ cells within the $CD14^-CD11c^-$ fraction (**Figure 3.19 A**).

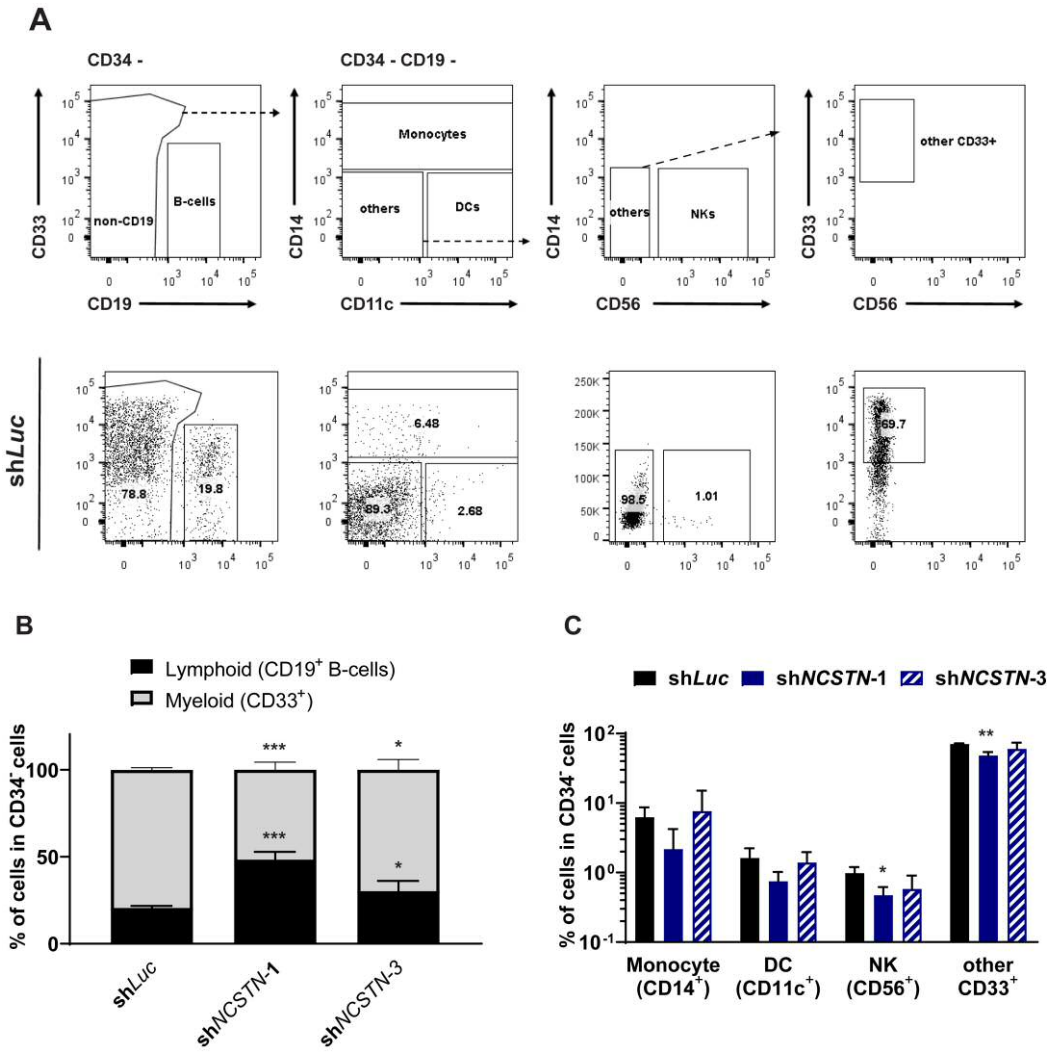

Figure 3.19. Nicastrin-KD HSPCs are skewed toward lymphoid development *in vitro*. (**A**) Representative dot plot of the differentiated fractions. Top row: $CD19^+$ B-cells and $CD19^-$ cells could be found in the $CD34^-$ compartment. The $CD19^-$ can be divided into DC-like cells, monocytes or other cells. $CD14^-CD11c^-$ cells can be NKs based on CD56 expression, or other myeloid precursors based on CD33 expression. Bottom three rows: representative dot plots for the conditions examined. (**B**) Quantification of myeloid versus lymphoid potential in the various conditions. (**C**) Quantification of non-$CD19^+$ cells present in the $CD34^-$ population. Results are the mean ± SD (n=3). Unpaired t-test. *p<0.05; **p<0.005; ***p<0.0005.

Notably, the balance between myeloid and lymphoid cells was perturbed by *NCSTN* silencing (**Figure 3.19 B**). Both Nicastrin-KD conditions had an increase in the lymphoid ($CD19^+$ B cell) compartment with concomitant reduction of the $CD33^+$ myeloid cells (**Figure 3.19**). Within non-$CD19^+$ compartment, a small reduction in the frequency of $CD56^+$ cells was observed in the sh*NCSTN-1* condition.

3.6 Pan-Notch inhibition leads to a depleted HSC pool in a cell-autonomous manner *in vivo*

Lastly, to address whether the effects of pan-Notch inhibition *in vivo* were cell-autonomous, HSPCs were transduced with the sh*Luc* or the sh*NCSTN-3* constructs. The latter was chosen over sh*NCSTN-1* given its stronger silencing efficiency. Following expansion and selection of HSPCs, 3800 to 5000 of FACS sorted GFP^+ HSPCs were injected intravenously into sub-lethally irradiated NSG mice. Twelve weeks after the transplantation, the recipients were sacrificed, and the bone marrows from three pairs of bones (tibiae, femurs and ileum) were analysed (**Figure 3.20**).

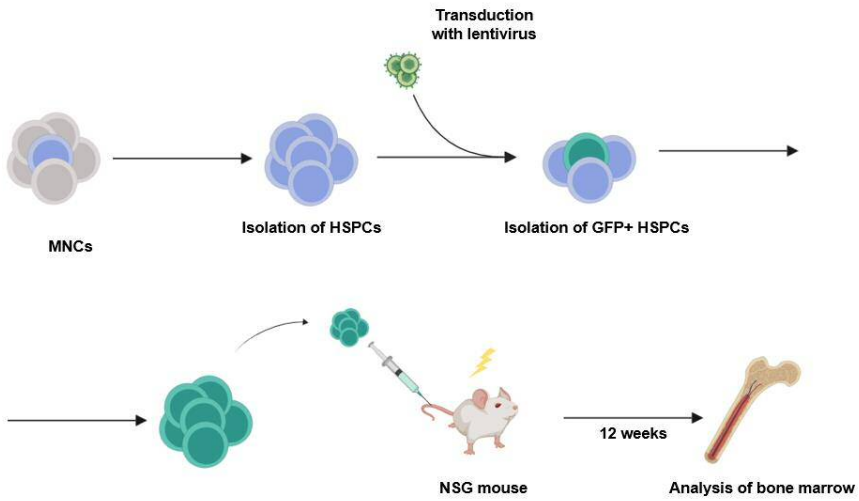

Figure 3.20 – Schematic representation of workflow. Human HSPCs isolated from CB MNCs were transduced with shRNA-carrying lentivirus constructs. Following selection and expansion of GFP^+ HSPCs, sub-lethally irradiated NSG mice were transplanted with the cells. Twelve weeks post-transplantation, the animals were sacrificed, and their BMs were analysed.

The flushed bone marrows were depleted of red blood cells. After that, the whole suspensions were stained with the HSPCs or differentiation antibody panels, and the outcomes were

analysed by FCM. Engraftment after xenotransplantation assays is usually done by the detection of human CD45$^+$CD33$^+$ and CD45$^+$CD19$^+$ which represents myelo-lymphoid engraftment. In this project, the transplanted HSPCs express the GFP reporter protein constitutively, and the measurement of GFP$^+$CD33$^+$ and GFP$^+$CD19$^+$ was used as an indication of the engraftment in the recipient animals. The sh*NCSTN-3* cohort had a 3-fold reduction in the myelo-lymphoid engraftment compared to that of the control, although this did not reach statistical significance due to the variability obtained (**Figure 3.21**).

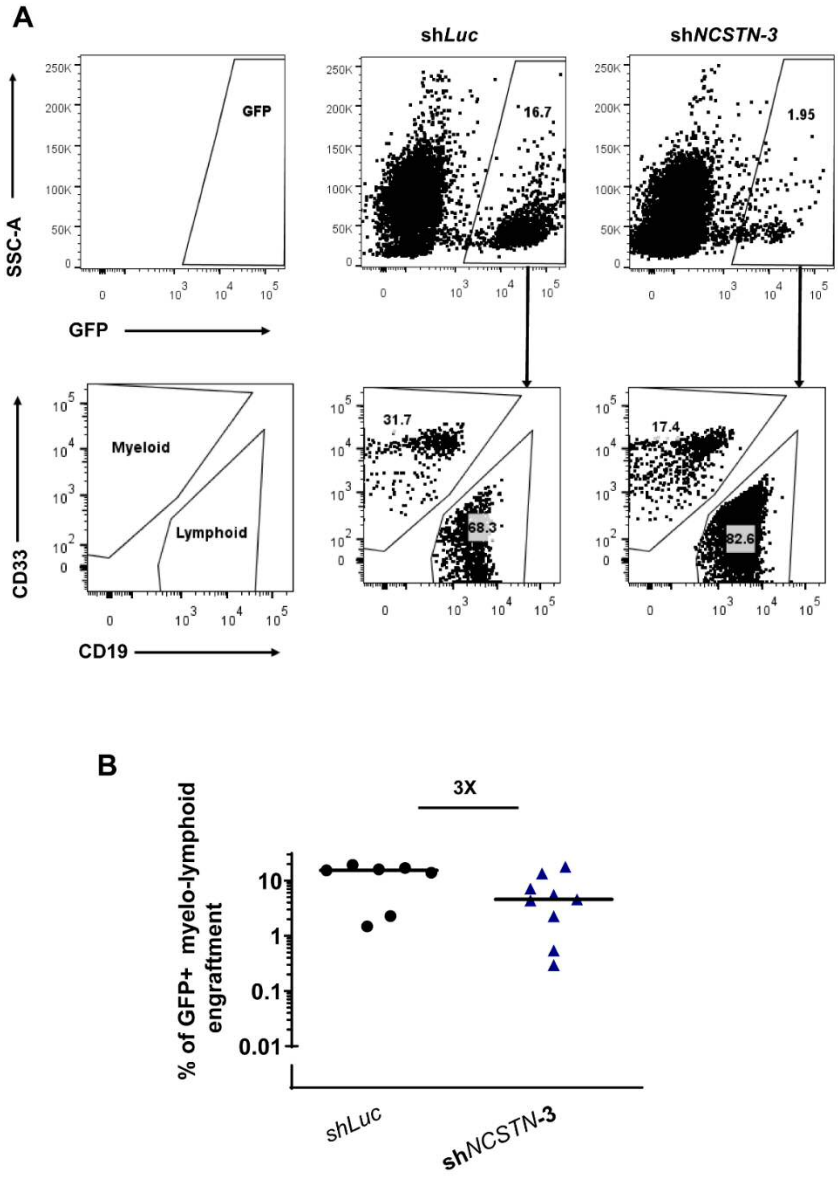

Figure 3.21 – Nicastrin-KD HSPCs have a reduced human myelo-lymphoid engraftment capacity. (**A**) Representative example of FCM analysis of Nicastrin-KD HSPCs. Live cells were gated on the GFP$^+$ population. (**B**) The sum of the frequencies of CD19$^+$ (Lymphoid) and CD33$^+$ (Myeloid) cells in GFP$^+$ cells are shown. Each dot represents a mouse and the bar is the median of the values (n=7 for the sh*Luc* cohort; n=9 for the sh*NCSTN-3* cohort). Mann-Whitney test.

Next, the frequencies of stem and progenitor cells in each cohort were measured. Representative dot plots showing the gating strategy can be found in **Figure 3.22**. A significant 5-fold reduction in the HSC fraction was found, while all other progenitor compartments remained largely unchanged (**Figure 3.22 B**).

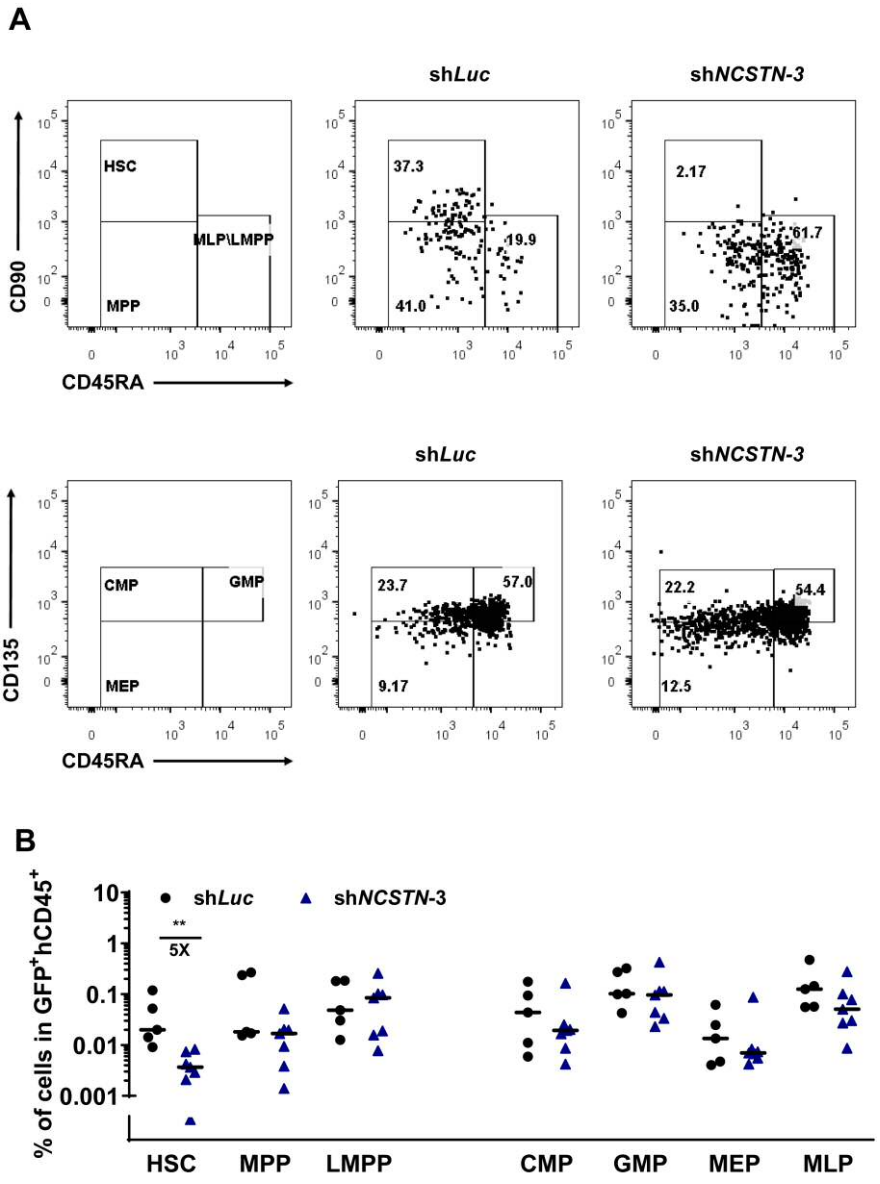

Figure 3.22 – NSG mice transplanted with Nicastrin-KD HSPCs have a reduced HSC compartment. (**A**) Representative dot plot of gating strategy for stem and progenitor cells with representative dot plots of sh*Luc* and sh*NCTSN-3*-transplanted NSG mice. (**B**) Quantification of stem and progenitor cells in the various conditions. Each dot represents a mouse. The bar is the median of the values (n=5 in the sh*Luc* cohort; n=7 in the sh*NCSTN-3* cohort). Mann-Whitney test. **p<0.005

The reduction of HSCs observed was consistent with the previous observations when pharmacological inhibition of Notch was employed *in vivo* (**Figure 3.4 C**) or shRNA mediated *NCSTN* silencing *in vitro* (**Figure 3.18**). This reinforces the notion that Notch is necessary for the maintenance of haematopoietic homeostasis and that its inhibition strongly affects the most primitive stem cell compartment. Interestingly, the effects seen are less striking than those previously observed with pharmacological inhibition of Notch. Even though we should be cautious with the direct comparison of the two approaches given their technical differences, this may be due to the nature of the experiments. DAPT, while being administered to the whole animal has the potential to affect all cells in the niche. On the other hand, cell autonomous inhibition of Nicastrin ensures Notch inhibition confined to the stem and progenitor cell compartment. Additionally, even though we observed a decrease in the total myelo-lymphoid engraftment from Nicastrin-KD cells, this did not translate into deregulated myeloid versus lymphoid balance, nor did it affect the frequencies of myeloid cells *in vivo* **(Figure 3.23 B and C).**

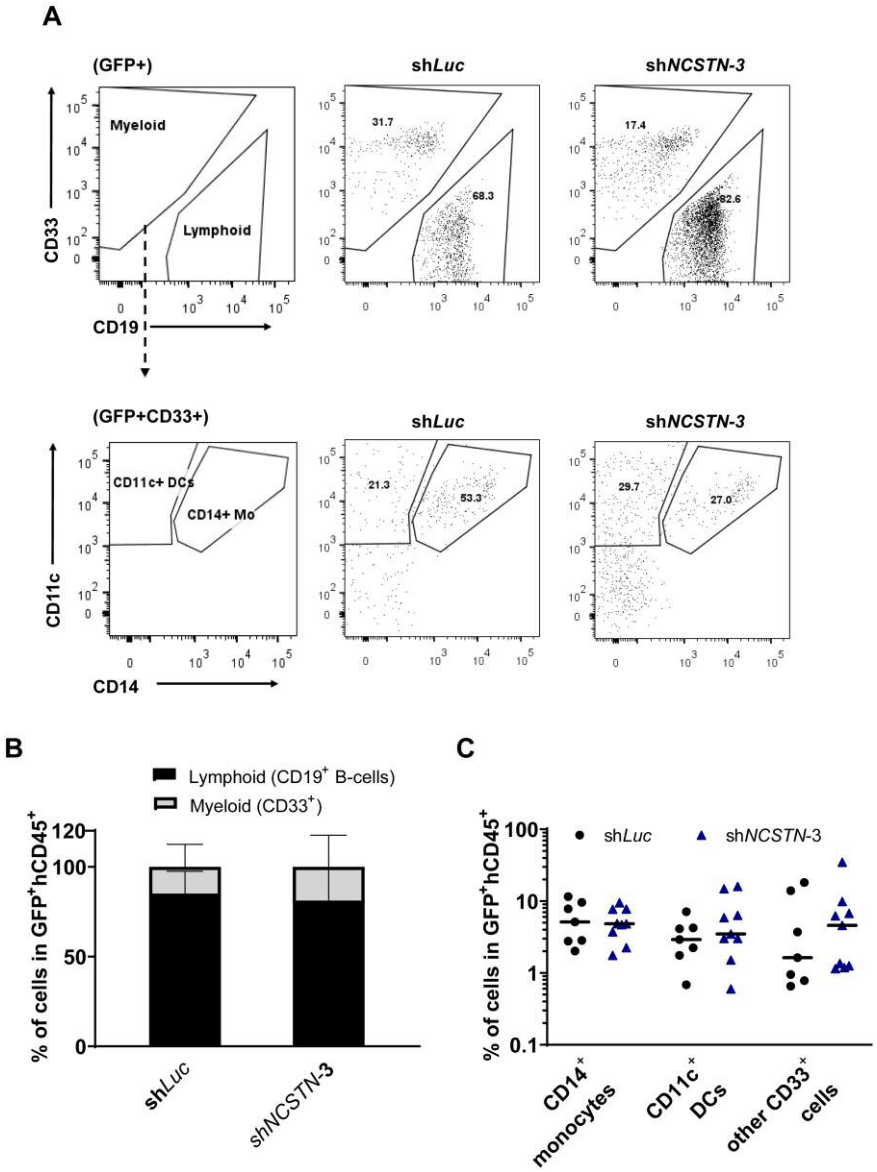

Figure 3.23 - NSG mice transplanted with Nicastrin-KD HSPCs have normally differentiated progenies. (**A**) Representative dot plot of gating strategy for stem and progenitor cells with representative dot plots of shLuc and shNCTSN-3-transplanted NSG mice. (**B**) Quantification of mature cells in the various conditions. Each dot represents a mouse (n=7 in the sh*Luc* cohort; n=9 in sh*NCSTN-3* cohort). Mann-Whitney test. The bar is the median of the values.

3.7 Discussion

Firstly, Notch signalling was shown to be highly expressed and active in various human haematopoietic stem and progenitor cell fractions. This agrees with early studies that first demonstrated Notch expression in human $CD34^{+}Lin^{-}$ cells (Milner *et al.*, 1994) which were later confirmed by others in both $CD34^{-}$ and $CD34^{+}$ HSCs (Anjos-Afonso *et al.*, 2013). Since then, Notch has been postulated as a regulator of human HSPCs self-renewal and

differentiation (Lauret *et al*., 2004), (Delaney *et al*., 2005). While canonical Notch signalling in murine BM cells appears to be dispensable *in vivo* (Maillard *et al*., 2008), whether Notch plays a role in human HSPCs *in vivo* remains unanswered. Benveniste *et al.,* have suggested human HSPCs require Notch signalling *in vitro* but not *in vivo* (Benveniste *et al*., 2014). However, a close inspection of the authors' results could infer a different interpretation. First, the percentage of the dnMAML1-HSC population within the human graft was half of that of the control. Second, the total number of dnMAML1 engrafted cells was more than double compared to controls. Given this, the authors concluded that the total number of engrafted dnMAML1 HSCs was unchanged relative to control HSCs *in vivo* (Benveniste *et al*., 2014). However, it can be interpreted that it did, as the frequency of dnMAML1 HSCs was reduced with a concomitant increase in total differentiated human cells. Here, employing a pan-Notch inhibition approach by using DAPT resulted in a significant reduction of various stem and progenitor cell compartments, including the HSC fraction. Pharmacological inhibition of Notch using DAPT non-selectively blocks the processing of all Notch receptors, as well as other γ-secretase substrates (CD44, ErbB4 among many others (Jurisch-Yaksi *et al*., 2013)). Non-haematopoietic cells in the bone marrow niche have been shown to express Notch ligands (Calvi *et al*., 2003), (Guezguez *et al*., 2013) and through them, regulate haematopoietic cells in the microenvironment. To address whether these outcomes were cell-autonomous, we challenged HSPCs with knockdown of the *NCSTN* gene (Nicastrin-KD HSPCs) under various assays *in vitro*. A miR-30 based shRNA-mediated silencing lentiviral construct was briefly tested for its capacity to block Notch processing. However, this system yielded very poor transduction efficiency in primitive human haematopoietic cells. To circumvent this issue, an H1 promoter-driven system was used instead which yielded very strong transduction and silencing efficiency.

The LTC-IC assay is the *in vitro* surrogate for xenotransplantation studies and challenges stem cells. The significant reduction (~60%) in the total number of CAFCs generated *in vitro* indicates the importance of Notch signalling in the maintenance of primitive cells. When re-plated onto differentiation-inducing conditions we noticed once more a significant reduction in the total number of colonies generated reinforcing the notion that physiological levels of Notch are fundamental for primitive cells with differentiation capacity *ex vivo*. Next, we carried out immunophenotypic analysis of the cells generated at the end of the LTC-IC assay. Interestingly, when assessing the frequency of HSPCs and differentiated cells at the end of the assay, a reduction in the HSC pool was found. A trending increase in the frequency of MLP/LMPP cells may be suggestive of the idea that there is differentiation of HSCs towards more committed progenitors. A fraction of those HSCs could also have undergone cell death as a result of Notch inhibition, although this was not observed (Anjos-Afonso *et al*, 2013) and

(Anjos-Afonso, personal observations). Additionally, a lower frequency of $CD33^+$ cells was also observed in Nicastrin-inhibited conditions *in vitro*. Of note, to formally test the various subpopulations detected under this assay, the cells should be harvested, sorted and rigorously tested for their true potential. Importantly, most of what is known about the role of Notch on HSPCs derives from gain-of-function studies, whereby Notch ligand stimulation or overexpression of NICD are employed. To the best of our knowledge, this is the first report showing the requirement for Notch signalling in human HSPCs *in vitro* by using a loss-of-function approach.

Lastly, to complement the *in vitro* functional characterisation of Notch-KD cells, sh*Luc* or sh*NCSTN*-3-transduced HSPCs were transplanted into NSG mice to gauge their potential *in vivo*. At 12 weeks post-transplantation, the HSC compartment was markedly reduced in NSG mice transplanted with Nicastrin-KD HSPCs (5-fold decrease compared to the control). We have previously shown that all stem and progenitor cell fractions expressed Notch receptors and possessed an active pathway. Pharmacological inhibition of Notch signalling most likely affected all those fractions to different extents which resulted in larger impact in many cell compartments. On the other hand, by inhibiting Notch in $CD34^+CD38^-$ the effects are initially confined to a smaller fraction of cells which are potentially extended to their immediate progeny later. Indeed, the 5-fold reduction in the frequency of HSCs in the Nicastrin-KD condition (that was equal to 15-fold in the total HSC pool) resulted in a total 3-fold reduction in total human engraftment, affecting equally all the lineages. Regarding the role of Notch signalling in the differentiation of haematopoietic cells, *in vitro* studies have yielded conflicting results. While some have argued that Notch signalling promotes myeloid differentiation (Tan-Pertel *et al*., 2000), (Schroeder *et al*., 2003), other studies have reported opposite effects, where Notch signalling indeed decreases myeloid potential (Milner *et al*., 1996), (de Pooter *et al*., 2006). It should be noted that most of these studies employed cell lines, which may not faithfully represent the behaviour of primary cells. On the other hand, *in vivo* studies have clearly established the role for Notch1 in T cell development (Radtke *et al*., 1999). More recently, it was shown to induce megakaryocyte development *in vitro* and *in vivo* (Mercher *et al*., 2008). In our study, even though we observed a lower frequency of $CD33^+$ cells *in vitro*, this effect was not evident *in vivo*. This could be due to the myeloid-bias nature of the LTC-IC which is better to reveal myeloid output variations as compared to the *in vivo* assay, which is biased toward lymphoid development. Still, the reduction of HSC frequency in all the assays performed indicates the requirement for Notch signalling in the maintenance of phenotypically defined HSCs both *in vitro* and *in vivo*. Yet. to confirm true impairment on stem cell activity, secondary transplantation into new recipients should be performed. Additionally, assuming Notch signalling maintains a quiescent and immature cell state, the cell cycle regulation of

cells recovered from these mice could be analysed. This would inform on the percentage of cells that exited the G0 phase of the cell cycle. Importantly, we observed differential Notch receptor activation in various HSPC compartments. To understand which receptor is responsible for the outcomes observed, knockdown of the individual receptors could be performed (which is an ongoing project in the lab). Collectively, these data indicate Notch signalling is active in haematopoietic stem and progenitor cells. Its inhibition by pharmacological or shRNA-mediated silencing of key Notch components results in destabilised primitive haematopoietic cell compartments, with exceptional effect on HSCs both *in vitro* and *in vivo*. The NICD has been shown to interact with molecules from many of the major signalling pathways. Hence, the effects described could partially be the result of impaired non-canonical Notch signalling. To address this subject, the Notch transcriptional co-activator RBPJκ molecule was silenced causing disruption of canonical Notch signalling exclusively. This is described in **Chapter 4**.

Chapter 4 - Exploring the roles of canonical Notch signalling in human HSPCs

4.1 Brief introduction

Canonical Notch signalling requires cell-cell interactions to be activated in a ligand- and RBPjκ-dependent manner. Non-canonical Notch signalling can be independent from RBPjκ and/or ligand-mediated activation. Notch receptors can interact with components of the major signalling pathways such as PI3K, AKT, mTORC2, Wnt, NFκβ, YY1 and HIF1α (Bigas and Espinosa, 2016), (Colombo *et al*., 2019). Although the functions of non-canonical Notch signalling have not been properly elucidated, some believe it may comprise a more efficient way to carry out cell-specific functions by activating specific transcription factors (Sanalkumar *et al*., 2010). As an example, Delta1 ligand was shown to activate STAT3 in $CD34^+$ cells and cause the loss of membrane bound IL-6 receptor through not yet defined mechanisms. The loss of IL-6 *cis*-signalling skewed the cells away from myeloid differentiation (Csaszar *et al*., 2014). Additionally, in the murine haematopoietic system, Notch signalling specifies T- or B cell commitment at the CLP stage (Wilson *et al*., 2001). RBPJκ/NICD-mediated signalling is required for T cell maintenance and differentiation (MacDonald *et al*., 2001), (De Smedt *et al*., 2002), (Han *et al*., 2002). On the other hand, a RBPjκ-independent Deltex-mediated mechanism inhibits expression of the E47 transcription factor that is required for B cell development (Bain *et al*., 1997), (Ordentlich *et al*., 1998), (Han *et al*., 2002). As explained in **Chapter 1**, RBPjκ interacts with NICD, MAML1 and other co-activators to initiate canonical Notch signalling. Disruption of the canonical Notch pathway has been achieved by deleting *Rbpj* in mouse models (Maillard *et al*., 2008), (Duarte *et al*., 2018), or by expressing a dominant negative form of Xenopus suppressor of hairless (dnXSu(H) – the xenopus homolog of CBF-1) (Duncan *et al*., 2005), or by expressing a dominant negative form of MAML1 (dnMAML1) (Maillard *et al*., 2008), (Benveniste *et al*., 2014). The outcomes of these studies were varied. Whereas some have reported no role for the canonical Notch signalling in murine BM cells *in vivo* (Maillard *et al.,* 2008) , (Duarte *et al*., 2018) others have shown a depletion of LT-HSCs (Duncan *et al*., 2005). In the human haematopoietic system, Benveniste and colleagues suggested a differential need for Notch *in vitro* and *in vivo* (Benveniste *et al*., 2014). Conversely, Anjos-Afonso *et al.,* have reported Notch activity in very primitive $CD34^-$ HSCs which produce more $CD34^+CD38^-$ progeny upon Notch inhibition (Anjos-Afonso *et al*., 2013).

As described in **Chapter 3**, disruption of pan-Notch signalling through pharmacological or shRNA-mediated methods resulted in deregulation of stem and progenitor cells compartments, with a particularly drastic reduction in HSC numbers and impairment of HSC repopulating capacity. Here, we focus on addressing the specific role of canonical Notch signalling by silencing the *RBPJ* gene which encodes for the essential Notch co-activator

RBPjκ. Importantly, the differential roles of the canonical and non-canonical Notch signalling pathway in human HSPCs have not been addressed.

Aims of Chapter 4

- Block canonical Notch signalling in HSPCs by using shRNA lentiviral vectors that inhibit the expression of *RBPJ* – an essential canonical Notch co-activator.
- Assess *in vitro* effects of canonical Notch inhibition by measuring colony-forming and differentiation capacity under the LTC-IC assay.
- Assess *in vivo* effects of canonical Notch inhibition by measuring myelo-lymphoid engraftment and frequencies of stem/progenitor and mature cells.

4.2 shRNA-mediated silencing of *RBPJ* in human HSPCs

4.2.1 Testing a miR-30-based shRNA system in human HSPCs

The miR30-based system previously cloned and tested in HSPCs was also investigated for its ability to silence the *RBPJ* in the HEK293T cell line. This was performed concurrently when this system was tested for *NCSTN* silencing. Despite achieving very efficient silencing of *RBPJ* in HEK293T cells (**Figure 4.1**), this construct was again unable to efficiently transduce human HSPCs (**Figure 4.2**).

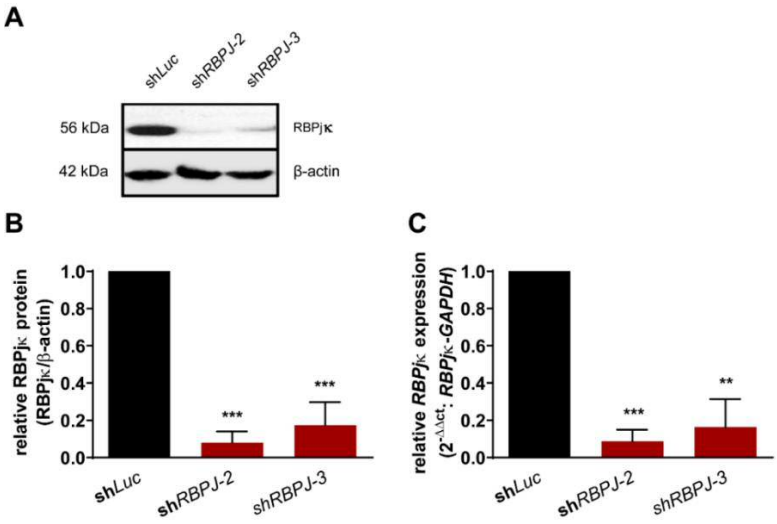

Figure 4.1 – shRNA-mediated knockdown of RBPjκ in HEK293T cells. (**A**) Representative WB of shRNA mediated knockdown of the RBPjκ protein. Quantification of (**B**) protein and (**C**) mRNA knockdown of *RBPJ*. Results are the mean ± SD (n=4). Unpaired t-test. **p<0.005; ***p<0.0005.

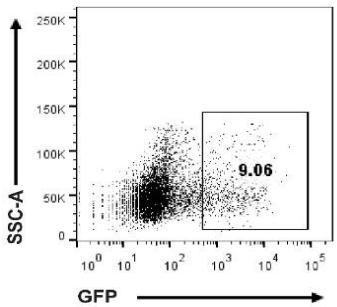

Figure 4.2 – miR-30 based shRNA lentiviral vector has low infectivity potential in human HSPCs. Representative dot plot of human CB $CD34^{+}CD38^{-}$ cells transduced at MOI 50 with the miR-30 lentiviral vector carrying a shRNA sequence targeting *RBPJ*. At day 4 post-transduction, the cells were analysed for GFP expression.

This indicates that the poor transduction efficiencies obtained were likely to be due to an intrinsically low ability of this specific construct to transduce primary primitive haematopoietic cells.

4.2.2 shRNA-mediated silencing of *RBPJ* using an H1 promoter-driven shRNA system

Given the poor efficiency of the miR-30 based system to transduce human HSPCs, the H1 promoter-driven shRNA system was again used for the remaining work. HEK293T cells were successfully transduced with the various constructs and showed a larger than 97% GFP expression 8 days post-transduction (**Figure 4.3**).

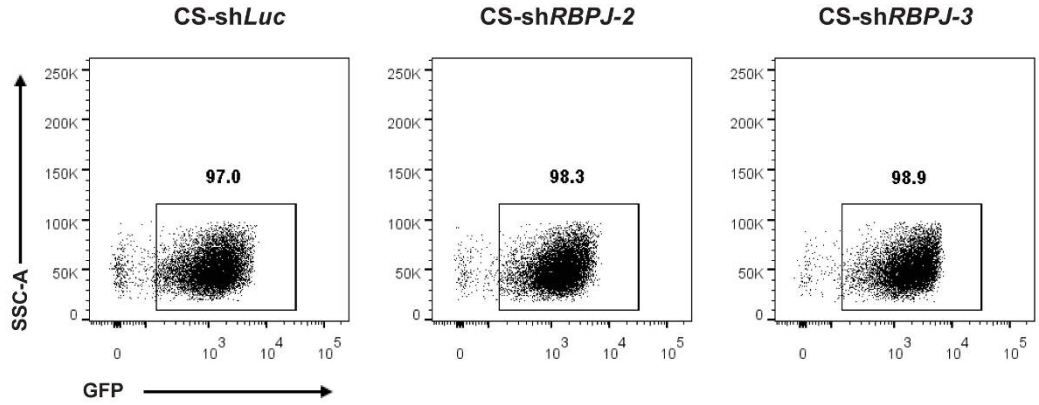

Figure 4.3 – HEK293T cells transduced with CS-shRNA constructs. HEK293T cells were analysed for their GFP expression 8 days post-transduction with CS-shRNA constructs.

Out of three sequences tested, the constructs termed sh*RBPJ*-2 and sh*RBPJ*-3 resulted in approximately 95% reduction of protein levels from both constructs as assessed by WB (**Figure 4.4 A** and **B**), and 80% and 90% reduction of *RBPJ* mRNA levels, respectively (**Figure 4.4 C**).

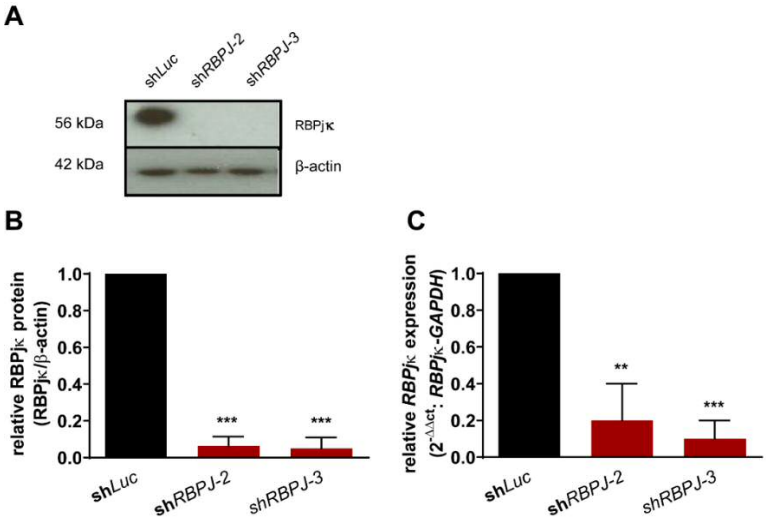

Figure 4.4 – The CS-shRNA lentiviral constructs induce potent RBPjκ knockdown in HEK293T cells. (**A**) Representative western blot of shRNA-mediated knockdown of the RBPjκ protein. Quantification of (**B**) protein and (**C**) mRNA knockdown of *RBPJ*. Results shown are the mean ± SD (n=4). Unpaired t-test. **p<0.005; ***p<0.0005.

4.3 Silencing of *RBPJ* results in reduced HSC compartment and perturbed B cell output *in vitro*

After validation of the constructs in the HEK293T cells, human HSPCs were transduced with the various lentiviral vectors at a MOI of 50. In contrast to the miR30-based system, the CS-shRNA constructs yielded high transduction efficiencies in human HSPCs (**Figure 4.5**).

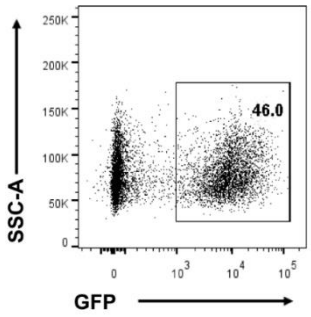

Figure 4.5 – The CS-shRNA lentiviral vector efficiently transduces human HSPCs. SSC-A – Side Scatter-Area; GFP – Green Fluorescent Protein.

A reduction of 63% and 80% of *RBPJ* mRNA levels was achieved by using sh*RBPJ*-2 and sh*RBPJ*-3, respectively (**Figure 4.6**).

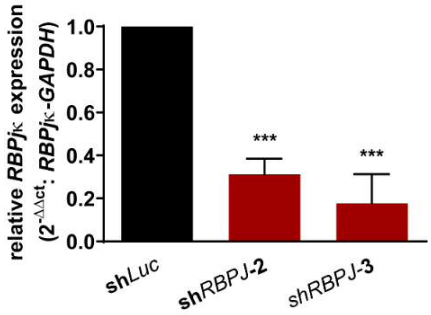

Figure 4.6 – The CS-shRNA lentiviral vector imparts potent *RBPJ* knockdown in human HSPCs. Quantification of *RBPJ* mRNA by qRT-PCR. Results shown are the mean ± SD (n=3). Unpaired t-test. ***p<0.0005.

Importantly, RBPJκ-knocked down (RBPJ-KD) cells proliferated largely at comparable rate without significant difference to control cells (**Figure 4.7**).

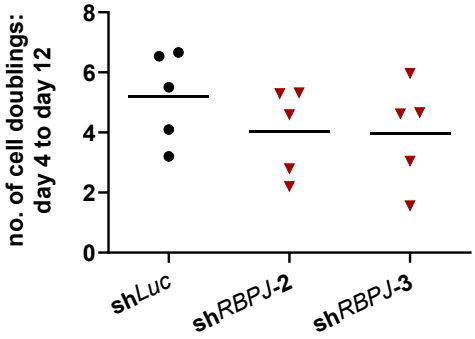

Figure 4.7 – RBPJ-KD HSPCs proliferate at a similar rate to control cells. The number of cell doublings from day 4 to day 12 of HSPCs expansion was plotted. Each dot represents an independent experiment and the bars are the mean of the values.

Then, at four days post-transduction GFP$^+$ HSPCs were sorted by FACS and challenged under the LTC-IC assay. At the fourth week of the assay, we observed a greater than 5-fold and 8-fold reduction in the total number of CAFCs generated in the sh*RBPJ-2* and sh*RBPJ-3* conditions, respectively as well as in the number of colonies generated at different cell doses (**Figure 4.8**). This was the same outcome that was observed in Nicastrin-KD HPSCs which suggests that Nicastrin acts via RBPjκ to maintain primitive cells *in vitro.*

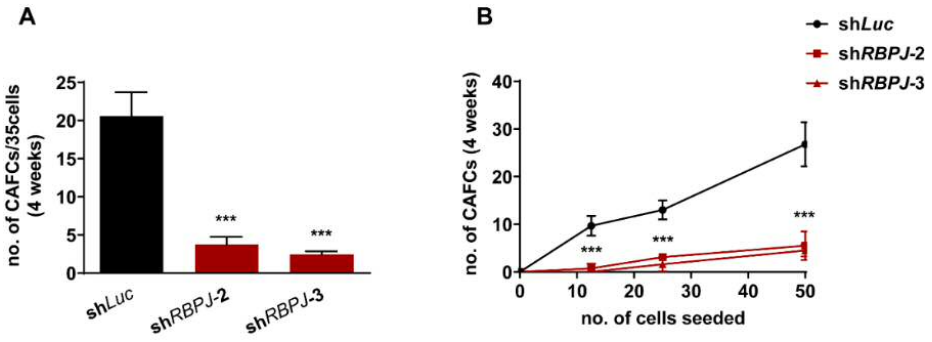

Figure 4.8 – RBPJ-KD HSPCs have defective CAFC capacity. (**A**) Total number of CAFCs generated at 4 weeks after HSPCs seeding and (**B**) number of CAFCs generated at various cell doses at 4 weeks after seeding. Both sh*RBPJ*-2 and sh*RBPJ*-3: p<0.0005. The results are the mean ± SD (n=4). Unpaired t-test. ***p<0.0005.

Accordingly, we also observed a strong 10-fold and 20-fold reduction in the number of LTC-IC-derived CFUs generated in sh*RBPJ-2* and sh*RBPJ-3* HSPCs, respectively (**Figure 4.9**).

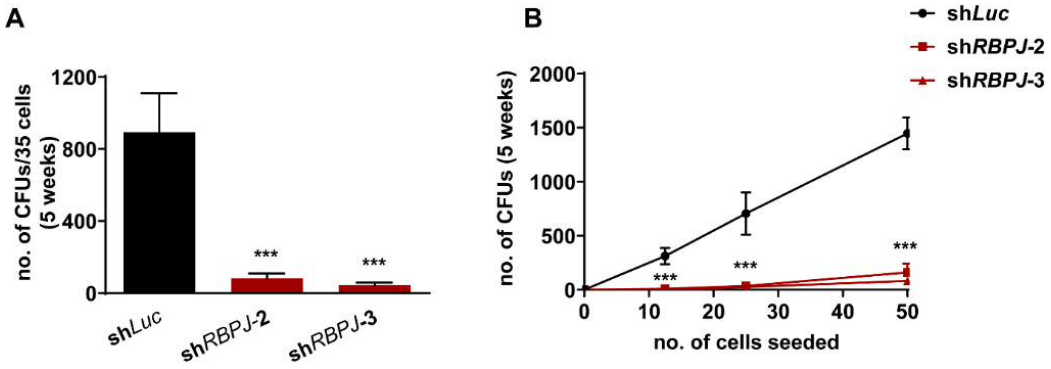

Figure 4.9 – RBPJ-KD HSPCs have defective LTC-IC derived CFU capacity. (**A**) The total number of CFUs generated two weeks after re-plating in methylcellulose (**B**) and the number of CFUs generated at the corresponding cell dose. Both sh*RBPJ*-2 and sh*RBPJ*-3: p<0.0005. The results are the mean ± SD (n=4). Unpaired t-test. ***p<0.0005.

A linear increase in the number of LTC-IC derived colonies can be seen in the control condition with increased number of cells seeded, which is almost completely abolished in the RBPJ-KD conditions (**Figure 4.9 B**) suggesting an almost complete loss of cells with primitive features in these cases. These data indicate that the reduction in LTC-IC activity observed among Nicastrin-KD HSPCs was at least in part due to impaired canonical Notch signalling.

To address the effects of *RBPJ* silencing in HSPCs *in vitro*, the cells were harvested at the end of the LTC-IC assay and analysed by FCM. We observed a significant 2.8-fold and 2.4-fold reduction in the number of human cells generated in the sh*RBPJ-2* and sh*RBPJ-3*

conditions at the end of assay, respectively (**Figure 4.10**). This indicates the cells were depleted during the assay when canonical Notch signalling was compromised.

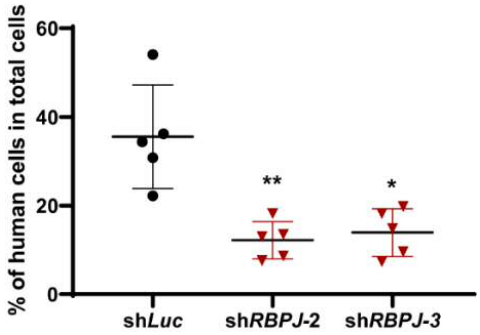

Figure 4.10 – Silencing of *RBPJ* reduces total human haematopoietic cell output in LTC-IC assay. Frequencies of GFP$^+$ cells in the total number of cells present at the end of the LTC-IC assay. Each dot or triangle represents one experiment. The bar is the mean ± SD (n=5). Unpaired t-test. *p<0.05; **p<0.005.

Additionally, a 6-fold and 3-fold decrease in the HSC frequency was observed in sh*RBPJ*-2 and sh*RBPJ*-3 transduced cells, respectively (**Figure 4.11**). This was accompanied by an increase in the frequency of subsequent progenies (e.g. increase in MPPs in sh*RBPJ-3* or in MLP/MLPPs in sh*RBPJ-2* transduced cells - see **Figure 4.11 B**), which again is suggestive of enforced differentiation from HSCs.

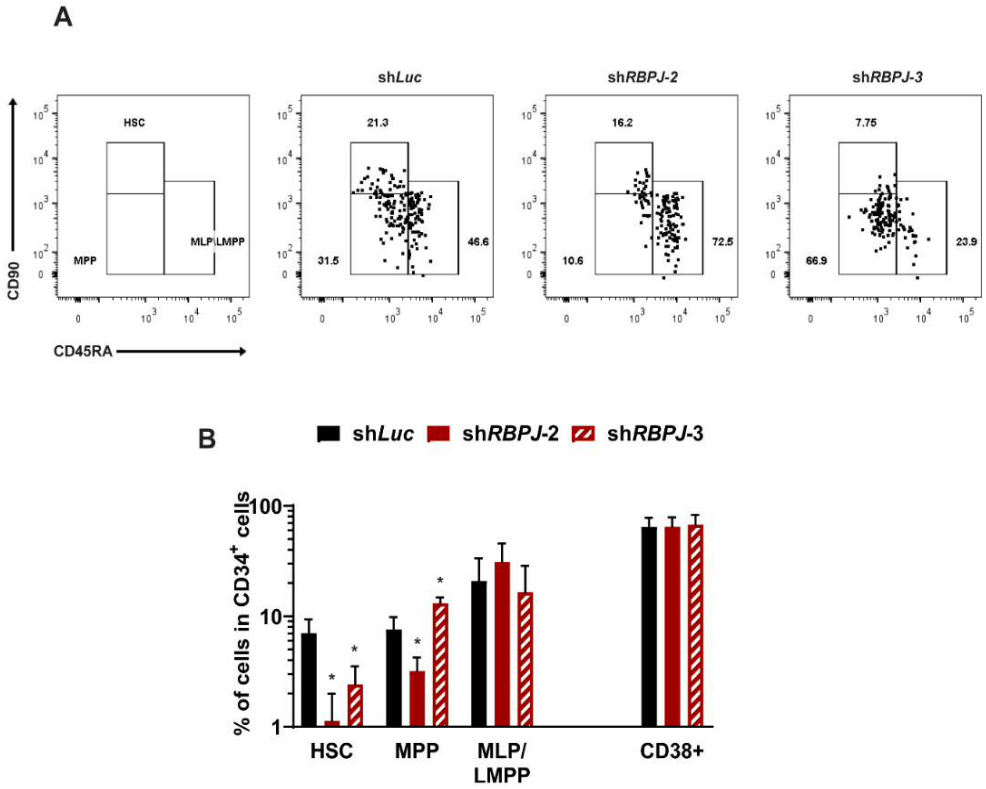

Figure 4.11 – *RBPJ* inhibition leads to reduced HSC compartment *in vitro*. (**A**) Representative dot plot of stem and progenitor cell frequencies. The cells were gated on the $GFP^+CD34^+CD38^-$ compartment. (**B**) Quantification of stem and progenitor cell frequency in control and RBPJ-KD HSPCs. Results are presented as mean ± SD (n=3). Unpaired t-test. *p<0.05.

Another fraction of cells was analysed for the expression of differentiation markers instead. Interestingly, a shift towards myeloid cell development was observed in RBPJ-KD cells, whereby an almost complete suppression of B cell development was observed (**Figure 4.12 B**). A deeper look into the non-$CD19^+$ compartment revealed deregulation of other mature cell types such as DCs and NKs (**Figure 4.12 C**). These perturbations were different than the ones observed upon *NCSTN* silencing, perhaps hinting at RBPJκ-independent mechanisms being also at play.

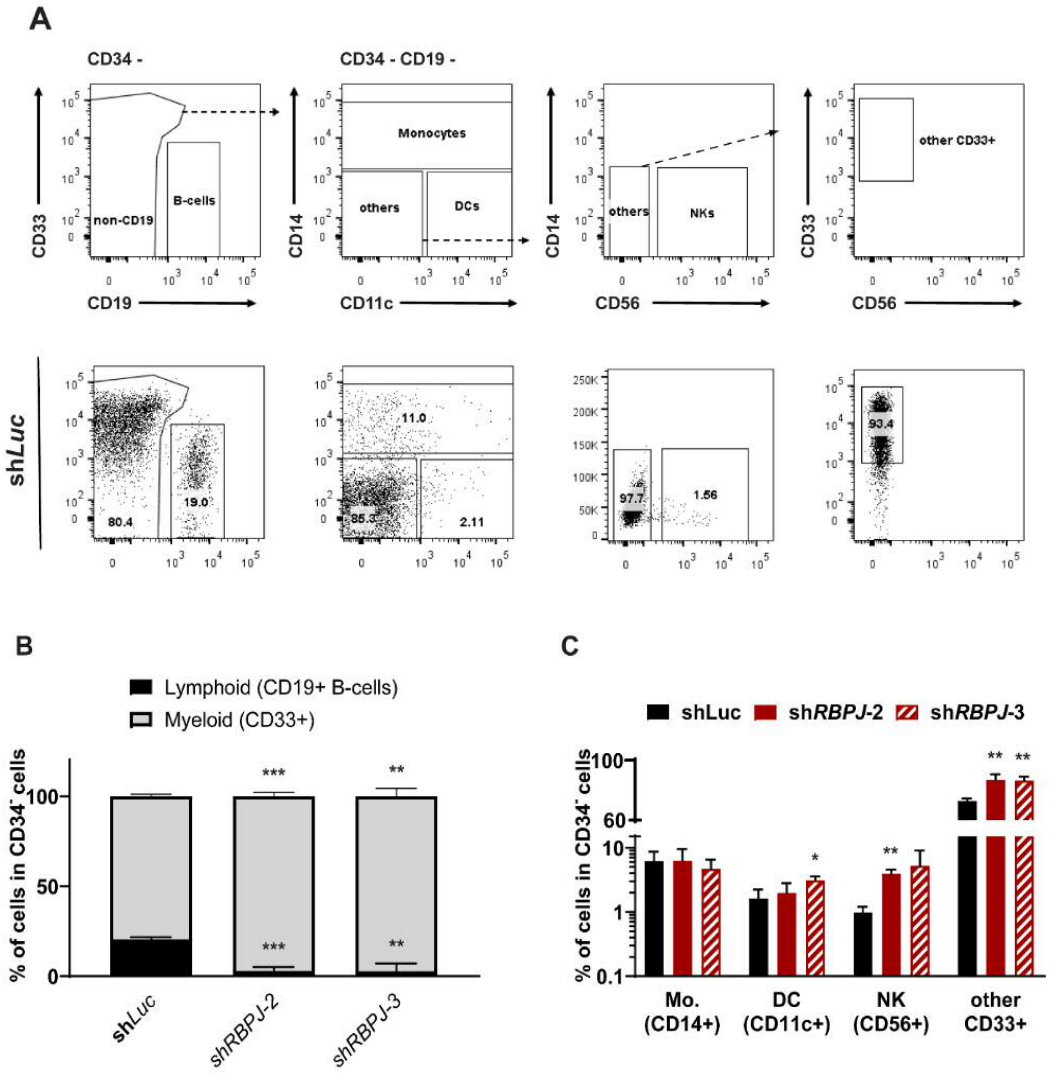

Figure 4.12. RBPJ-KD HSPCs have impaired B cell development *in vitro*. (**A**) Representative dot plot of the differentiated fractions. Top row: CD19^{+} B-cells and CD19^{-} cells could be found in the CD34^{-} compartment. The CD19^{-} can be divided into DC-like cells, monocytes or other cells. CD14^{-}CD11c^{-} cells can be NKs based on CD56 expression, or other myeloid precursors based on CD33 expression. Bottom row: representative dot plots for the control condition. (**B**) Quantification of lymphoid and myeloid cell compartments present in the CD34^{-} population. (**C**) Quantification of non-CD19^{+} cells present in the CD34^{-} population. Results are presented as mean ± SD (n=3). Unpaired t-test. *p<0.05; **p<0.005; ***p<0.0005.

4.4 Silencing of *RBPJ* results in reduced HSCs and reduced B cell output *in vivo*

At last, to address the effects of canonical Notch inhibition *in vivo*, sh*Luc* or sh*RBPJ*-3-transduced HSPCs were injected into NSG mice. Mouse bone marrows were harvested at 12 weeks post-transplant. sh*RBPJ*-3 was favoured over sh*RBPJ*-2 due to its stronger silencing

efficiency. A 68-fold decrease in the percentage of myelo-lymphoid engraftment was observed in RBPJ-KD cell recipients (**Figure 4.13**), demonstrating the significant deficiency on repopulating capacity that impaired canonical Notch signalling imparts.

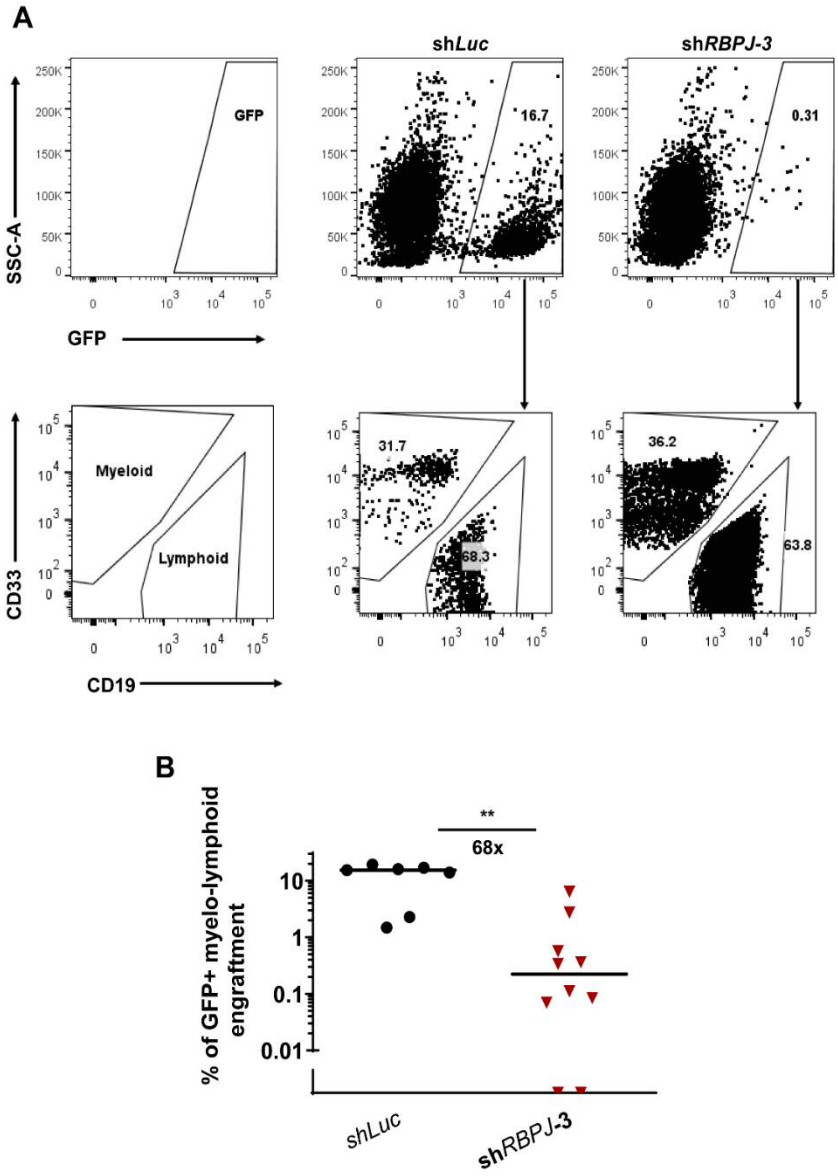

Figure 4.13 – NSG mice transplanted with RBPJ-KD HSPCs have reduced human (GFP⁺) myelo-lymphoid engraftment. (**A**) Representative example of FCM analysis of engraftment. Live cells were gated on the GFP⁺ population then verified for the presence of CD33⁺ and CD19⁺ cells in both conditions. (**B**) The sum of the frequencies of CD19⁺ (Lymphoid) and CD33⁺ (Myeloid) cells in GFP⁺ cells are shown. Each dot represents a mouse and the bar is the median of the values (n=7 for the sh*Luc* cohort; n=10 for the sh*RBPJ-3* cohort). Mann-Whitney test. **p<0.005.

Of note, due to the very low engraftment obtained in mice transplanted with RBPJ-KD HSPCs, this hampered a proper phenotypic analysis of the engrafted primitive sub-populations. Nevertheless, from the few mice that we were able to acquire enough events, we observed,

so far, a 2-fold reduction of the HSC population frequency at 12 weeks post-transplantation (**Figure 4.14**).

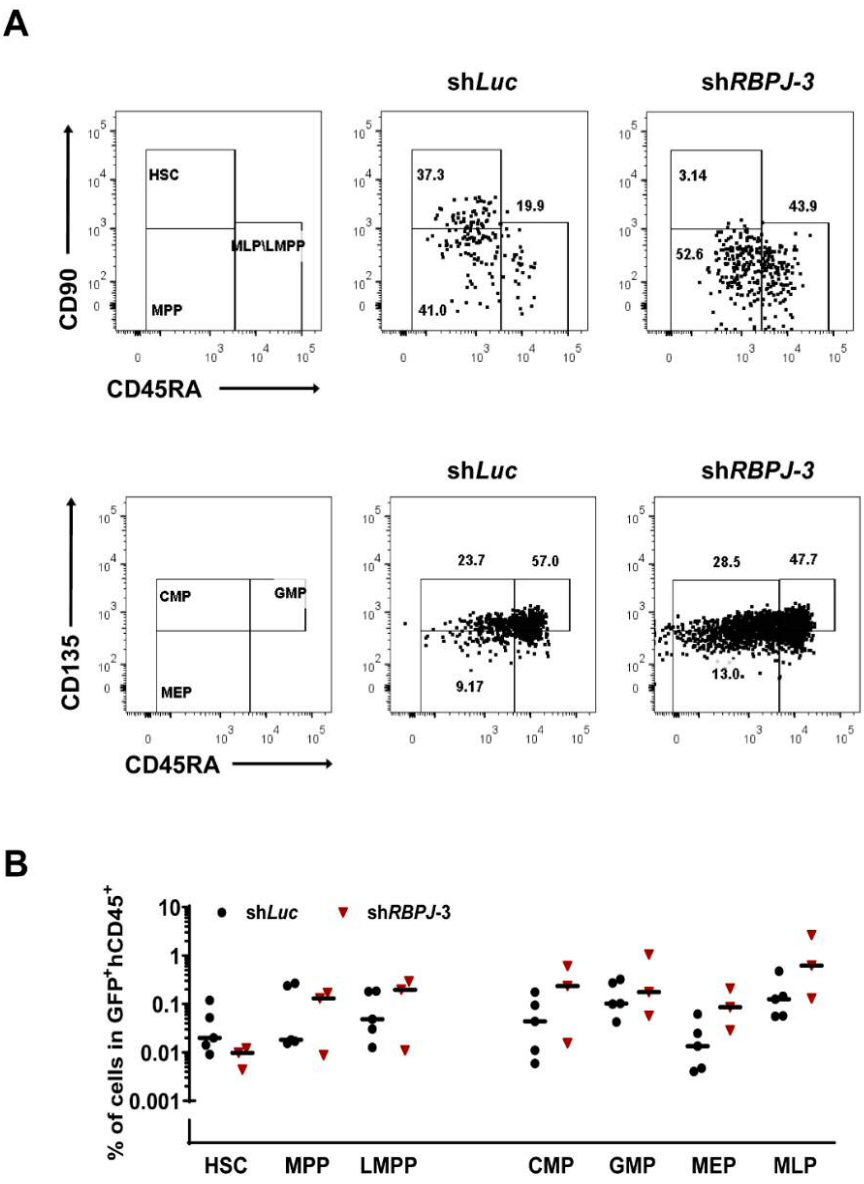

Figure 4.14 – NSG mice transplanted with RBPJ-KD HSPCs have a reduced HSC compartment. (**A**) Representative dot plot of gating strategy for stem and progenitor cells with representative dot plots of shLuc and shRBPJ-3-transplanted NSG mice. (**B**) Quantification of stem and progenitor cells in the various conditions. Each dot represents a mouse (n=5 for the sh*Luc* cohort; n=3 for the sh*RBPJ-3* cohort). Mann-Whitney test. The bar is the median of the values.

When assessing the effects on differentiation, we observed a drastic deficiency in B cell development from RBPJ-KD cells (**Figure 4.15 B**). In addition to this, a significant increase in the frequencies of $CD14^+$ monocytes and $CD11^+$ DCs was also be observed (**Figure 4.15 C**).

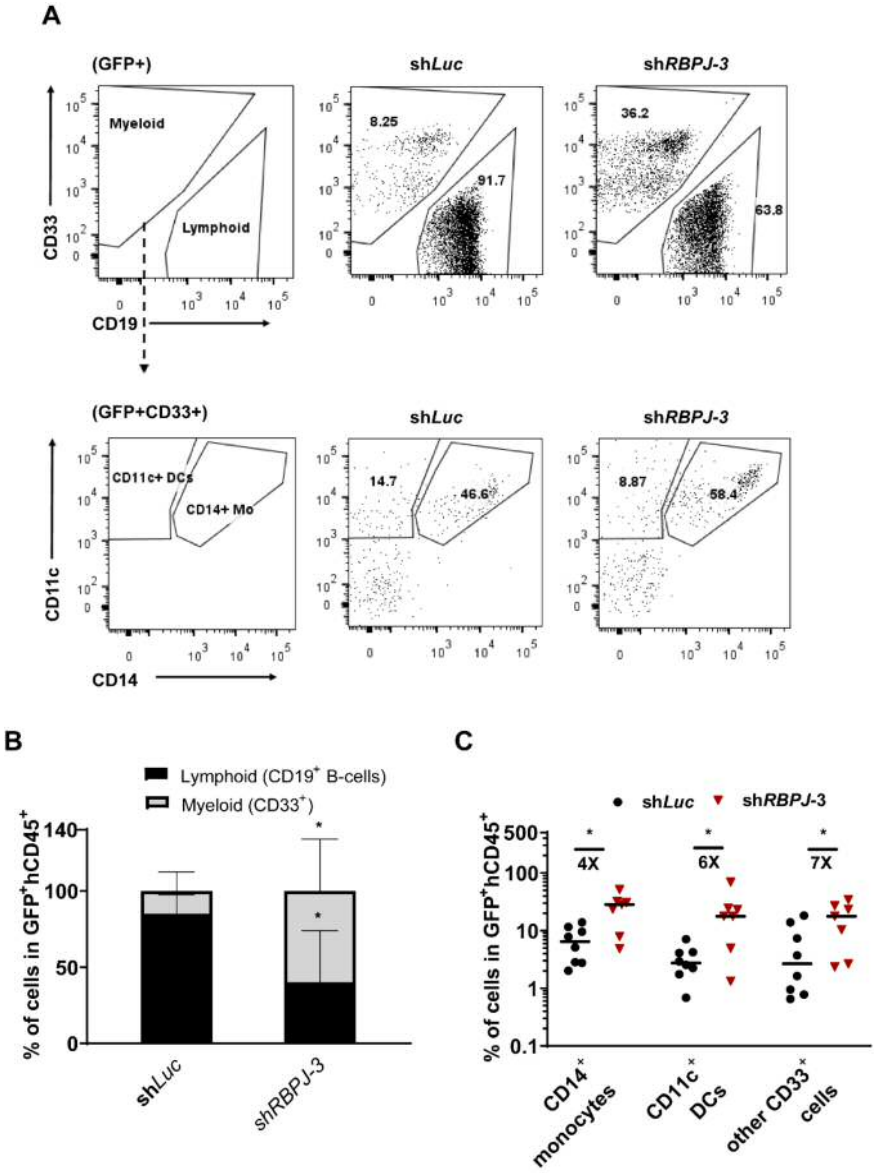

Figure 4.15 - NSG mice transplanted with RBPJ-KD HSPCs have impaired B cell development *in vivo*. (**A**) Representative dot plot of gating strategy for stem and progenitor cells with representative dot plots of sh*Luc* and sh*NCTSN-3*-transplanted NSG mice. (**B**) Quantification of mature cells in the various conditions within GFP^+CD45^+ cells. Each dot represents a mouse (n=8 for the sh*Luc* cohort; n=7 for the sh*RBPJ-3* cohort). The bar is the median of the values. Mann-Whitney test. *p<0.05.

4.5 Discussion

A miR30-based lentiviral system was tested for its ability to silence target gene expression in human HSPCs. However, this system yielded poor transduction efficiencies in this cell type irrespective of the shRNA sequences used. The CS-shRNA lentiviral vector was used instead which efficiently transduced human HSPCs and elicited potent knockdown of Notch target genes.

Blocking Notch signalling by expressing dnMAML1 or by conditional deletion of *Rbpj* had no impact on the preservation of mouse HSC function following transplantation into irradiated recipients (Maillard *et al.,* 2008), (Duarte *et al*., 2018). Additionally, Varnum-Finney and colleagues have not reported a role for Notch1 or Notch2 in murine haematopoiesis during homeostasis (Varnum-Finney *et al*., 2011). On one of the few studies carried out in the human haematopoietic system, Benveniste and colleagues have reported blocked in expansion of HSCs *in vitro* when dnMAML1 was employed but argued that blocking of Notch signalling has no impact in HSC repopulation capacity *in vivo* (Benveniste *et al*., 2014), although we have previously discussed how a different interpretation could be made. In contrast, Notch2 has been shown to modulate BM recovery under stress conditions (Varnum-Finney *et al*., 2011). Here, we showed that canonical Notch signalling inhibition severely impacted the maintenance of CAFCs and phenotypically defined HSCs *in vitro*. In addition, although both myeloid and lymphoid outputs were affected, the latter was even more affected. In fact, activating Notch mutations have been found in B cell leukaemias (Di Ianni *et al.,* 2009), (Puente *et al*., 2011b) implicating this pathway in B cell development. Accordingly, *RBPJ* silencing reduced engraftment and deregulated HSC frequency. However, due to the severe impact that the RBPJ-KD had on engraftment, the number of mice with sufficient engraftment was limited, preventing proper analysis of the stem/progenitor cell compartment. Nonetheless, the reduction in HSCs observed agrees with our previous observations when DAPT was employed, as well as with the *in vitro* studies. Further experiments where higher number of transplanted cells are required to fully appreciate the impact of *RBPJ* silencing in HSCs. Altogether this indicates that canonical Notch signalling is essential for the repopulation of human HSPCs *is vivo*.

As depicted above, most mouse studies revealed little impact on HSCs upon Notch signalling blockage. With the exception of the study performed by Duncan and colleagues in which the authors reported that transplanting dnXSu(H)-transduced c-Kit^{+}Thy1.1^{+}Lin$^{neg/lo}$Sca-1^{+} cells into lethally irradiated mice resulted in a significant decrease in HSC numbers when compared to recipients receiving control cells (Duncan *et al*., 2005). The authors also showed accelerated differentiation from dnXSu(H)- or dnMAML1-transduced haematopoietic stem/progenitor cells. In agreement with their latter observation, several studies have reported the expansion of myeloid cells upon Notch signalling disruption. A *Ncstn*$^{-/-}$ mouse model was shown to develop a CMML-like disease with expansion of GMPs (Klinakis *et al*., 2011). Furthermore, expression of Notch target gene *Hes1* appeared to supress the expression of granulocyte/monocyte-related genes such as *Cebpa* and *Spi1* (Klinakis *et al*., 2011). Also, Francis and colleagues have reported that a double heterozygous mouse model dnMAML1$^{f/-}$ Vav-Cre$^{+/-}$ possessed an increased GMP compartment, at the expense of CMPs. The results

obtained in this project with human HSPCs differ greatly from most mouse studies. Indeed, our data support that Notch is important in the maintenance of HSPCs' regenerative capacity and in the development of B cells, with no apparent role in regulating the GMP compartment.

Interestingly, the different *in vivo* xenotransplantation strategies employed here resulted in a varied degree of outcomes. Pharmacological inhibition of Notch resulted in a reduction of the HSC pool as well as most progenitors. Whole-animal administration of DAPT likely disrupted Notch signalling in all those cell compartments possessing Notch activity leading to major destabilisation of homoeostasis. Furthermore, disturbing Notch signalling in the non-haematopoietic niche also likely further disrupted haematopoietic cell maintenance. In contrast to this, cell-autonomous disruption of Notch signalling *via* shRNA-mediated knockdown of Notch key components caused mainly a reduction in the HSC compartment. By targeting the restricted $CD34^{+}CD38^{-}$ subset, the effects of Notch inhibition are only initially confined to this fraction. We can argue that sustained Notch signalling inhibition may have released HSCs from quiescence and/or enforced differentiation towards committed progenitors. Whether these observations would result in reduced self-renewal capacity could only be confirmed by secondary transplantation of Notch-inhibited cells. Still, the reduction of HSCs appears to be at least in part due to the impaired cell-autonomous of canonical Notch signalling.

Importantly, to better compare the experiments undertaking pharmacological or cell-autonomous Notch inhibition, an inducible shRNA expression system would be necessary. With this, sh*NCSTN-3* or sh*RBPJ-3*-transduced HSPCs could be transplanted into irradiated NSG mice and at 6-7 weeks post-transplantation, sh*RNA* expression would be induced, triggering Notch silencing. Then, the BM of the recipients would be analysed 5-6 weeks later. All in all, we suggest that canonical Notch modulates human HSC maintenance and cell fate *in vitro* and *in vivo*.

Chapter 5 - Exploring the roles of Notch signalling in Acute Myeloid Leukaemia

5.1 Brief introduction

AML is a type of blood cancer characterised by the proliferation of abnormally differentiated haematopoietic cells. The role of Notch signalling in the broad group of leukaemia diseases has been best characterised by the oncogenic role of Notch1 in T-ALL (Weng *et al*., 2004), (Aster *et al*., 2008). In addition, Notch mutations have also been identified in B cell leukaemias and lymphomas (Di Ianni *et al*., 2009), (Puente *et al*., 2011b), (Trøen *et al*., 2008). Conversely, the role of Notch signalling in AML has not been as well elucidated, although notable efforts in the past 20 years have mitigated this. Notch1 and Jag1 proteins were detected in AML (Tohda and Nara, 2001). However, the Notch1 intracellular fragment was determined to be absent in most primary AML samples tested (Tohda and Nara, 2001). Later, Chiaramonte and colleagues also reported Notch receptor expression in AML cells, but Notch target gene *HES1* was expressed at low levels (Chiaramonte *et al*., 2005). Reactivation of Notch signalling has since then emerged as a conceivable therapeutic approach. Tohda and Nara reported that Notch activation through immobilised ligands had a wide range of outcomes depending on the sample analysed (Tohda *et al*., 2005). Since, Notch activation was shown to inhibit proliferation of TF-1 AML cells (Chadwick *et al*., 2008) and CML cell line K562 (Yin *et al*., 2009). More recently and in agreement with these early studies, it was revealed that Notch signalling was silenced in most primary AML cells tested (Lobry *et al*., 2013), (Kannan *et al*., 2013). Lobry and colleagues have further reported Notch silencing in an MLL-AF9-driven mouse model of AML. Reactivation of the pathway prevented disease progression *in vivo*, which was correlated with the induction of apoptosis and differentiation (Lobry *et al*., 2013). Accordingly, Notch signalling reactivation was shown to induce apoptosis with downregulation of *BCL2* (Kannan *et al*., 2013). Interestingly, even though any of the four Notch intracellular domains was used to prevent proliferation of an AML cell line, different effects were observed (Kannan *et al*., 2013), reinforcing the notion that the various Notch-ICDs are not totally redundant. Indeed, several studies have indicated that maintenance of adequate Notch signalling in the BM microenvironment is essential to prevent myeloproliferative disorders in mouse models were introduced in Chapter 1 (Table 1.5). Despite this strong evidence pointing toward a tumour suppressor role for Notch in this context, activating β-catenin mutations in osteoblasts led to upregulated Jag1 ligand expression which subsequently activated Notch signalling in HSCs resulting in AML (Kode *et al*., 2014). In fact, the role of Notch in the crosstalk between the niche and AML cells have further supported stimulation of proliferation (Takam Kamga *et al*., 2016). Here, we proposed to characterise the Notch pathway in primary and AML cell lines, to explore the effects of Notch signalling reactivation and attempted to discriminate between the differential roles of Notch1 and Notch2 receptors in AML.

Aims of Chapter 5

- Measure the expression levels of Notch receptors and their active domains in primary and AML cell lines.
- Assess the effects of Notch activation on primary and AML cell lines on cell frequencies and apoptosis levels when co-cultured with stromal cells and by using Notch agonists such as peptides and small molecules.
- Evaluate the capacity of potential small molecule Notch agonists uncovered by virtual screenings to induce apoptosis in primary and AML cell lines.
- Determine the differential roles of Notch receptor activation on apoptosis of primary and AML cell lines.

5.2 Characterisation of the Notch pathway in primary and AML cell lines

We began by characterising Notch signalling in primary and AML cell lines. Cells and samples representing various cytogenetic background and risk profiles were used in order to have a general overview of the pathway in the several cases. The characteristics of the cells used in this study are summarised in **Table 5.1**.

Table 5.1 – Characteristics of AML cells used.

Denomination	Name	Karyotype/Cytogenetics	Risk profile
AML cell lines	**HL-60**		
	THP-1		
	OCI-AML3		
	KG-1		
	Kasumi-1		
Patient samples	**AML1**	49,xy,+5,+18,+19(5) / 46,xy(13)	Adverse
	AML2	47-48,XX,del(2)(p12),del(5)(p12),?t(6;7)(q21;q32),t(9;?)(q34;?);-11,del(12)(p11),+19,+4 markers[cp9]/46,XX[3]	Adverse
	AML3	(46,XX,+8, FLT3)	Adverse
	AML4	normal FLT3-ITD	Intermediate
	AML5	normal FLT3-ITD, NPM1a	Intermediate
	AML6	NPM1 mutated; Flt3 mutated	Intermediate
	AML7	normal	Intermediate
	AML8	normal	Intermediate
	AML9	NPM1 mutated	Favourable
	AML10	inv16	Favourable
	AML11	NPM1 mutated	Favourable
	AML12	inv16	Favourable
	AML13	t(8;21)	Favourable

Normal – normal karyotype, 46XX or 46XY

The expression of Notch receptors was measured by FCM. For primary AML samples, immunophenotyping was performed. CD99 is nowadays a well-recognised antigen for AML cells (Chung *et al*., 2017). Indeed, we found that all AML samples expressed high levels of CD99 antigen, and as such, after excluding low FSC and SCC cells such as lymphocytes, gating on $CD99^{hi}$ cells was then performed. Within the $CD34^{+}CD38^{+}$ compartment, GMP-like cells ($CD90^{-}CD45RA^{+}$) were found, while MLP-like cells (also $CD90^{-}CD45RA^{+}$) were present in the $CD34^{+}CD38^{-}$ fraction as described in (Goardon *et al*., 2011) (**Figure 5.1**).

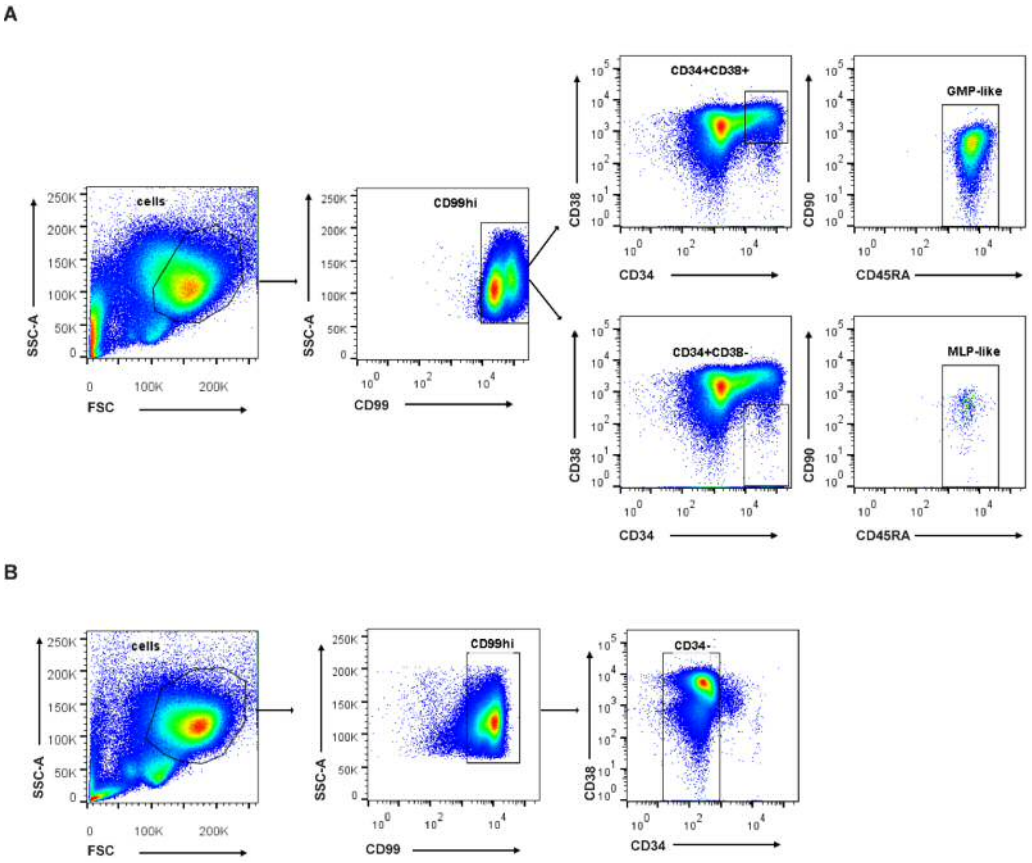

Figure 5.1 - Gating strategy for primary AML samples. Representative example of gating strategy for (**A**) CD34^{+} AMLs (AML3), CD99^{hi} cells contain the CD34^{+}CD38^{+} compartment which can be further separated into GMP-like cells (CD45RA^{+}CD90^{-}). Instead, in the CD34^{+}CD38^{-}, MLP-like cells can be found (CD45RA^{+}CD90^{-}). (**B**) In CD34^{-} AMLs (AML8), the CD99^{hi} compartment contains the population with less than 10% expression of the CD34 antigen. SSC-A – Side scatter-area.

Notch expression was analysed in the main population, which we considered as the whole fraction of CD34^{+} cells in the case of CD34^{+} AMLs (presenting at least 10% of CD34 expression) or the whole fraction of CD34^{-} cells for CD34^{-} cases (less than 10% CD34 expression). No significant differences were found in the expression levels of Notch receptors in the whole population when compared to the main population. Hence, only the expression for the whole population is shown (**Figure 5.2**). For AML cell lines, Notch receptors expression was simply measured on the unfractionated population (**Figure 5.2**).

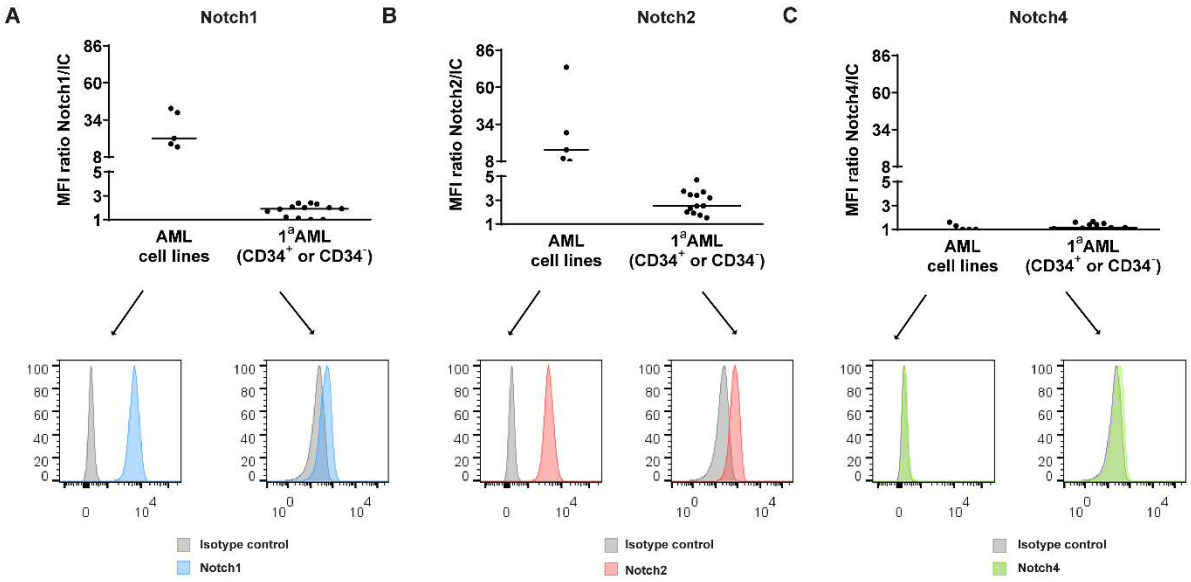

Figure 5.2 – Primary and AML cell lines express Notch1 and Notch2 receptors. FCM analysis of surface Notch receptors. The surface expression of (**A**) Notch1, (**B**) Notch2 and (**C**) Notch4 receptors were evaluated for each AML cell line and primary cell sample. On the bottom representative histograms are shown for AML cell lines (HL60) and primary cells (AML3). The MFI ratio of each receptor (anti-Notch/isotype controls) is shown. The bar is the median. Each dot represents a different sample or cell line.

We found both primary and AML cell lines to express Notch1 and Notch2 receptors. Notch4 receptor could not be detected in any of the samples analysed. In general, AML cell lines possessed greater expression of Notch1 and 2 receptors when compared to primary AML cells. Yet, several studies have reported silencing of the pathway despite expression of surface receptors (Chiaramonte *et al*., 2005), (Lobry *et al*., 2013), (Kannan *et al*., 2013). Hence, to complement this approach, cleaved Notch1 and Notch2 expressions were measured by WB. In agreement with the literature on the topic, we did not detect expression of active Notch components in both primary and AML cell lines for most cases (**Figure 5.3**).

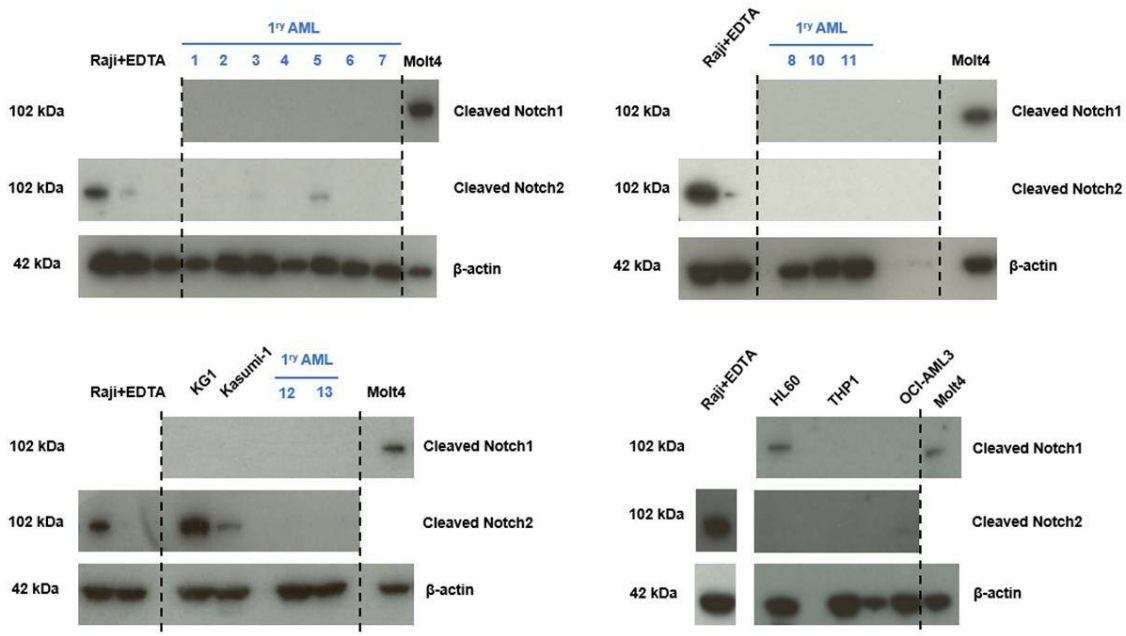

Figure 5.3 – Notch signalling is mostly silenced in primary and AML cell lines. Primary samples (in blue) and AML cell lines (in black) were probed for the expression of cleaved Notch1 or cleaved Notch2 antibodies. Raji cells treated with EDTA and Molt4 cells were used as positive controls for the expression of cleaved Notch2 and cleaved Notch1 receptors, respectively.

Still, we found that some primary AML cells express active Notch2 (AML3 and 5), albeit at low levels. Also, some AML cell lines expressed cleaved Notch1 (HL60) or Notch2 (KG1 and Kasumi-1), suggesting some Notch activity might be retained in some instances. Overall however, the pathway appears to be inactive especially in primary AML samples. Even though evidence can be found in support of both a tumour suppressor and an oncogenic role for Notch in AML, this likely depends on the presence of additional genetic lesions. In any case, given our observation that Notch signalling appears to be silenced in the samples analysed, we next tested the hypothesis that Notch reactivation may be of therapeutic value.

5.3 Notch activation in AML via Delta4-expressing stromal cells

To begin to investigate the potential roles that Notch signalling may have in AML, various AML cell lines were cultured in the presence of a feeder stromal cells layer expressing the Notch ligand Delta4 (S17-Delta4) or with parental S17 cells. The frequency of AML cells was measured four days after seeding. For this, AML cells and murine stromal cells were harvested and stained with human CD45 to distinguish human AML cells from the murine S17 cells. We

observed a significant reduction in the number of AML cells present at the end of culture with S17-Delta4 when compared to the culture on wild type S17s (**Figure 5.4**)

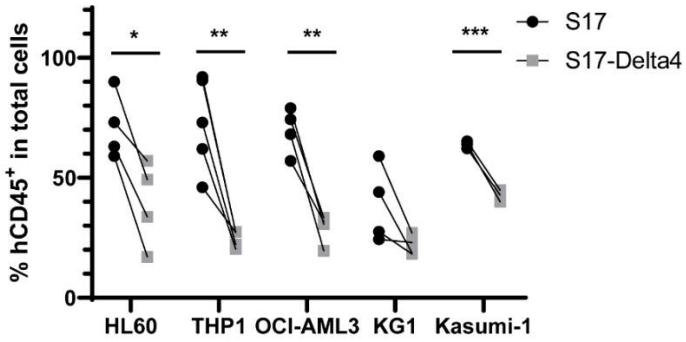

Figure 5.4 – Reduced frequency of AML cell lines when co-cultured in S17-Delta4. AML cell lines were co-cultured on wild type S17 or S17-Delta4 stromal cells. Four days after AML cell seeding, the frequency of human CD45 was analysed by FCM (n=3-5). Unpaired t-test. *p<0.05; **p<0.005 ***p<0.0005.

Simultaneously, apoptosis was quantified by Annexin-V staining at the end of the co-culture. We found a significant increase in total apoptosis (the sum of early and late apoptotic events) in cell lines HL60, OCI-AML3 and KG1 cells and a trending increase in apoptosis in Kasumi-1 cells cultured with S17-Delta4 when compared to the controls (**Figure 5.5**). Still, the THP1 cell line had comparable numbers of apoptotic events in both conditions. This may indicate that the reduction in cell numbers observed earlier may be the result of decreased proliferation and/or changes in the cell cycle.

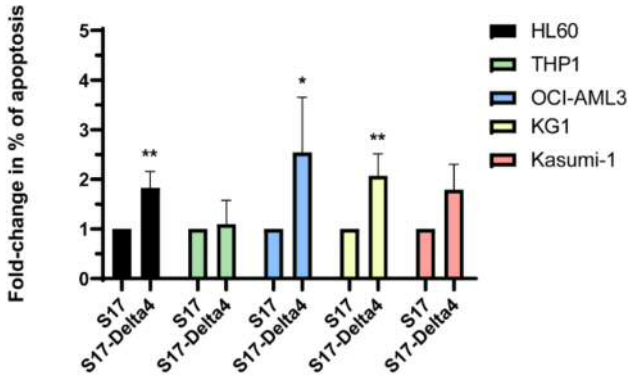

Figure 5.5 – Co-culturing AML cell lines on S17-Delta4 induces apoptosis. AML cell lines were co-cultured on wild type S17 or S17-Delta4 stromal cells. Four days after AML cell seeding, the percentage of Annexin-V+ cells were measured by FCM. (n=3-5) Unpaired t-test. *p<0.05; **p<0.005.

5.4 Notch activation in AML via a Jag1 ligand peptide

These results agree with reports in which membrane-bound ligands were shown to produce a similar effect (Tohda *et al*., 2005), (Kannan *et al*., 2013), (Klinakis *et al*., 2011) and conveyed that Notch signalling reactivation may be of therapeutic value. Nonetheless, a potential therapeutic approach with immobilised or membrane-bound ligands is not practical. For this reason, we tested the ability of a 17-aminoacid peptide based on the DSL domain of Jag1 ligand (herein termed Jag1 peptide) to induce apoptosis when supplemented in the growth media. Various AML cell lines were exposed to increasing concentrations of Jag1 peptide. Two days after treatment, the percentage of live cells was measured (**Figure 5.6**). The HL60 and Kasumi-1 cell lines had a significant response to the Jag1 peptide while OCI-AML3, THP1 and KG1 cells were affected by the DMSO in the vehicle solution. This peptide was reconstituted to the recommended concentration in a mix of DMSO and water (1:1). Serial dilutions were made in water and as such, for higher Jag1 concentrations a higher quantity of DMSO was used, which revealed to be toxic in the THP1 and OCI-AML3 cells above the 60 µM concentration threshold and above 20 µM for KG1 cells. Still, within the non-toxic window, no differences were found between the vehicle and Jag1 peptide conditions in these cell lines.

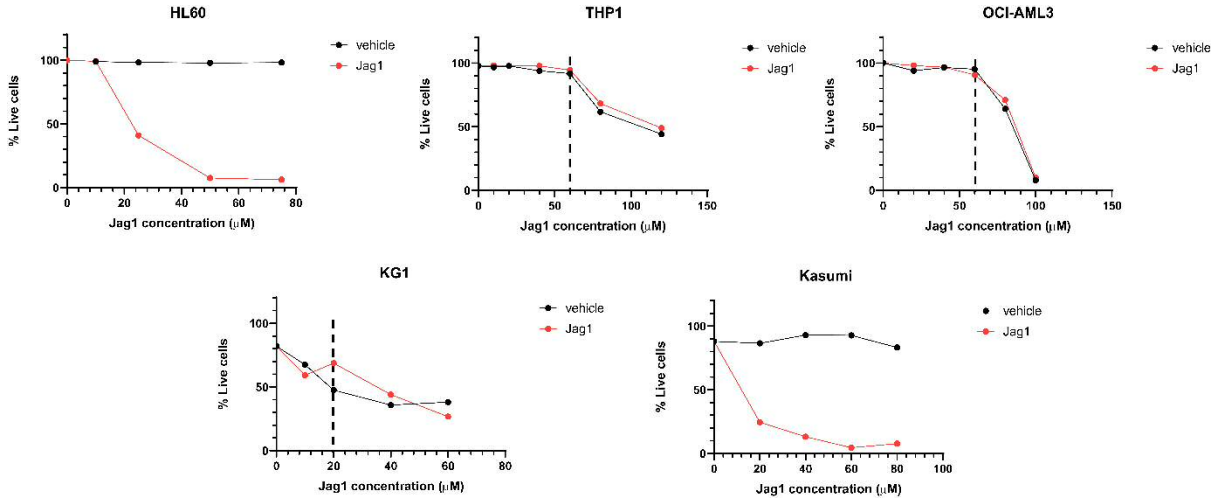

Figure 5.6 – Jag1 titration in AML cell lines. AML cells were treated with increasing concentrations of Jag1 peptide or vehicle and apoptosis was measured by FCM two days after treatment.

A Notch reporter lentiviral construct was generated as described on **Chapter 2** aiming to monitor Notch activity in a quicker and more practical manner (**Figure 5.7**). The vector contains a truncated nerve growth factor receptor (NGFR) sequence under the control of the

EF1α promoter allowing for positive selection by FACS using an anti-NGFR antibody. The mCherry fluorescent protein is controlled by Notch target gene *Hes1* allowing the monitorisation of Notch activity under various assays.

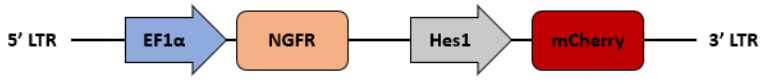

Figure 5.7 – Schematic representation of the Notch reporter lentiviral construct. The EF1α promoter controls the expression of the NGFR selection marker. mCherry expression is controlled by Notch target gene *Hes1*.

The HL60 cell line was transduced with the Notch reporter lentiviral construct at a MOI of 10 and then selected for NGFR expression by FACS. Attempting to distinguish conceivable diverse roles for Notch1 and Notch2 receptors in the regulation of AML cells, the Notch reporter HL60 cell line was then transduced with lentiviral constructs expressing shRNA sequences targeting the *NOTCH1* or *NOTCH2* genes (s*hLuc* was used as a control) previously validated and used in the lab for other projects. The cells were selected for GFP expression by FACS. As seen on **Figure 5.8**, the shRNA sequences were specific to the respective genes and did not affect the expression of the other Notch receptor.

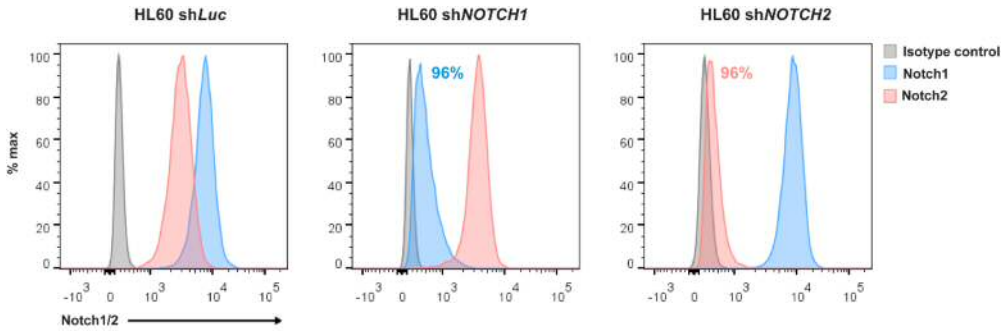

Figure 5.8 – Potent and specific knockdown of *NOTCH1* and *NOTCH2* in HL60 cells. Histograms of Notch1 (in blue) and Notch2 (in red) (isotype control in grey) expression in Notch reporter HL60 transduced with sh*Luc*, sh*NOTCH1* or sh*NOTCH2* lentiviral constructs.

Next, the Notch Reporter HL60 cell line with Notch1 or Notch2 knockdown (here termed NRep-HL60 sh*Luc*, NRep-HL60 sh*NOTCH1*, NRep-HL60 sh*NOTCH2*) were exposed to Jag1 peptide. The concentration chosen (20 μM) was the approximate dose needed to induce 50% cell death (IC50). Two days after the treatment, apoptosis was quantified (**Figure 5.9**).

Interestingly, the Jag1 peptide induced apoptosis in the NRep-HL60 sh*Luc* condition. However, this effect was greatly reduced when either of the Notch receptors was silenced (**Figure 5.9 A** and **B**). Although not pointing toward preferential activation through Notch1 or Notch2 receptors, these results may instead suggest that both receptors are required perhaps in a synergistic way, or that the levels of Notch activation are important in this setting. Additionally, upregulation of mCherry protein expression was detected upon Jag1 peptide treatment indicating Notch activation through *HES1* – an effect that was abolished when either Notch1 or Notch2 receptor was absent (**Figure 5.9 C**).

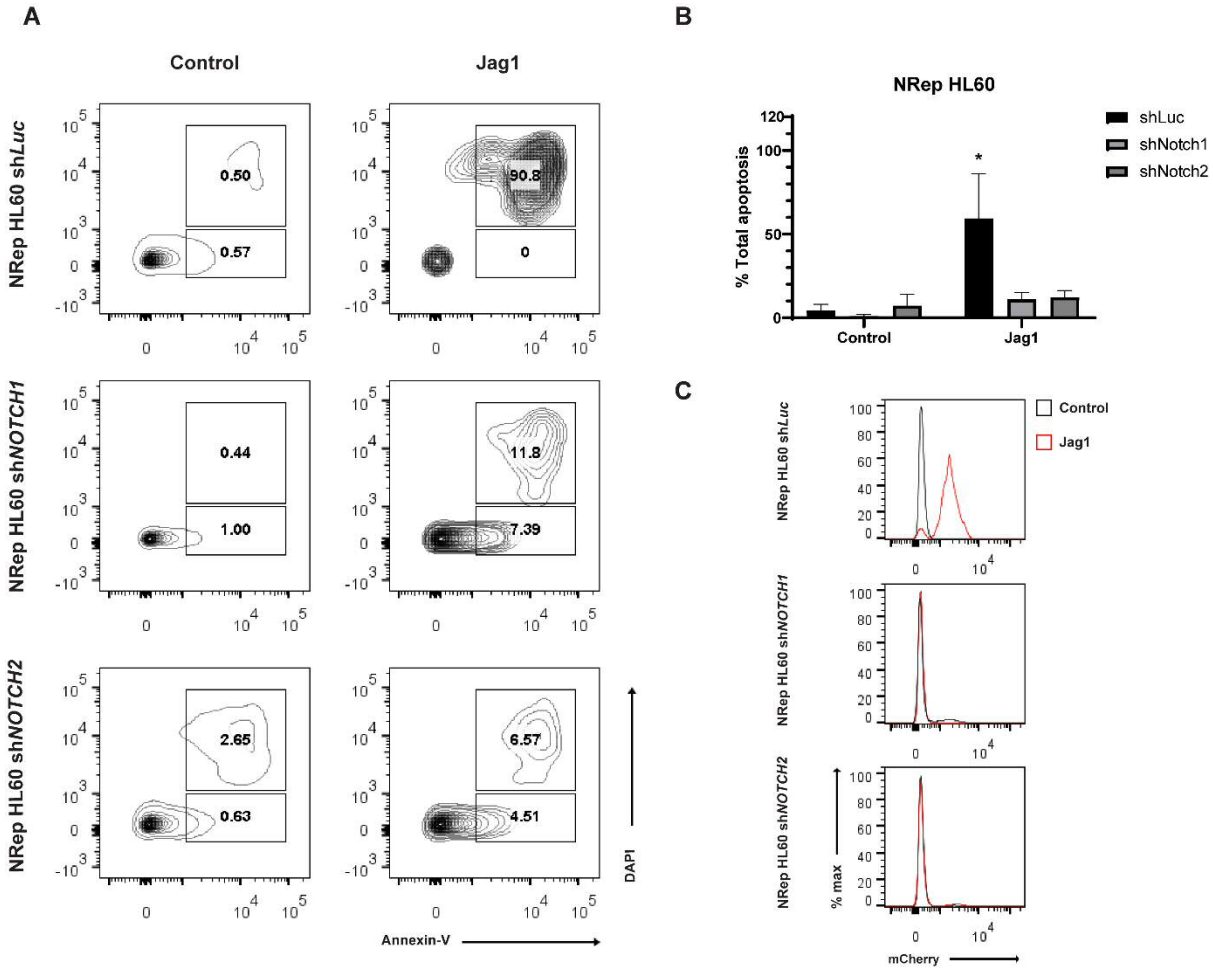

Figure 5.9 – Jag1 peptide induces apoptosis in the HL60 cell line via Notch activation. Jag1 peptide (20μM) was added to HL60 cells. After two days, Annexin-V⁺ cells were quantified. (**A**) Representative example of increased apoptosis in NRep HL60 cells upon Jag1 treatment, (**B**) quantification of apoptosis, (**C**) induction of mCherry expression upon Jag1 treatment. Bars are the mean ± SD (n=3). Unpaired t-test. *p<0.05; **p<0.005.

5.5 Notch activation in AML via small molecules

Next, we explored the use of small molecules with Notch agonistic properties to circumvent the limited bioavailability issues of peptide-based therapies (Craik *et al*., 2013). Thus, a collaboration with Professor Andrea Brancale from the School of Pharmacy at Cardiff University was established. The aim was to uncover small molecules with general Notch agonistic properties and/or agonists of specific receptors. By using a 3D generated model of the Notch1-Jag1 interaction (**Figure 5.10 A**), over three million compounds were virtually screened for their likeliness to interact with Notch receptors. Structure-based virtual screening uses the 3D structure of the target to find cognate partners, whereas ligand-based virtual screening uses the 3D structure of the ligand to filter a library of small molecules. After a series of filtering steps, a short list of 117 compounds was generated. Filtering steps included visual inspection for the ability of candidate molecules to interact and occupy with selected binding site. Molecules should also comply with Lipinski's rule of five (Lipinski *et al*., 2001). Briefly, this analysis shows that poor absorption of permeation of a compound is more likely when there are more than five hydrogen-bond donors; molecular mass is greater than 500 Da; high lipophilicity and the sum of nitrogen and oxygen atoms is more than 10 (Lipinski *et al*., 2001).

These guidelines determine the likeliness that a chemical compound can be used as an orally active drug in humans. In **Figure 5.10 A**, a predicted model for the Notch/Jag1 interaction is shown (Notch1 receptor in purple, Jag1 ligand in orange). Importantly, the natural structure of this interaction would be uncovered by protein crystallography. However, no data on this has been generated yet. In **Figure 5.10 B** and **C**, candidate molecules uncovered by ligand- or structure-based are depicted in green and red as docked on the Notch1 receptor binding domain (in purple), respectively. Aromatic rings can be observed in the same location that the Jag1 ligand (in orange) at Phe199 interacts with Notch1 receptor. This in addition with hydrogen interactions along the length of the compound may indicate a potential agonistic capacity from this and structurally similar compounds, mimicking the interaction between Jag1 ligand and Notch1 receptor. Of note, the drug screening and analysis of candidate molecules was performed by Professor Andrea Brancale lab members. To first assess whether the computational evaluation translated into biological activity, only 19 compounds were selected due to being commercially available at a trusted company. Of those, the top six scoring molecules were tested for this study.

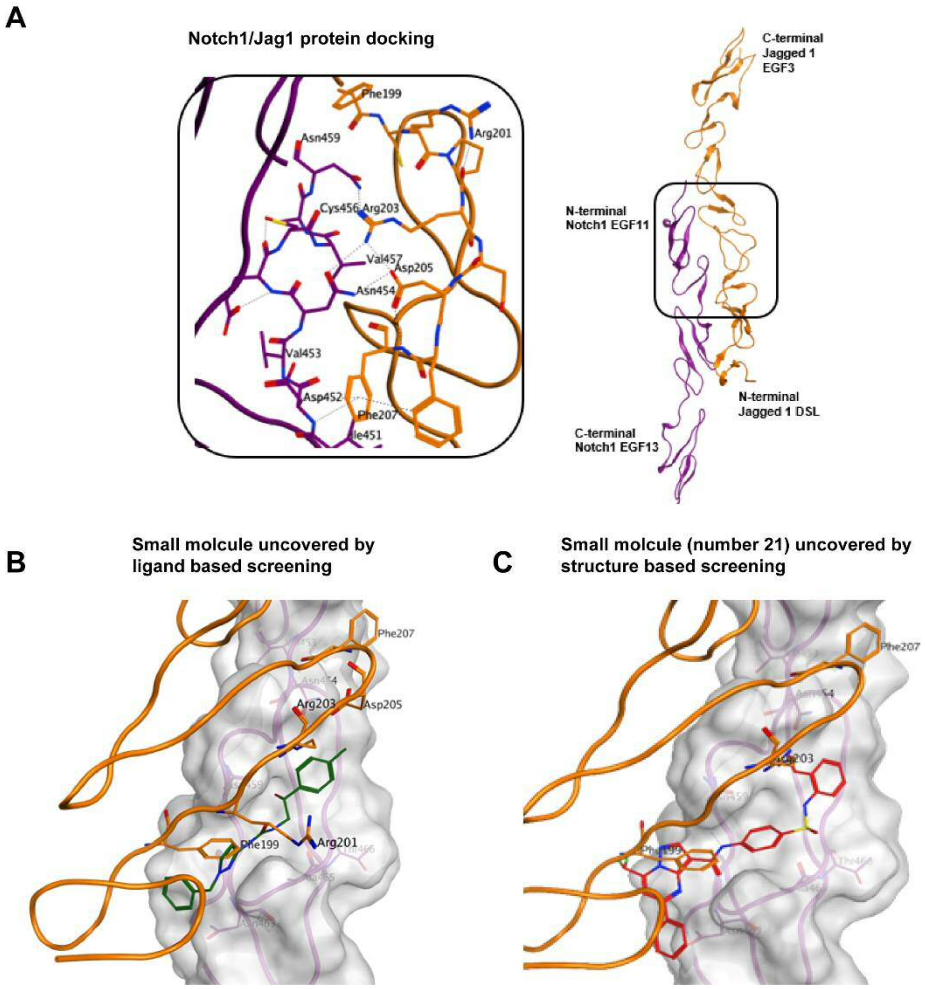

Figure 5.10 – Small molecule interaction with Notch1. After (**A**) 3D modelling of the Notch1/Jag1 interaction, ligand based (**B**) or structure based (**C**) screening uncovered molecules that theoretically interact with Notch1 receptor at the same positions as natural ligand Jag1. Notch1 receptor in purple, Jag1 ligand in orange, compound "X" in green and compound number 21 used in this study in red. (Adapted from the models generated by Julija Jotautaite at the School of Pharmacy from Cardiff University).

The five AML cell lines were exposed to the various compounds and apoptosis was measured the next day. Varied outcomes were observed, but compounds 24 and 31 induced the most apoptosis in various cell lines (**Figure 5.11**). As such, these compounds were selected for the remaining experiments.

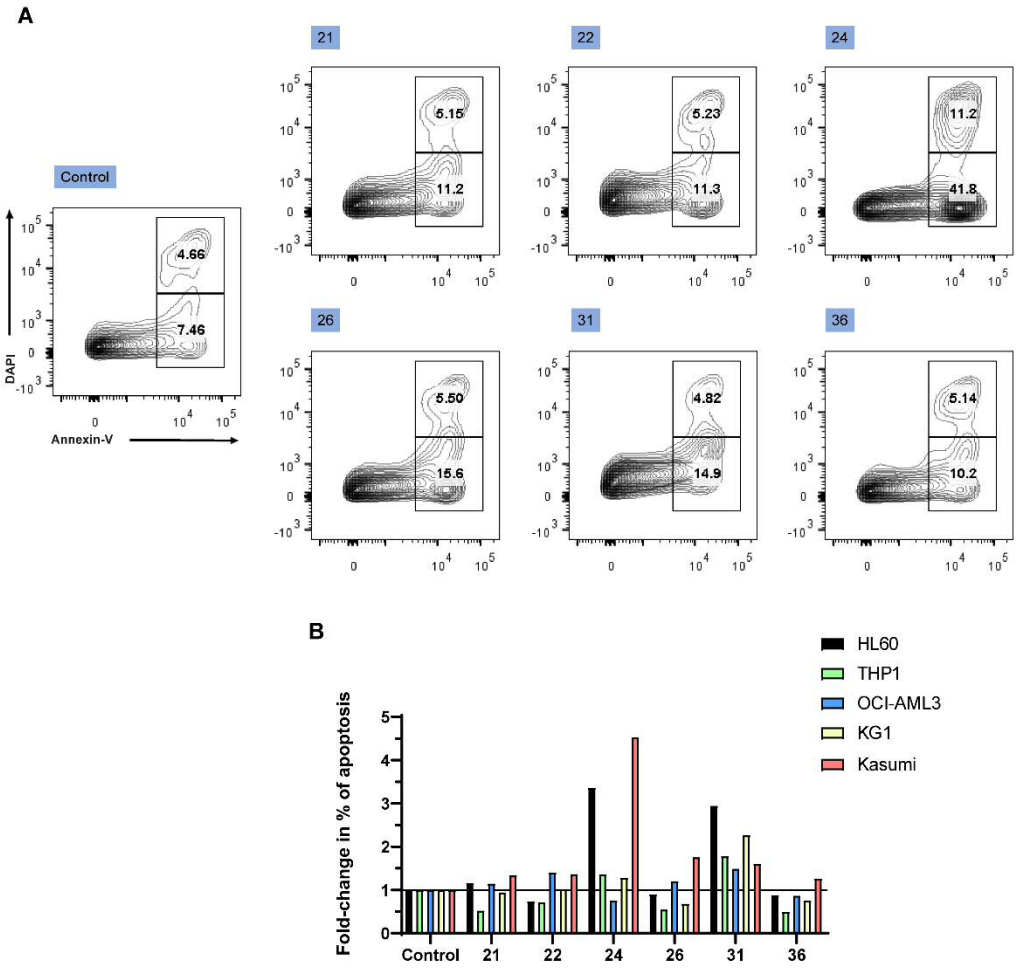

Figure 5.11 – Drug screening in AML cell lines. (**A**) Representative dot plot of an AML cell line (Kasumi) treated with the various drugs at a final concentration of 10 μM. The cells were analysed for the presence of Annexin-V 24 h after treatment. (**B**) Quantification of apoptosis induced by various compounds in the indicated AML cell lines.

In order to address whether any potential toxicity caused by these small molecule treatments is due to a reactivation of Notch pathway, AML cells were pre-treated with a γ-secretase inhibitor (compoundE, herein abbreviated to compE) or DMSO for 2 h prior drug treatment. After that, the compounds were added at a final concentration of 10 μM. The next day, apoptosis levels were measured by FCM (**Figure 5.12**). We noticed a generalised induction of apoptosis by both drugs in several cell lines. Unfortunately, this revealed to be independent of Notch activation. Therefore, future testing on these small molecules will address whether the cytotoxic effects are confined to AML cells. If so, dissection of the Notch-independent mechanisms by which these compounds induce apoptosis may be of therapeutic value.

A

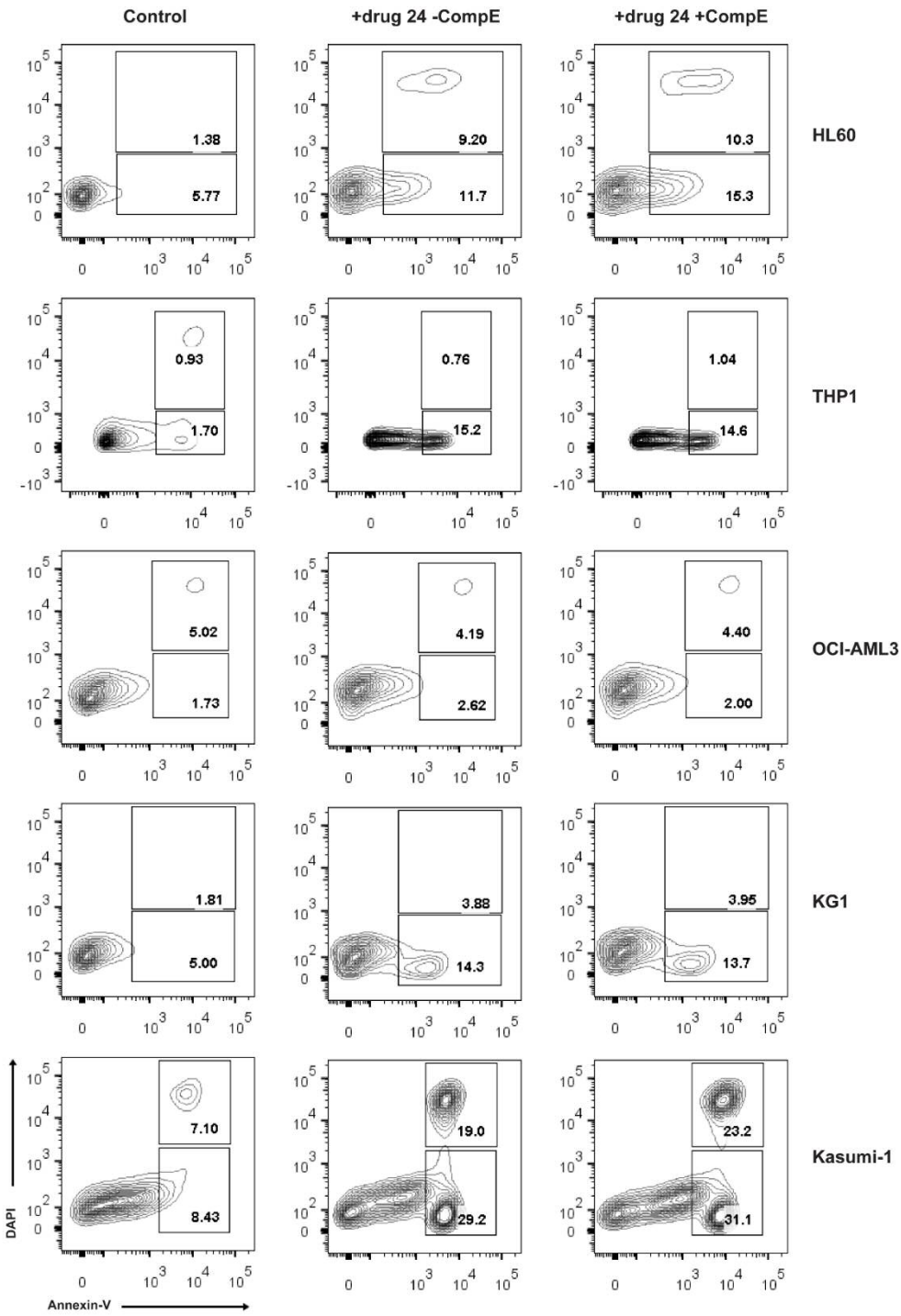
Control
+drug 24 -CompE
+drug 24 +CompE
HL60
1.38
5.77
9.20
11.7
10.3
15.3
THP1
0.93
1.70
0.76
15.2
1.04
14.6
OCI-AML3
5.02
1.73
4.19
2.62
4.40
2.00
KG1
1.81
5.00
3.88
14.3
3.95
13.7
Kasumi-1
7.10
8.43
19.0
29.2
23.2
31.1
DAPI
Annexin-V

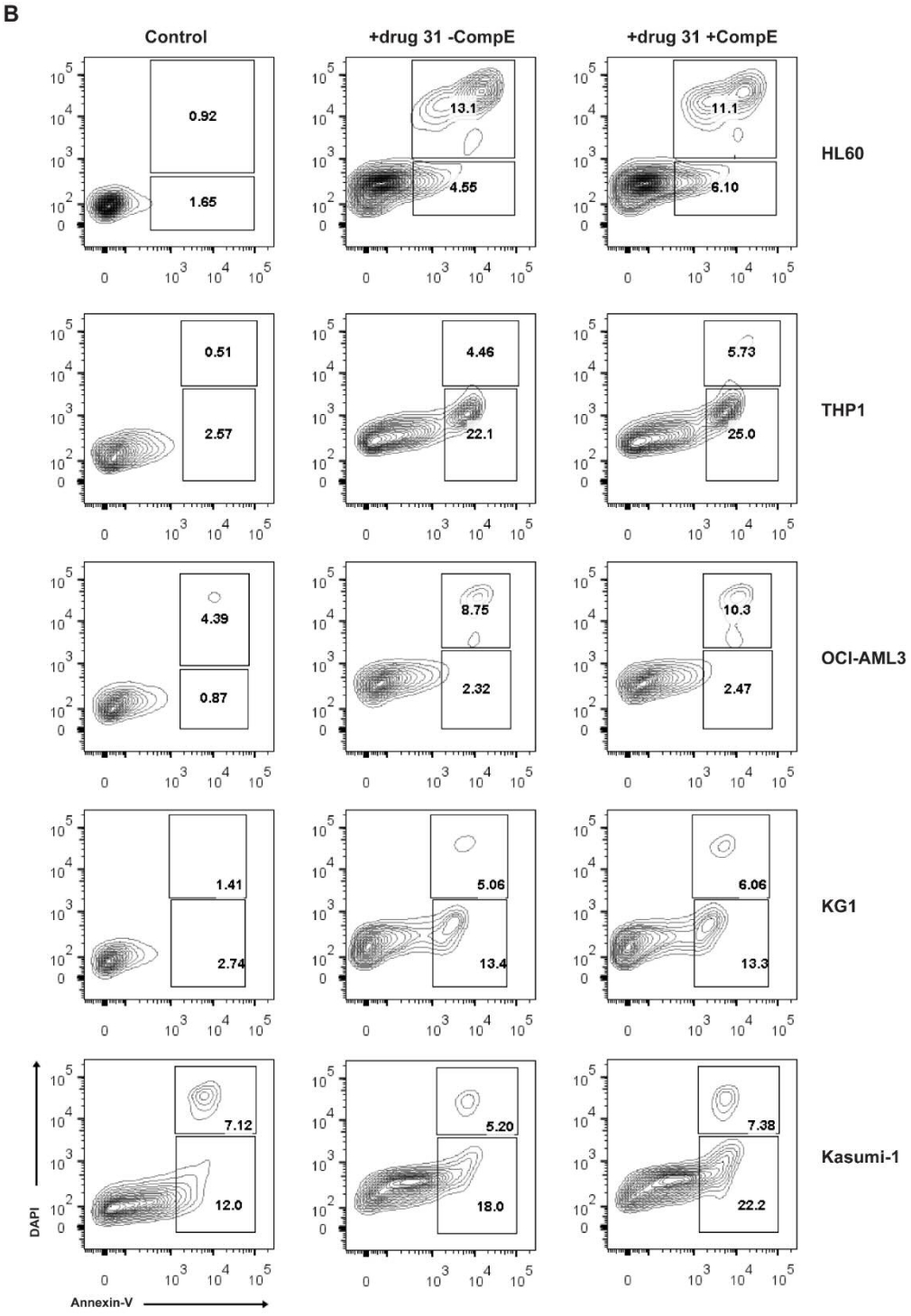

Figure 5.12 – Drugs 24 and 31 induce apoptosis in AML cell lines in a Notch-independent manner. Representative dot plots of AML cell lines treated with (**A**) drug number 24 and (**B**) drug number 31. The cells were analysed for the presence of Annexin-V 24 h after treatment (n=2).

5.6 Discussion

The results presented in this study support other published findings that despite Notch receptor expression on AML cells (especially on cell lines), the cleaved fractions of the receptors could not be detected in most samples analysed. Culturing AML cell lines on S17-Delta4 stroma resulted in decreased AML cell frequency in all cell lines tested and induced apoptosis in some. Still, in some cases, a reduced number of AML cells was detected without apparent changes in apoptotic levels. This may instead indicate altered cell cycle kinetics and proliferation as a result of Notch activation – an effect that has been reported before (Carlesso *et al*., 1999), (Sarmento *et al*., 2005). Even so, THP1 cells have been reported to undergo apoptosis following ligand stimulation (Lobry *et al*., 2013), (Kannan *et al*., 2013). Lobry and colleagues reported apoptosis induction 48 h following stimulation with immobilised plate bound Delta4 ligand (Lobry *et al*., 2013), while others presented induction of apoptosis 24 h after co-culturing THP1 cells on HS5 stromal cells expressing Delta1 (Kannan *et al*., 2013). Here, we determined that measuring apoptosis at the fourth day of the co-culture yielded higher percentages of apoptosis (personal observations). Therefore, this timepoint was used to better reveal putative differences between the conditions tested. Yet, future work will involve determining the kinetics of apoptosis for all cell lines tested as different timepoints may be required.

Following the observation that Notch reactivation through membrane bound ligand induces apoptosis and perhaps cell growth arrest in AML cell lines, we then used a Jag1 peptide in solution which would more closely resemble a possible therapy approach. This peptide was shown to possess cytotoxic activity in both primary and AML cell lines (Kannan *et al*., 2013). In our study, we observed a dose-dependent decrease in viability in HL60 and Kasumi-1 cells. To better measure Notch activity, HL60 cells were transduced with a Notch reporter and subsequently with shRNA sequences targeting the *NOTCH1* or *NOTCH2* genes. So far, only HL60 cells were tested given their response to membrane bound Delta4 and to soluble Jag1 peptide. Following validation of the Notch reporter and specificity of shRNA sequences, we observed an increase in the number of apoptotic cells in NRep-HL60 sh*Luc* treated with the Jag1 peptide when compared to vehicle treated. This effect was abolished in the HL60 cell line when either *NOTCH1* or *NOTCH2* were silenced, perhaps suggestive of the importance of signalling levels. Importantly, a Notch reporter construct indicated that apoptosis was mediated via Notch signalling activation. Still, cell lines representing other AML subtypes should be tested. While remaining a serious condition, the HL60 cell line represents the acute promyelocytic leukaemia subtype which owing to advances in diagnostics and treatments is

nowadays considered the most curable of adult acute myeloid leukaemias, with complete remission rates as high as 90% (Coombs *et al*., 2015).

Future confirmation of Notch reactivation should be done by detecting the cleaved forms of Notch receptors by WB with simultaneous use of Notch signalling inhibitors. Importantly, improvements on the Jag1 peptide experiments should be considered. The peptide was diluted in a mix of water and DMSO (1:1) at the recommended stock solution concentration. However, we observed high toxicity in OCI-AML3, THP1 and KG1 cell lines with vehicle only preventing its use in these cell lines. Therefore, requesting to synthesise larger amounts of the peptide in order to have a significantly lower DMSO/Jag1 peptide ratio to overcome the toxicity issues caused by DMSO in these cell lines would allow to uncover concentrations at which the peptide may have a potential effect in these cell lines. Additionally, the remaining AML cell lines used in this study should be transduced with the Notch reporter construct as well as the various Notch receptor silencing lentiviral vectors, providing valuable tools for the study of Notch signalling in AML with different genetic backgrounds.

The HL60 cell line with *NOTCH1* or *NOTCH2* KD generated during this study provided a tool for studying the role of Notch in AML. However, due to time constraints, limited testing was performed with these cell lines. In addition to stroma expressing Delta4, it would be interesting to assess whether different membrane bound ligands result in a different outcome. As mentioned earlier, mice constitutively expressing active β-catenin is osteoblasts exhibit upregulation of Jag1 ligand which promotes AML development (Kode *et al*., 2014) further showcasing the role of the niche in this context. It would be interesting to address the effect of membrane bound Jag1 ligand in AML cells. In combination with the several AML cell lines with *NOTCH1* or *NOTCH2* KD, these experiments could establish what are the consequences of each ligand/receptor pairing regarding cell growth, differentiation and apoptosis providing valuable insight into AML biology. In fact, mice with haematopoietic cells expressing the Notch1-ICD have been reported to develop aggressive T-ALL (Pear *et al*., 1996), (Lobry *et al*., 2013). On the contrary, expressing Notch2-ICD supressed MLL-AF9 driven AML development *in vivo* and did not result in T-ALL (Lobry *et al*., 2013). Therefore, the design of Notch2 specific agonists emerges as an attractive option. Still, given the different genetic background in the various AML subtypes, it would be relevant to address which specific cases might benefit from this approach. With the advent of molecular biology and recombinant protein tools, a new class of protein-based drugs have been explored since then. Within this class, antibodies have seen a tremendous success in their use for a variety of diseases (reviewed in (Craik *et al*., 2013). High potency and selectivity with potentially lower toxicity than small molecules turn peptide-based therapeutics into an attractive option. Still, disadvantages including poor metabolic stability and membrane permeability, limited oral bioavailability and rapid clearance limit their

usefulness (Craik *et al*., 2013). Improving peptide screening and new delivery formulations may circumvent some of these issues allowing for their more widespread use in clinical settings. Therefore, in addition to the Jag1 peptide, we attempted to uncover potential small molecule agonists of Notch signalling. Six small molecules were tested for their ability to induce apoptosis in AML cells. Despite two of the six molecules tested exhibited cytotoxicity effects, this was shown to be independent of Notch reactivation. Nonetheless, if cytotoxicity is proven to be specific to AML cells while sparing normal haematopoietic cells, these compounds should warrant further investigation. A vast array of small molecules has been tested for their antagonistic capacities toward Notch – particularly relevant in T-ALL cases (reviewed in (De Kloe and De Strooper, 2014). Conversely, with the growing body of evidence demonstrating a potential tumour suppressor role for Notch in AML, small molecules with Notch agonistic properties have instead emerged as promising potential therapies for AML. In one example, N-methylhemeanthidine chloride (NMHC), a compound derived from the plant *Zephyranthes candida* has shown promising and specific cytotoxicity toward AML cells, while sparing B-ALL, T-ALL and CML cells (Ye *et al*., 2016a). Remarkably, NMHC administration significantly reduced tumour development in a human AML xenograft model (Ye *et al*., 2016a).

Finally, due to time constraints, the various Notch signalling reactivation approaches could not be tested on primary AML cells. Future work will involve investigating whether the effects observed on AML cell lines are valid on primary AML cells which should provide further insight into the clinically relevant aspects of Notch in this disease. In summary, Notch appears to be silenced in human AML cells and reactivation of this pathway through different means indicated suppression of proliferation and induction of apoptosis. Pursuing the development of Notch receptor specific agonists should be a valuable strategy toward the development of more specific AML treatments.

Chapter 6 – Conclusions

The Notch pathway has a well characterised role in the emergence of HSCs during development (Kumano *et al.,* 2003). Further to this, several studies showed a positive role for Notch regulation in HSPCs (**Chapter 1**, **Table 1.3**). This was achieved by various methods such as direct exposure of stem and progenitor cells to Notch ligands *in vitro*, expressing Notch intracellular domains or downstream targets. These gain-of-function studies have consistently demonstrated that activation of this pathway is implicated in increased in HSC self-renewal (Varnum-Finney *et al*. (1998), (Carlesso *et al*., 1999), (Karanu *et al*., 2001), (Ohishi *et al*., 2002), (Kunisato *et al*., 2003), (Calvi *et al*., 2003), (Varnum-Finney *et al*., 2003), (Lauret *et al*., 2004). Consequently, Notch signalling has been exploited as a strategy for the *ex vivo* expansion of HSCs for clinical purposes (Delaney *et al*., 2010). On the other hand, loss-of-function studies have generated a variety of outcomes including depletion or no effect on HSCs (Duncan *et al*., 2005), (Maillard *et al*., 2008). The employment of varied mouse models, the loss of function approach undertaken (loss of specific Notch receptors, ligands, or Notch coactivators (RBPJκ) or overexpression of dominant negative molecules) all contributed to the variety of outcomes reported. In addition, researchers disagree on the levels of Notch signalling present in mouse HSCs. Maillard and colleagues have proposed that stem cells have low levels of Notch signalling *in vivo* under homeostatic conditions (Maillard *et al*., 2008). On the contrary, using transgenic Notch reporter mice, Duncan and colleagues have suggested that cells with primitive phenotype showed high Notch signalling activity *in vivo* and was downregulated when HSCs differentiated (Duncan *et al*., 2005). Despite all these controversies, little has been described on role of this signalling pathway in human HSPC regulation and this was one of the emphasis of this project. Thus, the work reported in this thesis set out to explore the role of Notch signalling in the regulation of human HSPCs and AML cells.

Firstly, we showed that Notch1 and 2 receptors were highly expressed in all stem and primitive progenitor cell compartments analysed. However, we observed slightly higher Notch1 and 2 receptor activation in HSCs despite that these cells did not harbour the highest cell surface expression as compared to other primitive populations. By employing DAPT as a pan-Notch inhibitor, we observed a significant reduction in myelo-lymphoid engraftment along with a decline in most stem/progenitor cell compartments, whereby the HSC frequency within the human graft was reduced by 7-fold when compared to the vehicle treated cohort. Cell-autonomous suppression of Nicastrin or RBPJκ expression led to reduced LTC-IC capacity with reduction of HSC fraction and deregulated mature progenies. Agreeing with these observations, cell-autonomous silencing of *NCSTN* or *RBPJ* resulted in decreased myelo-lymphoid engraftment in NSG mice, especially when *RBPJ* was silenced. The HSC fraction was significantly reduced by the silencing of either *NCSTN* or *RBPJ* and consequently reduced

numbers of mature cells were found as well. Overall, the results presented here contrast with most mouse studies and support the notion that the Notch pathway is important in the maintenance of HSPCs during regeneration. Nonetheless, secondary transplantation of Nicastrin-KD and RBPJ-KD HSPCs should be performed to reveal the roles of Notch signalling in HSC self-renewal.

Regarding the role of Notch pathway in the differentiation of haematopoietic cells, several studies have also reported varied results. Approximately 12% of B cell chronic lymphocytic leukaemia patient samples harbour Notch activation mutations suggesting a role for Notch signalling in B cell differentiation (Puente *et al*., 2011). In fact, deletion of *Rbpj* or *Notch2* in B cell progenitors impaired marginal zone B cells while enhancing follicular B cell development (Tanigaki *et al*., 2002), (Saito *et al*., 2003). Loss of Notch1 receptor or RBPJκ in adult BM cells prevents T cell development with concomitant ectopic appearance of B cells in the thymus (Han *et al*., 2002), (Radtke *et al*., 1999), (Wilson *et al*., 2001). Moreover, through lineage tracing experiments in mice, Oh *et al* proposed that Notch signalling acts at different nodes of differentiation in special localised niches, whereby Notch1 receptor has been implicated in commitment towards the lymphoid lineage while Notch2 receptor initiates erythroid differentiation (Oh *et al*., 2013). Conversely, the idea that Notch signalling imposes repression on myeloid transcription factor programme has been suggested (Klinakis *et al*., 2011). Approximately 12% of CMML patient samples possess Nicastrin loss of function mutations. Additionally, HES1 was suggested to supress GMP-associated genes *Cebpa* and *Spi1,* and when Nicastrin was lost, de-repression of a myeloid specific programme was observed (Klinakis *et al*., 2011). The authors further complemented this by showing that culturing CB $CD34^{+}CD38^{-}$ HSPCs with Notch ligands had supressed differentiation towards granulocyte and monocyte lineages (Klinakis *et al*., 2011). Even though we did not detect expansion of any specific cell lineage given the significant reduction of all cells analysed, B cell development was more affected than myeloid differentiation in the RBPJ-KD condition. As such, our observations of *in vitro* and *in vivo* B cell development impairment from RBPJ-KD cells indicate RBPJk to be required for proper B cell development. While it is difficult to pinpoint the reasons for these results, most likely non-canonical Notch-independent RBPJκ roles may be involved. This has been described in other systems, whereby for instance the pancreas specific RBPJκ loss phenotype is drastically different from the pancreas specific Notch1/2-deficient mice (Nakhai *et al*., 2008). Whereas RBPJκ loss in pancreatic progenitor cells led to premature differentiation and decrease in endocrine progenitor cells, the loss of Notch1 and Notch2 receptors only caused a moderate reduction in proliferation of pancreatic epithelial cells (Nakhai *et al*., 2008). Elucidation of Notch-independent RBPJκ functions revealed the interaction of RBPJκ with Ptf1a/p48 – a transcription factor indispensable for pancreas

development (Obata *et al*., 2001). The domain of RBPJκ interacting with Ptf1a is the same as the Notch receptor RAM binding domain and appears to be mutually exclusive. Therefore, competition for the RBPJκ binding site occurs between Ptf1a and the NICD (Beres *et al*., 2006). Still, mutations resulting in dominant negative effect of Nicastrin, but not the loss of RBPJκ, results in CMML-like disease in mice (Klinakis *et al*., 2011), (Han *et al*., 2002) thus, a similar mechanism may operate in this context as well. Adding to the complexity of the system, RBPJκ was initially considered a transcriptional repressor (Dou *et al*.,1994), (Hsieh *et al*., 1995). And in fact, it is believed that in some instances, in the absence of NICD, RBPJκ recruits co-repressors to supress target gene expression (reviewed in (Bray, 2016)). Recently, Duarte *et al* reported upregulation of *Hes1* and *Hes5* in the absence of *Rbpj* in megakaryocyte and erythrocyte progenitors, suggesting a repressive role for RBPJκ in the absence of Notch signalling (Duarte *et al*., 2018). Analysing the transcriptome of Nicastrin-KD and RBPJ-KD HSPCs by RNA sequencing should elucidate on the possible downstream mechanisms involved in the regulation of these cells. Additionally, chromatin immunoprecipitation assay (ChIP) sequencing may expose the DNA binding sites for the RBPJκ coactivator/corepressor complex.

Beyond the deletion of pathway members including *Ncstn* (Klinakis *et al*., 2011), *Rbpj* (Wang *et al*., 2014) and *Adam10* (Yoda *et al*., 2011), regulators of Notch receptor post-translational modifications such as Presenilins (Qyang *et al*., 2004), FX (Zhou *et al*., 2008) and Pofut (Yao *et al*., 2011) have been implicated in the generation of myeloproliferative diseases in mouse models (see **Table 1.5**), demonstrating the requirement for adequate levels of signalling in preventing malignant transformation. But determining the role of Notch pathway in myeloid malignancies has proved to be a complex task owing to the genetic diversity of the diseases, the pleiotropic roles of this pathway and the experimental differences in reported studies (mouse models, immortalised cell lines or primary cells, *in vitro* or *in vivo*). In chronic myeloid leukaemia (CML) mouse models - a myeloproliferative disease driven the *BCR-ABL1* fusion gene, HES1 appears to cooperate with BCR-ABL1 to promote CML blast crisis (Nakahara *et al*., 2010). On the other hand, *HES1* downregulation was associated with blast crisis in human samples (Sengupta *et al*., 2007) and Notch signalling reactivation supressed cell growth suggesting a tumour suppressor role in this case (Yang *et al*., 2013), (Yin *et al*., 2009). Therefore, mouse and human studies show conflicting results and as such, additional research might clarify these disagreements.

Whether Notch signalling has an oncogenic or tumour suppressor role in AML may depend on the presence of additional genetic lesions. For example, in a rare subset of acute megakaryocytic leukaemia, the OTT-MAL fusion protein activates *RBPJ* (Mercher *et al*., 2009). Also, indirect evidence of Notch signalling involvement in AML was shown by Notch

target Trib2 which enhanced proliferation of myeloid progenitors and promoted AML through degradation of C/EBPα (Keeshan *et al*., 2006). In acute promyelocytic leukaemia, an enhanced Notch expression signature was found in both human primary APL cells and in pre-leukemic cells derived from *Ctsg-PML-RARA* mice (Grieselhuber *et al*., 2013). The authors reported that the PML-RARA fusion protein caused Notch signalling activation, which promoted self-renewal in myeloid progenitors without affecting downstream commitment. However, other evidences support a tumour suppressor role for Notch signalling in myeloid leukaemias instead (Klinakis *et al*., 2011), (Lobry *et al*., 2013), (Kannan *et al*., 2013), (Chadwick *et al*., 2008), (Sengupta *et al*., 2007). In support of this, deletion of *Rbpj* accelerated MLL-AF9 driven AML. Mechanistically, the authors proposed that HES1 supresses MLL-AF9 driven AML likely through repression of *Flt3* (Kato *et al*., 2015). Additionally, Notch loss of function cooperates with Tet2 loss of function to induce AML *in vivo* (Lobry *et al*., 2013).

In our study, we showed that Notch pathway is silenced in most of the AML samples analysed. Possible mechanisms for Notch silencing in this context have been proposed (Lobry *et al*., 2014): (1) the possible absence of ligands in the AML niche – however, this has still yet to be demonstrated; (2) gene mutations; Mastermind-like 1 (*MAML1*) is a Notch coactivator frequently lost in 5q- AML (a type of AML lacking the long arm of chromosome 5). In cases where Mastermind like-1 is not lost (in 5q- AMLs), point mutations have been found in the *MAML1* (Jerez *et al*., 2012); (3) epigenetic modifications have also been implicated, as hypermethylation of Notch member genes *LFNG, MAML3 and HES5* have been uncovered in *IDH1*- or *IDH2*-mutated AML (Sasaki *et al*., 2012) and (4) alternative splicing, whereby *NOTCH2*, along with *FLT3* were found to be commonly mis-spliced in AML. In fact, up to 79% of AML patient samples analysed in that study expressed a *NOTCH2-Va* variant (Adamia *et al*., 2014). The authors correlated the expression of this variant with poor clinical outcome in the intermediate cytogenetic risk group. Moreover, *NOTCH2-Va* was associated with downregulation of Notch target genes *HES1*, *HEY1* and *DTX1* compared with AML cells expressing full length NOTCH2 (Adamia *et al*., 2014).

Given the apparent Notch signalling downregulation observed in AML cells analysed in our work, reactivation of this pathway was hypothesised as holding promising therapeutic value. Indeed, co-culturing AML cells on Delta4-expressing stroma or stimulating with soluble Jag1 ligand-based peptide induced apoptosis in some instances. A Notch reporter construct indicated the effects might be mediated through the reactivation of Notch signalling due to increased *Hes1*-controled mCherry expression, although future confirmation by qRT-PCR and WB is warranted. Future work will also involve generating more Notch reporter AML cell lines with *NOTCH1* or *NOTCH2* knockdown. This should allow the determination of the roles of

specific receptors in various contexts and be a valuable tool in the study of Notch signalling in AML.

Given its prominent oncogenic role in T-ALL and other haematological malignancies, a vast array of Notch antagonists such as γ -secretase inhibitors have been tested in pre-clinical and clinical trials (Hernandez Tejada *et al*., 2014). In addition, monoclonal antibodies targeting either Notch1 or Notch2 receptor were shown to possess anti-tumour and anti-angiogenic properties (Wu *et al*., 2010). An antibody targeting the γ-secretase complex has also shown promising results against T-ALL (Hayashi *et al*., 2012). Conversely, agonistic strategies have been developed aiming to treat diseases where Notch signalling appears to act as a tumour suppressor. Several ligand-mimicking proteins and peptides have been used as Notch agonists (reviewed in (Hernandez Tejada *et al.,* 2014)). We have used a Jag1 ligand peptide previously shown to possess *in vitro* effectiveness against AML (Kannan *et al*., 2013). Modifications to peptides that enhance their bioavailability while preserving their activity and improving on their delivery and transport strategies are key technical issues that should be addressed in order to facilitate the use of molecules that show *in vitro* efficiency. Of note, an anti-Notch2 agonist antibody has been useful in a mouse model of nephrosis (Tanaka *et al*., 2014) and could perhaps be of value in certain haematological malignancies. Even though re-activation of Notch pathway through immobilised ligands (Tohda *et al*., 2005), (Lobry *et al*., 2013) or overexpression of NICDs or downstream targets (Carlesso *et al*., 1999), (Kannan *et al*., 2013), (Lobry *et al*., 2013) has proven efficient in targeting myeloid leukaemic cells, this is not a practical strategy *in vivo*. We and others have reported peptide-based approaches to cause apoptosis in AML cells (Kannan *et al*., 2013). Still, these molecules have limited applications in AML due to peptide instability and low bioavailability (Craik *et al*., 2013). Other types of compounds have proven effective against AML cells *in vitro*. *N*-methylhemeanthidine chloride (NMHC) which can be found in the plant *Zephyranthes candida* proved to be toxic to several AML cell lines *in vitro*, by inducing cell cycle arrest, downregulation of cyclin B1 and upregulation of cell cycle regulator p21 (Ye *et al*., 2016b). This compound was also demonstrated to cause caspase-mediated apoptosis. The effects of NHMC are believed to be due to increased processing of Notch1 receptor as assessed by upregulation of N1-ICD, and Notch target genes *HES1* and *HEY1*. Notably, NHMC was shown to significantly reduce tumour burden in nude mice injected with HL60 cells. In another example, Resveratrol - commonly found in grapes, has been shown to synergise with HDAC inhibitors to induce apoptosis in leukaemia cells (Yaseen *et al*., 2012). Here, we attempted to find and test small molecule agonists of Notch signalling. Unfortunately, the compounds uncovered proved to cause cytotoxicity independent of Notch reactivation. Still, future investigation should address the specificity of the cytotoxic effects towards AML cells and the mechanisms behind it.

All in all, reactivation of Notch in some AML cases may hold a beneficial therapeutic potential. Therefore, the ever-increasing knowledge on the genetic background of this group of disease should allow for the development and use of more specific drugs targeting signalling pathways critical to AML cell regulation, of which Notch may be a useful candidate.

References

Adamia, S., Bar-Natan, M., Haibe-Kains, B., Pilarski, P.M., Bach, C., Pevzner, S., Calimeri, T., Avet-Loiseau, H., Lode, L., Verselis, S*., et al.* (2014). NOTCH2 and FLT3 gene mis-splicings are common events in patients with acute myeloid leukemia (AML): new potential targets in AML. Blood *123*, 2816-2825.

Adolfsson, J., Mansson, R., Buza-Vidas, N., Hultquist, A., Liuba, K., Jensen, C.T., Bryder, D., Yang, L., Borge, O.J., Thoren, L.A*., et al.* (2005). Identification of Flt3+ lympho-myeloid stem cells lacking erythro-megakaryocytic potential a revised road map for adult blood lineage commitment. Cell *121*, 295-306.

Ailles, L.E., Gerhard, B., Kawagoe, H., and Hogge, D.E. (1999). Growth Characteristics of Acute Myelogenous Leukemia Progenitors That Initiate Malignant Hematopoiesis in Nonobese Diabetic/Severe Combined Immunodeficient Mice. Blood *94*, 1761.

Andersen, P., Uosaki, H., Shenje, L.T., and Kwon, C. (2012). Non-canonical Notch signaling: emerging role and mechanism. Trends Cell Biol *22*, 257-265.

Andersson, E.R., Sandberg, R., and Lendahl, U. (2011). Notch signaling: simplicity in design, versatility in function. Development *138*, 3593-3612.

Andrawes, M.B., Xu, X., Liu, H., Ficarro, S.B., Marto, J.A., Aster, J.C., and Blacklow, S.C. (2013). Intrinsic selectivity of Notch 1 for Delta-like 4 over Delta-like 1. J Biol Chem *288*, 25477-25489.

Anjos-Afonso, F., Currie, E., Palmer, H.G., Foster, K.E., Taussig, D.C., and Bonnet, D. (2013). CD34(-) cells at the apex of the human hematopoietic stem cell hierarchy have distinctive cellular and molecular signatures. Cell Stem Cell *13*, 161-174.

Arber, D.A., Orazi, A., Hasserjian, R., Thiele, J., Borowitz, M.J., Le Beau, M.M., Bloomfield, C.D., Cazzola, M., and Vardiman, J.W. (2016). The 2016 revision to the World Health Organization classification of myeloid neoplasms and acute leukemia. Blood *127*, 2391-2405.

Arrighi, J.F., Hauser, C., Chapuis, B., Zubler, R.H., and Kindler, V. (1999). Long-term culture of human CD34(+) progenitors with FLT3-ligand, thrombopoietin, and stem cell factor induces extensive amplification of a CD34(-)CD14(-) and a CD34(-)CD14(+) dendritic cell precursor. Blood *93*, 2244-2252.

Aster, J.C., Pear, W.S., and Blacklow, S.C. (2008). Notch Signaling in Leukemia. Annual Review of Pathology: Mechanisms of Disease *3*, 587-613.

Bacher, U., Schnittger, S., Haferlach, C., and Haferlach, T. (2009). Molecular diagnostics in acute leukemias. Clin Chem Lab Med *47*, 1333-1341.

Bain, G., Robanus Maandag, E.C., te Riele, H.P., Feeney, A.J., Sheehy, A., Schlissel, M., Shinton, S.A., Hardy, R.R., and Murre, C. (1997). Both E12 and E47 allow commitment to the B cell lineage. Immunity *6*, 145-154.

Barbarulo, A., Grazioli, P., Campese, A.F., Bellavia, D., Di Mario, G., Pelullo, M., Ciuffetta, A., Colantoni, S., Vacca, A., Frati, L*., et al.* (2011). Notch3 and canonical NF-kappaB signaling pathways cooperatively regulate Foxp3 transcription. J Immunol *186*, 6199-6206.

Baum, C.M., Weissman, I.L., Tsukamoto, A.S., Buckle, A.M., and Peault, B. (1992). Isolation of a candidate human hematopoietic stem-cell population. Proc Natl Acad Sci U S A *89*, 2804-2808.

Bennett, J.M., Catovsky, D., Daniel, M.T., Flandrin, G., Galton, D.A., Gralnick, H.R., and Sultan, C. (1976). Proposals for the classification of the acute leukaemias. French-American-British (FAB) co-operative group. Br J Haematol *33*, 451-458.

Benveniste, P., Serra, P., Dervovic, D., Herer, E., Knowles, G., Mohtashami, M., and Zuniga-Pflucker, J.C. (2014). Notch signals are required for in vitro but not in vivo maintenance of human hematopoietic stem cells and delay the appearance of multipotent progenitors. Blood *123*, 1167-1177.

Berardi, A.C., Meffre, E., Pflumio, F., Katz, A., Vainchenker, W., Schiff, C., and Coulombel, L. (1997). Individual CD34+CD38lowCD19-CD10- progenitor cells from human cord blood generate B lymphocytes and granulocytes. Blood *89*, 3554-3564.

Bhatia, M., Bonnet, D., Murdoch, B., Gan, O.I., and Dick, J.E. (1998). A newly discovered class of human hematopoietic cells with SCID-repopulating activity. Nat Med *4*, 1038-1045.

Bhatia, M., Wang, J.C., Kapp, U., Bonnet, D., and Dick, J.E. (1997). Purification of primitive human hematopoietic cells capable of repopulating immune-deficient mice. Proc Natl Acad Sci U S A *94*, 5320-5325.

Bigas, A., and Espinosa, L. (2016). Notch Signaling in Cell–Cell Communication Pathways. Current stem cell reports *2*, 349-355.

Bonnet, D., and Dick, J.E. (1997). Human acute myeloid leukemia is organized as a hierarchy that originates from a primitive hematopoietic cell. Nat Med *3*, 730-737.

Borggrefe, T., and Oswald, F. (2009). The Notch signaling pathway: transcriptional regulation at Notch target genes. Cell Mol Life Sci *66*, 1631-1646.

Bosma, G.C., Custer, R.P., and Bosma, M.J. (1983). A severe combined immunodeficiency mutation in the mouse. Nature *301*, 527-530.

Bowers, M., Zhang, B., Ho, Y., Agarwal, P., Chen, C.C., and Bhatia, R. (2015). Osteoblast ablation reduces normal long-term hematopoietic stem cell self-renewal but accelerates leukemia development. Blood *125*, 2678-2688.

Bray, S.J. (2006). Notch signalling: a simple pathway becomes complex. Nat Rev Mol Cell Biol *7*, 678-689.

Buenrostro, J.D., Corces, M.R., Lareau, C.A., Wu, B., Schep, A.N., Aryee, M.J., Majeti, R., Chang, H.Y., and Greenleaf, W.J. (2018). Integrated Single-Cell Analysis Maps the Continuous Regulatory Landscape of Human Hematopoietic Differentiation. Cell *173*, 1535-1548 e1516.

Butler, J.M., Nolan, D.J., Vertes, E.L., Varnum-Finney, B., Kobayashi, H., Hooper, A.T., Seandel, M., Shido, K., White, I.A., Kobayashi, M.*, et al.* (2010). Endothelial cells are essential for the self-renewal and repopulation of Notch-dependent hematopoietic stem cells. Cell Stem Cell *6*, 251-264.

Calvi, L.M., Adams, G.B., Weibrecht, K.W., Weber, J.M., Olson, D.P., Knight, M.C., Martin, R.P., Schipani, E., Divieti, P., Bringhurst, F.R.*, et al.* (2003). Osteoblastic cells regulate the haematopoietic stem cell niche. Nature *425*, 841-846.

Carlesso, N., Aster, J.C., Sklar, J., and Scadden, D.T. (1999). Notch1-induced delay of human hematopoietic progenitor cell differentiation is associated with altered cell cycle kinetics. Blood *93*, 838-848.

Chadwick, N., Fennessy, C., Nostro, M.C., Baron, M., Brady, G., and Buckle, A.M. (2008). Notch induces cell cycle arrest and apoptosis in human erythroleukaemic TF-1 cells. Blood Cells Mol Dis *41*, 270-277.

Chang, A.N., Cantor, A.B., Fujiwara, Y., Lodish, M.B., Droho, S., Crispino, J.D., and Orkin, S.H. (2002). GATA-factor dependence of the multitype zinc-finger protein FOG-1 for its essential role in megakaryopoiesis. Proc Natl Acad Sci U S A *99*, 9237-9242.

Chen, L., Kostadima, M., Martens, J.H.A., Canu, G., Garcia, S.P., Turro, E., Downes, K., Macaulay, I.C., Bielczyk-Maczynska, E., Coe, S.*, et al.* (2014). Transcriptional diversity during lineage commitment of human blood progenitors. Science *345*, 1251033.

Chen, X., Skutt-Kakaria, K., Davison, J., Ou, Y.L., Choi, E., Malik, P., Loeb, K., Wood, B., Georges, G., Torok-Storb, B.*, et al.* (2012). G9a/GLP-dependent histone H3K9me2 patterning during human hematopoietic stem cell lineage commitment. Genes Dev *26*, 2499-2511.

Chiaramonte, R., Basile, A., Tassi, E., Calzavara, E., Cecchinato, V., Rossi, V., Biondi, A., and Comi, P. (2005). A wide role for NOTCH1 signaling in acute leukemia. Cancer Lett *219*, 113-120.

Chung, S.S., Eng, W.S., Hu, W., Khalaj, M., Garrett-Bakelman, F.E., Tavakkoli, M., Levine, R.L., Carroll, M., Klimek, V.M., Melnick, A.M.*, et al.* (2017). CD99 is a therapeutic target on disease stem cells in myeloid malignancies. Science translational medicine *9*, eaaj2025.

Civin, C.I., Strauss, L.C., Brovall, C., Fackler, M.J., Schwartz, J.F., and Shaper, J.H. (1984). Antigenic analysis of hematopoiesis. III. A hematopoietic progenitor cell surface antigen defined by a monoclonal antibody raised against KG-1a cells. J Immunol *133*, 157-165.

Clarkson, B., Ohkita, T., Ota, K., and Fried, J. (1967). Studies of cellular proliferation in human leukemia. I. Estimation of growth rates of leukemic and normal hematopoietic cells in two adults with acute leukemia given single injections of tritiated thymidine. J Clin Invest *46*, 506-529.

Colombo, M., Platonova, N., Giannandrea, D., Palano, M.T., Basile, A., and Chiaramonte, R. (2019). Re-establishing Apoptosis Competence in Bone Associated Cancers via Communicative Reprogramming Induced Through Notch Signaling Inhibition. Front Pharmacol *10*, 145.

Conneally, E., Cashman, J., Petzer, A., and Eaves, C. (1997). Expansion in vitro of transplantable human cord blood stem cells demonstrated using a quantitative assay of their lympho-myeloid repopulating activity in nonobese diabetic-scid/scid mice. Proc Natl Acad Sci U S A *94*, 9836-9841.

Coombs, C.C., Tavakkoli, M., and Tallman, M.S. (2015). Acute promyelocytic leukemia: where did we start, where are we now, and the future. Blood Cancer Journal *5*, e304-e304.

Cornelissen, J.J., Gratwohl, A., Schlenk, R.F., Sierra, J., Bornhauser, M., Juliusson, G., Racil, Z., Rowe, J.M., Russell, N., Mohty, M.*, et al.* (2012). The European LeukemiaNet AML Working Party consensus statement on allogeneic HSCT for patients with AML in remission: an integrated-risk adapted approach. Nat Rev Clin Oncol *9*, 579-590.

Corselli, M., Chin, C.J., Parekh, C., Sahaghian, A., Wang, W., Ge, S., Evseenko, D., Wang, X., Montelatici, E., Lazzari, L.*, et al.* (2013). Perivascular support of human hematopoietic stem/progenitor cells. Blood *121*, 2891-2901.

Craik, D.J., Fairlie, D.P., Liras, S., and Price, D. (2013). The Future of Peptide-based Drugs. Chemical Biology & Drug Design *81*, 136-147.

Crane, G.M., Jeffery, E., and Morrison, S.J. (2017). Adult haematopoietic stem cell niches. Nat Rev Immunol *17*, 573-590.

Csaszar, E., Wang, W., Usenko, T., Qiao, W., Delaney, C., Bernstein, I.D., and Zandstra, P.W. (2014). Blood stem cell fate regulation by Delta-1-mediated rewiring of IL-6 paracrine signaling. Blood *123*, 650-658.

D'Souza, B., Meloty-Kapella, L., and Weinmaster, G. (2010). Canonical and non-canonical Notch ligands. Curr Top Dev Biol *92*, 73-129.

Danet, G.H., Luongo, J.L., Butler, G., Lu, M.M., Tenner, A.J., Simon, M.C., and Bonnet, D.A. (2002). C1qRp defines a new human stem cell population with hematopoietic and hepatic potential. Proc Natl Acad Sci U S A *99*, 10441-10445.

De Kloe, G.E., and De Strooper, B. (2014). Small Molecules That Inhibit Notch Signaling. In Notch Signaling: Methods and Protocols, H.J. Bellen, and S. Yamamoto, eds. (New York, NY: Springer New York), pp. 311-322.

De Kouchkovsky, I., and Abdul-Hay, M. (2016). 'Acute myeloid leukemia: a comprehensive review and 2016 update'. Blood Cancer J *6*, e441.

de Pooter, R.F., Schmitt, T.M., de la Pompa, J.L., Fujiwara, Y., Orkin, S.H., and Zúñiga-Pflücker, J.C. (2006). Notch Signaling Requires GATA-2 to Inhibit Myelopoiesis from Embryonic Stem Cells and Primary Hemopoietic Progenitors. The Journal of Immunology *176*, 5267.

De Smedt, M., Reynvoet, K., Kerre, T., Taghon, T., Verhasselt, B., Vandekerckhove, B., Leclercq, G., and Plum, J. (2002). Active form of Notch imposes T cell fate in human progenitor cells. J Immunol *169*, 3021-3029.

Delaney, C., Heimfeld, S., Brashem-Stein, C., Voorhies, H., Manger, R.L., and Bernstein, I.D. (2010). Notch-mediated expansion of human cord blood progenitor cells capable of rapid myeloid reconstitution. Nat Med *16*, 232-236.

Delaney, C., Varnum-Finney, B., Aoyama, K., Brashem-Stein, C., and Bernstein, I.D. (2005). Dose-dependent effects of the Notch ligand Delta1 on ex vivo differentiation and in vivo marrow repopulating ability of cord blood cells. Blood *106*, 2693-2699.

Dexter, J.S. (1914). The Analysis of a Case of Continuous Variation in Drosophila by a Study of Its Linkage Relations. The American Naturalist *48*, 712-758.

Dexter, T.M., Allen, T.D., and Lajtha, L.G. (1977). Conditions controlling the proliferation of haemopoietic stem cells in vitro. J Cell Physiol *91*, 335-344.

Di Ianni, M., Baldoni, S., Rosati, E., Ciurnelli, R., Cavalli, L., Martelli, M.F., Marconi, P., Screpanti, I., and Falzetti, F. (2009). A new genetic lesion in B-CLL: a NOTCH1 PEST domain mutation. British Journal of Haematology *146*, 689-691.

DiNardo, C., de Botton, S., Pollyea, D.A., Stein, E.M., Fathi, A.T., Roboz, G.J., Collins, R., Swords, R.T., Flinn, I.W., Altman, J.K.*, et al.* (2015). Molecular Profiling and Relationship with Clinical Response in Patients with IDH1 Mutation-Positive Hematologic Malignancies Receiving AG-120, a First-in-Class Potent Inhibitor of Mutant IDH1, in Addition to Data from the Completed Dose Escalation Portion of the Phase 1 Study. Blood *126*, 1306.

DiNardo, C.D., Rausch, C.R., Benton, C., Kadia, T., Jain, N., Pemmaraju, N., Daver, N., Covert, W., Marx, K.R., Mace, M.*, et al.* (2018). Clinical experience with the BCL2-inhibitor venetoclax in combination therapy for relapsed and refractory acute myeloid leukemia and related myeloid malignancies. American Journal of Hematology *93*, 401-407.

Ding, L., Saunders, T.L., Enikolopov, G., and Morrison, S.J. (2012). Endothelial and perivascular cells maintain haematopoietic stem cells. Nature *481*, 457-462.

Dohner, H., Estey, E., Grimwade, D., Amadori, S., Appelbaum, F.R., Buchner, T., Dombret, H., Ebert, B.L., Fenaux, P., Larson, R.A.*, et al.* (2017). Diagnosis and management of AML in adults: 2017 ELN recommendations from an international expert panel. Blood *129*, 424-447.

Dong, Z., Yang, N., Yeo, S.Y., Chitnis, A., and Guo, S. (2012). Intralineage directional Notch signaling regulates self-renewal and differentiation of asymmetrically dividing radial glia. Neuron *74*, 65-78.

Doulatov, S., Notta, F., Eppert, K., Nguyen, L.T., Ohashi, P.S., and Dick, J.E. (2010). Revised map of the human progenitor hierarchy shows the origin of macrophages and dendritic cells in early lymphoid development. Nat Immunol *11*, 585-593.

Duarte, S., Woll, P.S., Buza-Vidas, N., Chin, D.W.L., Boukarabila, H., Luis, T.C., Stenson, L., Bouriez-Jones, T., Ferry, H., Mead, A.J., *et al.* (2018). Canonical Notch signaling is dispensable for adult steady-state and stress myelo-erythropoiesis. Blood *131*, 1712-1719.

Duncan, A.W., Rattis, F.M., DiMascio, L.N., Congdon, K.L., Pazianos, G., Zhao, C., Yoon, K., Cook, J.M., Willert, K., Gaiano, N., *et al.* (2005). Integration of Notch and Wnt signaling in hematopoietic stem cell maintenance. Nat Immunol *6*, 314-322.

Estey, E., Karp, J.E., Emadi, A., Othus, M., and Gale, R.P. (2020). Recent drug approvals for newly diagnosed acute myeloid leukemia: gifts or a Trojan horse? Leukemia.

Fabbri, G., Rasi, S., Rossi, D., Trifonov, V., Khiabanian, H., Ma, J., Grunn, A., Fangazio, M., Capello, D., Monti, S., *et al.* (2011). Analysis of the chronic lymphocytic leukemia coding genome: role of NOTCH1 mutational activation. J Exp Med *208*, 1389-1401.

Falini, B., Martelli, M.P., Bolli, N., Sportoletti, P., Liso, A., Tiacci, E., and Haferlach, T. (2011). Acute myeloid leukemia with mutated nucleophosmin (NPM1): is it a distinct entity? Blood *117*, 1109-1120.

Farge, T., Saland, E., de Toni, F., Aroua, N., Hosseini, M., Perry, R., Bosc, C., Sugita, M., Stuani, L., Fraisse, M., *et al.* (2017). Chemotherapy-Resistant Human Acute Myeloid Leukemia Cells Are Not Enriched for Leukemic Stem Cells but Require Oxidative Metabolism. Cancer Discov *7*, 716-735.

Fellmann, C., Hoffmann, T., Sridhar, V., Hopfgartner, B., Muhar, M., Roth, M., Lai, D.Y., Barbosa, I.A., Kwon, J.S., Guan, Y., *et al.* (2013). An optimized microRNA backbone for effective single-copy RNAi. Cell Rep *5*, 1704-1713.

Fernandez, L., Rodriguez, S., Huang, H., Chora, A., Fernandes, J., Mumaw, C., Cruz, E., Pollok, K., Cristina, F., Price, J.E., *et al.* (2008). Tumor necrosis factor-alpha and endothelial cells modulate Notch signaling in the bone marrow microenvironment during inflammation. Exp Hematol *36*, 545-558.

Flanagan, S.P. (1966). 'Nude', a new hairless gene with pleiotropic effects in the mouse. Genet Res *8*, 295-309.

Flores-Figueroa, E., Varma, S., Montgomery, K., Greenberg, P.L., and Gratzinger, D. (2012). Distinctive contact between CD34+ hematopoietic progenitors and CXCL12+ CD271+ mesenchymal stromal cells in benign and myelodysplastic bone marrow. Lab Invest *92*, 1330-1341.

Fortini, M.E. (2009). Notch signaling: the core pathway and its posttranslational regulation. Dev Cell *16*, 633-647.

Fortunel, N.O., Hatzfeld, J.A., Monier, M.N., and Hatzfeld, A. (2003). Control of hematopoietic stem/progenitor cell fate by transforming growth factor-beta. Oncol Res *13*, 445-453.

Francis, O.L., Chaudhry, K.K., Lamprecht, T., and Klco, J.M. (2017). Impact of Notch disruption on myeloid development. Blood Cancer J *7*, e598.

Galy, A., Travis, M., Cen, D., and Chen, B. (1995). Human T, B, natural killer, and dendritic cells arise from a common bone marrow progenitor cell subset. Immunity *3*, 459-473.

Gama-Norton, L., Ferrando, E., Ruiz-Herguido, C., Liu, Z., Guiu, J., Islam, A.B.M.M.K., Lee, S.-U., Yan, M., Guidos, C.J., López-Bigas, N., *et al.* (2015). Notch signal strength controls cell fate in the haemogenic endothelium. Nature Communications *6*, 8510.

Gartner, S., and Kaplan, H.S. (1980). Long-term culture of human bone marrow cells. Proc Natl Acad Sci U S A *77*, 4756-4759.

Goardon, N., Marchi, E., Atzberger, A., Quek, L., Schuh, A., Soneji, S., Woll, P., Mead, A., Alford, K.A., Rout, R., *et al.* (2011). Coexistence of LMPP-like and GMP-like leukemia stem cells in acute myeloid leukemia. Cancer Cell *19*, 138-152.

Goldman, D.C., Bailey, A.S., Pfaffle, D.L., Al Masri, A., Christian, J.L., and Fleming, W.H. (2009). BMP4 regulates the hematopoietic stem cell niche. Blood *114*, 4393-4401.

Gordon, W.R., Vardar-Ulu, D., Histen, G., Sanchez-Irizarry, C., Aster, J.C., and Blacklow, S.C. (2007). Structural basis for autoinhibition of Notch. Nat Struct Mol Biol *14*, 295-300.

Gorgens, A., Radtke, S., Mollmann, M., Cross, M., Durig, J., Horn, P.A., and Giebel, B. (2013). Revision of the human hematopoietic tree: granulocyte subtypes derive from distinct hematopoietic lineages. Cell Rep *3*, 1539-1552.

Grimwade, D., Walker, H., Oliver, F., Wheatley, K., Harrison, C., Harrison, G., Rees, J., Hann, I., Stevens, R., Burnett, A.*, et al.* (1998). The importance of diagnostic cytogenetics on outcome in AML: analysis of 1,612 patients entered into the MRC AML 10 trial. The Medical Research Council Adult and Children's Leukaemia Working Parties. Blood *92*, 2322-2333.

Gruszka, A.M., Valli, D., and Alcalay, M. (2017). Understanding the molecular basis of acute myeloid leukemias: where are we now? Int J Hematol Oncol *6*, 43-53.

Gu, S., Jin, L., Zhang, Y., Huang, Y., Zhang, F., Valdmanis, P.N., and Kay, M.A. (2012). The loop position of shRNAs and pre-miRNAs is critical for the accuracy of dicer processing in vivo. Cell *151*, 900-911.

Guan, Y., Gerhard, B., and Hogge, D.E. (2003). Detection, isolation, and stimulation of quiescent primitive leukemic progenitor cells from patients with acute myeloid leukemia (AML). Blood *101*, 3142-3149.

Guezguez, B., Campbell, C.J., Boyd, A.L., Karanu, F., Casado, F.L., Di Cresce, C., Collins, T.J., Shapovalova, Z., Xenocostas, A., and Bhatia, M. (2013). Regional localization within the bone marrow influences the functional capacity of human HSCs. Cell Stem Cell *13*, 175-189.

Guiu, J., Shimizu, R., D'Altri, T., Fraser, S.T., Hatakeyama, J., Bresnick, E.H., Kageyama, R., Dzierzak, E., Yamamoto, M., Espinosa, L.*, et al.* (2013). Hes repressors are essential regulators of hematopoietic stem cell development downstream of Notch signaling. J Exp Med *210*, 71-84.

Guo, M., Jan, L.Y., and Jan, Y.N. (1996). Control of daughter cell fates during asymmetric division: interaction of Numb and Notch. Neuron *17*, 27-41.

Han, H., Tanigaki, K., Yamamoto, N., Kuroda, K., Yoshimoto, M., Nakahata, T., Ikuta, K., and Honjo, T. (2002). Inducible gene knockout of transcription factor recombination signal binding protein-J reveals its essential role in T versus B lineage decision. Int Immunol *14*, 637-645.

Hannon, G.J., and Rossi, J.J. (2004). Unlocking the potential of the human genome with RNA interference. Nature *431*, 371-378.

Hao, Q.-L., Zhu, J., Price, M.A., Payne, K.J., Barsky, L.W., and Crooks, G.M. (2001). Identification of a novel, human multilymphoid progenitor in cord blood. Blood *97*, 3683.

Hayakawa, F., Towatari, M., Kiyoi, H., Tanimoto, M., Kitamura, T., Saito, H., and Naoe, T. (2000). Tandem-duplicated Flt3 constitutively activates STAT5 and MAP kinase and introduces autonomous cell growth in IL-3-dependent cell lines. Oncogene *19*, 624-631.

Haylock, D.N., Horsfall, M.J., Dowse, T.L., Ramshaw, H.S., Niutta, S., Protopsaltis, S., Peng, L., Burrell, C., Rappold, I., Buhring, H.-J.*, et al.* (1997). Increased Recruitment of Hematopoietic Progenitor Cells Underlies the Ex Vivo Expansion Potential of FLT3 Ligand. Blood *90*, 2260.

Hills, R.K., Castaigne, S., Appelbaum, F.R., Delaunay, J., Petersdorf, S., Othus, M., Estey, E.H., Dombret, H., Chevret, S., Ifrah, N.*, et al.* (2014). Addition of gemtuzumab ozogamicin to induction chemotherapy in adult patients with acute myeloid leukaemia: a meta-analysis of individual patient data from randomised controlled trials. Lancet Oncol *15*, 986-996.

Hoebeke, I., De Smedt, M., Stolz, F., Pike-Overzet, K., Staal, F.J., Plum, J., and Leclercq, G. (2007). T-, B- and NK-lymphoid, but not myeloid cells arise from human CD34(+)CD38(-)CD7(+) common lymphoid progenitors expressing lymphoid-specific genes. Leukemia *21*, 311-319.

Holmfeldt, P., Ganuza, M., Marathe, H., He, B., Hall, T., Kang, G., Moen, J., Pardieck, J., Saulsberry, A.C., Cico, A.*, et al.* (2016). Functional screen identifies regulators of murine hematopoietic stem cell repopulation. J Exp Med *213*, 433-449.

Hozumi, K., Mailhos, C., Negishi, N., Hirano, K.-i., Yahata, T., Ando, K., Zuklys, S., Holländer, G.A., Shima, D.T., and Habu, S. (2008). Delta-like 4 is indispensable in thymic environment specific for T cell development. The Journal of Experimental Medicine *205*, 2507.

Ilyas, A.M., Ahmad, S., Faheem, M., Naseer, M.I., Kumosani, T.A., Al-Qahtani, M.H., Gari, M., and Ahmed, F. (2015). Next generation sequencing of acute myeloid leukemia: influencing prognosis. BMC Genomics *16 Suppl 1*, S5.

Ishii, M., Matsuoka, Y., Sasaki, Y., Nakatsuka, R., Takahashi, M., Nakamoto, T., Yasuda, K., Matsui, K., Asano, H., Uemura, Y.*, et al.* (2011). Development of a high-resolution purification method for precise functional characterization of primitive human cord blood-derived CD34-negative SCID-repopulating cells. Exp Hematol *39*, 203-213 e201.

Iso, T., Kedes, L., and Hamamori, Y. (2003). HES and HERP families: multiple effectors of the Notch signaling pathway. J Cell Physiol *194*, 237-255.

Issaad, C., Croisille, L., Katz, A., Vainchenker, W., and Coulombel, L. (1993). A murine stromal cell line allows the proliferation of very primitive human CD34++/CD38- progenitor cells in long-term cultures and semisolid assays. Blood *81*, 2916-2924.

Itkin, T., Ludin, A., Gradus, B., Gur-Cohen, S., Kalinkovich, A., Schajnovitz, A., Ovadya, Y., Kollet, O., Canaani, J., Shezen, E.*, et al.* (2012). FGF-2 expands murine hematopoietic stem and progenitor cells via proliferation of stromal cells, c-Kit activation, and CXCL12 down-regulation. Blood *120*, 1843-1855.

Ito, M., Hiramatsu, H., Kobayashi, K., Suzue, K., Kawahata, M., Hioki, K., Ueyama, Y., Koyanagi, Y., Sugamura, K., Tsuji, K.*, et al.* (2002). NOD/SCID/gamma(c)(null) mouse: an excellent recipient mouse model for engraftment of human cells. Blood *100*, 3175-3182.

Iwasaki, M., Liedtke, M., Gentles, A.J., and Cleary, M.L. (2015). CD93 Marks a Non-Quiescent Human Leukemia Stem Cell Population and Is Required for Development of MLL-Rearranged Acute Myeloid Leukemia. Cell Stem Cell *17*, 412-421.

Jacobson, L.O., Simmons, E.L., Marks, E.K., and Eldredge, J.H. (1951). Recovery from radiation injury. Science *113*, 510-511.

Jan, M., Snyder, T.M., Corces-Zimmerman, M.R., Vyas, P., Weissman, I.L., Quake, S.R., and Majeti, R. (2012). Clonal evolution of preleukemic hematopoietic stem cells precedes human acute myeloid leukemia. Sci Transl Med *4*, 149ra118.

Jerez, A., Gondek, L.P., Jankowska, A.M., Makishima, H., Przychodzen, B., Tiu, R.V., O'Keefe, C.L., Mohamedali, A.M., Batista, D., Sekeres, M.A.*, et al.* (2012). Topography, clinical, and genomic correlates of 5q myeloid malignancies revisited. J Clin Oncol *30*, 1343-1349.

Jitschin, R., Saul, D., Braun, M., Tohumeken, S., Völkl, S., Kischel, R., Lutteropp, M., Dos Santos, C., Mackensen, A., and Mougiakakos, D. (2018). CD33/CD3-bispecific T-cell engaging (BiTE®) antibody construct targets monocytic AML myeloid-derived suppressor cells. Journal for ImmunoTherapy of Cancer *6*, 116.

Jurisch-Yaksi, N., Sannerud, R., and Annaert, W. (2013). A fast growing spectrum of biological functions of gamma-secretase in development and disease. Biochim Biophys Acta *1828*, 2815-2827.

Kannan, S., Sutphin, R.M., Hall, M.G., Golfman, L.S., Fang, W., Nolo, R.M., Akers, L.J., Hammitt, R.A., McMurray, J.S., Kornblau, S.M., *et al.* (2013). Notch activation inhibits AML growth and survival: a potential therapeutic approach. J Exp Med *210*, 321-337.

Karamitros, D., Stoilova, B., Aboukhalil, Z., Hamey, F., Reinisch, A., Samitsch, M., Quek, L., Otto, G., Repapi, E., Doondeea, J., *et al.* (2018). Single-cell analysis reveals the continuum of human lympho-myeloid progenitor cells. Nature Immunology *19*, 85-97.

Karanu, F.N., Murdoch, B., Miyabayashi, T., Ohno, M., Koremoto, M., Gallacher, L., Wu, D., Itoh, A., Sakano, S., and Bhatia, M. (2001). Human homologues of Delta-1 and Delta-4 function as mitogenic regulators of primitive human hematopoietic cells. Blood *97*, 1960-1967.

Keeshan, K., He, Y., Wouters, B.J., Shestova, O., Xu, L., Sai, H., Rodriguez, C.G., Maillard, I., Tobias, J.W., Valk, P., *et al.* (2006). Tribbles homolog 2 inactivates C/EBPalpha and causes acute myelogenous leukemia. Cancer cell *10*, 401-411.

Kelly, L.M., and Gilliland, D.G. (2002). Genetics of myeloid leukemias. Annu Rev Genomics Hum Genet *3*, 179-198.

Kidd, S., Kelley, M.R., and Young, M.W. (1986). Sequence of the notch locus of Drosophila melanogaster: relationship of the encoded protein to mammalian clotting and growth factors. Mol Cell Biol *6*, 3094-3108.

Kim, H., Huang, L., Critser, P.J., Yang, Z., Chan, R.J., Wang, L., Carlesso, N., Voytik-Harbin, S.L., Bernstein, I.D., and Yoder, M.C. (2015). Notch ligand Delta-like 1 promotes in vivo vasculogenesis in human cord blood-derived endothelial colony forming cells. Cytotherapy *17*, 579-592.

Kim, Y.W., Koo, B.K., Jeong, H.W., Yoon, M.J., Song, R., Shin, J., Jeong, D.C., Kim, S.H., and Kong, Y.Y. (2008). Defective Notch activation in microenvironment leads to myeloproliferative disease. Blood *112*, 4628-4638.

Kimura, S., Roberts, A.W., Metcalf, D., and Alexander, W.S. (1998). Hematopoietic stem cell deficiencies in mice lacking c-Mpl, the receptor for thrombopoietin. Proc Natl Acad Sci U S A *95*, 1195-1200.

Klinakis, A., Lobry, C., Abdel-Wahab, O., Oh, P., Haeno, H., Buonamici, S., van De Walle, I., Cathelin, S., Trimarchi, T., Araldi, E., *et al.* (2011). A novel tumour-suppressor function for the Notch pathway in myeloid leukaemia. Nature *473*, 230-233.

Kode, A., Manavalan, J.S., Mosialou, I., Bhagat, G., Rathinam, C.V., Luo, N., Khiabanian, H., Lee, A., Murty, V.V., Friedman, R., *et al.* (2014). Leukaemogenesis induced by an activating beta-catenin mutation in osteoblasts. Nature *506*, 240-244.

Kojika, S., and Griffin, J.D. (2001). Notch receptors and hematopoiesis. Exp Hematol *29*, 1041-1052.

Komatsu, H., Chao, M.Y., Larkins-Ford, J., Corkins, M.E., Somers, G.A., Tucey, T., Dionne, H.M., White, J.Q., Wani, K., Boxem, M., *et al.* (2008). OSM-11 facilitates LIN-12 Notch signaling during Caenorhabditis elegans vulval development. PLoS Biol *6*, e196.

Krebs, L.T., Xue, Y., Norton, C.R., Shutter, J.R., Maguire, M., Sundberg, J.P., Gallahan, D., Closson, V., Kitajewski, J., Callahan, R., *et al.* (2000). Notch signaling is essential for vascular morphogenesis in mice. Genes Dev *14*, 1343-1352.

Kronke, J., Bullinger, L., Teleanu, V., Tschurtz, F., Gaidzik, V.I., Kuhn, M.W., Rucker, F.G., Holzmann, K., Paschka, P., Kapp-Schworer, S., *et al.* (2013). Clonal evolution in relapsed NPM1-mutated acute myeloid leukemia. Blood *122*, 100-108.

Kumano, K., Chiba, S., Kunisato, A., Sata, M., Saito, T., Nakagami-Yamaguchi, E., Yamaguchi, T., Masuda, S., Shimizu, K., Takahashi, T., *et al.* (2003). Notch1 but not Notch2 is essential for generating hematopoietic stem cells from endothelial cells. Immunity *18*, 699-711.

Kunisato, A., Chiba, S., Nakagami-Yamaguchi, E., Kumano, K., Saito, T., Masuda, S., Yamaguchi, T., Osawa, M., Kageyama, R., Nakauchi, H.*, et al.* (2003). HES-1 preserves purified hematopoietic stem cells ex vivo and accumulates side population cells in vivo. Blood *101*, 1777-1783.

Kurooka, H., and Honjo, T. (2000). Functional interaction between the mouse notch1 intracellular region and histone acetyltransferases PCAF and GCN5. J Biol Chem *275*, 17211-17220.

La Motte-Mohs, R.N., Herer, E., and Zuniga-Pflucker, J.C. (2005). Induction of T-cell development from human cord blood hematopoietic stem cells by Delta-like 1 in vitro. Blood *105*, 1431-1439.

Ladi, E., Nichols, J.T., Ge, W., Miyamoto, A., Yao, C., Yang, L.T., Boulter, J., Sun, Y.E., Kintner, C., and Weinmaster, G. (2005). The divergent DSL ligand Dll3 does not activate Notch signaling but cell autonomously attenuates signaling induced by other DSL ligands. The Journal of cell biology *170*, 983-992.

Lagadinou, E.D., Sach, A., Callahan, K., Rossi, R.M., Neering, S.J., Minhajuddin, M., Ashton, J.M., Pei, S., Grose, V., O'Dwyer, K.M.*, et al.* (2013). BCL-2 inhibition targets oxidative phosphorylation and selectively eradicates quiescent human leukemia stem cells. Cell Stem Cell *12*, 329-341.

Lai, C., Doucette, K., and Norsworthy, K. (2019). Recent drug approvals for acute myeloid leukemia. Journal of Hematology & Oncology *12*, 100.

Lampreia, F.P., Carmelo, J.G., and Anjos-Afonso, F. (2017). Notch Signaling in the Regulation of Hematopoietic Stem Cell. Curr Stem Cell Rep *3*, 202-209.

Lancet, J.E., Uy, G.L., Cortes, J.E., Newell, L.F., Lin, T.L., Ritchie, E.K., Stuart, R.K., Strickland, S.A., Hogge, D., Solomon, S.R.*, et al.* (2018). CPX-351 (cytarabine and daunorubicin) Liposome for Injection Versus Conventional Cytarabine Plus Daunorubicin in Older Patients With Newly Diagnosed Secondary Acute Myeloid Leukemia. J Clin Oncol *36*, 2684-2692.

Lansdorp, P.M., Sutherland, H.J., and Eaves, C.J. (1990). Selective expression of CD45 isoforms on functional subpopulations of CD34+ hemopoietic cells from human bone marrow. J Exp Med *172*, 363-366.

Lapidot, T., Sirard, C., Vormoor, J., Murdoch, B., Hoang, T., Caceres-Cortes, J., Minden, M., Paterson, B., Caligiuri, M.A., and Dick, J.E. (1994). A cell initiating human acute myeloid leukaemia after transplantation into SCID mice. Nature *367*, 645-648.

Laurenti, E., Doulatov, S., Zandi, S., Plumb, I., Chen, J., April, C., Fan, J.B., and Dick, J.E. (2013). The transcriptional architecture of early human hematopoiesis identifies multilevel control of lymphoid commitment. Nat Immunol *14*, 756-763.

Lauret, E., Catelain, C., Titeux, M., Poirault, S., Dando, J.S., Dorsch, M., Villeval, J.L., Groseil, A., Vainchenker, W., Sainteny, F.*, et al.* (2004). Membrane-bound delta-4 notch ligand reduces the proliferative activity of primitive human hematopoietic CD34+CD38low cells while maintaining their LTC-IC potential. Leukemia *18*, 788-797.

Lechman, E.R., Gentner, B., Ng, S.W., Schoof, E.M., van Galen, P., Kennedy, J.A., Nucera, S., Ciceri, F., Kaufmann, K.B., Takayama, N.*, et al.* (2016). miR-126 Regulates Distinct Self-Renewal Outcomes in Normal and Malignant Hematopoietic Stem Cells. Cancer Cell *29*, 214-228.

Lee, J.S., Thomas, D.M., Gutierrez, G., Carty, S.A., Yanagawa, S., and Hinds, P.W. (2006). HES1 cooperates with pRb to activate RUNX2-dependent transcription. J Bone Miner Res *21*, 921-933.

Lee, M.O., Song, S.H., Jung, S., Hur, S., Asahara, T., Kim, H., Kwon, S.M., and Cha, H.J. (2012). Effect of ionizing radiation induced damage of endothelial progenitor cells in vascular regeneration. Arterioscler Thromb Vasc Biol *32*, 343-352.

Lee, S.-y., Kumano, K., Nakazaki, K., Sanada, M., Matsumoto, A., Yamamoto, G., Nannya, Y., Suzuki, R., Ota, S., Ota, Y.*, et al.* (2009). Gain-of-function mutations and copy number increases of Notch2 in diffuse large B-cell lymphoma. Cancer Science *100*, 920-926.

Ley, T.J., Ding, L., Walter, M.J., McLellan, M.D., Lamprecht, T., Larson, D.E., Kandoth, C., Payton, J.E., Baty, J., Welch, J.*, et al.* (2010). DNMT3A mutations in acute myeloid leukemia. N Engl J Med *363*, 2424-2433.

Ley, T.J., Mardis, E.R., Ding, L., Fulton, B., McLellan, M.D., Chen, K., Dooling, D., Dunford-Shore, B.H., McGrath, S., Hickenbotham, M.*, et al.* (2008). DNA sequencing of a cytogenetically normal acute myeloid leukaemia genome. Nature *456*, 66-72.

Li, L., Piloto, O., Nguyen, H.B., Greenberg, K., Takamiya, K., Racke, F., Huso, D., and Small, D. (2008). Knock-in of an internal tandem duplication mutation into murine FLT3 confers myeloproliferative disease in a mouse model. Blood *111*, 3849-3858.

Lipinski, C.A., Lombardo, F., Dominy, B.W., and Feeney, P.J. (2001). Experimental and computational approaches to estimate solubility and permeability in drug discovery and development settings. Adv Drug Deliv Rev *46*, 3-26.

Liu, Z.H., Dai, X.M., and Du, B. (2015). Hes1: a key role in stemness, metastasis and multidrug resistance. Cancer Biol Ther *16*, 353-359.

Livak, K.J., and Schmittgen, T.D. (2001). Analysis of relative gene expression data using real-time quantitative PCR and the 2(-Delta Delta C(T)) Method. Methods *25*, 402-408.

Lobry, C., Ntziachristos, P., Ndiaye-Lobry, D., Oh, P., Cimmino, L., Zhu, N., Araldi, E., Hu, W., Freund, J., Abdel-Wahab, O.*, et al.* (2013). Notch pathway activation targets AML-initiating cell homeostasis and differentiation. J Exp Med *210*, 301-319.

Lorenz, E., Uphoff, D., Reid, T.R., and Shelton, E. (1951). Modification of irradiation injury in mice and guinea pigs by bone marrow injections. J Natl Cancer Inst *12*, 197-201.

MacDonald, H.R., Wilson, A., and Radtke, F. (2001). Notch1 and T-cell development: insights from conditional knockout mice. Trends Immunol *22*, 155-160.

Maillard, I., Koch, U., Dumortier, A., Shestova, O., Xu, L., Sai, H., Pross, S.E., Aster, J.C., Bhandoola, A., Radtke, F.*, et al.* (2008). Canonical notch signaling is dispensable for the maintenance of adult hematopoietic stem cells. Cell Stem Cell *2*, 356-366.

Majeti, R., Park, C.Y., and Weissman, I.L. (2007). Identification of a hierarchy of multipotent hematopoietic progenitors in human cord blood. Cell Stem Cell *1*, 635-645.

Mancini, S.J., Mantei, N., Dumortier, A., Suter, U., MacDonald, H.R., and Radtke, F. (2005). Jagged1-dependent Notch signaling is dispensable for hematopoietic stem cell self-renewal and differentiation. Blood *105*, 2340-2342.

Manz, M.G., Miyamoto, T., Akashi, K., and Weissman, I.L. (2002). Prospective isolation of human clonogenic common myeloid progenitors. Proc Natl Acad Sci U S A *99*, 11872-11877.

Mazurier, F., Doedens, M., Gan, O.I., and Dick, J.E. (2003). Rapid myeloerythroid repopulation after intrafemoral transplantation of NOD-SCID mice reveals a new class of human stem cells. Nat Med *9*, 959-963.

Mercher, T., Cornejo, M.G., Sears, C., Kindler, T., Moore, S.A., Maillard, I., Pear, W.S., Aster, J.C., and Gilliland, D.G. (2008). Notch signaling specifies megakaryocyte development from hematopoietic stem cells. Cell Stem Cell *3*, 314-326.

Metzeler, K.H., Maharry, K., Radmacher, M.D., Mrozek, K., Margeson, D., Becker, H., Curfman, J., Holland, K.B., Schwind, S., Whitman, S.P.*, et al.* (2011). TET2 mutations improve the new European LeukemiaNet risk classification of acute myeloid leukemia: a Cancer and Leukemia Group B study. J Clin Oncol *29*, 1373-1381.

Miller, C.L., and Lai, B. (2005). Human and mouse hematopoietic colony-forming cell assays. Methods Mol Biol *290*, 71-89.

Milner, L.A., Bigas, A., Kopan, R., Brashem-Stein, C., Bernstein, I.D., and Martin, D.I.K. (1996). Inhibition of granulocytic differentiation by <em>mNotch1</em&gt. Proceedings of the National Academy of Sciences *93*, 13014.

Milner, L.A., Kopan, R., Martin, D.I., and Bernstein, I.D. (1994). A human homologue of the Drosophila developmental gene, Notch, is expressed in CD34+ hematopoietic precursors. Blood *83*, 2057-2062.

Mohr, S.E., and Perrimon, N. (2012). RNAi screening: new approaches, understandings, and organisms. Wiley Interdiscip Rev RNA *3*, 145-158.

Mori, Y., Chen, J.Y., Pluvinage, J.V., Seita, J., and Weissman, I.L. (2015). Prospective isolation of human erythroid lineage-committed progenitors. Proc Natl Acad Sci U S A *112*, 9638-9643.

Mupo, A., Celani, L., Dovey, O., Cooper, J.L., Grove, C., Rad, R., Sportoletti, P., Falini, B., Bradley, A., and Vassiliou, G.S. (2013). A powerful molecular synergy between mutant Nucleophosmin and Flt3-ITD drives acute myeloid leukemia in mice. Leukemia *27*, 1917-1920.

Nandagopal, N., Santat, L.A., LeBon, L., Sprinzak, D., Bronner, M.E., and Elowitz, M.B. (2018). Dynamic Ligand Discrimination in the Notch Signaling Pathway. Cell *172*, 869-880 e819.

Ng, S.W., Mitchell, A., Kennedy, J.A., Chen, W.C., McLeod, J., Ibrahimova, N., Arruda, A., Popescu, A., Gupta, V., Schimmer, A.D.*, et al.* (2016). A 17-gene stemness score for rapid determination of risk in acute leukaemia. Nature *540*, 433-437.

Notta, F., Doulatov, S., Laurenti, E., Poeppl, A., Jurisica, I., and Dick, J.E. (2011). Isolation of single human hematopoietic stem cells capable of long-term multilineage engraftment. Science *333*, 218-221.

Notta, F., Zandi, S., Takayama, N., Dobson, S., Gan, O.I., Wilson, G., Kaufmann, K.B., McLeod, J., Laurenti, E., Dunant, C.F.*, et al.* (2016). Distinct routes of lineage development reshape the human blood hierarchy across ontogeny. Science *351*, aab2116.

Novershtern, N., Subramanian, A., Lawton, L.N., Mak, R.H., Haining, W.N., McConkey, M.E., Habib, N., Yosef, N., Chang, C.Y., Shay, T.*, et al.* (2011). Densely interconnected transcriptional circuits control cell states in human hematopoiesis. Cell *144*, 296-309.

Nowell, C.S., and Radtke, F. (2017). Notch as a tumour suppressor. Nat Rev Cancer *17*, 145-159.

Oh, P., Lobry, C., Gao, J., Tikhonova, A., Loizou, E., Manet, J., van Handel, B., Ibrahim, S., Greve, J., Mikkola, H.*, et al.* (2013). In vivo mapping of notch pathway activity in normal and stress hematopoiesis. Cell Stem Cell *13*, 190-204.

Ohishi, K., Varnum-Finney, B., and Bernstein, I.D. (2002). Delta-1 enhances marrow and thymus repopulating ability of human CD34(+)CD38(-) cord blood cells. J Clin Invest *110*, 1165-1174.

Ordentlich, P., Lin, A., Shen, C.P., Blaumueller, C., Matsuno, K., Artavanis-Tsakonas, S., and Kadesch, T. (1998). Notch inhibition of E47 supports the existence of a novel signaling pathway. Mol Cell Biol *18*, 2230-2239.

Palomero, T., Sulis, M.L., Cortina, M., Real, P.J., Barnes, K., Ciofani, M., Caparros, E., Buteau, J., Brown, K., Perkins, S.L.*, et al.* (2007). Mutational loss of PTEN induces resistance to NOTCH1 inhibition in T-cell leukemia. Nat Med *13*, 1203-1210.

Palu, G., Selby, P., Powles, R., and Alexander, P. (1979). Spontaneous regression of human acute myeloid leukaemia xenografts and phenotypic evidence for maturation. Br J Cancer *40*, 731-735.

Papaemmanuil, E., Gerstung, M., Bullinger, L., Gaidzik, V.I., Paschka, P., Roberts, N.D., Potter, N.E., Heuser, M., Thol, F., Bolli, N.*, et al.* (2016). Genomic Classification and Prognosis in Acute Myeloid Leukemia. N Engl J Med *374*, 2209-2221.

Pear, W.S., Aster, J.C., Scott, M.L., Hasserjian, R.P., Soffer, B., Sklar, J., and Baltimore, D. (1996). Exclusive development of T cell neoplasms in mice transplanted with bone marrow expressing activated Notch alleles. J Exp Med *183*, 2283-2291.

Perl, A.E. (2019). Gilteritinib significantly prolongs overall survival in patients with FLT3-mutated (FLT3mut+) relapsed/refractory (R/R) acute myeloid leukemia (AML): Results from the Phase III ADMIRAL trial. AACR Annual Meeting, vol 2019.

Poulos, M.G., Guo, P., Kofler, N.M., Pinho, S., Gutkin, M.C., Tikhonova, A., Aifantis, I., Frenette, P.S., Kitajewski, J., Rafii, S.*, et al.* (2013). Endothelial Jagged-1 is necessary for homeostatic and regenerative hematopoiesis. Cell Rep *4*, 1022-1034.

Prochazka, M., Gaskins, H.R., Shultz, L.D., and Leiter, E.H. (1992). The nonobese diabetic scid mouse: model for spontaneous thymomagenesis associated with immunodeficiency. Proc Natl Acad Sci U S A *89*, 3290-3294.

Puente, X.S., Pinyol, M., Quesada, V., Conde, L., Ordóñez, G.R., Villamor, N., Escaramis, G., Jares, P., Beà, S., González-Díaz, M.*, et al.* (2011a). Whole-genome sequencing identifies recurrent mutations in chronic lymphocytic leukaemia. Nature *475*, 101-105.

Puente, X.S., Pinyol, M., Quesada, V., Conde, L., Ordóñez, G.R., Villamor, N., Escaramis, G., Jares, P., Beà, S., González-Díaz, M.*, et al.* (2011b). Whole-genome sequencing identifies recurrent mutations in chronic lymphocytic leukaemia. Nature *475*, 101-105.

Qian, H., Buza-Vidas, N., Hyland, C.D., Jensen, C.T., Antonchuk, J., Mansson, R., Thoren, L.A., Ekblom, M., Alexander, W.S., and Jacobsen, S.E. (2007). Critical role of thrombopoietin in maintaining adult quiescent hematopoietic stem cells. Cell Stem Cell *1*, 671-684.

Quek, L., Otto, G.W., Garnett, C., Lhermitte, L., Karamitros, D., Stoilova, B., Lau, I.J., Doondeea, J., Usukhbayar, B., Kennedy, A.*, et al.* (2016). Genetically distinct leukemic stem cells in human CD34-acute myeloid leukemia are arrested at a hemopoietic precursor-like stage. J Exp Med *213*, 1513-1535.

Qyang, Y., Chambers, S.M., Wang, P., Xia, X., Chen, X., Goodell, M.A., and Zheng, H. (2004). Myeloproliferative disease in mice with reduced presenilin gene dosage: effect of gamma-secretase blockage. Biochemistry *43*, 5352-5359.

Radtke, F., Wilson, A., Stark, G., Bauer, M., van Meerwijk, J., MacDonald, H.R., and Aguet, M. (1999). Deficient T cell fate specification in mice with an induced inactivation of Notch1. Immunity *10*, 547-558.

Ramasamy, S.K., and Lenka, N. (2010). Notch exhibits ligand bias and maneuvers stage-specific steering of neural differentiation in embryonic stem cells. Mol Cell Biol *30*, 1946-1957.

Rangarajan, A., Talora, C., Okuyama, R., Nicolas, M., Mammucari, C., Oh, H., Aster, J.C., Krishna, S., Metzger, D., Chambon, P.*, et al.* (2001). Notch signaling is a direct determinant of keratinocyte growth arrest and entry into differentiation. EMBO J *20*, 3427-3436.

Rathinam, C., Matesic, L.E., and Flavell, R.A. (2011). The E3 ligase Itch is a negative regulator of the homeostasis and function of hematopoietic stem cells. Nat Immunol *12*, 399-407.

Rebay, I., Fleming, R.J., Fehon, R.G., Cherbas, L., Cherbas, P., and Artavanis-Tsakonas, S. (1991). Specific EGF repeats of Notch mediate interactions with Delta and serrate: Implications for notch as a multifunctional receptor. Cell *67*, 687-699.

Robert-Moreno, A., Espinosa, L., de la Pompa, J.L., and Bigas, A. (2005). RBPjkappa-dependent Notch function regulates Gata2 and is essential for the formation of intra-embryonic hematopoietic cells. Development *132*, 1117-1126.

Rodriguez-Fraticelli, A.E., Wolock, S.L., Weinreb, C.S., Panero, R., Patel, S.H., Jankovic, M., Sun, J., Calogero, R.A., Klein, A.M., and Camargo, F.D. (2018). Clonal analysis of lineage fate in native haematopoiesis. Nature *553*, 212.

Ronchini, C., and Capobianco, A.J. (2001). Induction of cyclin D1 transcription and CDK2 activity by Notch(ic): implication for cell cycle disruption in transformation by Notch(ic). Mol Cell Biol *21*, 5925-5934.

Rongvaux, A., Willinger, T., Martinek, J., Strowig, T., Gearty, S.V., Teichmann, L.L., Saito, Y., Marches, F., Halene, S., Palucka, A.K.*, et al.* (2014). Development and function of human innate immune cells in a humanized mouse model. Nature Biotechnology *32*, 364.

Rossi, D., Rasi, S., Fabbri, G., Spina, V., Fangazio, M., Forconi, F., Marasca, R., Laurenti, L., Bruscaggin, A., Cerri, M.*, et al.* (2012). Mutations of NOTCH1 are an independent predictor of survival in chronic lymphocytic leukemia. Blood *119*, 521-529.

Russler-Germain, D.A., Spencer, D.H., Young, M.A., Lamprecht, T.L., Miller, C.A., Fulton, R., Meyer, M.R., Erdmann-Gilmore, P., Townsend, R.R., Wilson, R.K.*, et al.* (2014). The R882H DNMT3A mutation associated with AML dominantly inhibits wild-type DNMT3A by blocking its ability to form active tetramers. Cancer Cell *25*, 442-454.

Saito, T., Chiba, S., Ichikawa, M., Kunisato, A., Asai, T., Shimizu, K., Yamaguchi, T., Yamamoto, G., Seo, S., Kumano, K.*, et al.* (2003). Notch2 Is Preferentially Expressed in Mature B Cells and Indispensable for Marginal Zone B Lineage Development. Immunity *18*, 675-685.

Sallmyr, A., Fan, J., Datta, K., Kim, K.T., Grosu, D., Shapiro, P., Small, D., and Rassool, F. (2008). Internal tandem duplication of FLT3 (FLT3/ITD) induces increased ROS production, DNA damage, and misrepair: implications for poor prognosis in AML. Blood *111*, 3173-3182.

Sanalkumar, R., Dhanesh, S.B., and James, J. (2010). Non-canonical activation of Notch signaling/target genes in vertebrates. Cell Mol Life Sci *67*, 2957-2968.

Santaguida, M., Schepers, K., King, B., Sabnis, A.J., Forsberg, E.C., Attema, J.L., Braun, B.S., and Passegue, E. (2009). JunB protects against myeloid malignancies by limiting hematopoietic stem cell proliferation and differentiation without affecting self-renewal. Cancer Cell *15*, 341-352.

Sarmento, L.M., Huang, H., Limon, A., Gordon, W., Fernandes, J., Tavares, M.J., Miele, L., Cardoso, A.A., Classon, M., and Carlesso, N. (2005). Notch1 modulates timing of G₁-S progression by inducing SKP2 transcription and p27^{Kip1} degradation. The Journal of Experimental Medicine *202*, 157.

Schmittgen, T.D., Zakrajsek, B.A., Mills, A.G., Gorn, V., Singer, M.J., and Reed, M.W. (2000). Quantitative reverse transcription-polymerase chain reaction to study mRNA decay: comparison of endpoint and real-time methods. Anal Biochem *285*, 194-204.

Schroeder, T., Kohlhof, H., Rieber, N., and Just, U. (2003). Notch signaling induces multilineage myeloid differentiation and up-regulates PU.1 expression. J Immunol *170*, 5538-5548.

Segre, J.A., Nemhauser, J.L., Taylor, B.A., Nadeau, J.H., and Lander, E.S. (1995). Positional cloning of the nude locus: genetic, physical, and transcription maps of the region and mutations in the mouse and rat. Genomics *28*, 549-559.

Shang, Y., and Zhou, F. (2019). Current Advances in Immunotherapy for Acute Leukemia: An Overview of Antibody, Chimeric Antigen Receptor, Immune Checkpoint, and Natural Killer. Frontiers in Oncology *9*.

Shimizu, K., Chiba, S., Kumano, K., Hosoya, N., Takahashi, T., Kanda, Y., Hamada, Y., Yazaki, Y., and Hirai, H. (1999). Mouse jagged1 physically interacts with notch2 and other notch receptors. Assessment by quantitative methods. J Biol Chem *274*, 32961-32969.

Shivdasani, R.A., Fujiwara, Y., McDevitt, M.A., and Orkin, S.H. (1997). A lineage-selective knockout establishes the critical role of transcription factor GATA-1 in megakaryocyte growth and platelet development. EMBO J *16*, 3965-3973.

Shlush, L.I., Mitchell, A., Heisler, L., Abelson, S., Ng, S.W.K., Trotman-Grant, A., Medeiros, J.J.F., Rao-Bhatia, A., Jaciw-Zurakowsky, I., Marke, R.*, et al.* (2017). Tracing the origins of relapse in acute myeloid leukaemia to stem cells. Nature *547*, 104-108.

Shlush, L.I., Zandi, S., Mitchell, A., Chen, W.C., Brandwein, J.M., Gupta, V., Kennedy, J.A., Schimmer, A.D., Schuh, A.C., Yee, K.W.*, et al.* (2014). Identification of pre-leukaemic haematopoietic stem cells in acute leukaemia. Nature *506*, 328-333.

Shultz, L.D., Lyons, B.L., Burzenski, L.M., Gott, B., Chen, X., Chaleff, S., Kotb, M., Gillies, S.D., King, M., Mangada, J.*, et al.* (2005). Human lymphoid and myeloid cell development in NOD/LtSz-scid IL2R gamma null mice engrafted with mobilized human hemopoietic stem cells. J Immunol *174*, 6477-6489.

Singbrant, S., Karlsson, G., Ehinger, M., Olsson, K., Jaako, P., Miharada, K., Stadtfeld, M., Graf, T., and Karlsson, S. (2010). Canonical BMP signaling is dispensable for hematopoietic stem cell function in both adult and fetal liver hematopoiesis, but essential to preserve colon architecture. Blood *115*, 4689-4698.

Sirinoglu Demiriz, I., Tekgunduz, E., and Altuntas, F. (2012). What is the most appropriate source for hematopoietic stem cell transplantation? Peripheral stem cell/bone marrow/cord blood. Bone Marrow Res *2012*, 834040.

Six, E.M., Bonhomme, D., Monteiro, M., Beldjord, K., Jurkowska, M., Cordier-Garcia, C., Garrigue, A., Dal Cortivo, L., Rocha, B., Fischer, A.*, et al.* (2007). A human postnatal lymphoid progenitor capable of circulating and seeding the thymus. The Journal of experimental medicine *204*, 3085-3093.

Song, S.J., Ito, K., Ala, U., Kats, L., Webster, K., Sun, S.M., Jongen-Lavrencic, M., Manova-Todorova, K., Teruya-Feldstein, J., Avigan, D.E.*, et al.* (2013). The oncogenic microRNA miR-22 targets the TET2 tumor suppressor to promote hematopoietic stem cell self-renewal and transformation. Cell Stem Cell *13*, 87-101.

Stegmeier, F., Hu, G., Rickles, R.J., Hannon, G.J., and Elledge, S.J. (2005). A lentiviral microRNA-based system for single-copy polymerase II-regulated RNA interference in mammalian cells. Proc Natl Acad Sci U S A *102*, 13212-13217.

Stein, E.M., DiNardo, C., Altman, J.K., Collins, R., DeAngelo, D.J., Kantarjian, H.M., Sekeres, M.A., Fathi, A.T., Flinn, I.W., Frankel, A.E.*, et al.* (2015). Safety and Efficacy of AG-221, a Potent Inhibitor of Mutant IDH2 That Promotes Differentiation of Myeloid Cells in Patients with Advanced Hematologic Malignancies: Results of a Phase 1/2 Trial. Blood *126*, 323.

Stein, E.M., DiNardo, C.D., Fathi, A.T., Pollyea, D.A., Stone, R.M., Altman, J.K., Roboz, G.J., Patel, M.R., Collins, R., Flinn, I.W.*, et al.* (2019). Molecular remission and response patterns in patients with mutant-IDH2 acute myeloid leukemia treated with enasidenib. Blood *133*, 676-687.

Stone, R.M., Mandrekar, S.J., Sanford, B.L., Laumann, K., Geyer, S., Bloomfield, C.D., Thiede, C., Prior, T.W., Döhner, K., Marcucci, G.*, et al.* (2017). Midostaurin plus Chemotherapy for Acute Myeloid Leukemia with a FLT3 Mutation. New England Journal of Medicine *377*, 454-464.

Sugimura, R., He, X.C., Venkatraman, A., Arai, F., Box, A., Semerad, C., Haug, J.S., Peng, L., Zhong, X.B., Suda, T.*, et al.* (2012). Noncanonical Wnt signaling maintains hematopoietic stem cells in the niche. Cell *150*, 351-365.

Sugiyama, T., Kohara, H., Noda, M., and Nagasawa, T. (2006). Maintenance of the hematopoietic stem cell pool by CXCL12-CXCR4 chemokine signaling in bone marrow stromal cell niches. Immunity *25*, 977-988.

Sutherland, H.J., Lansdorp, P.M., Henkelman, D.H., Eaves, A.C., and Eaves, C.J. (1990). Functional characterization of individual human hematopoietic stem cells cultured at limiting dilution on supportive marrow stromal layers. Proc Natl Acad Sci U S A *87*, 3584-3588.

Takam Kamga, P., Bassi, G., Cassaro, A., Midolo, M., Di Trapani, M., Gatti, A., Carusone, R., Resci, F., Perbellini, O., Gottardi, M.*, et al.* (2016). Notch signalling drives bone marrow stromal cell-mediated chemoresistance in acute myeloid leukemia. Oncotarget *7*, 21713-21727.

Tan-Pertel, H.T., Walker, L., Browning, D., Miyamoto, A., Weinmaster, G., and Gasson, J.C. (2000). Notch Signaling Enhances Survival and Alters Differentiation of 32D Myeloblasts. The Journal of Immunology *165*, 4428.

Tanigaki, K., Han, H., Yamamoto, N., Tashiro, K., Ikegawa, M., Kuroda, K., Suzuki, A., Nakano, T., and Honjo, T. (2002). Notch–RBP-J signaling is involved in cell fate determination of marginal zone B cells. Nature Immunology *3*, 443-450.

Taussig, D.C., Miraki-Moud, F., Anjos-Afonso, F., Pearce, D.J., Allen, K., Ridler, C., Lillington, D., Oakervee, H., Cavenagh, J., Agrawal, S.G.*, et al.* (2008). Anti-CD38 antibody-mediated clearance of human repopulating cells masks the heterogeneity of leukemia-initiating cells. Blood *112*, 568-575.

Thomas, D., and Majeti, R. (2017). Biology and relevance of human acute myeloid leukemia stem cells. Blood *129*, 1577-1585.

Tian, C., Tang, Y., Wang, T., Yu, Y., Wang, X., Wang, Y., and Zhang, Y. (2015). HES1 is an independent prognostic factor for acute myeloid leukemia. Onco Targets Ther *8*, 899-904.

Till, J.E., and McCulloch, E.A. (1961). A direct measurement of the radiation sensitivity of normal mouse bone marrow cells. Radiat Res *14*, 213-222.

Tohda, S., Kogoshi, H., Murakami, N., Sakano, S., and Nara, N. (2005). Diverse effects of the Notch ligands Jagged1 and Delta1 on the growth and differentiation of primary acute myeloblastic leukemia cells. Exp Hematol *33*, 558-563.

Tohda, S., and Nara, N. (2001). Expression of Notch1 and Jagged1 proteins in acute myeloid leukemia cells. Leuk Lymphoma *42*, 467-472.

Trøen, G., Wlodarska, I., Warsame, A., Hernández Llodrà, S., De Wolf-Peeters, C., and Delabie, J. (2008). NOTCH2 mutations in marginal zone lymphoma. Haematologica *93*, 1107.

Tsang, A.P., Visvader, J.E., Turner, C.A., Fujiwara, Y., Yu, C., Weiss, M.J., Crossley, M., and Orkin, S.H. (1997). FOG, a multitype zinc finger protein, acts as a cofactor for transcription factor GATA-1 in erythroid and megakaryocytic differentiation. Cell *90*, 109-119.

Tzeng, Y.S., Li, H., Kang, Y.L., Chen, W.C., Cheng, W.C., and Lai, D.M. (2011). Loss of Cxcl12/Sdf-1 in adult mice decreases the quiescent state of hematopoietic stem/progenitor cells and alters the pattern of hematopoietic regeneration after myelosuppression. Blood *117*, 429-439.

Van Den Berg, D.J., Sharma, A.K., Bruno, E., and Hoffman, R. (1998). Role of members of the Wnt gene family in human hematopoiesis. Blood *92*, 3189-3202.

Vanheusden, K., Van Coppernolle, S., De Smedt, M., Plum, J., and Vandekerckhove, B. (2007). In vitro expanded cells contributing to rapid severe combined immunodeficient repopulation activity are CD34+38-33+90+45RA. Stem Cells *25*, 107-114.

Varnum-Finney, B., Brashem-Stein, C., and Bernstein, I.D. (2003). Combined effects of Notch signaling and cytokines induce a multiple log increase in precursors with lymphoid and myeloid reconstituting ability. Blood *101*, 1784-1789.

Varnum-Finney, B., Halasz, L.M., Sun, M., Gridley, T., Radtke, F., and Bernstein, I.D. (2011). Notch2 governs the rate of generation of mouse long- and short-term repopulating stem cells. J Clin Invest *121*, 1207-1216.

Varnum-Finney, B., Purton, L.E., Yu, M., Brashem-Stein, C., Flowers, D., Staats, S., Moore, K.A., Le Roux, I., Mann, R., Gray, G.*, et al.* (1998). The Notch ligand, Jagged-1, influences the development of primitive hematopoietic precursor cells. Blood *91*, 4084-4091.

Velten, L., Haas, S.F., Raffel, S., Blaszkiewicz, S., Islam, S., Hennig, B.P., Hirche, C., Lutz, C., Buss, E.C., Nowak, D.*, et al.* (2017). Human haematopoietic stem cell lineage commitment is a continuous process. Nat Cell Biol *19*, 271-281.

Wang, J., Sun, Q., Morita, Y., Jiang, H., Gross, A., Lechel, A., Hildner, K., Guachalla, L.M., Gompf, A., Hartmann, D.*, et al.* (2012). A differentiation checkpoint limits hematopoietic stem cell self-renewal in response to DNA damage. Cell *148*, 1001-1014.

Wang, J.C., Doedens, M., and Dick, J.E. (1997). Primitive human hematopoietic cells are enriched in cord blood compared with adult bone marrow or mobilized peripheral blood as measured by the quantitative in vivo SCID-repopulating cell assay. Blood *89*, 3919-3924.

Wang, L., Zhang, H., Rodriguez, S., Cao, L., Parish, J., Mumaw, C., Zollman, A., Kamoka, M.M., Mu, J., Chen, D.Z.*, et al.* (2014). Notch-dependent repression of miR-155 in the bone marrow niche regulates hematopoiesis in an NF-kappaB-dependent manner. Cell Stem Cell *15*, 51-65.

Weerkamp, F., Luis, T.C., Naber, B.A., Koster, E.E., Jeannotte, L., van Dongen, J.J., and Staal, F.J. (2006). Identification of Notch target genes in uncommitted T-cell progenitors: No direct induction of a T-cell specific gene program. Leukemia *20*, 1967-1977.

Weisberg, E., Boulton, C., Kelly, L.M., Manley, P., Fabbro, D., Meyer, T., Gilliland, D.G., and Griffin, J.D. (2002). Inhibition of mutant FLT3 receptors in leukemia cells by the small molecule tyrosine kinase inhibitor PKC412. Cancer Cell *1*, 433-443.

Welch, J.S., Ley, T.J., Link, D.C., Miller, C.A., Larson, D.E., Koboldt, D.C., Wartman, L.D., Lamprecht, T.L., Liu, F., Xia, J.*, et al.* (2012). The origin and evolution of mutations in acute myeloid leukemia. Cell *150*, 264-278.

Welch, J.S., Westervelt, P., Ding, L., Larson, D.E., Klco, J.M., Kulkarni, S., Wallis, J., Chen, K., Payton, J.E., Fulton, R.S.*, et al.* (2011). Use of whole-genome sequencing to diagnose a cryptic fusion oncogene. JAMA *305*, 1577-1584.

Weng, A.P., Ferrando, A.A., Lee, W., Morris, J.P.t., Silverman, L.B., Sanchez-Irizarry, C., Blacklow, S.C., Look, A.T., and Aster, J.C. (2004). Activating mutations of NOTCH1 in human T cell acute lymphoblastic leukemia. Science *306*, 269-271.

Weng, A.P., Millholland, J.M., Yashiro-Ohtani, Y., Arcangeli, M.L., Lau, A., Wai, C., Del Bianco, C., Rodriguez, C.G., Sai, H., Tobias, J.*, et al.* (2006). c-Myc is an important direct target of Notch1 in T-cell acute lymphoblastic leukemia/lymphoma. Genes Dev *20*, 2096-2109.

Wertheim, G.B.W. (2015). Molecular characterization and testing in acute myeloid leukemia. Journal of Hematopathology *8*, 177-189.

Wharton, K.A., Johansen, K.M., Xu, T., and Artavanis-Tsakonas, S. (1985). Nucleotide sequence from the neurogenic locus notch implies a gene product that shares homology with proteins containing EGF-like repeats. Cell *43*, 567-581.

Wilson, A., MacDonald, H.R., and Radtke, F. (2001). Notch 1-deficient common lymphoid precursors adopt a B cell fate in the thymus. The Journal of experimental medicine *194*, 1003-1012.

Winer, J., Jung, C.K., Shackel, I., and Williams, P.M. (1999). Development and validation of real-time quantitative reverse transcriptase-polymerase chain reaction for monitoring gene expression in cardiac myocytes in vitro. Anal Biochem *270*, 41-49.

Wouters, B.J., and Delwel, R. (2016). Epigenetics and approaches to targeted epigenetic therapy in acute myeloid leukemia. Blood *127*, 42-52.

Wu, A.M., Till, J.E., Siminovitch, L., and McCulloch, E.A. (1967). A cytological study of the capacity for differentiation of normal hemopoietic colony-forming cells. Journal of Cellular Physiology *69*, 177-184.

Wunderlich, M., Chou, F.S., Link, K.A., Mizukawa, B., Perry, R.L., Carroll, M., and Mulloy, J.C. (2010). AML xenograft efficiency is significantly improved in NOD/SCID-IL2RG mice constitutively expressing human SCF, GM-CSF and IL-3. Leukemia *24*, 1785-1788.

Xiao, X., Lai, W., Xie, H., Liu, Y., Guo, W., Liu, Y., Li, Y., Li, Y., Zhang, J., Chen, W.*, et al.* (2019). Targeting JNK pathway promotes human hematopoietic stem cell expansion. Cell Discovery *5*, 2.

Yao, D., Huang, Y., Huang, X., Wang, W., Yan, Q., Wei, L., Xin, W., Gerson, S., Stanley, P., Lowe, J.B.*, et al.* (2011). Protein O-fucosyltransferase 1 (Pofut1) regulates lymphoid and myeloid homeostasis through modulation of Notch receptor ligand interactions. Blood *117*, 5652-5662.

Yaseen, A., Chen, S., Hock, S., Rosato, R., Dent, P., Dai, Y., and Grant, S. (2012). Resveratrol sensitizes acute myelogenous leukemia cells to histone deacetylase inhibitors through reactive oxygen species-mediated activation of the extrinsic apoptotic pathway. Mol Pharmacol *82*, 1030-1041.

Ye, Q., Jiang, J., Zhan, G., Yan, W., Huang, L., Hu, Y., Su, H., Tong, Q., Yue, M., Li, H.*, et al.* (2016a). Small molecule activation of NOTCH signaling inhibits acute myeloid leukemia. Scientific Reports *6*, 26510.

Ye, Q., Jiang, J., Zhan, G., Yan, W., Huang, L., Hu, Y., Su, H., Tong, Q., Yue, M., Li, H.*, et al.* (2016b). Small molecule activation of NOTCH signaling inhibits acute myeloid leukemia. Sci Rep *6*, 26510.

Yin, D.D., Fan, F.Y., Hu, X.B., Hou, L.H., Zhang, X.P., Liu, L., Liang, Y.M., and Han, H. (2009). Notch signaling inhibits the growth of the human chronic myeloid leukemia cell line K562. Leuk Res *33*, 109-114.

Yoda, M., Kimura, T., Tohmonda, T., Uchikawa, S., Koba, T., Takito, J., Morioka, H., Matsumoto, M., Link, D.C., Chiba, K.*, et al.* (2011). Dual functions of cell-autonomous and non-cell-autonomous ADAM10 activity in granulopoiesis. Blood *118*, 6939-6942.

Yoshihara, H., Arai, F., Hosokawa, K., Hagiwara, T., Takubo, K., Nakamura, Y., Gomei, Y., Iwasaki, H., Matsuoka, S., Miyamoto, K.*, et al.* (2007). Thrombopoietin/MPL signaling regulates hematopoietic stem cell quiescence and interaction with the osteoblastic niche. Cell Stem Cell *1*, 685-697.

Young, A.L., Challen, G.A., Birmann, B.M., and Druley, T.E. (2016). Clonal haematopoiesis harbouring AML-associated mutations is ubiquitous in healthy adults. Nat Commun *7*, 12484.

Yu, X., Alder, J.K., Chun, J.H., Friedman, A.D., Heimfeld, S., Cheng, L., and Civin, C.I. (2006). HES1 inhibits cycling of hematopoietic progenitor cells via DNA binding. Stem Cells *24*, 876-888.

Zeng, Y., Wagner, E.J., and Cullen, B.R. (2002). Both natural and designed micro RNAs can inhibit the expression of cognate mRNAs when expressed in human cells. Mol Cell *9*, 1327-1333.

Zhao, M., Ross, J.T., Itkin, T., Perry, J.M., Venkatraman, A., Haug, J.S., Hembree, M.J., Deng, C.X., Lapidot, T., He, X.C.*, et al.* (2012). FGF signaling facilitates postinjury recovery of mouse hematopoietic system. Blood *120*, 1831-1842.

Zhao, Y., Katzman, R.B., Delmolino, L.M., Bhat, I., Zhang, Y., Gurumurthy, C.B., Germaniuk-Kurowska, A., Reddi, H.V., Solomon, A., Zeng, M.S.*, et al.* (2007). The notch regulator MAML1 interacts with p53 and functions as a coactivator. J Biol Chem *282*, 11969-11981.

Zhou, L., Li, L.W., Yan, Q., Petryniak, B., Man, Y., Su, C., Shim, J., Chervin, S., and Lowe, J.B. (2008). Notch-dependent control of myelopoiesis is regulated by fucosylation. Blood *112*, 308-319.

Zweidler-McKay, P.A., He, Y., Xu, L., Rodriguez, C.G., Karnell, F.G., Carpenter, A.C., Aster, J.C., Allman, D., and Pear, W.S. (2005). Notch signaling is a potent inducer of growth arrest and apoptosis in a wide range of B-cell malignancies. Blood *106*, 3898-3906.

Appendix I

Solutions

Annealing buffer
100 mM $C_2H_3KO_2$ (Merck)
30 mM HEPES pH7.4 (Merck)
2 mM $Mg(CH_3COO)_2$ (Merck)
This should be stored at -20 °C and is ok to freeze-thaw.

SDS Running buffer
50 ml 20X NuPAGE™ MOPS SDS Running buffer solution (Thermo)
950 ml distilled miliQ water

Transfer buffer
50 ml 20X NuPAGE™ Transfer Buffer (Thermo)
100 ml 100% methanol (Merck)
850 ml distilled miliQ water

Blocking solution
5 g of non-fat milk powder
100 ml TBS-T

20X TBS
60.57 g Tris base (Fisher)
88 g NaCl (Merck)
Dissolve in 400 ml miliQ water
Adjust to pH 7.6 with HCl
Make up to 500 ml with miliQ water

TBS-T
250 ml 2X TBS
249.5 ml miliQ water
0.5 ml Tween 20 (Merck)

Appendix II

Table II.1 - Oligos used to generate the miR30-based lentiviral constructs

Gene	Clone		Oligo sequences (5' to 3')	Reference
Luc	**sh*Luc***	Fwd	5' pho - TCGAGAAGGTATATTGCTGTTGACAGTGAGCGCTACGCTGAGTACTTCGAAATGTAGTGAAGCCACAGATGTACATTTCGAAGTACTCAGCGTAATGCCTACTGCCTCGG	
		Rev	5' pho - AATTCCGAGGCAGTAGGCATTACGCTGAGTACTTCGAAATGTACATCTGTGGCTTCACTACATTTCGAAGTACTCAGCGTAGCGCTCACTGTCAACAGCAATATACCTTC	
NCSTN	**sh*NCSTN-1***	Fwd	5'pho-TCGAGAAGGTATATTGCTGTTGACAGTGAGCGCCACCACTTATGTTGTACAGTATAGTGAAGCCACAGATGTATACTGTACAACATAAGTGGTG TTGCCTACTGCCTCGG	Dharmacon (V3LHS_300630)
		Rev	5'pho-AATTCCGAGGCAGTAGGCAACACCACTTATGTTGTACAGTATACATCTGTGGCTTCACTATACTGTACAACATAAGTGGTGGCGCTCACTGTCAACAGCAATATACCTTC	
NCSTN	**sh*NCSTN-2***	Fwd	5'pho-TCGAGAAGGTATATTGCTGTTGACAGTGAGCGCGTGCGTTCTACTGCACGATTATAGTGAAGCCACAGATGTATAATCGTGCAGTAGAACGCACATGCCTACTGCCTCGG	Sigma (TRCN0000308211)
		Rev	5'pho-AATTCCGAGGCAGTAGGCATGTGCGTTCTACTGCACGATTATACATCTGTGGCTTCACTATAATCGTGCAGTAGAACGCACGCGCTCACTGTCAACAGCAATATACCTTC	
NCSTN	**sh*NCSTN-3***	Fwd	5'pho-TCGAGAAGGTATATTGCTGTTGACAGTGAGCGACAGTTAGAGAATGTTGACTCATAGTGAAGCCACAGATGTATGAGTCAACATTCTCTAACTGCTGCCTACTGCCTCGG	Dharmacon (V3LHS_300634)
		Rev	5'pho-AATTCCGAGGCAGTAGGCAGCAGTTAGAGAATGTTGACTCATACATCTGTGGCTTCACTATGAGTCAACATTCTCTAACTGTCGCTCACTGTCAACAGCAATATACCTTC	
NCSTN	**sh*NCSTN-4***	Fwd	5'pho-TCGAGAAGGTATATTGCTGTTGACAGTGAGCGCCTCAGTGGAGAGGAAGATATATAGTGAAGCCACAGATGTATATATCTTCCTCTCCACTGAGTTGCCTACTGCCTCGG	Dharmacon (V3LHS_300632)
		Rev	5'pho - AATTCCGAGGCAGTAGGCAACTCAGTGGAGAGGAAGATATATACATCTGTGGCTTCACTATATATCTTCCTCTCCACTGAGGCGCTCACTGTCAACAGCAATATACCTTC	
NCSTN	**sh*NCSTN-5***	Fwd	5'pho - TCGAGAAGGTATATTGCTGTTGACAGTGAGCGCGGTGCCTTCCATAACAAATATTAGTGAAGCCACAGATGTAATATTTGTTATGGAAGGCACCATGCCTACTGCCTCGG	Dharmacon (V2LHS_255892)
		Rev	5'pho - AATTCCGAGGCAGTAGGCATGGTGCCTTCCATAACAAATATTACATCTGTGGCTTCACTAATATTTGTTATGGAAGGCACCGCGCTCACTGTCAACAGCAATATACCTTC	
NCSTN	**sh*NCSTN-6***	Fwd	5'pho - TCGAGAAGGTATATTGCTGTTGACAGTGAGCGAATCTTCAAGAAGAAAGATGGGTAGTGAAGCCACAGATGTACCCATCTTTCTTCTTGAAGATGTGCCTACTGCCTCGG	Dong *et al* 2010
		Rev	5'pho - AATTCCGAGGCAGTAGGCACATCTTCAAGAAGAAAGATGGGTACATCTGTGGCTTCACTACCCATCTTTCTTCTTGAAGATTCGCTCACTGTCAACAGCAATATACCTTC	
NCSTN	**sh*NCSTN-7***	Fwd	5'pho - CGAGAAGGTATATTGCTGTTGACAGTGAGCGCATGTAGAGTATTCAGTAGAGCTAGTGAAGCCACAGATGTAGCTCTACTGAATACTCTACATTTGCCTACTGCCTCGG	Dong *et al* 2010
		Rev	5'pho - AATTCCGAGGCAGTAGGCAAATGTAGAGTATTCAGTAGAGCTACATCTGTGGCTTCACTAGCTCTACTGAATACTCTACATGCGCTCACTGTCAACAGCAATATACCTTC	
RBPJ	**sh*RBPJ-1***	Fwd	5'pho - TCGAGAAGGTATATTGCTGTTGACAGTGAGCGCGGGAAGCTATGCGAAATTATTTAGTGAAGCCACAGATGTAAATAATTTCGCATAGCTTCCCTTGCCTACTGCCTCGG	Dharmacon (V2LHS_263385)
		Rev	5'pho - AATTCCGAGGCAGTAGGCAAGGGAAGCTATGCGAAATTATTTACATCTGTGGCTTCACTAAATAATTTCGCATAGCTTCCCGCGCTCACTGTCAACAGCAATATACCTTC	
RBPJ	**sh*RBPJ-2***	Fwd	5'pho - TCGAGAAGGTATATTGCTGTTGACAGTGAGCGCGGACAGAATTTCACTCCAAATTAGTGAAGCCACAGATGTAATTTGGAGTGAAATTCTGTCCTTGCCTACTGCCTCGG	Dharmacon (V2LHS_1148633)
		Rev	5'pho - AATTCCGAGGCAGTAGGCAAGGACAGAATTTCACTCCAAATTACATCTGTGGCTTCACTAATTTGGAGTGAAATTCTGTCCGCGCTCACTGTCAACAGCAATATACCTTC	
RBPJ	**sh*RBPJ-3***	Fwd	5'pho - TCGAGAAGGTATATTGCTGTTGACAGTGAGCGCCAGGACAGAATTTCACTCCAATAGTGAAGCCACAGATGTATTGGAGTGAAATTCTGTCCTGTTGCCTACTGCCTCGG	Dharmacon (V3LHS_342058)
		Rev	5'pho - AATTCCGAGGCAGTAGGCAACAGGACAGAATTTCACTCCAATACATCTGTGGCTTCACTATTGGAGTGAAATTCTGTCCTGGCGCTCACTGTCAACAGCAATATACCTTC	

sense; loop; anti-sense

Table II.2 - Oligos used to generate H1 promoter-driven shRNA constructs (CS-shRNA)

Gene	Clone		Oligo sequences (5' to 3')
Luc	**sh*Luc***	Fwd	5' pho - GATCCCCACGCTGAGTACTTCGAAATGTTTCAAGAGAACATTTCGAAGTACTCAGCGTTTTTTGGAAAT
		Rev	5' pho - CTAGATTTCCAAAAAACGCTGAGTACTTCGAAATGTTCTCTTGAAACATTTCGAAGTACTCAGCGTGGG
NCSTN	**sh*NCSTN-1***	Fwd	5' pho - GATCCCCACCACTTATGTTGTACAGTATTTCAAGAGAATACTGTACAACATAAGTGGTTTTTTGGAAAT
		Rev	5' pho - CTAGATTTCCAAAAAACCACTTATGTTGTACAGTATTCTCTTGAAATACTGTACAACATAAGTGGTGGG
NCSTN	**sh*NCSTN-3***	Fwd	5' pho - GATCCCCAGTTAGAGAATGTTGACTCATTTCAAGAGAATGAGTCAACATTCTCTAACTTTTTTGGAAAT
		Rev	5' pho - CTAGATTTCCAAAAAAGTTAGAGAATGTTGACTCATTCTCTTGAAATGAGTCAACATTCTCTAACTGGG
RBPJ	**sh*RBPJ-2***	Fwd	5' pho - GATCCCCGGACAGAATTTCACTCCAAATTTCAAGAGAATTTGGAGTGAAATTCTGTCCTTTTTTGGAAAT
		Rev	5' pho - CTAGATTTCCAAAAAGGACAGAATTTCACTCCAAATTCTCTTGAAATTTGGAGTGAAATTCTGTCCGGG
RBPJ	**sh*RBPJ-3***	Fwd	5' pho - GATCCCCAGGACAGAATTTCACTCCAAATTCAAGAGATTTGGAGTGAAATTCTGTCCTTTTTTGGAAAT
		Rev	5' pho - CTAGATTTCCAAAAAAGGACAGAATTTCACTCCAAATCTCTTGAATTTGGAGTGAAATTCTGTCCTGGG
NOTCH1	**sh*NOTCH1***	Fwd	5' pho - GATCCCCAGGTGCAGCCACAAAACTTACTTCAAGAGAGTAAGTTTTGTGGCTGCACCTTTTTTGGAAAT
		Rev	5' pho - CTAGATTTCCAAAAAAGGTGCAGCCACAAAACTTACTCTCTTGAAGTAAGTTTTGTGGCTGCACCTGGG
NOTCH2	**sh*NOTCH2***	Fwd	5' pho - GATCCCCACCACATCCTCTCCAATGATTTTCAAGAGAAATCATTGGAGAGGATGTGGTTTTTTGGAAAT
		Rev	5' pho - CTAGATTTCCAAAAAACCACATCCTCTCCAATGATTTCTCTTGAAAATCATTGGAGAGGATGTGGTGGG

sense; loop; anti-sense

Table II.3 – Starting plasmids used for the generation of lentiviral constructs

Plasmid name	Source
pLV.EF1α-premiRNA30-RFP	Biossettia Inc. (USA)
pSIN.Tet-HPGK-rtTA2-hDKK-Ires-GFP	Generated *in-house*
pGIPZ™	Dharmacon – Horizon Discovery Group plc (UK)
pmCherry	Clontech (Takara Bio, Japan)
pECFP-C1	Clontech (Takara Bio, Japan)
pEntr4-H1	Riken (Japan)
CS-RfA-EG	Riken (Japan)
pCCL-NGFR	a gift from Prof. Luigi Naldini (San Raffaele Telethon Institute for Gene Therapy)
CSII-EF-MCS	Riken (Japan)
pHes1-GFPd20 plasmid	Addgene (plasmid #14808)

Table II.4 – Primers used for molecular cloning

Primer name	Sequence (5' to 3')
Fwd cherry for reporter	ACTGACACCGGTCGCCACCATGG
Rev cherry for reporter	GCTAAGCTTCTTGTACAGCTCGTCCATGCC
Fwd Hes1 GFP	ACTGACCTCGAGACTGACTGCCTCTAGGCATATGACACGCACGCACACACAC
Rev Hes1 GFP	ACTGACGTCGACCTACACATTGATCCTAGCAGAAGCAC
Fwd NGFR	ACTGACCTCGAGCGCCACCATGGGGGCAGG
Rev NGFR	ACTGACCATATGACTGACGCGTCTAGAGGATCCCCCTGTTCCACC
Fwd GFP	TACCCCTCTAGAGTCGAGCTACCGGTCGCCACCATGGTGAGCAAGGGCGAGG
Rev GFP	TTGGAACCTAAGTCGACACGCGTTTACTTGTACAGCTCGTCCATGCC
Fwd miR30shrna	TCTCGAGGATCCACAGAATCGTTGCCTGCAC
Rev miR30shrna	GCTCGAGCTAGCTTCAGCTTTGTAAAAATGTATCAAAG

Table II.5 – Primers used in DNA sequencing

Primer name	Sequence (5' to 3')
Fwd Seq NGFR	GTTCTCCGACGTGGTGAGC
Rev Seq NGFR	CTCATCCTGGTAGTAGCC
Rev Seq Hes1	CTAATGTCTTCCGGAATTCC
Fwd Seq cherry	AAGCTGAAGGTGACCAAG
Rev Seq cherry	TTCACGTAGGCCTTGGAG
Seq rev SHMIR30 EF1	TTACATCAAGTGCCAAGCTG
Seq Fwd SHMIR30 pECFP	CCAAAATGTCGTAACAACTCC
pH1up2seq	CAGGAAGATGGCTGTGAGG
Seq Fwd GFP	CCTCTAGAGTCGAGCTACC

Table II.6 – Primers used in qRT-PCR.

Gene		Primers (5' to 3')	Melting temperature (°C)
NCSTN	Fwd	GCAATGGTTTGGCTTATGAAG	63.2
	Rev	ATGCATGTGTGAAAAGAGCTG	62.9
RBPJ	Fwd	AGAGTCTCAACCGTGTGCATT	63.7
	Rev	GTGCTTTCGCTTGTCTGAGTC	64
GAPDH	Fwd	GGGAAGGTGAAGGTCGGAGT	66.6
	Rev	GGGTCATTGATGGCAACAATA	64.4

Appendix III

Table III.1 – Antibodies used in FCM/FACS

Antigen	Reactivity	Fluorochrome	Clone	Dilution	Company
CD10	Human	APC	CB-CALLA	1:10	eBiosciences, USA
CD11c	Human	PE	B-ly6	1:10	BD Biosciences, USA
CD11c	Human	APC	MJ4-27G12	1:10	Miltenyi Biotec, Germany
CD14	Human	PE-Cy7	61D3	1:10	eBiosciences
CD19	Human	AF780	HIB19	1:10	ebiosciences
CD33	Human	APC	P67.6	1:10	BD Biosciences
CD33	Human	BV711	WM53	1:10	BD Biosciences
CD34	Human	APC	581	1:10	BD Biosciences
CD34	Human	PerCP	8G12	1:10	BD Biosciences
CD38	Human	APC-eFluor 780	HIT2	1:10	eBiosciences
CD38	Human	PE-Cy7	HB7	1:10	eBiosciences
CD45RA	Human	PE-Cy7	HI100	1:10	eBiosciences
CD45RA	Human	APC Fire 750	HI100	1:10	Biolegend
CD56	Human	BV605	5.1H11	1:10	Biolegend
CD62L	Human	PE	DREG-56	1:10	Biolegend
CD90	Human	BV605	5E10	1:10	BD Biosciences
CD90	Human	PE	eBio5E10 (5E10)	1:10	eBiosciences
CD135	Human	BV711	4G8	1:10	BD Biosciences
CD271	Human	AF647	C40-1457	1:10	BD Biosciences
NOTCH1	Human	PE	MHN1-519	1:10	BD Biosciences
NOTCH2	Human	PE	MHN2-25	1:10	BD Biosciences
NOTCH4	Human	PE	MHN4-2	1:20	BD Biosciences
Lineage	Human	eFluor 450	RPA-2.10, OKT3, 61D3, CB16, HIB19, TULY56, HIR2	1:10	eBiosciences
Nicastrin	Human	PE	polyclonal	1:40	Sino biological, China
Rabbit IgG isotype control		PE	polyclonal	1:10	BIOSS antibodies, USA
Mouse IgG1, k isotype control		PE	MOPC-21	1:5	BD Biosciences
Mouse IgG1 negative control		AF647	MOPC-21	1:10	BD Biosciences

Table III.2 – Antibodies used in WB.

Antigen	Reactivity	Conjugate	Clone	Dilution	Company
Notch1	Human	unconjugated	D1E11	1/750	Cell Signaling Technology, USA
Notch2	Human	unconjugated	D76A6	1/500	Cell Signaling Technology, USA
Notch4	Human	unconjugated	L5C5	1/1000	Cell Signaling Technology, USA
Cleaved Val1744 Notch1	Human	unconjugated	Rabbit monoclonal D3BA	1/500	Cell Signaling Technology, USA
Cleaved Ala1734 Notch2	Human	unconjugated	polyclonal	1/300	Thermo
Nicastrin	Human	unconjugated	polyclonal	1/1500	Abcam, UK
RBP-Jκ	Human	unconjugated	E-7	1/25	Santa Cruz Biotechnology, USA
β-actin	Human	unconjugated	AC-15	1/10000	Merck
Goat anti-mouse Immunoglobulins	Mouse	HRP	polyclonal	1/5000	DAKO, USA
Goat anti-rabbit Immunoglobulins	Rabbit	HRP	polyclonal	1/5000	DAKO, USA

Appendix IV

Table IV.1 – Characteristics of small molecules.

Compound number	Structure	Molecular Weight
21	AK-968/41024176 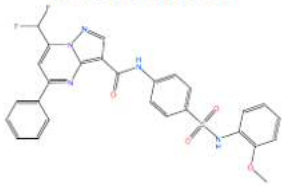	549.55
22	AK-778/11863058 	371.44
24	AJ-292/42226209 	407.91
26	AP-970/43337797 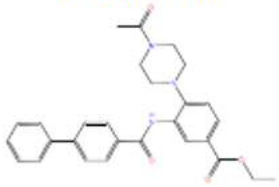	471.55
31	AK-968/40318875 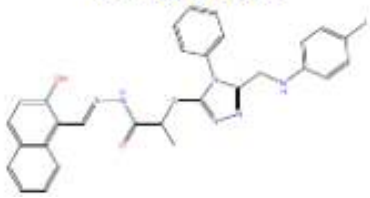	648.53
36	AO-081/40681397 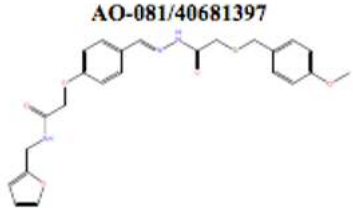	467.54